

CURRENT PRACTICES FOR MODIFICATION OF PAVING ASPHALTS

Hussain U. Bahia and Dario Perdomo
The Asphalt Institute, Research Park Dr., PO Box 14052, Lexington, KY, 40512.

Keywords: Modified Asphalts, Superpave, Asphalt Additives

Introduction

The Superpave binder specification, AASHTO MP1 (1), has introduced new concepts for selecting paving asphalt binders. The specification, in addition to using rheological and failure measurements that are more related to performance, is based on the idea that the criteria to maintain a satisfactory contribution of asphalt binders to the resistance of pavement failures remains the same but have to be satisfied at critical application temperatures. The test procedures require that the material be characterized within certain ranges of strains or stresses to ensure that material and geometric nonlinearities are not confounded in the measurements.

These new specification concepts have resulted in re-evaluation of asphalt modification by the majority of modified asphalt suppliers. The philosophy of asphalt modification is expected to change, following these new concepts, from a general improvement of quality to more focus on using modifiers based on the most critical need as defined by two factors:

- The application temperature domain
- The type of distress to be remedied

The new specification requirements should result in a more effective use of modifiers as the amount and type of modifier will be directly related to the application environment and the engineering requirements.

Modification to meet the Superpave Binder Specifications

The Superpave binder specification parameters have been selected such that one or more material properties are used to evaluate the potential contribution of asphalt binders to resistance of critical pavement distress types (2,3):

Workability: Rotational viscosity is used as the indicator of workability. This is a requirement that is not related to climatic conditions, but is necessary to ensure that binders are workable enough so that mineral aggregates can be properly coated and asphalt mixtures can be compacted efficiently to reach the required density.

This requirement is critical for many modifiers currently used because they tend to increase in consistency and thus result in less workability. To achieve required workability, temperatures for mixing and compaction are usually increased. This can result in increased production cost, more volatile loss, increased oxidative aging, and possible degradation of certain modifiers.

Permanent Deformation: Complex shear modulus (G^*) is used as the indicator of total resistance to deformation (rigidity) under cyclic loading. Sine of the phase angle ($\sin \delta$) is used as the indicator of relative elasticity of the binder under cyclic loading. Both parameters are combined in the parameter ($G^*/\sin \delta$) to ensure that the binder will have acceptable contribution to resistance of permanent deformation.

This requirement indicates that modification of asphalts, to resist permanent deformation, can be done either by increasing rigidity, elasticity, or both. Rigidity is a material characteristic that is much easier to alter because of the nature of the asphalt. Rigidity can be increased by oxidation in the refinery process, by using low cost additives that will work as inert fillers, or by using stiffeners that will react with asphalt and change its consistency. Elasticity, on the other hand, requires creating an elastic structure using certain types of elastomeric materials. These materials, mostly polymeric in nature, should exhibit compatibility with the asphalt and be resistant to changes due to oxidation, phase separation, and unstable reaction. Elasticity has been identified as an important property needed to improve pavement performance. This concept is based mostly on few pavement tests sections and accelerated failure tests in the laboratory. How much elasticity is needed, and what is the elastic structure's contribution to the resistance to permanent deformation, is difficult to quantify. In the Superpave specification the parameter $\sin \delta$ was selected based on the concept of dissipated energy. It is derived with the consideration that asphalts are compared within the linear visco-elastic region. This has important ramifications for some modifiers because their elastic response is different at different strain or stress levels. Strain dependency is discussed in a following section.

Fatigue Cracking: Same parameters (G^* and $\sin \delta$) are used as the indicators of resistance to fatigue cracking. An important distinction is that the specification targeted only strain controlled fatigue as the main fatigue distress. The whole Superpave system (binder and mixture) does not focus on stress controlled fatigue. Using the same energy concepts, the parameter $G^*\sin \delta$ is used to indicate that resistance to strain-controlled fatigue can be achieved by decreasing rigidity (G^*) and/or increasing elasticity (lower $\sin \delta$).

From a modification perspective, decreasing rigidity (measured by G^*) is simpler than increasing elasticity. Rigidity can be decreased in the refining process, by using fluxing agents, or with other low cost hydrocarbons that are compatible with asphalts. Increasing elasticity requires the same basic modifications discussed earlier in relation to permanent deformation. It is, however, more complex at intermediate temperatures because most asphalts show a significant amount of elasticity at intermediate temperatures. To add more elasticity, a highly elastic structure created by an elastomer is needed. The same complications discussed in regard to the strain dependency apply at intermediate temperatures. Unmodified asphalts have a narrow range of linear visco-elastic behavior at intermediate temperatures. In the nonlinear range unmodified asphalts show tendency to lose their elastic behavior (increase in δ) differently than asphalts modified with elastomeric materials. This difference can result in dissimilar performance of modified asphalts in the non-linear range.

Low Temperature Thermal Cracking: Because of the important role of the binder in thermal cracking, the Superpave specification includes three parameters that are combined in any one parameter. Creep stiffness, $S(@60\text{sec})$, is used as an indicator of the amount of thermal stresses that can be built in the asphalt due to a given thermal gradient induced strain induced by temperature change. Logarithmic creep rate, $m(@60\text{sec})$, is an indicator of the relative elasticity; higher m (60) values indicate less elasticity and more ability to relax stresses by viscous flow. Failure strain, ϵ_f , is used as an indicator of brittleness or the ability to stretch without cracking (strain tolerance).

Modification of low temperature properties can be achieved by changing one or more of these parameters. In most cases it is difficult to use modifiers that will change one of these indicators while keeping the others constant. Unlike fatigue, thermal cracking indicators favor modification that results in less elastic binders. This should be easier to achieve since refining processes and additives that result in softer binders either reduce or do not affect the elasticity (higher δ and higher m values). Strain tolerance can be increased by many several mechanisms. Elastomeric polymers can improve strain tolerance. Plastomers and certain fillers can work as crack arresters and increase strain tolerance. Certain hydrocarbons, because of their low glass transition temperature, can significantly improve strain tolerance.

Types and Amounts of Modified Asphalts

There is a large number of modifiers used in paving applications at the present time. In a survey published in 1993 (4), there were a total of 48 commercial brands of asphalt modifiers. These modifiers were classified in 5 classes including 10 fillers/extenders, 16 thermoplastic polymers, 3 thermosets polymers, 1 liquid polymer, 4 aging inhibitors, and 10 adhesion promoters. During the Strategic Highway Research Program (5, 6) 82 asphalt modifiers or modified asphalts were obtained, documented and stored at the Material Reference Library. These 82 sources of modifiers were classified in 8 classes including 39 thermoplastics, 27 anti-stripping agents, 5 anti-oxidants, 2 fibers, 2 extenders, 1 recycling agent, and 1 oxidant. In an internal report by the Engineering Staff of the Asphalt Institute (7), 48 types of modifiers were identified. They were classified into 13 polymers, 10 hydrocarbons, 6 mineral fillers, 6 antioxidants, 6 antistripping additives, 4 fibers, 2 extenders, and 1 oxidant.

The classification of asphalt modifiers can be done based on the composition and physical nature of the modifier, based on the mechanism by which it alters asphalt properties, or based on the target asphalt property that needs to be modified. Table 1 is generated, based on a review of literature (4, 5, 6, 7), to summarize the generic types of asphalt modifiers classified according to the nature of the modifier. The target distress shown in the table is the main distress or property that the additive is expected, or claimed, to affect favorably. The information is based on interpretation of the published information for brands of modifiers that belong to the modifier classes shown. In many cases the reported effects are based on limited data, which means that the effects cannot be generalized to all asphalt and/or aggregate sources.

Typical Effects of Modification On Superpave Binder Parameters

A sample of effect of modification on the Superpave Binder parameters is shown in figures 1 to 4. In all these figures the relative changes (modified/unmodified) in the performance indicators are shown. The base asphalts vary among the modifiers but not for a modifier. Figure 1 shows the effects of some elastomeric polymers (SB and SBR). The ratios are calculated using values measured at temperatures for which the base asphalt meets the respective requirements for each of the parameters. As depicted in Figure 1, the elastomeric polymers show favorable effects on all performance related parameters. $G^*/\sin \delta$ increases, $G^*\sin \delta$ and $S(60)$ decrease, and $m(60)$ and strain at failure increase. The relative changes are however higher for the $G^*/\sin \delta$ and failure strain than the other parameters.

Figure 2 depicts the changes for another asphalt modified with 3 different plastomeric additives at 4% by weight of asphalt. These vary in their molecular weight but all are polyethylene based. The only significant change is seen at high temperatures for the parameter $G^*/\sin \delta$. It appears that these plastomers are not effective with this particular asphalt at intermediate or low temperatures.

Figure 3 depicts the effects of three different types of crumb rubbers. These are all mixed at 15% by weight of asphalt. The effect on the values of $G^*/\sin \delta$ are more pronounced than the

plastomeric modifiers but the effects on the other parameters are not very significant. These rubbers are not reacted and no extender oils were used in preparation of their mixtures with the asphalt.

Figure 4 depicts the effects of two mineral fillers (C: Calcite and Q: quartz) mixed at 50 % volume concentration. As depicted, these fillers significantly increase $G^*/\sin \delta$, which is a favorable effect. They, however, also increase $G^*\sin \delta$, $S(60)$ and they decrease $m(60)$. These effects are not favorable and may contribute to significant increase in fatigue and thermal cracking.

The data presented in Figures 1 to 4 are samples of data collected for specific asphalts. They cannot be generalized for all asphalts. Several of these modifiers/additives react with asphalts and their effects are therefore asphalt specific. They are presented here to give an overview of the general trends of effects. The data clearly shows that the most significant effect is seen at high temperatures in the parameter $G^*/\sin \delta$. This is expected since asphalts exhibit the least stiffness at higher temperatures. If the effects on G^* and $\sin \delta$ for these modifiers are considered separately, it is clear that the most significant effect is on the value of G^* . Even for the elastomeric modifiers, the phase angle did not drop by more than 25 degrees. For an asphalt with a phase angle of 80 degrees, this change will only result in a 15% reduction of $\sin \delta$. This finding substantiates the concept that it is more difficult to induce elasticity at high temperatures than to enhance rigidity with most of the modification techniques used currently.

Characteristics not Considered by the Superpave Binder Specifications and Test Protocols

The Superpave binder specification is based on important assumptions that are justified for unmodified asphalts. Several of these assumptions may not be valid for some modified asphalts. Following are some of the critical assumptions or characteristics that are not considered and which are currently being discussed by asphalt researchers.

Dependency of viscosity on shear rate: The rotational viscosity is measured at 135 C at a recommended rate of 20 rpm. This shear rate was selected because most unmodified asphalts show Newtonian behavior (viscosity is independent of shear rate) at this rate. It was also selected to simulate shear rates during pumping and handling in refineries and asphalt plants. Many modified asphalts are highly shear dependent at and above the value of 20 rpm. Modified asphalts can also exhibit elasticity at these high temperatures, which cannot be measured with a viscometer. The current rotational viscosity protocol for Superpave does not include a procedure to measure shear rate dependency and the criteria for workability do not address this characteristic of modified asphalts. In the mixture design requirements of Superpave, it is required to mix at a viscosity of approximately 0.17 Pa-s and compact at 0.28 Pa-s. These low viscosities cannot be achieved for many modified asphalts unless they are heated to extremely high temperatures.

Strain dependency of rheological response under cyclic loading: The rheological properties in the Superpave specification are measured at selected strain levels. These strain levels are selected to be within the linear viscoelastic range for unmodified asphalts. The basis for the selection was the relation between limit of linear behavior and the value of G^* . For modified asphalts it is known that this relation may not hold true. Figures 5 to 7 depict strain dependency of selected modified asphalts. Figure 5 is for an asphalt modified with two polymeric modifiers, including both an elastomeric and a plastomeric modifier. Figure 6 is for an asphalt modified with crumb rubber, and Figure 7 is for an asphalt modified with a rigid filler. In all cases it is apparent that there is a shear thinning effect. The G^* decreases with strain while the δ increases. Unmodified asphalts also show a shear thinning effect; the linearity limit on the strain scale decreases as the temperature decreases. The Superpave specification does not allow for consideration of strain dependency nor does it refer to a range of strains that are typically encountered in the field.

The concept in the Superpave specification is to select asphalts based on their performance within the small strain (linear) range because pavements should not be designed to encounter large strains. In other words asphalts should be compared within the (safe) pre-failure region within which they do not undergo high deformation or stresses. It should be mentioned however that it is very difficult to estimate the true strain distribution in an asphalt-aggregate mixture under loading. It is difficult because of the irregular shape of aggregates and the random distribution of voids and binder between aggregates. For the specification to be applicable for materials that do not show a wide linear region, a range of strains should be defined and used in testing. Strain dependency should not be considered as an inferior property. Strain dependent materials (nonlinear materials) can perform well if their strain/stress dependency is taken into account.

Thixotropy and effect of mechanical working: Effect of repeated loading at constant rates on G^* and δ is another behavior that is not considered in the Superpave specifications. Certain additives can result in a thixotropic network structure that can be destroyed or altered by repeated shearing. Such structure can be destroyed permanently by mechanical working or can be affected temporarily and regained when material is left to rest. Not many asphalt modifiers that are currently used are known to show such a behavior. Figure 8 depicts a typical example of a time sweep for an asphalt before and after modification with polymeric additives. The figure shows that neither the G^* nor the δ are changing in this experiment where the asphalts are being sheared at 10 rad/s every 6 seconds for more approximately 66 seconds. Some asphalts modified with Tall oil and some gel-like compounds can show significant changes due to

mechanical working. Similar to strain dependency, thixotropy should not be considered as an inferior material property. If thixotropy is considered properly in testing and evaluation, thixotropic materials can outperform non-thixotropic materials.

Loading rate dependency: The testing in the specification is conducted at selected loading rates that are assumed to be typical under traffic on open highways. It is well recognized that traffic does not move at one speed. It is also known that thermal cooling cycles vary significantly in their cooling and warming rates. Dependency on loading rates is material specific, not only for modified binders but also for unmodified asphalts. The testing rate of 10 rad/s used for cyclic testing, and the loading time of 60 seconds used for the creep testing, are based on simplifications of asphalt behavior. Modification may result in nullifying the assumptions used in these simplifications. The effect of modification on loading rate dependency should be considered in selecting modifiers and a more comprehensive procedure should be included in the specification to evaluate this property.

Time-Temperature Equivalency: Testing for low temperature creep is done at 10 °C higher than the lowest pavement design temperatures. Also in the guidelines for considering slow moving traffic and traffic amount, it is recommended to shift temperature of testing rather than loading frequency. These requirements and guidelines are based on the assumption that the time-temperature equivalency factors are similar for most asphalts. Although there are similarities in time-temperature equivalency factors for asphalts (8), the equivalency factors can vary for asphalts with different glass transition behavior and asphalts that are heavily modified. One of the common modification techniques is to use softer asphalts with good low temperature properties, and use additives to improve high temperature properties. Such a modified asphalt may have a glass transition region that is significantly lower than an unmodified asphalt with equivalent high temperature properties. These two asphalts can show significantly different time-temperature shift factors due to the difference in transition temperature range. The glass transition region and time-temperature equivalency of asphalts are important properties that are not fully considered in the specifications.

Concluding Remarks

The Superpave binder specification introduces a new system that can more accurately evaluate the effect of modifiers on performance related properties of asphalt binders. There is a variety of additives that are used as asphalt modifiers in paving applications. These can be classified based on their composition and/or effects as polymers (elastomeric and plastomeric), fillers, fibers, hydrocarbons, anti-stripping agents, oxidants, antioxidants, crumb rubber, and extenders. A sample of polymers, fillers, and crumb rubber modifiers was evaluated using the Superpave binder tests. The results indicate that they can impart significant changes on the properties measured in the Superpave specification. The main changes they can impart reflect on the rigidity of the binder (G^*) at the intermediate to high pavement temperatures encountered in the field.

The testing protocols included in the Superpave specification are not inclusive of certain important characteristics that are typical of modified binders. Among these characteristics are strain dependency, thixotropy, loading rate dependency, and time-temperature equivalency. These characteristics are modifier specific and ignoring them in selecting modifiers may lead to underestimating or overestimating the effect of the modifier on pavement performance. Typical results for strain dependency and mechanical working were presented for a group of selected modifiers. The Superpave specifications should include provisions to measure these characteristics, and guidelines to assess their effects on pavement performance.

References

1. "Standard Specification for Performance Graded Asphalt Binder", AASHTO Designation MP1-93, AASHTO, Gaithersburg, Md., September, 1993.
2. Anderson, D.A., and T.W. Kennedy, "Development of SHRP Binder Specification", Journal of the Association of Asphalt Paving Technologists, Vol. 62, 1993, P. 481
3. Bahia, H.U., and Anderson, D.A. "The New Proposed Rheological Properties: Why are They Required and How They Compare to Conventional Properties," Transportation Research Board record 1488, Washington, DC, 1995, pp. 32-39.
4. Kristin Peterson, "Specifier's Guide to Asphalt Modifiers", Roads and Bridges Magazine, May 1993, pp. 42-46.
5. M. Mortazavi, and J.S. Moulthrop, "The SHRP Materials Reference Library," SHRP-A-646 report, National Research Council, Washington, D.C. 1993.
6. Rowlett, R.D. et al., "Performance of Asphalt Modifiers: Classification of Modifiers and Literature Review," Center for Construction Materials Technology, SWL, Houston, Texas, April 1990.
7. McGennis, R.B., "Asphalt Modifiers are here to Stay", Asphalt Contractor, April 1995, pp. 38-41.
8. Anderson, D.A., Christensen, D.W., Bahia, H.U., Dongre, R., Sharma, M.G., Button, J. J. "Binder Characterization and Evaluation, Volume 3: Physical Characterization," Report No. SHRP-A-369, The Strategic Highway Research Program, National Research Council, Washington, DC 1994.

Table 1. Generic types of asphalt modifiers currently used for paving applications.

The classification of CLASS		EFFECT ON DISTRESS				AGN ⁵
		PD ¹	FC ²	LTC ³	MD ⁴	
1. Mineral Fillers	Carbon black	x				x
	Hydrated lime	x				x
	Fly ash	x				
	Portland cement	x				
	Silica fume	x				
	Baghouse fines	x				
2. Extenders	Sulphur	x	x	x		
	Some fillers (baghouse dust)					
3a. Polymers Elastomers	<i>Styrene block copolymers</i>	x	x	x		
	Styrene butadiene diblock (SB)	x		x	x	
	Styrene butadiene triblock/radial block (SBS)	x	x	x		
	Styrene Isoprene (SIS)	x				
	Styrene ethylbutylene (SEBS)					
	<i>Styrene butadiene rubber latex (SBR)</i>	x		x		
3b. Polymers Plastomers	Polychloroprene latex	x	x			
	Polyisoprene (natural and synthetic)	x				
	Ethylene Propylene diene monomer (EDPM)	x				
	Polyisobutylene	x				
	<i>Ethylene vinyl acetate (EVA)</i>	x	x			
	<i>Ethylene methacrylates (EMA)</i>					
	<i>Polyethylene (low density and high density)</i>	x		x		
	Polypropylene	x				
Polyolefin	x					
4. Crumb rubber	Different sizes, treatments, and processes	x	x	x		
5. Oxidants	Manganese compounds	x				
6. Hydrocarbons	Aromatics			x		
	Napthenics					
	Paraffinics/wax				x	
	Vacuum gas oil			x		
	ROSE process resins	x				
	Asphaltenes	x				
	Tall oil	x	x			
	Natural asphalts	x				
7. Antistrips	Fatty amidoamines					x
	Imidazolines					x
	Polyamines					x
	Hydrated lime					x
	Organo-metallics					x
	Acids					x
8. Fibers	Polypropylene	x	x	x		
	Polyester	x		x		
	Cellulose	x				
	Mineral	x				
	Reinforcement	x	x	x		
9. Antioxidants	Carbamates					
	Lead			x		x
	Zinc			x		x
	Carbon black	x				x
	Hydrated lime				x	x
	Phenols					x
	Ethyoxylated amine				x	x

1: PD: Permanent Deformation

3. LTC: Low Temperature Cracking

2. FC: Fatigue Cracking

4. MD: Moisture Damage

5. AGN: Oxidative Aging

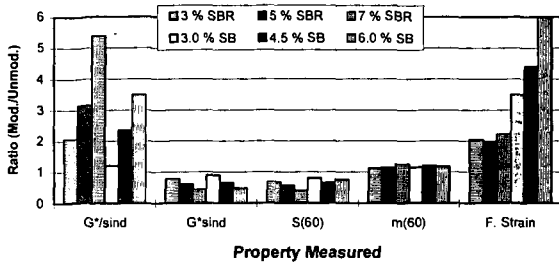


Figure 1. Relative Change in Superpave binder properties after modification with SBR and SB-based modifiers

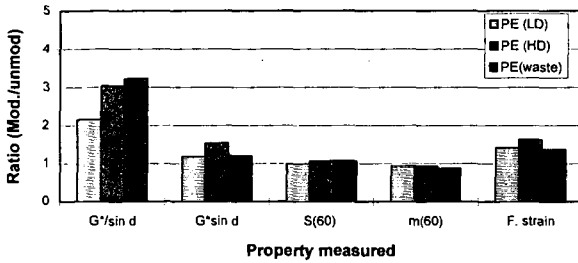


Figure 2. Relative Change in Superpave binder properties after addition of Plastomers

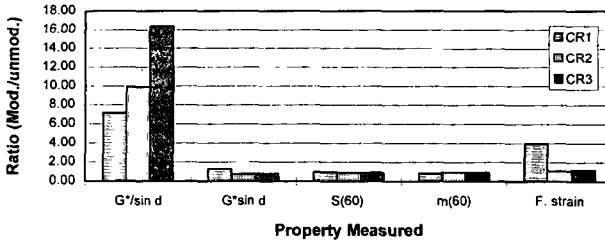


Figure 3. Relative change in Superpave binder properties after modification with 3 types of crumb rubber

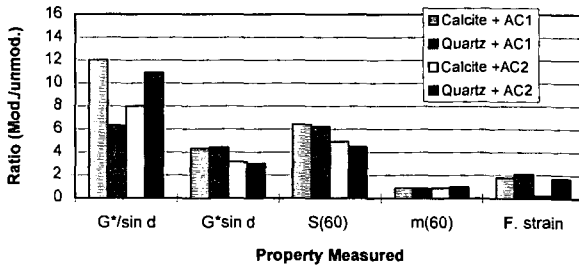


Figure 4. Relative change in Superpave binder properties after addition of mineral fillers

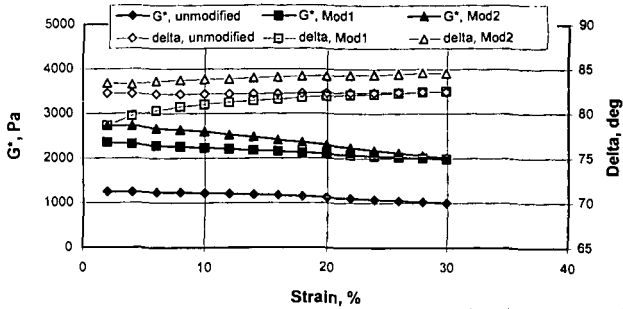


Figure 5. Effect of testing strain on properties of a typical asphalt before and after modification with polymers

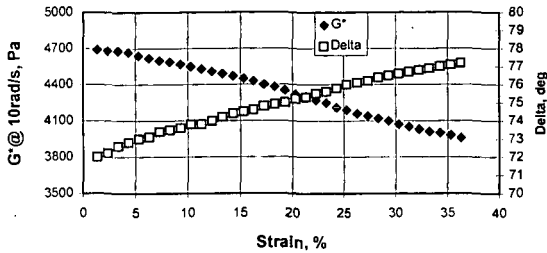


Figure 6. Effect of testing strain on properties of a typical asphalt modified with crumb rubber

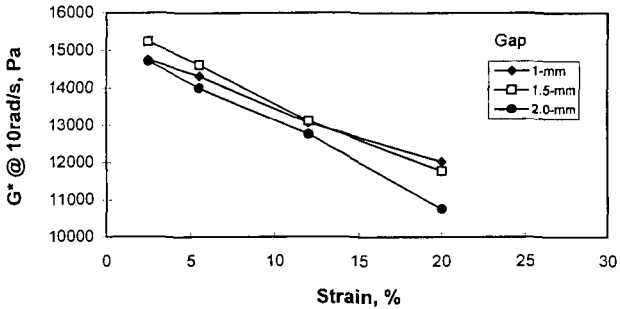


Figure 7. Strain dependency of asphalt filled with rigid filler (Ottawa sand < 0.25 mm) Filler/Asphalt ratio= 0.5 by volume

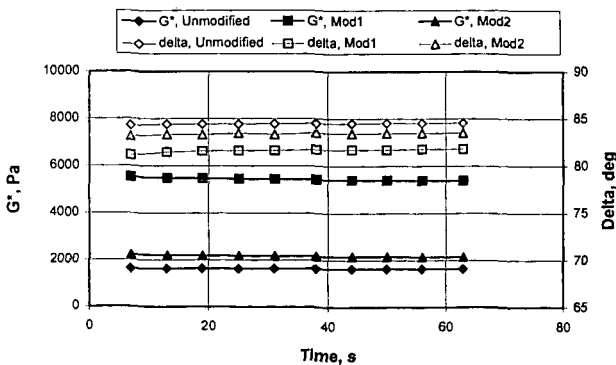


Figure 8. Effect of mechanical working on asphalt properties before and after modification with polymers

FURFURAL MODIFIED ASPHALT OBTAINED BY USING A LEWIS ACID AS A CATALYST

G. Mohammed Memon, FHWA/ EBA Engineering Inc.
Brian H. Chollar, FHWA
6300 Georgetown Pike
McLean, VA 22101

INTRODUCTION

Asphalt is solid or semi-solid at room temperature, becomes soft and starts flowing upon heating, and becomes hard and brittle at very low temperatures.

States have been facing problems such as cracking, rutting, and asphalt adhesion to aggregates in their asphaltic pavements for years. Many polymer additives have been used in asphalt to reduce these problems, but little work has been done using chemically modified products of asphalt to attempt to solve these serious problems of asphalt pavements⁽¹⁻³⁾. The above mentioned problems decrease the life of the pavements, resulting in an increase of maintenance and/or replacement costs. There are two types of cracking which can occur in asphalt pavement; one related to load, and the other related to thermal stress. The load-related cracking is known as fatigue cracking and is defined as fracture under repeated or cyclic stress having a maximum value of less than the tensile strength of the material. The thermal cracking occurs due to pavement shrinkage at low temperatures causing the shrinkage stresses to exceed the tensile strength.

FHWA researchers have found furfural to be a suitable candidate for functional group modification of asphalt. The modified product shows improved performance as well as improved rheological properties.⁴ The furan ring in the product was found to be the principal component responsible for the product high temperature stiffness, whereas the furan ring (with or without an aldehyde group) was also important in improving the product low temperature properties². The nature of this reaction was determined by FHWA laboratories using different analytical instruments. Phenolic moieties present in asphalt were found to be reacting with furfural (in the presence of an acid as a catalyst) forming a polymeric material³. However, mix testing showed corrosive fumes (due to HCl) escaping from the furfural modified asphalt⁵.

Thus, a chemically modified asphalt is needed which: has low creep stiffness, has less temperature susceptibility, can resist thermal stress to alleviate thermal cracking, can maintain a high stiffness at high temperatures to resist rutting, and is an environmentally accepted modified product. The major objective of this study was to obtain a furfural modified asphalt with the above properties using a non-polluting Lewis acid, para-toluene sulfonic acid (PTSA), as a catalyst for the reaction.

EXPERIMENTAL METHOD

Materials used: The asphalts [AAD-1 (California Coast), AAV-1 (North Alaskan Slope), and AAM-1 (West Texas Intermediate)] used in this study were obtained from the Strategic Highway Research Program (SHRP) Material Reference Library (MRL), Reno, Nevada. The aggregate used was traprock screenings (#10 diabase) from Vulcan Materials Co. All reagents were of analytical grade from Baxter Scientific Products unless otherwise specified.

Furfural Reaction: 200 g of asphalt was placed in a 500-ml three-necked round-bottomed flask equipped with a mechanical stirrer and a thermometer. The asphalt was heated to 93°C, followed by the addition of PTSA (0.07-0.12 milimoles/gram of asphalt) and then furfural (0.15-0.20 milimoles/gram of asphalt) drop wise with continuous stirring. The contents of the flask were then

heated for 1.5 hours at the same temperature.

Test Methods: Standard tests used to measure the properties of asphalts are given below:

Freeze-Thaw Pedestal Test.⁶ The wet environment has an impact on the asphalt-aggregate bond. This bond can be weakened or destroyed if water penetrates into the pavement.

This test measures the water susceptibility of the adhesion of virgin and modified asphalt to the aggregate. The briquettes of the asphalt-aggregate mixture were made according to the Wyoming pedestal test developed by Plancher et al⁶. The samples in jars filled over the top of the briquette level with water were stored in a freezer at -10 to -12°C for 24 hours, cooled to the room temperature, stored in an oven at 60°C for 24 hours, and then examined for surface cracks or breakage. This cycle was continued until the failure of the briquets occurred due to repeated freeze-thaw cycling.

Test Methods:

1. Rolling Thin Film Oven Test (RTFOT), ASTM-D1754-87.
2. Standard Practice for Accelerated Aging of Asphalt Binder Using a Pressurized Aging Vessel (PAV), AASHTO PP1-93 (1A).
3. Test Method for Determining the Flexural Creep Stiffness of Asphalt Binder Using the Bending Beam Rheometer (BBR), AASHTO TP1-93.
4. Test Method for Determining the Rheological Properties of Asphalt Binder Using a Dynamic Shear Rheometer (DSR), AASHTO TP5-93.
5. Corbett Separation Analysis, ASTM D-4124-86.
6. Thin Layer Chromatography (TLC)³.
7. Fourier Transform Infrared (FTIR), & Stokes Data Analysis Method³.

RESULTS AND DISCUSSION:

TLC results of the model polymer made by the interaction of phenol and furfural, using PTSA as a catalyst, shows more polarity in the model polymer than in phenol or furfural. The IR spectrum (figure I) shows that the modified asphalt has more mono and poly substitution on the benzene ring as compared to the corresponding virgin asphalt.

Rheological Properties: Chemical modification of an asphalt with furfural was conducted using a method developed at the Federal-Highway Administration⁴. Figure II shows the continuous SHRP PG grading for virgin and Furfural-Modified asphalts using HCl as a catalyst. The rheological properties of the asphalts used (AAD-1, AAV, & AAM-1)⁷, Fu-Modified using HCl and Fu-Modified asphalt using PTSA, are illustrated in figures II, III, IV, and V, respectively. Virgin asphalt AAV passes the criteria for stiffness at 57°C, and the modified binder passes at 63°C. The low temperature rheological data for both virgin and the modified binder pass the SHRP specification at -28°C. The useful temperature range (the sum of the high and low PG grades) for virgin binder AAV is 85°C; that for the modified binder is 91°C. The temperature difference of 6°C is equal to 1 PG grading and is a significant change. From an economic point of view, 1 PG grading will result in a significant cost savings, but the corrosivity of HCl is a major problem. To solve that problem, a new catalyst (p-toluene sulfonic acid, PTSA) was used. The use of PTSA (figure III) provided a modified asphalt product of AAV which showed PG 63-31 continuous PG grading and 94°C as the useful temperature range. The temperature difference between the virgin and the modified product of 9°C is equal to 1.5 PG grading and is slightly better than that of the HCl modified product. Figure IV demonstrates the rheological behavior of virgin AAM-1 and its Fu-modified binder. The continuous high temperature grading for the virgin binder and for the modified binder is at 67 and 78°C respectively. The low temperature grading for both virgin and the Fu-modified binders were found to be -23°C and -

30°C respectively. The useful temperature range for the virgin binder is 90°C; that for Fu-modified binder is 108°C. The difference in the useful temperature range is 18°C (or 3 PG grades), which is extremely significant. Figure V depicts the rheological continuous grading for the third asphalt used in this study, binder AAD-1. The virgin binder passes the high temperature stiffness specification at 62°C; the modified binder passes it at 71°C. The creep stiffness and slope for both the virgin and the modified binders pass the specification at -31° and -34°C respectively. The useful temperature range is 90° and 105°C for virgin and modified binder respectively, a 12°C range or 2 PG grades. Thus, these modifications are improving the PG grading simultaneously at both high and low temperatures, but the degree of improvement is asphalt source-dependent. Moisture susceptibility was checked through the Wyoming freeze thaw pedestal tests and is shown in figure VI. The virgin asphalt AAV-1 failed after 4 freeze-thaw cycles, whereas Fu-modified by HCl and Fu-modified by PTSA failed after 16 and 18 freeze-thaw cycles, respectively. This indicates that the modified binder is significantly (four times) less moisture susceptible than its corresponding virgin binder.

CONCLUSION: The use of furfural for asphalt modification in presence of a Lewis acid (catalyst) produces a product which is:

- Environmentally acceptable
- Easy to prepare.
- Economical.
- Less temperature and moisture susceptible.
- Improves both the high and low temperature rheological properties simultaneously.
- Asphalt source-dependent in terms of performance.
- Shows potential for higher fatigue and rutting resistance as compared to the corresponding virgin binder.

REFERENCES

1. B. H. Chollar, G. M. Memon, N. Shashidhar, J. G. Boone, and J. A. Zenewitz, "Characteristics of Furfural Modified Asphalt" 73rd TRB Meeting Paper No. 930913, Jan. 1993.
2. G. M. Memon, J. G. Boone, and B. H. Chollar, "Furfural Substitutes for Chemical Modification of Asphalt", ASTM STP 1241, Philadelphia, 1994.
3. G. M. Memon and B. H. Chollar, "Nature of the Chemical Reaction for Furfural Modified Asphalt", 208th ACS National Meeting, Washington, D.C., Aug. 20-25, 1994, 39 # 3, pp870-78.
4. D. Kumari, B. H. Chollar, J. G. Boone, and J. A. Zenewitz, "Chemical Modification of asphalt" FHWA Report No. FHWA/RD-91-193, August, 1992.
5. K. D. Stuart, "Asphalt Mixtures Containing Modified Binders" FHWA Report No. FHWA/RD-92-101, August, 1992.
6. H. Plancher, G. Miyake, R. L. Venable and J. C. Petersen, "A Simple Laboratory Test to Indicate the Susceptibility of Asphalt-Aggregate Mixtures to Moisture Damage During Repeated Freeze-Thaw Cycling," Proceedings of the Canadian Technical Asphalt Association, Vol. 25, pp. 247-262, 1980.
7. G. M. Memon and B. H. Chollar, "Environmentally Benign Asphalt Having Improved Rheological Properties" (Patent applied for), July, 1995.

Figure I
 Infrared Spectra of: a) Asphalt
 AAD-1 and b) Fu-Mod. AAD-1

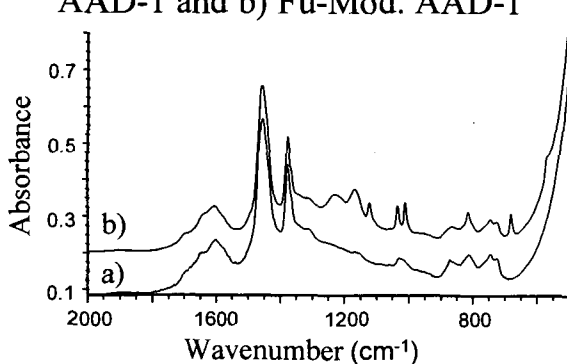


Figure II
 PG Grades for Virgin (AAV) and Fu-
 Mod., Using HCl as the Catalyst

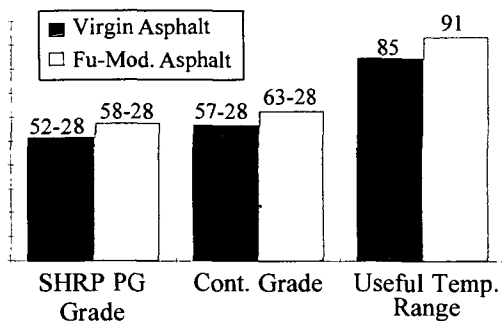


Figure III
 PG Grades for Virgin (AAV) and Fu-
 Mod., Using PTSA as the Catalyst

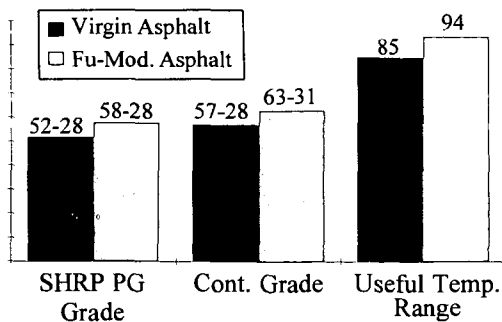


Figure IV
 PG Grades for Virgin (AAM-1) and
 Fu-Mod., Using PTSA as the Catalyst

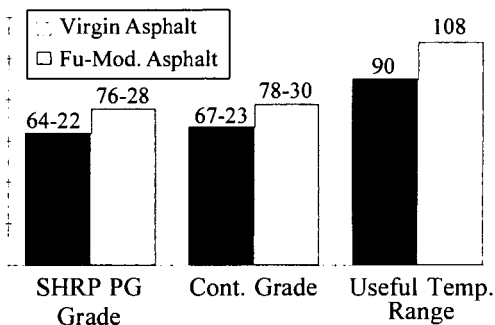


Figure V
 PG Grades for Virgin (AAD-1) and
 Fu-Mod., Using PTSA as the Catalyst

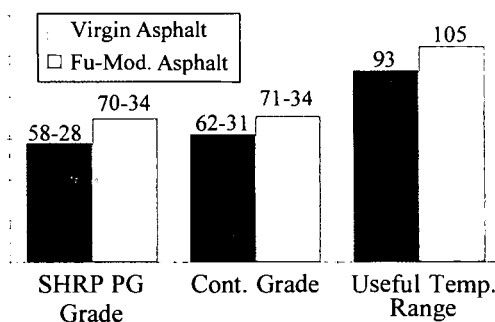
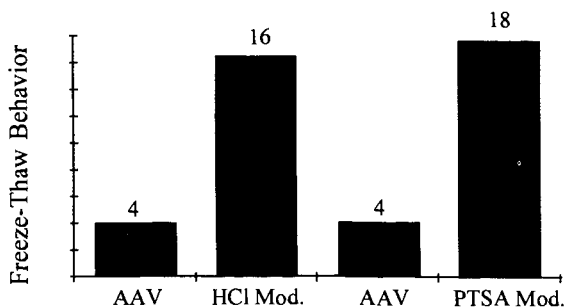


Figure VI
 Comparison of Freeze-Thaw
 Pedestal Tests



THE UTILITY OF PHENOL-ALDEHYDE CROSS LINKING RESINS IN
POLYMER MODIFIED ASPHALT - THE BUTAPHALT(tm) PROCESS

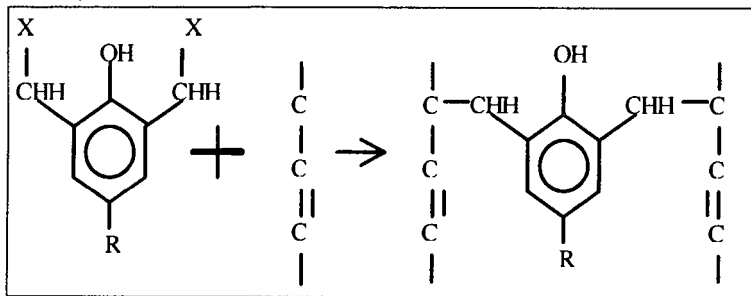
Dennis D. Krivohlavek
Asphalt Technology & Consulting, Inc.
4201 S.W. Hwy. 66
Claremore, Oklahoma 74107

Keywords: Cross Linking, Phenol-Aldehyde Resins, Polymer Modified Asphalt

The use of Phenol-Aldehyde cross linking or vulcanizing resin is well known in the rubber and plastics industry. Previous to our work little (if any) understanding of the utility of these compounds in polymer modified asphalt (or bitumen) was known. This presentation will hopefully enlighten practitioners of the art of asphalt modification on this subject. This art is commercially known as the Butaphalt(tm) Process.

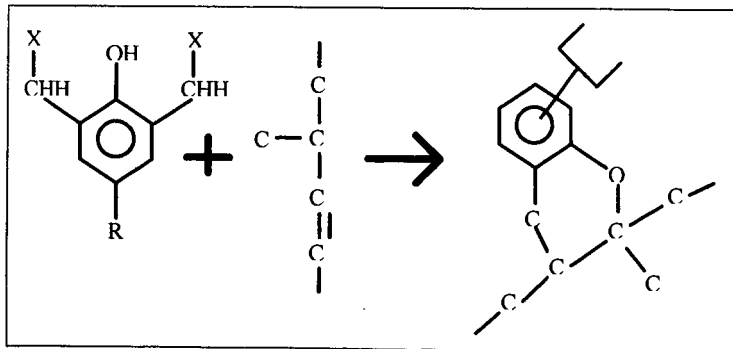
Of initial interest is the mechanism of reaction of Phenol-Aldehyde cross linking resins. As the quantitative analysis of such a mechanism in asphalt would likely need years of effort to resolve, we will look at possible mechanisms in a rubber system. Several publications offer excellent discussions on the art of vulcanization. Science and Technology of Rubber, Second Edition, edited by James E. Mark, et. al., Academic Press, page 366, is such a publication. Therefore, a possible mechanism is illustrated in Figure 1 below.

Figure 1



Another possible mechanism for the reactive phenolic resins involves the formation of a quinone across the double bond of the rubber molecule. Again, several sources of information in the literature are available. Science and Technology of Rubber, Second Edition, edited by James E. Mark, et. al., Academic Press, page 368, makes such reference. This mechanism is thought to create a chroman or chromane structure. This chroman(e) structure is illustrated in Figure 2 below.

Figure 2



Evidence of some form of a chemical and resulting physical change has taken place in the asphalt can be observed by testing Conventional (abbreviated as Cnvntal in tables below) and Butaphalt(tm) Processing. Such a test program with Lloydminster asphalt was performed. It should be noted that this asphalt is generally considered to be a good to excellent candidate for polymer modification. These select tests and their results are also compared at various concentrations of a commercially available high molecular weight radial styrene butadiene styrene (SBS) polymer. Test results are given in Table 1 below.

Table 1

Tests Results in Celsius	3.50% SBS Cnvntal	3.50% SBS Butaphalt	2.50% SBS Cnvntal	2.50% SBS Butaphalt
Separation @ 162	16.11	-0.14	15.14	-0.14
SoftPt B/4 TFOT	70.00	79.44	54.31	58.33
SoftPt Aft TFOT	50.97	63.89	49.17	56.67
B/4-Aft Soft Pt	-19.03	-15.55	-5.14	-1.66

The Separation Test involved static heated storage for each specimen for 48 hours. Although Lloydminster asphalt is normally considered very good for modification, the Separation value is unacceptable under the Conventional Process. However the Butaphalt(tm) Process corrected this deficiency completely. Notice that these results are independent of the SBS concentrations.

The Softening points are always higher with the Butaphalt Process (tm) for a given polymer level. This is true whether observing these results either before or after the Thin Film Oven Test. The Butaphalt(tm) Process consistently yielded minimum decrease Softening Point differential values through the Thin Film Oven Test. These results would indicate longer storage life at in service storage temperatures. These results should also indicate a better product through the hot mix plant and on the road.

We will next look at an asphalt that is considered to be a "problem" for polymer modification. This asphalt is known to be from a wide variety of combined crude oil feed stocks. Among the possible crude oil selections is Alaskan North Slope. Asphalt made from or containing significant quantities of Alaskan North Slope crude oil have been known to have problems when modified with either SBS or styrene butadiene random polymerized latex (SBR) polymers. This next asphalt was not only reported to have significant Alaskan North Slope crude oil but is also reported to have slightly air blown components used in its manufacturing process. Generally speaking, limited air blowing of an asphalt or its component parts will not be severely detrimental to the final traditional product. But, air blowing an asphalt or its component parts are not desirable for a candidate asphalt for polymer modification. We will again examine the Butaphalt(tm) Process in comparison to a Conventional Process in this asphalt. The same high molecular weight SBS polymer at 2.50% by weight dosage level as previously discussed will be used again. In this study, slightly more of the Butaphalt(tm) compound (commercially known as BLC-720 OR B-720) was used over the previous study given above. We will also look at a different set of physical test results. Selecting different physical tests to examine in this study was purposely done to give the reader a better overall understanding of what Phenol-Aldehyde cross linking resins as used by the Butaphalt(tm) Process offer the asphalt polymer formulation. One such physical test that indicates chemical change in polymer modified asphalt is the Force Ductility test. Figure 3 (on the last page) are the Force Ductility curves generated at 4 Celsius, 5 cm/min pull rate from or by the Butaphalt(tm) Process and the Conventional Process. The solid line represents the Butaphalt(tm) Process with its higher initial peak and higher values throughout its elongation. It is the authors opinion that this over all increased value indicates some form of chemical modification to the asphalt polymer composition. It is further the authors opinion that the binder made by the

Butaphalt(tm) Process with these improved Force Ductility values will yield a final product with better overall service life.

Table 2 below gives test results on Ball and Ring Softening Point. Results are given as before and after the Thin Film Oven Test (TFOT).

Table 2

Test (Celsius)	Cnvntal	Butaphalt
Soft Pt B/4 TFOT	51.11	80.56
Soft Pt Aft TFOT	55.00	65.00
B/4-Aft Soft Pt	+3.89	-15.56

In this case, the Butaphalt(tm) Process had higher overall values both before and after the Thin Film Oven Test. The Conventional Process indicated an increasing softening point value through the TFOT with the Butaphalt(tm) Process indicating the opposite trend.

Table 3 below gives test results on ASTM Kinematic Viscosity. Results are given as before and after the Thin Film Oven Test (TFOT). In this table the Percent Change is calculated as [(B/4 TFOT) - (Aft TFOT) / (B/4 TFOT)] X 100.

Table 3

Kinematic Visc.	Cnvntal	Butaphalt
B/4 TFOT, cStk	495	1500
Aft TFOT, cStk	835	1457
B/4-Aft, cStk	+40	-43
Percent Change	+8.08	-2.87

In this case, the Butaphalt(tm) Process had higher but decreasing values through the TFOT than the Conventional Process. The Butaphalt(tm) Process did have the lowest percent change from the original Kinematic Viscosity.

This same asphalt was also modified with a commercially available SBR latex. The dosage level was 2.50% rubber solids (the same amount as was SBS rubber above) but the amount of Butaphalt(tm) compound BLC-720 was used as with the Lloydminster asphalt of Table 1 above. The process of incorporating the SBR latex into the asphalt is some what proprietary.

The proprietary process of incorporating SBR latex may account for the possibly better than expected Conventional Processing results. This is especially true in Figure 4 (on the last page) illustrating the Force Ductility results. Again, the sample with the Butaphalt(tm) compound BLC-720 (the dashed line) had higher initial peak and overall values. As before, it is the author's opinion that this increased value Butaphalt Process will result in superior binder performance.

As before, we will examine Ring and Ball Softening Point both before and after Thin Film Oven Testing. This work is summarized in Table 4 below.

Table 4

Test (Celsius)	Cnvntal	Butaphalt
Soft Pt B/4 TFOT	51.11	51.11
Soft Pt Aft TFOT	53.33	56.67
B/4-Aft Soft Pt	+2.22	+5.56

Results from this work indicate that this combination of asphalt and SBR latex are equal on initial softening point values. In this case, the Butaphalt(tm) process gave higher values through the TOFT than the Conventional Process. The increase is significant but not to the degree of being detrimental to the product. As a result, the final product in the field may well be very acceptable.

One test parameter that has been historically difficult for SBR latex is Elastic Recoverv (ER). In this studv, the Elastic

Recovery is improved by the Butaphalt(tm) Process over the Conventional Process. Further, the Elastic Recovery value through the TFOT is still acceptable for the Butaphalt(tm) Process. The ER procedure used a standard ductilometer and to elongate the specimen at 5 cm/min at 10 degrees Celsius to 20cm., relax for 5 minutes, cut about the center and leave undisturbed for sixty (60) minutes. The ends were then brought together and the ductilometer reading recorded. The calculation was as follows: [(initial elongation) - (final reading) / (initial elongation)] X 100 = E R. These results are given in Table 5 below.

Table 5

Elastic Recovery	Conventional	Butaphalt
E R B/4 TFOT	53	61
E R Aft TFOT	49	58
B/4-Aft E R	4	3

From this information, one may find that the Butaphalt(tm) Process will allow formulations with improved Elastic Recovery. This improvement could likely mean the difference between acceptable and non acceptable specification product. The change in E R from before TFOT to after TFOT is acceptable for both Conventional and Butaphalt(tm) Processing.

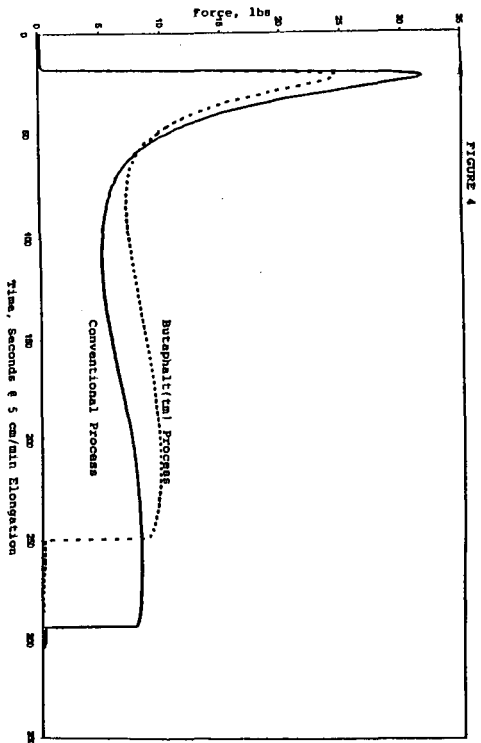
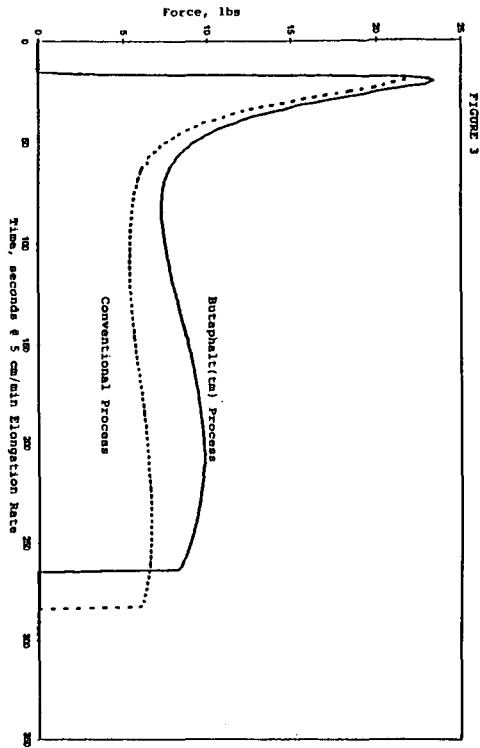
The last area we will discuss deals with the newer test methods as developed by the Strategic Highway Test Program (SHRP). These tests cumulate in a PG grading system. For our purposes, we will look at the PG grading system as a continuous grading system. A continuous grading is determined by the absolute value sum of the high and low PG grading values. In this study, 3.00% by weight of a styrenic block copolymer of a different physical structure and chemical ratio than those previously discussed was processed with a "typical" or "average" asphalt. The PG grading results in a high and a low Celsius temperature service value. These values for the Unmodified or Control asphalt, Conventional and Butaphalt(tm) Processing are given below in Table 6 below.

Table 6

Test Range	Control	Conventional	Butaphalt
High Value	+59	+69	+74
Low Value	-30	-29	-32
Continuous	89	98	106

These results illustrate conclusively that the Butaphalt(tm) process can create superior products in the PG grading system. Improvements are consistent with previous results presented in this discussion. Notice in particular the ability of the Butaphalt(tm) Process to significantly improve both the high and low end of the PG grading. These improvements are a desirable direction over the Control and that provided by the Conventional Process.

In conclusion, the use of Phenol-Aldehyde cross linking resins as reduced to practice in the Butaphalt(tm) Process (Patented) can provide useful tools to improving polymer modified asphalt.



COMPATIBILIZER FOR CRUMB RUBBER MODIFIED ASPHALT

M.E.Labib¹, G.M.Memon², and B.H.Chollar²

¹Civil and Environmental Engineering Department, New Jersey Institute of Technology, Newark, N.J. 07102

²Federal Highway Administration, 6300 Georgetown Pike
McLean, Va. 22101

KEY WORDS: Asphalt, Crumb Rubber, Compatibilizer, Epoxy Ring, Crumb Rubber Compatible Asphalt.

INTRODUCTION: The United States of America discards more than 300 million tires each year, and out of that, a large fraction of the tires is dumped into stock piles. This large quantity of tires creates an environmental problem. The use of scrap tires is limited. There is a usage potential in such fields as fuel for combustion and Crumb Rubber-Modified Asphalt binder (CRMA)¹.

The use of crumb rubber in modifying asphalt is not a new technique; it has been used since early 1960 by pavement engineers².

Crumb rubber is a composite of different blends of natural and synthetic rubber (natural rubber, processing oils, polybutadiene, polystyrene butadiene, and filler)³.

Prior research had concluded that the performance of crumb rubber modified asphalt is asphalt dependent. In some cases it improves the rheological properties and in some cases it degrades the properties of modified asphalt⁴.

Typical problems encountered in crumb rubber modified asphalt pavement include: raveling of pavement, poor mixing, and inconsistent application in the field.

The major objectives of this research were to achieve proper dispersion of crumb rubber particulates into asphalt and to make crumb rubber compatible modified asphalt with improvement both in high and low temperature properties, which can lead to reduced cracking, rutting, and raveling tendencies of the CRMA pavement. The approach of this study was to join the crumb rubber and asphalt molecules with small bifunctional molecules called compatibilizers.

MATERIALS AND METHODS:

Materials used: Three SHRP core asphalts, a California Coast (AAD-1), a lime treated California Valley (AAG-1), and a solvent treated West Texas intermediate (AAM-1) asphalt, were used in this study. They are representative of many of the asphalts used in the United States. These asphalts cover extended ranges of compositional characteristics such as oxygen concentration, nitrogen concentration, carboxylic acid concentration, amine concentration, asphaltene level, polar aromatic concentration, and others. All of the reagents used were analytical grade from Baxter Scientific Products, McGraw Park, IL, unless otherwise specified. The compatibilizers (polyfunctional epoxides with ethylenic and acrylic backbones) used in this study were made by the DuPont Corporation & Elf Atochem respectively. Crumb rubber (-80 mesh) was supplied by Rouse Rubber Industries Inc.

EXPERIMENTAL METHOD: The crumb rubber compatible asphalt was prepared from 400 g asphalt heated at 163°C in a 600 ml beaker, followed by the addition of the compatibilizer having the epoxy ring with a glycidyl backbone (0.006-0.023 milimoles compatibilizer per g asphalt) to the asphalt with continuous stirring for 15-20 minutes. The crumb rubber (6-15%) was then dispersed into the hot asphalt compatibilizer mixture with continuous stirring and heating for 3 hours.

TEST METHODS: 1. The American Association of State Highway and Transportation Officials (AASHTO) Standard Method, No. PP5-93, was used for the separation test.

2. The AASHTO Standard Test Method, No. TP1-93, was used for determining the flexural creep stiffness of the asphalt binder

²To whom correspondence is to be made.

using the Bending Beam Rheometer (BBR).

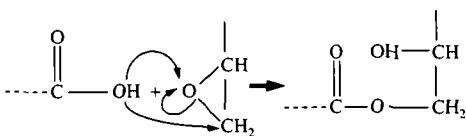
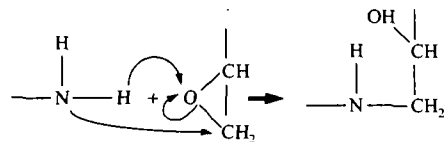
3. The AASHTO Standard Test Method, No. TP5-93, was used for determining the rheological properties of asphalt binder using a Dynamic Shear Rheometer (DSR).

Rheological Characterization:

High temperature behavior by DSR: A Dynamic Shear Rheometer (Rheometrics DSR II) was used to determine the high temperature rheological properties of the virgin, control, and compatible modified binders by using parallel plate geometry. A time sequence (3 minutes) at three temperatures from 52-76°C, with a torque of 20.66 g.cm at a frequency of 10 rad/s was used. The rheological behavior of the binders was calculated by $G'/\sin \delta$.

Low Temperature Behavior by BBR: A Cannon Bending Beam Rheometer (BBR) was used to determine the low temperature rheological properties of the virgin, control, and compatible modified binders. Samples were run in triplicate at -24, -18, and -12°C to measure the creep stiffness (S value) and the change of stiffness with time (m value).

RESULTS & DISCUSSION: The possible reaction between the asphalt functional groups (carboxylic or amino) and the epoxy groups of the compatibilizer is as follows:



This type of mechanism is already reported in literature⁵. In this mechanism, the hydrogen atom of the secondary amine or carboxylic group can open the epoxy ring very easily and bring about the bonding. Physically, formation of clumps was not observed occurring in the compatible modified binder reaction, as it was in the control, an indication of proper dispersion of the crumb rubber into asphalt.

RHEOLOGICAL PROPERTIES:

Rheological properties of the asphalts used (AAD-1, AAG-1, & AAM-1), the control (asphalt mixed with crumb rubber (CRM) under the same reaction conditions), and the crumb rubber compatible modified asphalt are illustrated in figures I through VI. Figures I and II show continuous SHRP performance grading (PG grading) of AAD-1; the virgin asphalt passes the criteria for stiffness at 63°C, the control and modified binder pass at 80°C. Figure I also shows the low temperature rheological data for the virgin, control, and modified binders; the virgin passes the SHRP performance specification at -31°C, the control passes at -28°C, and the modified binder passes at -35°C. Asphalt AAD-1 shows high temperature improvement as compared to the virgin on addition with the CRM (control). The same observation was observed with the modification. However, the low temperature shows a different behavior; the control was degraded as compared to the virgin, but the modified binder shows significant improvement, i.e. by 7°C (more than one PG grading interval). Thus, the addition of crumb rubber to asphalt does not always improve the low temperature properties; asphalt AAD-1 is a case in point. The addition of crumb rubber to asphalt is asphalt dependent. Figure II shows the useful temperature range (the sum of the high and low temperature PG grades) for the virgin, control, and the modified binder of AAD-1. The virgin asphalt shows 94°C as the useful temperature range; whereas, the control and modified binder shows 108°C and

115°C. The product from the addition of crumb rubber and a compatibilizer to asphalt is improved by 2.3 and 3.5 PG-grading intervals (6°C), which, in this economically driven era, is very significant from the refinery point of view. The use of crumb rubber in asphalt is also advantageous in that CRM contains UV resistant additives.

Figure III indicates the rheological properties (continuous PG grading) of asphalt AAG-1, its control, and its modified compatible binder. The addition of crumb rubber to this Californian asphalt shows simultaneous improvement of low and high temperature properties, i.e. from PG 62-19 to PG 66-24. The modified compatible binder shows further improvement for both high and low temperature rheological properties, i.e. PG 72-29. The asphalt, AAG-1, shows low temperature rheological properties that are different from those of asphalt AAD-1. Figure IV shows the useful temperature range for asphalt AAG-1, its control, and its compatible modified binder. The virgin asphalt in this case has a useful temperature range of 81°C, whereas, its control and the modified compatible binder have useful temperature ranges of 90 and 101°C respectively. In this case the addition of crumb rubber and its compatible product shows an increase of 1.5 and 3.3 PG-grading intervals. This is very significant as compared to the virgin material.

Figure V shows the rheological properties of the virgin, control, and modified compatible binder asphalt AAM-1 (Californian valley solvent treated asphalt). The continuous PG-grading for the virgin binder shows PG 66-23°C; whereas, its corresponding control and compatible modified binder shows PG 68-30 and PG 73-32 respectively. The improvement in the PG grading of this asphalt is not as significant as it was for the other two asphalts, but it is still significant. Figure VI shows the useful temperature ranges for the virgin, its control, and its compatible modified binder, as 89, 101, and 105°C respectively. Therefore the addition of crumb rubber shows improvement by 2 and 2.7 PG-grading intervals as compared with the control and the compatible modified binder respectively.

From the above discussion it is clear that the compatible modified binder rheologically performs better than its control or its virgin binder. The process to prepare crumb rubber modified compatible asphalt may be accomplished with some degree of success. In this study the compatible modified binder was not only properly dispersed but reproducible results were also obtained.

CONCLUSION: The use of a compatibilizer can 1)enhance the solubility of crumb rubber into asphalt and 2)improve the rheological properties of crumb rubber modified asphalt. Modified compatible asphalt is advantageous over the virgin and its control by having a wider useful temperature range. The use of modified compatible asphalt has the potential to prevent asphaltic pavement from raveling and may increase the use of scrap tires. The amount of compatibilizer used in asphalt is dependent on the source of asphalt.

REFERENCES:

1. Scrap Tire Management Council, Scrap Tire Use/Disposal Study, Sept. 1990.
2. Charles McDonald, "Sahuaro Concept of Asphalt-Rubber Binders", Proceeding - First Asphalt-Rubber User-Producer Workshop, May 1980.
3. Michael Wm. Rouse, "Production Identification and Application of Crumb Rubber Modifier (CRM) for Asphalt Pavements", presented at the 52nd Annual meeting of the Southeastern Association of State Highway and Transportation Officials, August, 1993.
4. G.M.Memon and B.H.Chollar, "Thermal Characteristics of Crumb Rubber Modified Asphalt", 24th NATAS Conference, San Francisco, CA, Sept. 10-13, 1995, pp 27-32.
5. J.W.Nicholson, "The Chemistry of Polymers", Royal Society of Chemistry, p 73, 1991.

Figure I

**Continuous Rheological Grading
of Asphalt AAD -1 (Glycidyl)**

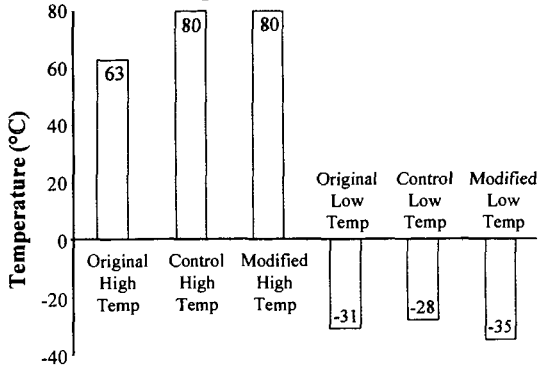


Figure II

**Useful Temperature Range for Asphalt AAD-1,
Control, and Compatible Modified Binder**

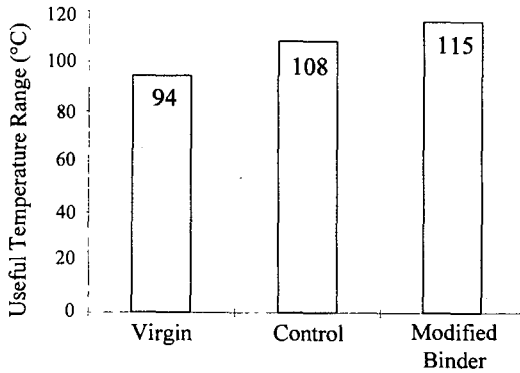


Figure III

**Continuous Rheological Grading
of Asphalt AAG -1 (Glycidyl)**

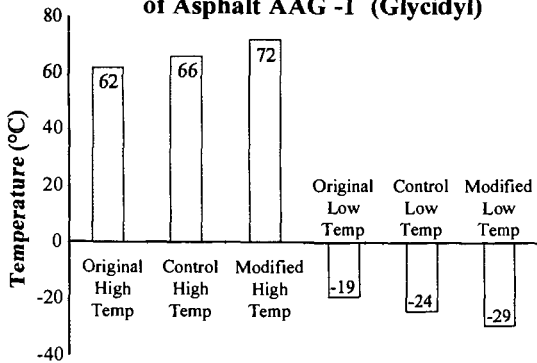


Figure IV

Useful Temperature Range for Asphalt AAG-1,
Control, and Compatible Modified Binder

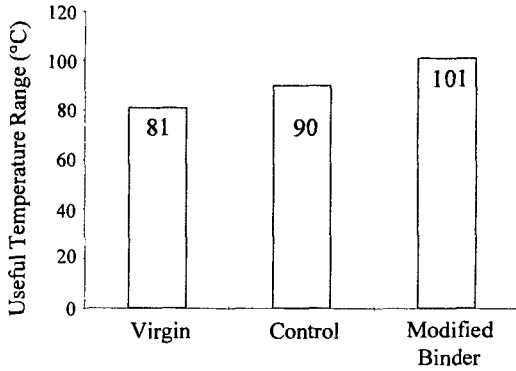


Figure V

Continuous Rheological Grading
of Asphalt AAM -1 (Glycidyl)

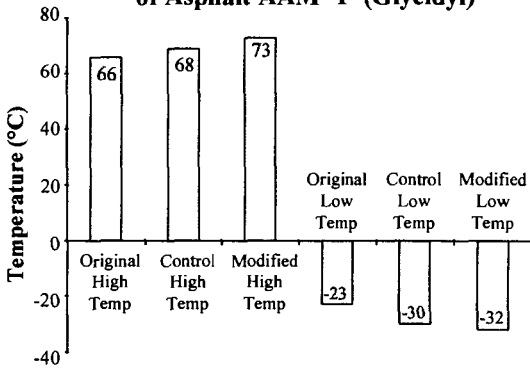
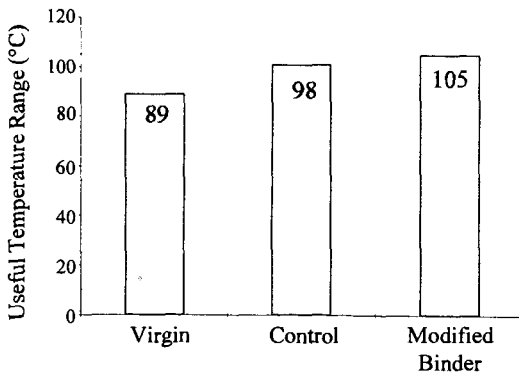


Figure VI

Useful Temperature Range for Asphalt AAM-1,
Control, and Compatible Modified Binder



EFFECTS OF CARBOXYLIC ACIDS ON THE RHEOLOGICAL PROPERTIES OF CRUMB RUBBER MODIFIED ASPHALT

Jane E. Tauer and Raymond E. Robertson
Western Research Institute
365 North 9th Street
Laramie, Wyoming 82070

Keywords: Crumb Rubber, Crumb Rubber Modified Asphalt, Asphalt

ABSTRACT

The Federal mandate of 1991-1995 on the use of scrap tires in Federal roadway construction sparked a major interest in gaining a fundamental understanding of the behavior of rubber in asphalt. This study is a systematic elucidation of what chemistry controls the final crumb rubber modified asphalt (CRMA) product quality. We discovered that the type and total acid content in the asphalt are the most influential chemical factors that determine the changes in the important roadway properties of shear modulus (G^*) and loss angle (δ) of CRMA. Low acid (<0.005 mL) asphalts were modified with three types of carboxylic acid and each made into CRMA using typical field mixing conditions of 1 hour at 175°C. Rheological measurements were then made at various storage times up to 192 hours following storage at both 156 and 200°C. We found the changes in CRMA rheological properties correspond to the acid type spiked into the asphalt.

INTRODUCTION

In December 1991 the Intermodal Surface Transportation Efficiency Act (ISTEA) mandated the use of large amounts of rubber from scrap tires in Federally funded roadway construction. In 1995 this mandate was removed but in the time between 1991 and 1995 the mandate sparked much interest in gaining a better understanding of the use of rubber tire material in roadways. Some successful use of tire rubber had been demonstrated for up to twenty years before the mandate in the states of Arizona, California, and Florida. These three states had experimented with the use of finely ground rubber (crumb rubber) mixed with asphalt to make asphalt concrete. Upon examination of their successful uses of this crumb rubber modifier (CRM) to make crumb rubber modified asphalt (CRMA), it became obvious that each state gained a good understanding of the material properties of the CRMA and further employed good engineering design and construction practices in using CRMA to build roads. To a lesser degree, it became obvious that CRMA used in Florida was substantially different from that used in California. This suggested that there were unrecognized differences in materials used by the two states. An attempt was made to trace the sources of CRM and asphalt crude oil sources used by each state. What became apparent quickly was that both Florida and California used consistent supplies of asphalt in their respective states, but that the asphalt crude sources used in the two states were very different from each other. The California DOT reported the asphalt binder behaved somewhat like a mineral filled asphalt. On the other hand, the Florida DOT reported building with a homogeneous material which suggested that the CRM had dissolved, or digested into the asphalt. The experiences with CRMA related above strongly suggested to us that some unique set of CRMA properties can be expected and can be related back to the crude oil source used to produce each asphalt.

To control the rheological properties of crumb rubber-asphalt mixtures, an understanding of the chemistry involved in the CR-asphalt interaction is necessary. We began our study with a systematic analysis of the variables involved in this interaction, i.e., asphalt type, CR type, mixing time and temperature, and particle size and concentration

BACKGROUND

In previous experiments we found CRMs do not swell significantly in whole asphalt at temperatures of 200°C and times up to 1000 hours, but we found a portion of the crumb rubber (CR) appears to dissolve which leads to changes in the rheology of the CRMA. The rheological changes are different among various asphalts and greater than the effect imparted by Teflon of the same particle size. These changes in rheological properties led to an investigation into what component(s) of the asphalt is (are) interacting with the CR. In order to determine the component(s) involved, asphalts from different crude sources were used in mix experiments. The CRMAs were prepared using standard blending procedures (blended for one hour at 175°C) then tested and stored at 200°C. The CRMAs were checked visually and microscopically each day for changes in the CR. Several of the asphalts had no apparent effect on the CR, however one asphalt had a dramatic effect on CR appearance. After five days at 200°C this mixture had the appearance of a neat asphalt (i.e., very smooth and shiny). We repeated the experiment with this particular asphalt, Strategic Highway Research Program (SHRP) asphalt ABD-1, with the same results. This asphalt has a lime treated counterpart (SHRP AAG-1) which had been tested earlier with no apparent interaction with the CR. Lime is added to this asphalt

to neutralize its high carboxylic acid content. It then seemed logical that carboxylic acid had something to do with the dissolution of the CR. The experiment was repeated with another high acid asphalt, SHRP AAK-2, with the same results (i.e., the CR dissolved). We then removed the acid fraction from the ABD-1, using ion exchange chromatography, and added it to a low acid asphalt, SHRP AAM-1. Asphalt AAM-1 had also been used in the earlier experiment with no dissolution. Crumb rubber was mixed with both samples and stored for several days at 200°C. After several days the acid free ABD-1-CR mixture showed no signs of interaction, crumb particles were still visible in the mixture. However the acid modified AAM-1-CR mixture had the appearance of a neat asphalt. We now had enough evidence of the involvement of carboxylic acid as the active component or a marker of the active component to begin a series of controlled acid doping experiments.

EXPERIMENTAL

The experimental procedure involves the doping of two low acid asphalts, AAB-1 and AAM-1 with various carboxylic acids (9-anthracene carboxylic acid, stearic acid and cholic acid) at 0.01, 0.02 and 0.03 weight percent. The acid was mixed with asphalt by mechanical stirring at 175°C. The acid-doped asphalts were then mixed using a low shear mixer for one hour at 175°C with U.S. Standard #40 mesh (420µm) CRM and U.S. Standard #40 mesh natural tire rubber (NR). Rheological measurements were taken immediately after mixing. Suitable control samples were prepared and rheological measurements were taken for comparison to the CRMA. The remainder of the CRMAs and control samples were then split. Half of the samples were stored at 156°C for up to 192 hours and the other half at 200°C for up to 192 hours. This experiment is still in progress, but the work to date is presented here. All samples were analyzed using an Rheometrics RDA II rheometer, operated in strain control mode.

RESULTS

Figures 1 through 10 show the results of the acid doping experiments for asphalt AAB-1. The time sequence for all of the data points in the figures, except for figures 3 and 4, are not shown; the data are plotted versus the loss angle or G' . Figures 1 and 5 show the shear modulus and the loss angle data taken at 60° and 25°C for samples stored at 156°C. Figures 2 and 6 show the storage and loss moduli data taken at 60° and 25°C for samples stored at 156°C. Figures 3 and 4 show the storage and loss moduli for CR4-9-anthracene carboxylic acid doped AAB-1 and CR4-AAB-1, and CR4-stearic acid doped AAB-1 and CR4-AAB-1 stored at 156°C and measured at 60°C, respectively. In these figures the storage times of the data points are noted. Figures 7 and 9 show the shear modulus and the loss angle data taken at 60° and 25°C for samples stored at 200°C. Figures 8 and 10 show the storage and loss moduli data taken at 60° and 25°C for samples stored at 200°C.

DISCUSSION

Asphalts are viscoelastic fluids and are evaluated using dynamic mechanical analyzers (DMA). When analyzing asphalts the DMA is run in an oscillatory mode which supplies a periodic deformation at a given frequency, ω . The DMA can calculate several material constants including the magnitude of complex shear modulus, loss angle, storage modulus, and loss modulus. The complex shear modulus, $G^*(\omega)$, is a complex function of frequency, as shown in equation (1),

$$G^*(\omega) = \frac{\sigma_0}{\epsilon_0} e^{i\delta} = G' + iG'' \quad (1)$$

where δ is the loss angle at a given frequency, σ_0 is the stress amplitude at a given frequency, and ϵ_0 is the strain amplitude at a given frequency. The loss or phase angle, δ , is a function of the internal friction of the material. For a viscous material the loss angle would be 90° and for an elastic material the loss angle would be 0°. The magnitude of $G^*(\omega)$ is found using equation (2).

$$|G^*(\omega)| = G^* = \sqrt{G'^2 + G''^2} \quad (2)$$

The storage modulus, G' , is the real part of the complex shear modulus and is associated with the storage and loss of energy during the periodic deformation (recoverable deformation). The loss modulus, G'' , represents the imaginary part of the complex shear modulus and is associated with the dissipation of energy and its transformation into heat (permanent deformation). G' and G'' can be found using equations (3) and (4).

$$G' = G^* \cos \delta \quad (3)$$

$$G'' = G^* \sin \delta \quad (4)$$

It is obvious from the figures that not only are the acids involved in the interaction of asphalt with CRM, but the type of acid is very important in the interaction. Figure 1 shows G^* and δ for AAB-1, acid doped AAB-1, CR4-AAB-1 and CR4-acid doped AAB-1. The samples were stored at 156°C and measurements were taken at 60°C. The data here represent all storage times up to and including the 192 hour. Neat asphalt AAB-1 and acid doped AAB-1 are grouped together in the lower right corner

of the figure. This indicates that the acid doping of AAB-1 has not changed G^* and δ (at 60°C) by any significant amount. The next group of data points are found higher up on the right side of the figure. Each of the data points in this set represents a CR4 mixture, measured immediately after the one hour mix time. A significant increase in G^* due to the addition of the CR4 is observed. The loss angle has gone from -89° to -86° for CR4-AAB-1 (CR4) and to -85° for the CR4-9-anthracene carboxylic acid doped AAB-1 (A), but G^* has increased from 128 Pa to 702 Pa and 1150 Pa, respectively. From Equation (2) it can be seen that this increase in G^* must be accompanied by an increase in G' and/or G'' . Figure 2 shows G' and G'' for these samples. Again the AAB-1 and acid doped AAB-1 are grouped together in the lower left corner. The one hour CR4 mixtures data start in the lower right of the figure and are above the majority of points running from left to right. The CR4-9-anthracene carboxylic acid doped AAB-1 (A) has the largest increase in both G' and G'' , compared to the other CR4 mixtures. The CR4-stearic acid AAB-1 (S) shows the least change in rheological properties, while the CR4-cholic acid AAB-1 (C) is very close to the CR4-AAB-1 (CR4). The data points for the longer storage times run from -82° loss angle to -74° loss angle in figure 1 and from G'' of 300 Pa to -1700 Pa in figure 2. This main stream of data points include the 24 hour to 192 hour storage times. It is important to note that the rheology undergoes the greatest change between the one and 24 hour time period for all CR mixtures. Figure 1 shows that the 24 hour through the 192 hour samples group according to acid type. The CR4-9-anthracene carboxylic acid data is found in the upper left hand side of the figure, the CR4-AAB-1 and CR4-cholic acid AAB-1 are in the next group and finally the CR4-stearic acid AAB-1. Figures 3 and 4 show selected data from figure 2 and the storage times are noted on the data points. In figure 3 we see the data for CR4-9-anthracene carboxylic acid doped AAB-1 and CR4-AAB-1. The CR4-9-anthracene carboxylic acid doped AAB-1 has substantially higher G' 's and G'' 's. The addition of 9-anthracene carboxylic acid to AAB-1 has improved the rheological properties in terms of high (60°C) temperature flow. It is believed that somehow the 9-anthracene carboxylic acid is preventing or favorably controlling the dissolution of the CR. The mechanism involved in this process is not yet understood. Stearic acid, however (figure 4) has the opposite effect. It appears to increase the dissolution of the CR, leading to a degradation of high temperature properties when compared to CR4-AAB-1. Stearic acid is used in rubber production as a processing aid and an accelerant and may accelerate the dissolution of rubber in asphalt. Also, it is important to note that the improvement in properties is time dependent. Each reaches a maximum value of G' and G'' at a different storage time. The CR4-AAB-1 reaches the maximum G' and G'' at 24 hours and then begins to decline. CR4-9-anthracene carboxylic acid doped AAB-1 reaches its maximum at 96 hours, while the CR4-stearic acid doped AAB-1 reaches its maximum values at 24 hours.

The data pattern in figures 5 and 6 are similar to that in figures 1 and 2, though the AAB-1 and acid doped AAB-1 data points show a slight change rheological properties (figure 6). The effect of the acid type is quite apparent from the data in all of the figures. In figure 1, CR4-stearic acid doped AAB-1 samples show less of a change in G^* and δ than the CR4-AAB-1 samples for all storage times. Figures 7 through 10 show comparable data for samples stored at 200°C with the addition of natural rubber AAB-1 mixtures (NR). In these figures the contrast between the one hour sample (G^* 's -480 Pa to 1150 Pa) and the 24 through 192 hour samples (G^* 's under 400 Pa) is quite dramatic. Also the loss angles in figure 5 are higher than those in figure 1. After 24 hours at 200°C, the increase in G' and G'' due to the addition of CR4 has been negated by the increased dissolution of the CR4. The G'' has decreased from 1150 Pa for CR4-9-anthracene carboxylic acid doped AAB-1 to 189 Pa, and G' from 105 Pa to 19 Pa. Figures 7 and 8 show the data for the samples stored at 200°C and measures at 25°C. The data show that NR-AAB-1 has properties similar to the acid doped AAB-1, and the effect of the rubber is minor after 24 hours. In previous studies it was found that the natural rubber dissolved in all asphalts tested within a few hours of mixing. The data points at a loss angle of $70^\circ+$ are those for the long storage time.

CONCLUSIONS

The addition of carboxylic acids to asphalt AAB-1 produces varying amounts of rheological change in the crumb rubber mix. The interaction is acid type and temperature dependant. The rheological changes occur at a fairly low temperatures in asphalts (typically mixed at 165° to 175°C) in a relatively short time. This is similar to the mixing conditions commonly employed at a CRMA road construction site. At higher temperatures, the interaction proceeds more rapidly. The effect of carboxylic acid type is fairly pronounced. The improvement in high temperature properties for the CR4-9-anthracene carboxylic acid doped AAB-1 is striking, while the CR4 stearic acid doped AAB-1 exhibits a decrease in rheologic properties. The cholic acid added to AAB-1 appears to have almost no effect on the rheology of the CRMA. Each asphalt contains varying types and amounts of naturally occurring carboxylic acids; therefore each crumb rubber mixture will have different properties based on the asphalt composition. The most important aspect for CRMA in roadways may be the fact that the CRMA undergoes a dramatic change in rheologic properties within 24 hours of mixing the CRM and asphalt. It is during this time period that the CRMA is combined with aggregate and the pavement is laid. If the CRMA is graded immediately after mixing, then by the time it is

mixed with aggregate the properties will have changed. It is not until 48, or in some cases 72 hours, after mix that the rheological properties appear to stabilize (figures 1 through 4).

The addition of crumb rubber to asphalt poses many challenges to the paving industry. Only by understanding the chemistry of these systems will we be able to predict the rheological properties of the CRMA.

ACKNOWLEDGMENTS

The authors gratefully acknowledge the Federal Highway Administration for financial support of this work under Contract No. DTFH61-92C-00170. The authors express thanks to Mr. Jack Van Kirk, California DOT, and Mr. Gale Page, Florida DOT, for many helpful discussions. Thanks are also expressed to WRI personnel. Bruce Thomas acquired most of the rheological data. Jan Hart and Paul Holper prepared all of the samples.

DISCLAIMER

This document is disseminated under the sponsorship of the Department of Transportation in the interest of information exchange. The United States Government assumes no liability for its contents or use thereof.

The contents of this report reflect the views of Western Research Institute which is responsible for the facts and accuracy of the data presented herein. The contents do not necessarily reflect the official views of the policy of the Department of Transportation.

REFERENCES

Findley, William N., James S. Lai and Kasif Onaran, Creep and Relaxation of Nonlinear Viscoelastic Materials, Dover Publications, Mineola, N.Y., 1989.

Tschoegl, Nicholas W., The Phenomenological Theory of Linear Viscoelastic Behavior, An Introduction, Springer-Verlag, New York, 1989.

Hofman, Werner, Rubber Technology Handbook, Hanser Publishers, Oxford University Press, New York, 1988.

Key for figures: Neat→AAB-1, A→9-anthracene carboxylic acid modified AAB-1, S→stearic acid modified AAB-1, C→cholic acid modified AAB-1, CR4→AAB-1 and CR4, A-CR4→9-anthracene carboxylic acid modified AAB-1 and CR4, S-CR4→stearic acid modified AAB-1 and CR4, C-CR4→cholic acid modified AAB-1 and CR4 and NR→AAB-1 and natural rubber.

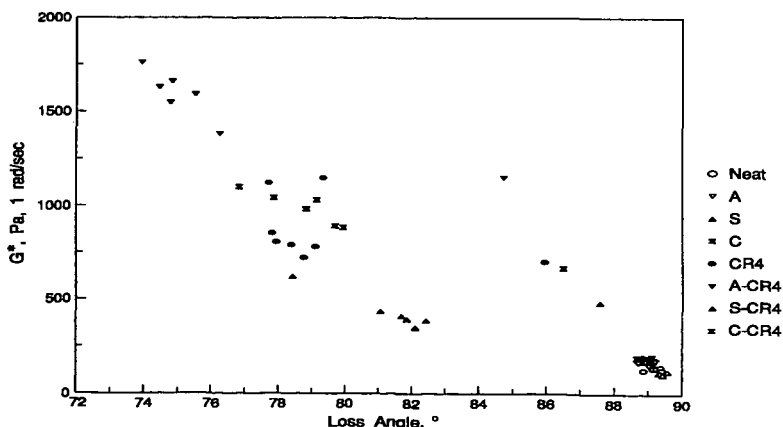


Figure 1. Shear modulus and loss angle of asphalt AAB-1, acid doped AAB-1, and CR mixtures at 60°C and storage temperature of 156°C.

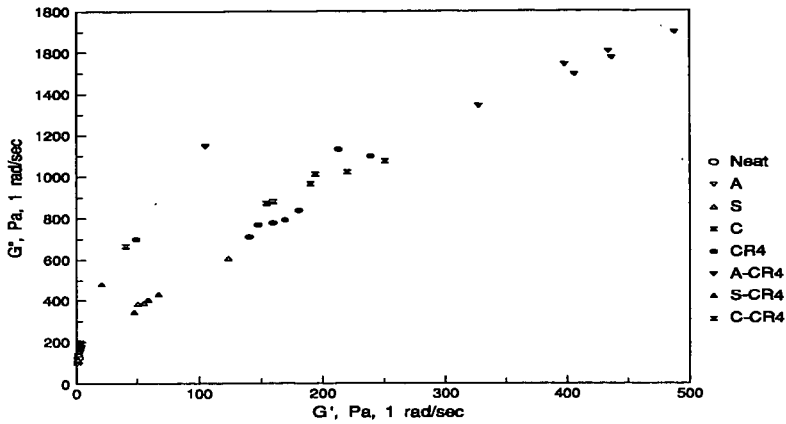


Figure 2. Storage and loss moduli of asphalt AAB-1, acid doped AAB-1 and CR mixtures at 60°C and storage temperature of 156°C.

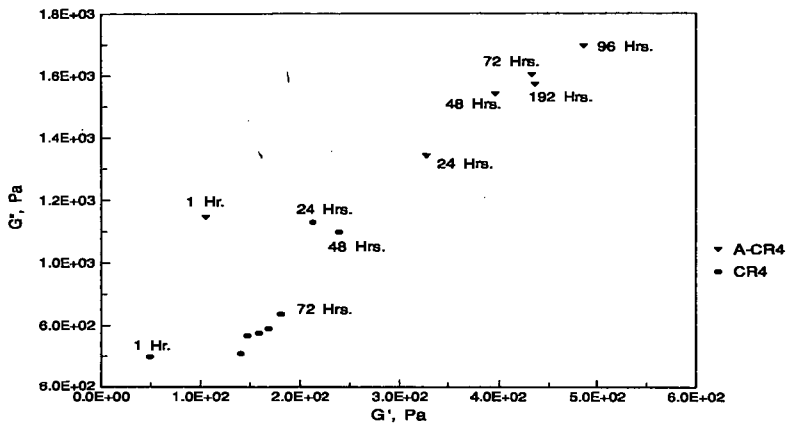


Figure 3. Storage and loss moduli for CR4 9-anthracene carboxylic acid doped AAB-1 and CR4 AAB-1 at 60°C and storage temperature of 156°C.

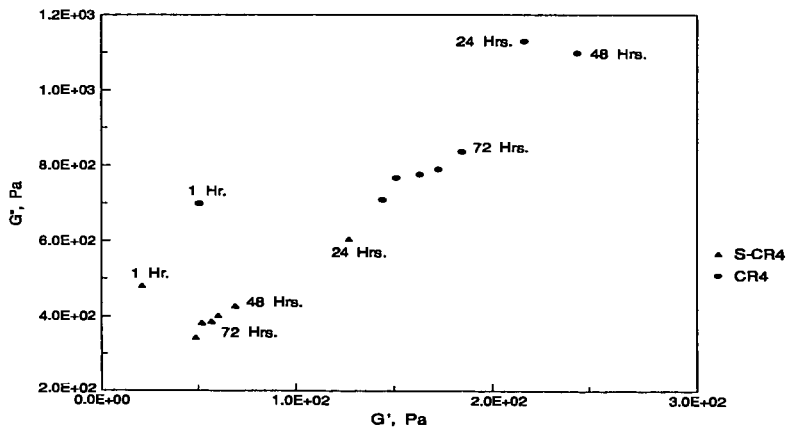


Figure 4. Storage and loss moduli for CR4 stearic acid doped AAB-1 and CR4 AAB-1 at 60°C and storage of 156°C.

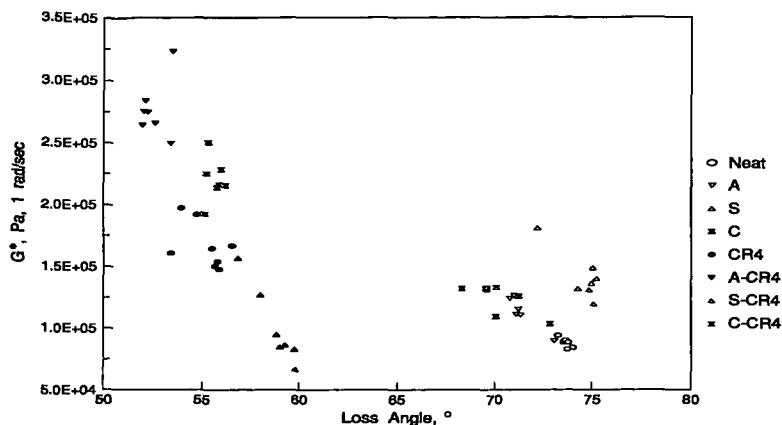


Figure 5. Shear modulus and loss angle of asphalt AAB-1, acid doped AAB-1 and CR mixtures at 25°C and storage temperature of 156°C

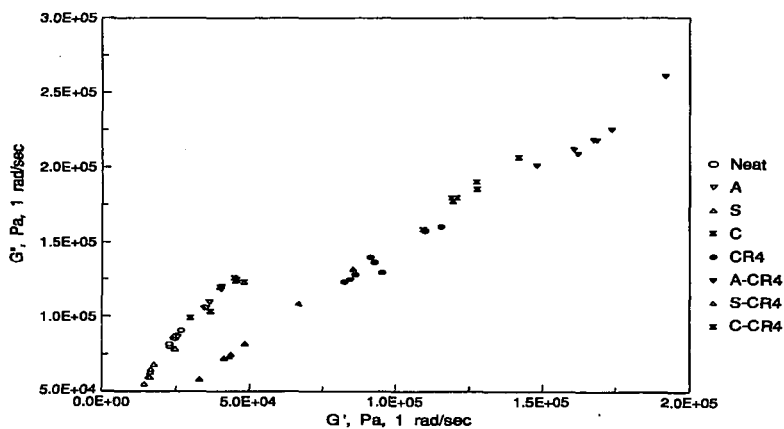


Figure 6. Storage and loss moduli of asphalt AAB-1, acid doped AAB-1 and CR mixtures at 25°C and storage temperature of 156°C.

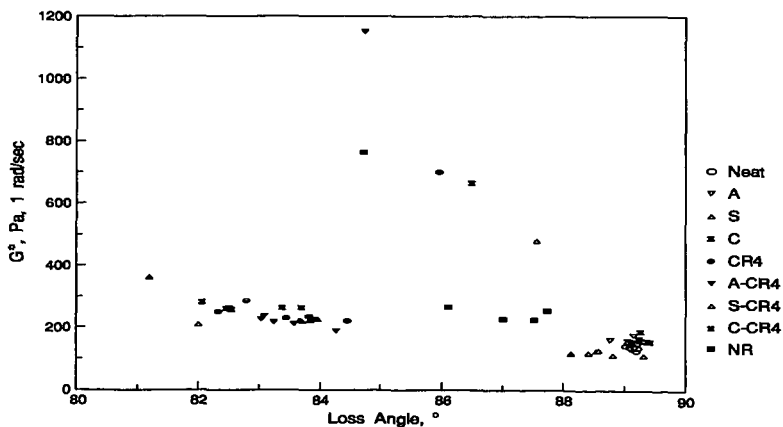


Figure 7. Shear modulus and loss angle of asphalt AAB-1, acid doped AAB-1 and CR mixtures at 60°C and storage temperature of 200°C.

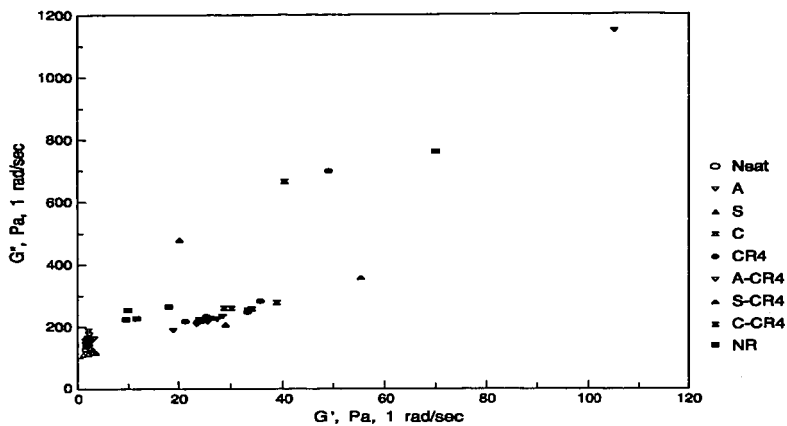


Figure 8. Storage and loss moduli of asphalt AAB-1, acid doped AAB-1 and CR mixtures at 60°C and storage temperature of 200°C.

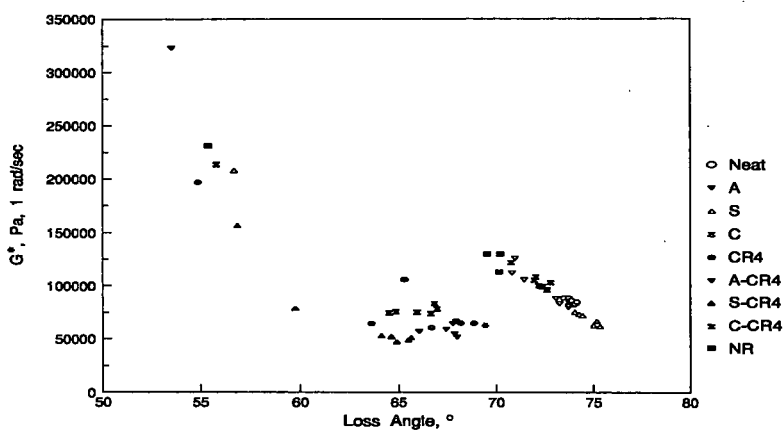


Figure 9. Shear modulus and loss angle of asphalt AAB-1, acid doped AAB-1 and CR mixtures at 25°C and storage temperature of 200°C.

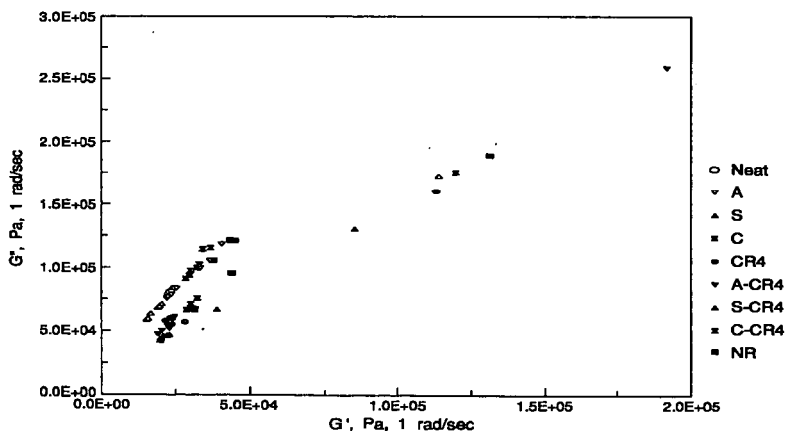


Figure 10. Storage and loss moduli of asphalt AAB-1, acid doped AAB-1 and CR mixtures at 25°C and storage temperature of 200°C.

INVESTIGATION OF THE CURING VARIABLES OF ASPHALT-RUBBER BINDER

T.C. Billiter, J.S. Chun, R.R. Davison, C.J. Glover, and J.A. Bullin
Department of Chemical Engineering
Texas A&M University
College Station, Texas 77843-3122

Keywords: Asphalt-Rubber, Asphalt, Rubber Dissolution

INTRODUCTION

Currently, the paving industry utilizes a curing time of 1 hour at 177°C (350°F) for producing asphalt-rubber binder (1). Billiter et al. (2) showed that at these curing conditions, 1 hour at 177°C (350°F), adding rubber to asphalt was beneficial, with the rubber improving the low-temperature creep stiffness at (-15°C (5°F)), the temperature susceptibility in the 0°C-90°C (32°F-194°F) temperature region, increasing G^* and η^* at 60°C (140°F) and 1.0 rad/sec, and decreasing δ at 60°C (140°F) and 1.0 rad/sec. On the other hand, Billiter et al. (2) showed that the addition of rubber was also detrimental, in that the viscosity increased significantly in the compaction temperature region of 149°C-193°C (300°F-380°F). This increased viscosity can cause compaction problems, with Allison (3) reporting that engineers blamed the compaction problems of asphalt-rubber on undissolved crumb rubber, which they believed had no beneficial effect. Additionally, the engineers reported that improper compaction led to early road failure. High compaction viscosities also led to high air void content for dense-graded mixes (4), which is detrimental since Linden et al. (5) reported a correlation between air voids and performance.

Engineers could solve these problems by producing an asphalt-rubber binder with a non-detrimental compaction viscosity. If Allison (3) is correct, then eliminating undissolved rubber from asphalt-rubber binder would help produce such a binder. Apparently, eliminating undissolved rubber is possible, since Billiter et al. (2), Franta (6), and Zanzotto and Kennepohl (7) have reported that rubber devulcanizes and depolymerizes during the application of high shear and high temperature in the presence of asphalt. Obviously, the production of such an asphalt-rubber binder will require a study of the variables of curing time, curing temperature, and the type and amount of mechanical energy. This work investigates these variables in an attempt to produce such an asphalt-rubber binder.

MATERIALS

Three asphalts were used in this study. Asphalt #1, an AC-10, and Asphalt #2, an AC-5, were acquired from refineries in Texas. Asphalt #3, an AC-10, was produced in the laboratory by blending a commercially available asphalt and a commercially available recycling agent. The asphalt comprised 78% by weight of Asphalt #3 and had a viscosity of 40,710 poise at 60°C (140°F). The recycling agent comprised 22% by weight of Asphalt #3 and had a viscosity of 5.5 poise at 60°C (140°F). Asphalt #3 was produced to study the effect of adding a light aromatic fraction to an asphalt.

Minus 10 and minus 40 mesh rubber were acquired from Granular Products, also known as Tire Gator (TG), located in Mexia, Texas. Additionally, minus 10, 40, and 80 mesh rubber were acquired from Rouse (RS) Rubber located in Vicksburg, Mississippi.

EXPERIMENTAL METHODS

The bending beam rheometer, dynamic shear rheometer, Brookfield rotational viscometer, Fourier transform infrared spectrometer, and size exclusion chromatograph that were in this study are described in Billiter et al. (2).

Mixing Apparatus

To produce the asphalt-rubber binders, asphalts and rubbers were 'cured' or mixed at high temperatures (177, 191, or 204°C (350, 375, or 400°F)). Curing is the application of heat and mixing to an asphalt and crumb rubber mixture in which the rubber may be swelled, disintegrated, dissolved, and/or reduced in molecular size. The curing process, as carried out in this laboratory, involved mixing at high temperatures with a 5.1 cm (2") diameter blade driven at 500 rpm or 1550 rpm by a variable speed motor. The blends were cured in 1 gallon paint cans under a nitrogen blanket to prevent the binder from oxidizing.

Rubber Dissolution Test

The extent to which the rubber had dissolved into the asphalt was determined with the following gravimetric procedure. The analysis was performed using a pre-weighed 0.45 μm syringe filter. A 0.2 gram asphalt-rubber sample was dissolved in 10 ml of THF. The asphalt-rubber/THF solution was sonicated for 30 minutes. The solution was then strained through the syringe filter. The filter was heated in a vacuum oven at 100°C (212°F) for 3 hours, removed from the oven and placed at ambient conditions for 24 hours, and finally weighed. The difference between the final filter weight and the initial filter weight is the weight of the rubber that did not dissolve into the asphalt. This weight, the initial sample size weight, and percent rubber content of the initial sample were used to determine the amount of rubber that dissolved into the asphalt.

EXPERIMENTAL DESIGN

Table 1 shows combinations of temperature, mixer speed, weight percent rubber, rubber mesh size, rubber source, and asphalt used in these sets of experiments. The total curing time was 48 hours for the blends cured at 500 rpm, with samples being taken at 3, 6, 12, 24, 36, and 48 hours. For the 1550 rpm blends, the total curing time was 3 hours, with samples being taken at 1, 2, and 3 hours. Experimental Plan (EP) #1, EP #2, and EP #3 were done to study the variable of curing time. EP #3 was done to study the variable of curing temperature and EP #2 was done to study the variable of mixing power, the authors assuming power is approximately proportional to the square of the blending speed. The asphalt rubber products were evaluated in terms of high-temperature viscosities ($>121^{\circ}\text{C}$ ($>250^{\circ}\text{F}$)), intermediate-temperature rheological properties (0°C - 90°C , (32°F - 194°F)), low-temperature creep stiffness at -15°C (5°F), rubber dissolution, molecular weight distribution, and Fourier Transform Infrared Spectrometer (FTIR).

RESULTS AND DISCUSSION

As discussed in the introduction, previous results in the literature suggest that the dissolution of rubber during the curing process should lead to better binder properties. Consequently, the primary objective of this research was to study the effect of various curing variables on the dissolution of rubber. Specifically, the curing variables of curing time, curing temperature, and rate of mixing are of greatest interest, with the results of the variables of asphalt type, rubber content, rubber mesh size, and rubber source also being presented.

Each figure focuses on a particular variable. If a graph is referenced, at least one example of the comparison being made will be presented.

Experimental Plan #1

Percent Rubber and Mesh Size

For the asphalts studied, the addition of rubber was positive for the low- and intermediate-temperature properties of a binder; the higher the rubber content, within the range studied, the better the results. For a given mesh size, the 10% rubber level lowered the creep stiffness, and therefore improved the elasticity, more than the 5% rubber level, Figure 1. Obviously, the benefits of the elastic additive were more pronounced at the higher concentration levels, thus producing a more flexible binder. Furthermore, the smaller rubber particles were slightly better at improving low-temperature properties, Figure 1. It is theorized that the smaller rubber particles are better able to interact because of their greater surface area per unit mass. The 60°C complex viscosities were higher for the 10% blends and for the larger rubber particles, Figure 2, thereby producing a binder more resistant to rutting. The increase in complex viscosity is probably more of a particle effect than a surface area effect, thus explaining the larger particles' enhanced performance. In the intermediate temperature region, the temperature susceptibility was lower, and therefore better, for the 10% blends and for the smaller rubber particles, Figure 3. In this work the temperature susceptibility is defined in terms of the Andrade equation (8), $\ln(\eta) = \text{Constant} - E_a/RT$, in which E_a is a viscosity activation energy and is a measure of temperature susceptibility. Adding rubber was detrimental to the high-temperature viscosity of an asphalt. The high-temperature viscosity was higher for the 10% blends and the larger particles, Figure 4.

All binder properties were a function of curing time. Although creep stiffness did not improve substantially with curing time, there was always a slight improvement in creep stiffness with curing time, Figure 1. The 60°C complex viscosity increased with curing time, Figure 2. The high-temperature viscosity decreased with curing time, which is desirable, Figure 4. This phenomenon can be explained qualitatively by imaging the rubber particles as rigid spheres and applying an equation derived by Einstein for the viscosity of a dilute suspension of rigid spheres: $\eta = \eta_s(1+2.5\phi)$, where η is the viscosity of the solution, η_s is the viscosity of the solvent, and ϕ the volume fraction of spheres (9). Obviously, the higher the percent rubber the higher the effective ϕ and thus, the higher the viscosity. Furthermore, the significant decrease in high-temperature viscosity with curing time has to be caused by the rubber particles being reduced in size, thus lowering the effective ϕ , because the viscosity of the asphalt, η_s , is definitely increasing as the particles are devulcanized and depolymerized into the asphalt phase of the solution.

The improvements with curing time in the low- and intermediate-temperature properties, as well as the reduction of high-temperature viscosity, are most certainly explained by the rubber devulcanizing and depolymerizing during the curing process. As noted earlier, the devulcanizing and depolymerizing of rubber during the curing process has been discussed by Billiter et al. (2) and Zanzotto and Kennepohl (7), with support from Franta (6). This phenomenon is represented in Figure 5, a GPC chromatograph of the data of an Asphalt #1 blend as measured by an intrinsic viscosity detector. Figure 5 shows that with curing time there is mass transfer into the asphalt phase. The growth of the peak in the 20 to 25 minute retention time region represents the flux of devulcanized and depolymerized rubber into the asphalt phase of the binder. The molecular weight distribution in this region varies from approximately 190,000 at a retention time of 20.63 minutes to 5,970 at a retention time of 24.37 minutes. Please note that the dissolved rubber molecules represented by the data in Figure 5 are smaller than $0.45 \mu\text{m}$ (0.45 microns , 4500\AA), since each sample was prepared for GPC injection with a filter that had a pore membrane size of $0.45 \mu\text{m}$. In fact they are generally smaller than 1000\AA , the pore size of the largest GPC column, as the

chromatograms show little indication of exclusion. The particles are most certainly being devulcanized and depolymerized since they are being reduced from a size of 400-2000 microns to smaller than 1000Å during the curing process.

Comparison of Asphalt Type

The interaction of the rubber and the base asphalt was very much dependent upon the asphalt composition. Asphalt #3, produced by combining a highly asphaltenic 40,000 poise asphalt with a lower molecular weight 5.5 poise recycling agent, initially interacted with the rubber much better than the other asphalts. This interaction is most certainly explained by the presence of the lower molecular weight recycling agent, which could have just as easily been called a rubber extending oil since such oils are used in the rubber processing industry. Asphalt #3 was able to dissolve much more rubber with curing time, Figure 6. Apparently, the light aromatics of Asphalt #3 are able to interact with the rubber at a much faster rate than the other asphalts, and thus improve the binder properties faster. Similarly, the increase in the 60°C complex viscosity, Figure 2, and the initial improvement in temperature susceptibility, Figure 3, were much greater for Asphalt #3. Although the temperature susceptibility of Asphalt #3 did not continue to improve with time as fast as the other asphalts, the initial improvement offsets this.

The low-temperature performance of Asphalt #3 without rubber, which had a creep stiffness of 377 MPa, was much worse than either Asphalt #1, 208 MPa, or Asphalt #2, 101 MPa. Apparently, not enough of the light aromatics are present to sufficiently peptize the substantial amount of larger molecular weight material present in Asphalt #3. However, with the addition of rubber, the low-temperature properties of Asphalt #3 improved more than the other asphalts, Figure 1. Once again, the other asphalts improve with curing time at a faster rate than Asphalt #3, but the initial decrease in creep stiffness more than offsets this.

At the other end of the temperature scale, the high-temperature viscosity was also very dependent on both asphalt type and curing time. The high-temperature viscosity of Asphalt #1 blends was the most dependent on curing time, Figure 4.

Comparison of Tire Gator and Rouse

Ground rubbers from two sources were used in this curing study. Rouse rubber was perhaps slightly better at improving the creep stiffness, Figure 1, and 60°C complex viscosity, Figure 2, of Asphalt #1. Sieve analysis showed that for a given mesh size, the size gradation of Rouse rubber was finer than Tire Gator rubber, and thus with more surface area per unit mass, reacted more rapidly, Figure 6. Please note that initially the Rouse -10 mesh particles dissolved faster than even the Tire Gator -40 mesh particles. At high-temperatures the Rouse rubber particles were less detrimental to the viscosity of Asphalt #1, Figure 4. Once again, the Rouse -10 mesh particles are initially better for the binder property than even the Tire Gator -40 particles.

The relative performance of Tire Gator and Rouse rubber was somewhat asphalt dependent. Like Asphalt #1, Asphalt #2 was better able to dissolve the Rouse Rubber, Figure 6. As expected, the creep stiffness, Figure 1, and the temperature susceptibility were better for the Rouse blends. On the other hand, the Rouse rubber was not better for the high-temperature viscosity and the Tire Gator blends actually have a higher 60°C complex viscosity than the Rouse blends, Figure 2. This oddity can most likely be explained by the mesh size, but one of the crumb rubbers may contain more natural than synthetic rubber and be better able to interact with an asphalt of a certain composition.

Experimental Plan #2

Utilizing a higher shear rate significantly increased the interaction of the rubber and the asphalt. Figure 6 shows that as much crumb rubber dissolves in 2-3 hours utilizing a mixing speed of 1550 rpm as dissolves in 48 hours utilizing a mixing speed of 500 rpm. This strongly indicates that the devulcanization and depolymerization of crumb rubber during the curing process is a mass transfer limited process, with the increased dispersion of the higher mixing speed allowing improved swelling of the rubber and therefore, increased interaction between the asphalt and rubber. As with previous results, the flux of rubber into the asphalt phase improved the low-, intermediate, and high-temperature rheological properties of a binder. Thus, curing at a higher shear rate for a shorter period of time produced similar binder properties as curing the same binder at lower shear for a much longer period of time. In fact, corresponding roughly to the power input it is estimated that increasing the mixing speed three fold, decreases the required curing time nine fold.

Experimental Plan #3

Increasing the curing temperature significantly increased the interaction between the crumb rubber and the asphalt. Figure 6 shows that the higher the curing temperature the higher the amount of rubber dissolving. Some of the increased interaction can be explained by the lower asphalt viscosity at the higher temperatures causing increased mass transfer between the asphalt and rubber. However, the majority of the increased interaction is probably due to the rubber-asphalt reaction, like any chemical reaction, being very dependent upon temperature. The rubber-asphalt reaction is one of devulcanization and depolymerization in which breaking of the cross-linking network and shortening of the main chains takes place (6). As before, all rheological properties improved with increased rubber dissolution.

CONCLUSIONS

These results are a powerful indicator that the 1 hour curing time at 177°C (350°F) and relatively low shear, used in the field, are not optimal. On the other hand, the extended curing times utilized in this study would not be agreeable with field personal. However, the results of this study strongly imply that increasing curing temperature and shear rate can reduce the required curing time to an acceptable level. In fact, by utilizing high temperature and high shear, along with extended curing time, the rubber particles can be devulcanized and depolymerized into the asphalt to produce an asphalt-rubber binder that is both homogeneous and truly elastic. This can be done with no trade off in binder properties, in fact binder performance may be enhanced

ACKNOWLEDGMENTS

Support for this work by the U.S. Department of Energy (DOE), Assistant Secretary for Energy Efficiency and Renewable Energy, Office of Industrial Technologies, under DOE Albuquerque Operations Office Cooperative Agreement DE-FC04-94AL94AL99567, the Texas Department of Transportation (TxDot), in cooperation with the Federal Highway Administration (FHWA), and the U.S. Department of Transportation, is gratefully acknowledged. The technical contributions of Mrs. Ann Ferry are greatly appreciated.

DISCLAIMER

The contents of this report reflect the views of the authors who are responsible for the facts and the accuracy of the data presented herein. The contents do not necessarily reflect the official views or policies of the TxDOT, the DOE, or the FHWA. This report does not constitute a standard, specification, or regulation.

REFERENCES

- (1) Takallou, H.B., and Takallou, M.B., *Elastomerics*, **123**(7), 19 (1991).
- (2) Billiter, T.C., Davison, R.R., Glover, C.J., and Bullin, J.A., *Fuel Sci. And Tech. Int'l.* (in press).
- (3) Allison, K., *Rubber World*, March and April, 47 and 91 respectively (1967).
- (4) Jimenez, R.A., *Trans. Res. Rec.*, **843**, 4 (1982).
- (5) Linden, R.N., Mahoney, J.P., and Jackson, N.C., Preprint No. 880178 presented at Trans. Res. Board's 68th Annual Meeting, (1989).
- (6) Franta, I., *Elastomers and Rubber Compounding Materials*, Elsevier, New York, N.Y., 302-315 (1989).
- (7) Zanzotto, L., and Kennepohl, G.J., Preprint No. 960241 present at Trans. Res. Board's 75th Annual Meeting, (1996).
- (8) Andrade, E.N. da C., *Nature*, **125**(3148), 309 (1930).
- (9) Rosen, S.L., *Fundamental Principles of Polymeric Materials*, John Wiley and Sons, 2nd ed., New York, N.Y., 95 (1993).

Table 1. Experimental Plans (EPs)

EP	Asphalt	Rubber Source	Mesh Size	Weight Percent	Mixer Speed	Temperature (°C)
#1	#1	Rouse	-10	10	500	191
		Tire Gator	-10, -40	5, 10		
	#2	Rouse	-10, -40, -80	5, 10		
		Tire Gator	-10, -40	10		
	#3	Rouse	-40, -80	5, 10		
		Tire Gator	-10	5, 10		
#2	#1	Rouse	-10	10	500, 1550	191
	#2	Tire Gator	-40	10		
#3	#1	Tire Gator	-40	10	500	177, 191, 204

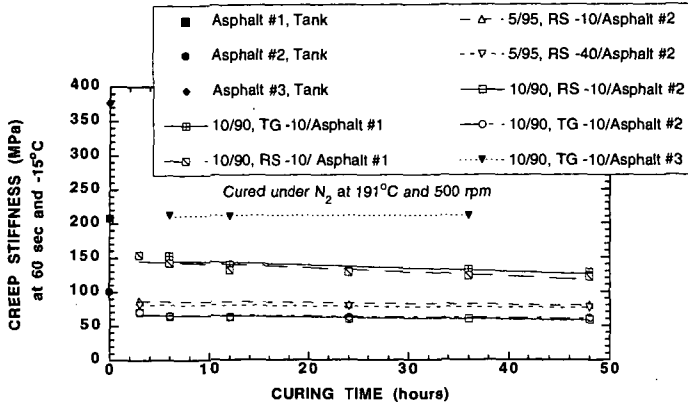


Figure 1. Low-Temperature Data

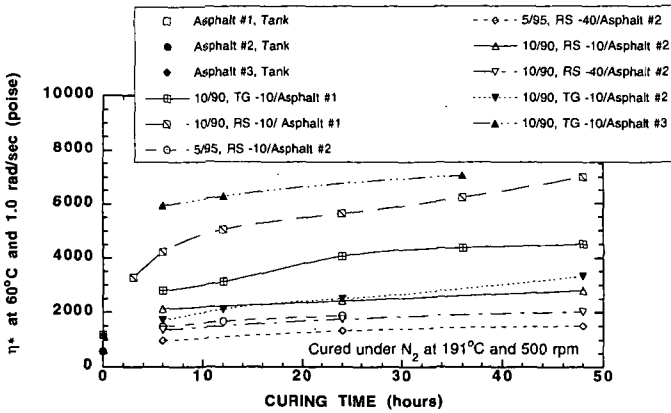


Figure 2. Intermediate-Temperature Data, Complex Viscosity

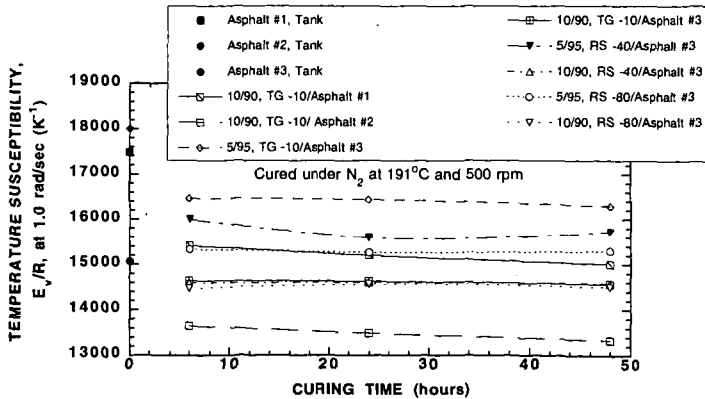


Figure 3. Intermediate-Temperature Data, Temperature Susceptibility

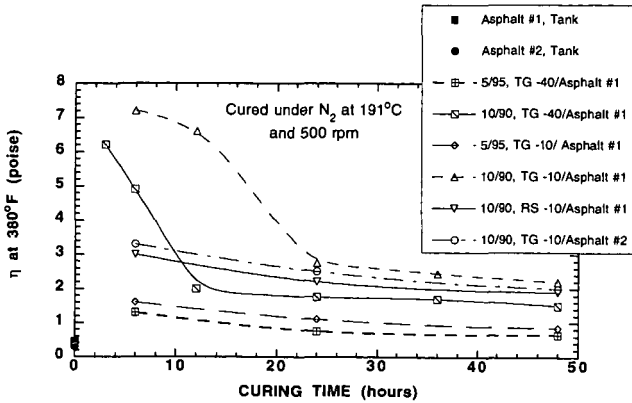


Figure 4. High-Temperature Data

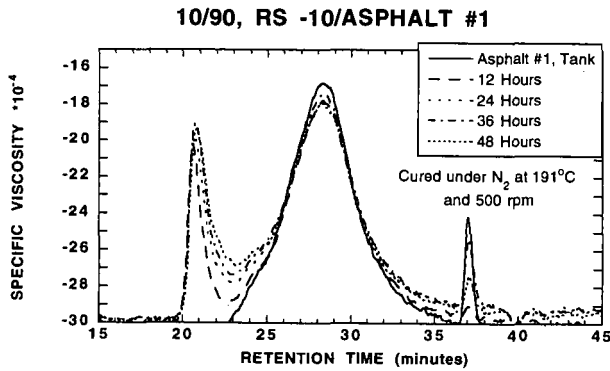


Figure 5. GPC Data for Asphalt #1

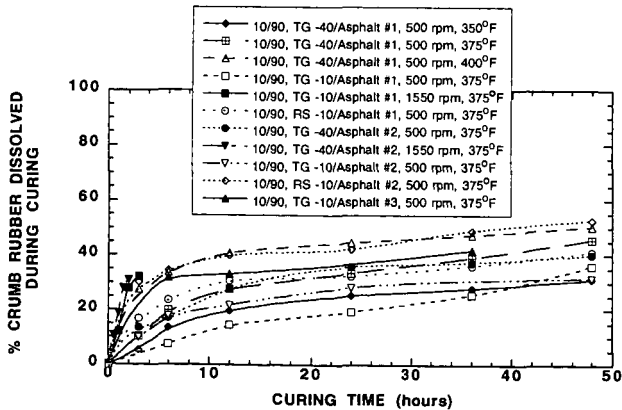


Figure 6. Rubber Dissolution Data

EVALUATION OF THE EFFECTS OF CRUMB RUBBER AND SBR ON RUTTING RESISTANCE OF ASPHALT CONCRETE

Chuang-Tsair Shih, Mang Tia & Byron E. Ruth
Department of Civil Engineering
University of Florida
Gainesville, FL 32611

Keywords: Crumb rubber, SBR, rutting resistance.

ABSTRACT

This paper presents the results of a study to evaluate the effects of addition of crumb rubber (CR) and styrene-butadiene rubber (SBR) on the rutting resistance of asphalt concrete. These two additives were blended with an AC-20 and an AC-30 grade asphalt cements at different levels of concentrations. These modified and unmodified asphalt blends were tested at intermediate and high temperatures to evaluate their rutting resistance characteristics. They were also used to make Florida type S-1 structural surface mixtures. These mixtures were made into Marshall-size specimens by using Gyrotory Testing Machine (GTM) equipped with air-roller to compact and densify to three compaction levels which simulate three different conditions in the pavement. The FDOT's (Florida Department of Transportation) Loaded Wheel Tester was also used to evaluate the rutting resistance of these asphalt mixtures. The test results indicate that the modified asphalt mixtures show relatively better rutting resistance and shear resistance as compared with the unmodified asphalt mixtures.

INTRODUCTION

With the increasing load and pressure of vehicles tires which are applied to our highway pavements today, one of the major distresses seen on our highway pavements is rutting. One of the promising options to lessen this problem is the use of polymers to modify the asphalt binders. The addition of polymers usually has the effect of increasing the stiffness of the binders at high service temperatures without increasing the stiffness at low service temperatures. This modification of binder properties means that the asphalt mixture could be more rut resistant at high service temperatures while its cracking resistance at low temperatures would not be lessened. Crumb rubber (CR) and styrene-butadiene rubber (SBR) are two of the commonly used asphalt additives for this purpose. The purpose of this study was to conduct a laboratory evaluation of the effects of the addition of crumb rubber and SBR on the rutting resistance of typical asphalt paving mixtures used in Florida.

MATERIALS AND TESTING PROGRAM

Binders Used

Two asphalts, namely an AC-20 and an AC-30 grade asphalts, which are commonly used in Florida, were used as the reference asphalt cements. The additives used were (1) a crumb rubber with a nominal size of #80 mesh (0.177 mm), which has been used in several paving projects in Florida, and (2) a SBR, which was a copolymer of styrene and butadiene. The crumb rubber was blended with the asphalt cements in the laboratory at a temperature of 190 °C. The blending of SBR with the asphalt was done by the company that supplied these modifiers. The asphalts and modified asphalts which were used in this testing program include the following:

- (1) AC-20
- (2) AC-20 + 15% CR
- (3) AC-20 + 3% SBR
- (4) AC-30
- (5) AC-30 + 10% CR
- (6) AC-30 + 3% SBR

Table 1 displays the medium- and high-temperature properties of these six binders. These properties include the (1) penetration at 25 °C (ASTM D5) [ASTM, 1995], (2) Brookfield viscosity at 60 °C (ASTM D4402) and (3) $G^*/\sin\delta$ values as determined by the dynamic shear rheometer test (AASHTO Designation TP5) [AASHTO, 1993] at 60 °C of these six binders at their original state and after the standard Thin Film Oven Test process (ASTM D1754), which simulates the short-term aging effect that occurs in the hot-mixing process.

It can be seen that at 60 °C, which represents a typical high pavement service temperature, both the CR-modified and SBR-modified asphalts are substantially stiffer than their corresponding base asphalts. However, at 25 °C, the CR-modified asphalts are only slightly harder than the base asphalts, while the SBR-modified asphalts are softer than the base asphalts, as seen from the penetration values.

Preparation of Asphalt Mixtures

Each of these six binders was mixed with a limestone aggregate blend at a binder content of 6.5% to produce mixtures which meet the requirements for a Florida DOT S-1 structural mix. Table 2 shows the specific gravities and the gradation of the aggregate blend used, along with the gradation limits for a FDOT S-1 mix.

Compaction and Testing of Asphalt Mixtures in the GTM

The Gytratory Testing Machine (GTM) (ASTM D3387) was used to compact and test these different types of asphalt mixtures. The GTM settings selected were based on the results of a previous study on simulation of traffic compaction [Ruth et al, 1994]. Nine Marshall-size specimens for each of these six different asphalt mixtures were tested. Three of the specimens were compacted to a level that simulates the initial field condition. This was achieved by applying 18 GTM revolutions at 135-149 °C (275-300 °F) using a gyratory angle of 3 degrees, 690 kPa (100 psi) of ram pressure and 62 kPa (9 psi) of air roller pressure. Another three specimens were compacted to a level that simulates the condition after two to three years of traffic. This was achieved by applying an additional 50 GTM revolutions at 60 °C at the same settings after the initial compaction. Three other specimens were compacted to a level that simulates the ultimate condition in the pavement. This was achieved by applying an additional 300 GTM revolutions at 60 °C after the initial compaction.

The gyratory shear, which is an indicator of the shear strength of the materials tested, was also measured during the GTM compaction process.

Preparation of Asphalt Mixture Specimens for Loaded Wheel Tests

The asphalt mixtures were heated to 149 °C (300 °F), mixed and then returned to the oven prior to compaction to 7.6 cm (width) X 3.8 cm (thickness) X 38.1 cm (3" X 1.5" X 15") beam specimens for the FDOT Loaded Wheel Tests. Compaction was achieved by applying a load of 60,000 lbs across the top of the beam and then releasing it, for four cycles. Then, the load of 60,000 lbs was applied for the fifth time, and held for six minutes. The compacted beams were demolded the next day, and allowed to cure at room temperature for seven days. Each beam was preheated in the test chamber at 40.5 °C (105 °F) for 24 hours before testing in the Loaded Wheel Tester.

Loaded Wheel Tests

The Loaded Wheel Tester was intended to simulate the repeated applications of moving wheel loads on the asphalt mixtures tested. A stiff pressurized hose mounted along the top of the beam acted as a tire to transfer the load from the wheel of the moving chassis to the beam. The hose pressure was set at 690 kPa (100 psi) and the moving chassis was loaded with 543 N (122 lb) of steel plates centered above the wheel. The test temperature was set at 40.5 °C (105 °F) and monitored with a thermometer embedded in a dummy specimen placed inside the Loaded Wheel Tester. One loading cycle consisted of a forward and return pass of the loaded chassis. Rut depth measurements were made with a dial gauge at seven different locations on the top of the beam at an interval of 5.1 cm (2 inches), each at 0, 1000, 4000, and 8000 cycles.

The average of three rut measurements at the center was used. This was found to be more consistent in comparison with the average of all seven measurements. The measurements at the ends of the beams tended to be exaggerated due to the combined effects of abrasion by the hose, slower moving loads at the ends and the change in pitch of the chassis.

RESULTS OF GTM TESTS

Tables 3 through 5 display the gyratory shear and the volumetric properties of the mixtures as measured by the GTM at the initial, medium and ultimate compaction, respectively. It can be seen that at the same compactive efforts, the CR-modified mixtures had lower air voids than the unmodified mixtures and the SBR-modified mixtures had the lowest air voids. It is speculated that the lower air voids of the modified mixtures were possibly due to a higher compaction temperature used for these mixtures. However, in spite of their lower air voids, the modified mixtures generally showed a higher gyratory shear strength than the unmodified mixtures, and the difference increased as the compactive effort increased.

RESULTS OF LOADED WHEEL TESTS

The results of the Loaded Wheel tests are displayed in Table 6. It can be seen that the SBR-modified asphalt mixtures show the highest reduction in rut depth as compared with the unmodified reference mixtures (up to 38% at 8000 cycles). The CR-modified mixtures showed a reduction in rut depth of 17 to 21% as compared with the unmodified mixtures. The standard deviations of rut measurements ranged between 0.03 and 0.05 inch. Results of a statistical Duncan's grouping indicate that the SBR-modified asphalt mixtures (AC-20+3%SBR and AC-30+3%SBR) had the least rut depths while the unmodified asphalt mixtures (AC-20 and AC-30) had the highest rut depths among all six types of asphalt mixtures tested.

SUMMARY AND CONCLUSION

The results of this laboratory study show that the addition of crumb rubber and SBR could increase the rutting resistance of asphalt paving mixtures. The CR-modified and SBR-modified asphalts had higher stiffness at 60 °C than the unmodified base asphalts. The modified asphalt mixtures had higher gyratory shear strengths than the unmodified mixtures. The modified mixtures exhibited substantially lower rut depths in the Loaded Wheel tests than the unmodified mixtures. It is also interesting to note, from the results of the GTM tests, that having a low air voids at ultimate compaction condition does not necessarily result in a mixture with lower shear strength.

REFERENCES

- American Association of State Highway and Transportation Officials 1993. *AASHTO Provisional Standards*, AASHTO, Washington, D.C.
- American Society for Testing and Materials 1995. *Annual Book of ASTM Standard*, ASTM, Philadelphia, Pennsylvania.
- Ruth, B.E., Tia, M., Shen, X. and Wang, L.H. 1994. Improvement of Asphalt Mix Design to Prevent Rutting, Technical Report, Department of Civil Engineering, University of Florida, Gainesville, Florida.

Table 1 Medium- and high-temperature properties of the binders used

Asphalt Binder	Penetration at 25°C, 5sec, 100g, (dmm)		Brookfield Viscosity at 60°C at Shear Rate=1/s (poise)		G*/sinδ at 60°C at 10 rad/s (Pa)	
	Original	TFOT Residue	Original	TFOT Residue	Original	TFOT Residue
AC-20	72.5	42.2	2526	5936	3542	7383
AC-20+15%CR	51.7	38.8	20605	25352	13115	22672
AC-20+3.0%SBR	58.5	58.5	10709	14341	9304	11771
AC-30	55.0	35.8	3785	8251	4687	9330
AC-30+10%CR	47.3	34.3	9779	20424	11020	18493
AC-30+3%SBR	57.0	47.0	17407	16426	6593	12917

Table 2 Bulk specific gravities and gradation of the aggregate blend used

Sieve Size	Bulk Specific Gravity of Aggregates Retained	Gradation (% Passing)	FDOT S-I Specification (% Passing)
3/4"	---	100	100
1/2"	2.375	99	88 - 100
3/8"	2.379	90	75 - 93
No.4	2.345	63	47 - 75
No.10	2.298	47	31 - 53
No.40	2.333	35	19 - 35
No.80	2.655	13	7 - 21
No.200	2.784	4	2 - 6

Table 3 Mix Properties as Measured by the Gyratory Testing Machine at Initial Compaction

Mix Type	Gyratory Shear (psi)	Bulk Density (pcf)	Air Void (%)	VMA (%)
AC-20	61.00	137.2	5.90	16.04
AC-20+15%CR	63.23	137.5	5.30	15.83
AC-20+3%SBR	60.19	140.5	2.20	13.98
AC-30	59.37	137.4	4.93	15.90
AC-30+10%CR	63.38	137.7	5.20	15.75
AC-30+3%SBR	61.25	139.9	2.68	14.40

Table 4 Mix Properties as Measured by the Gyratory Testing Machine at Medium Compaction

Mix Type	Gyratory Shear (psi)	Bulk Density (pcf)	Air Void (%)	VMA (%)
AC-20	63.54	139.4	4.37	14.68
AC-20+15%CR	66.60	141.1	2.84	13.64
AC-20+3%SBR	66.76	142.1	1.10	13.01
AC-30	55.98	139.8	3.27	14.43
AC-30+10%CR	70.28	141.5	2.58	13.41
AC-30+3%SBR	67.41	142.4	0.94	12.87

Table 5 Mix Properties as Measured by the Gyrotory Testing Machine at Ultimate Compaction

Mix Type	Gyrotory Shear (psi)	Bulk Density (pcf)	Air Void (%)	VMA (%)
AC-20	61.55	141.4	3.02	13.47
AC-20+15%CR	66.09	142.0	2.17	13.05
AC-20+3%SBR	52.33	143.0	0.47	12.45
AC-30	61.93	141.1	3.99	14.62
AC-30+10%CR	63.41	142.4	1.93	12.84
AC-30+3%SBR	73.60	142.8	0.63	12.59

Table 6 Results of Loaded Wheel Test

	Average Rut Depth (inch)			Reduction in Rut Depth as compared with Base AC
	At 1000 Cycles	At 4000 Cycles	At 8000 Cycles	
AC-20	0.146	0.210	0.276	--
AC-20+15%CR	0.136	0.188	0.228	17%
AC-20+3%SBR	0.093	0.144	0.177	36%
AC-30	0.109	0.176	0.262	--
AC-30+10%CR	0.118	0.176	0.207	21%
AC-30+3%SBR	0.092	0.135	0.162	38%

FACTORS AFFECTING THE KINETICS AND MECHANISMS OF ASPHALT OXIDATION AND THE RELATIVE EFFECTS OF OXIDATION PRODUCTS ON AGE HARDENING

J. Claine Petersen
Western Research Institute (retired)
1316 Jennifer Court, Loveland, CO 80537

P. Michael Harnsberger and Raymond E. Robertson
Western Research Institute
365 North 9th Street, Laramie, WY 82070

Keywords: Oxidation kinetics, Oxidation mechanisms, Oxidation products-viscosity relationships

ABSTRACT

The ketones and sulfoxides formed in asphalts are the major determinants of viscosity increase on oxidation. Asphalts initially exhibit a high reactivity with oxygen causing a rapid spurt in the formation of both oxidation products and viscosity increase. This spurt is followed by a slower rate of oxidation and hardening. Different oxidation mechanisms appear operative during these two periods. During the spurt, sulfoxides are the major oxidation product and determinant of viscosity increase, particularly at lower temperatures. Following the spurt, ketones are usually the major product and determinant of viscosity increase. Molecular moieties that are converted to ketones and sulfoxides compete for the reactive oxidant. The ratio of ketones to sulfoxides formed was found dependent on oxygen concentration (pressure), temperature and sulfur content. The relative amounts of sulfoxides and ketones formed under different internal and external environments, and their differing effects on viscosity, are rationalized by the microstructural model of asphalt.

INTRODUCTION

Asphalt oxidation is important because it is the major cause of asphalt hardening, resulting in the deterioration of many desirable asphalt performance properties. In asphalt concrete pavements, oxidative hardening contributes to pavement embrittlement and excessive pavement cracking. Factors affecting the rate of oxidative hardening and the mechanisms of asphalt oxidation are the subjects of this paper.

Oxidation produces polar functional groups in asphalt molecules; ketones (1) and sulfoxides (2) are the major oxidation products; only minor amounts of dicarboxylic anhydrides (3) and carboxylic acids (4) are formed during the advanced stages of oxidation. Methods for their quantification have been developed (5). Viscosity increase accompanies the introduction of the polar functional groups; however, the relative sensitivity to viscosity increase is highly asphalt source (composition) dependent and is related to the component compatibility of the asphalts (6). The more compatible asphalts show lower sensitivity to viscosity increase from oxidation (6-8). Component compatibility is defined as the relative amount of molecular aggregation of the polar asphalt components to form micellar structuring, often referred to as microstructure. The use of the term micellar with reference to asphalt does not imply well defined or spherical components as is common in aqueous systems. In fact, just the opposite is probably true in which irregular shaped molecular agglomerates with poorly defined boundaries and gradual polarity gradients exist within the asphalt matrix.

On oxidation, all asphalts exhibit a hyperbolic-like kinetic curve when log viscosity is plotted versus oxidation time, showing an initial rapid rate of viscosity increase (referred to in this paper as the spurt) followed by a slower, nearly linear rate of viscosity increase (8). Following the viscosity spurt, viscosity increase correlates directly with ketone formation (8-11), with each asphalt having its unique ketone-viscosity relationship. The formation of polar asphaltene components on oxidation also correlates with viscosity increase (12); thus, it follows that the rate of asphaltene formation should correlate with the rate of ketone formation, which relationship has been demonstrated (13,14).

The shape of the kinetic plot, and the effect of asphalt component compatibility on

oxidative aging are shown in Figure 1 for two asphalts studied in the Strategic Highway Research Program (SHRP). Asphalt AAG-1 is a highly compatible asphalt with well dispersed microstructure, while asphalt AAD-1 is at the other end of the compatibility spectrum. The time scales have been time-temperature shifted to offset the effect of temperature on the increase in oxidation rate so that changes in kinetics as a function of temperature can be visually compared. This procedure will be used throughout this paper. Data in Figure 1 are presented to illustrate the effects of component compatibility on oxidation kinetics. The data show that for the highly compatible asphalt AAG-1, there were no significant changes in microstructure on oxidation between 60°C and 80°C that affected the oxidation kinetics, presumably because the oxidation products were solubilized in the asphalt dispersed phase ("solvent" component) precluding their interaction to form significantly larger molecular agglomerates. Thus, the asphalt behaved more like a true solution. However, for the less compatible, more highly associated asphalt AAD-1, lowering the oxidation temperature from 80°C to 60°C significantly reduced the rate of oxidative hardening following the spurt. This lowering is believed the result of molecular immobilization from the formation of microstructure, reducing the reactivity of precursor molecules that form ketones. These effects are discussed in detail elsewhere (8).

In the present paper, the chemical and physicochemical factors that control the phenomena cited above are identified and their effects interpreted and rationalized by the microstructural model of asphalt. A new model for the chemical mechanisms of asphalt oxidation is also presented. Because of the large number of variables affecting asphalt oxidation kinetics, only selected examples can be presented within the scope of this paper. A sequence of papers are planned for future publication in which the subjects presented are discussed in more detail and on larger sets of asphalts.

RESULTS AND DISCUSSION

Oxidation Kinetics and Oxidation Products-Viscosity Relationships. As stated in the Introduction, ketones and sulfoxides are the major identifiable functional groups formed in asphalt on oxidation. Recent data of Liu, et al. (10) relating carbonyl formation with oxygen uptake for SHRP asphalts AAA-1 and AAG-1 were compared by us with total ketones plus sulfoxides formed in these same two asphalts oxidized at Western Research Institute (WRI) using the same oxidation method. Analysis of Liu's data showed that the ratio of oxygen uptake for AAA-1/AAG-1 was 1.32; the corresponding ratio of total ketones plus sulfoxides calculated from the WRI data was 1.31, confirming that ketones and sulfoxides account for essentially all of the oxygen that reacted with these asphalts. It therefore follows, that except for variable volatile loss in asphalt pavement mix plants, nonreversible age hardening of asphalts in pavements is a direct result of ketone and sulfoxide formation.

The rates (kinetics) of chemical oxidation and viscosity increase of asphalts are influenced by asphalt composition, oxidation products formed, temperature, oxygen partial pressure (concentration and/or diffusion rate) and physicochemical effects. These factors are demonstrated for selected asphalts in Figures 2-6. It has been shown (15, 16) that asphalts exposed to 100% oxygen or air at 300 psi (2.07×10^6 Pa) pressure are saturated with oxygen, thus eliminating the need to consider oxygen concentration (diffusion) as a variable in the oxidation kinetics. Elimination of this complicating factor greatly simplifies the study of the kinetics of the oxidation chemistry.

In Figures 2-4, the oxidation and age hardening kinetics of three selected SHRP asphalts having different sulfur contents are considered. The asphalts were aged at 60°C and 100°C using the SHRP TF0-PAV method (300 psi (2.07×10^6 Pa, air)). Data for AAF-1 (3.4% sulfur) are shown in Figure 2. Kinetic data are shown at the left of the figure and oxidation functional group-viscosity relationships at the right. The time scales are time-temperature shifted as explained for Figure 1. Note that during the initial oxidation spurt that sulfoxides are formed at a much faster rate than ketones. This has been found true for all asphalts studied. Further, the relative amounts of ketones and sulfoxides formed and viscosity increase during the spurt are nearly independent of temperature in the absence of oxygen diffusion effects. This was found to hold for all eight SHRP core study asphalts. Following the spurt, the rate of formation of ketones at 60°C is lower than at 100°C, resulting in a corresponding reduction in viscosity increase. These results are interpreted as follows based on the microstructural model

of asphalt (6-8).

First, it is proposed that the mechanisms of oxidation during and after the spurt are different. This is discussed later in the paper. The present discussion relates to oxidation following the spurt. Asphalt AAF-1 is of intermediate compatibility; therefore, as temperatures are decreased, polar, more aromatic components (related to the polar aromatics and asphaltenes generic fractions) associate into agglomerates, thus reducing their molecular mobility and reactivity with oxygen from physicochemical effects (7, 8). That is, the effective concentrations of mobile reactants are reduced by being buried in the microstructure. This is somewhat analogous to what has been observed in micellar catalysis where reaction sites on whole molecules can be buried in the micelle (17). Because the reactive components that form ketones (benzylic carbons, (1, 6)) are highly concentrated in the polar, more aromatic fractions (6), ketone formation is inhibited in the less compatible asphalt AAF-1 at lower temperatures. Lin, et al. (14) recently showed that the new asphaltenes which form on oxidation are produced primarily from the maltenes fraction. Based on the known composition of the precursors to ketone formation, the new asphaltenes are probably formed primarily from the polar aromatics fraction. The new asphaltenes are reported (14) to have the same effect of viscosity as original asphaltenes, although chemically quite different.

Next, consider the relative effects of ketones and sulfoxides on viscosity increase from data at the right in Figure 2. Note that the ketones formed correlate with viscosity increase as previously mentioned. During the oxidation spurt, for which limited data points are available, it is difficult to assess the relative contribution of sulfoxides and ketones to viscosity increase. However, the linear ketone-viscosity plot and major change in the slope of the sulfoxide-viscosity plot at the point corresponding to the end of the spurt indicate that the ketones are the major determinants of viscosity increase in asphalt AAF-1 oxidized between 60°C and 100°C. The lower concentration of sulfoxides at 60°C following the change in direction of the sulfoxide plot at the point corresponding to the end of the spurt in the kinetic plots could result from either greater thermal instability of the sulfoxides at 100°C and/or the depletion of highly reactive sulfides which form sulfoxides. Obviously, there is no additional contribution to viscosity increase by the sulfoxides formed during 100°C oxidation past the change in slope of the curve represented by about 0.25 mol/L sulfoxides, since the concentration of sulfoxides remains constant. Note also that the slope of the ketone plot is steeper (viscosity increase more sensitive to ketone formation) for 100°C oxidation than for 60°C oxidation, even in the absence of sulfoxide formation. This is evidence that at the higher temperature, ketones are formed deeper in the microstructure because their precursors are liberated for reaction by thermal dissociation of the microstructure.

Before discussing the remaining figures, the following hypothesis based on the microstructural model is presented to explain how ketones and sulfoxides produce viscosity increase. Sulfoxides and ketones are both polar, containing an electronegative oxygen producing a dipole that can interact or associate with other dipoles or induced dipoles. From a polarity standpoint, the sulfoxide functional group is probably as polar or more polar than the ketone. Yet, the ketones formed beyond the oxidation spurt show the major effect on viscosity increase. Thus, it is concluded that the polar nature of the ketones and/or sulfoxides alone is not the fundamental factor responsible for the significant effects on viscosity increase. It is proposed that the size of the associated molecular agglomerates on which these function groups are formed is the primary reason for their profound effects on viscosity. It is well known that the viscosity of polymers is directly related to molecular weight. The ketones are formed predominantly on molecules of the polar, aromatic components where the benzylic carbons are concentrated (6). These ketone precursors are also the molecules believed to be associated in molecular agglomerates in asphalt. As previously mentioned, the maltenes (which contain the polar aromatics) have been shown (14) to be involved in asphaltene formation and viscosity increase. Thus, it logically follows that the ketones, which are most likely formed on already associated molecular species, cause much larger molecular agglomerates to form through their association with other large associated species. As a result, the formation of a single ketone moiety could cause the formation of a much larger agglomerate with significantly greater effective molecular weight, and thus a significant effect on viscosity increase.

On the other hand, the sulfides which are precursors of sulfoxides should be found in

relative abundance in the weakly associated dispersing phase of asphalt, thus sulfoxides formed following the spurt could be concentrated in the dispersing phase. Also, if the sulfide moieties are located in the physical vicinity of the associated phase, the molecules of which they are a part may not have sufficient polarity or aromaticity to cause them to be strongly associated with larger agglomerates. Once sulfoxides are formed, they may then interact with polar constituents present in either the weakly or strongly associated components. However, in either case, they would have limited effect on effective molecular weight increase, and thus viscosity increase, for the following reasons. If the association of sulfoxides occurred in the dissociated (solvent) phase, the association of the sulfoxide with otherwise weakly associated molecules would only about double the effective molecular weight. For typical asphalt molecules, this might be a molecular weight increase from 1000 to 2000 Daltons. If a sulfoxide-containing molecule with no additional highly polar molecular components were to associate with a large agglomerate in the dispersed phase, for example and agglomerate with an effective molecular weight of 30,000 Daltons, this would only increase the effective molecular weight to 31,000 Daltons --- as rather insignificant relative increase. Thus, oxidation of sulfides to form sulfoxides under the conditions just described should have a relatively small effect on viscosity increase. Of course, another reason for the reduced effect of sulfoxides on viscosity following the spurt in some asphalts might be that the concentration of reactive sulfides in the vicinity of the ketone-forming precursors for which they compete to form sulfoxides might simply be depleted.

With the theory presented, consider the data for asphalt AAM-1 and AAA-1 in Figures 3 and 4, respectively. Asphalt AAM-1 (Figure 3) is a compatible asphalt with low sulfur content (1.2%). Because the polar components of this compatible asphalt are well dispersed, the lowering of the oxidation temperature from 100°C to 60°C does not significantly change the state of dispersion (immobilization of the aromatic molecules containing the ketone-forming benzylic carbons) of the asphalt. As a result, no significant physicochemical effect is seen in the kinetic plot at the left in Figure 3 for AAM-1 between 60°C and 100°C, as was seen for the more incompatible asphalt AAF-1 (Figure 2). The similarities of the ketone kinetics at both the high and low temperatures is also reflected in the viscosity plots, again confirming the relationship between ketone formation and viscosity increase. The decrease in sulfoxides with time following the oxidation spurt is unique for asphalt AAM-1 among the asphalt studied to date and is as yet unexplained.

The relatively large increase in viscosity with ketone formation as seen for AAM-1 is not typical for compatible asphalts (compare with the much-studied compatible asphalt AAG-1 (Figure 2)). Asphalt AAM-1 has a very low heptane asphaltenes content and its molecules are inherently much larger than those of most other asphalts (16). Recent solid state NMR measurements at WRI (18) indicate that asphalt AAM-1 has much larger condensed aromatic ring structures than the other SHRP asphalts. The authors propose that these large polarizable condensed ring structures provide for increased molecular association in this asphalt, and thus its high sensitivity to viscosity increase with ketone formation.

A change in slope of the ketone-viscosity plot at the right in the figure corresponding to the end of the spurt is evident. The combined effect of ketones and sulfoxides on viscosity during the spurt (below 0.15 mol/L ketones) is less than that of the ketones alone following the spurt. This is believed to result from the different oxidation mechanisms operating during the spurt, with the initial major oxidation product being sulfoxides. Further, the spurt oxidation mechanism proposed later on would dictate that during the spurt, oxidation products may be formed on molecules having a different state of dispersion than molecules on which they are formed after the spurt, thus having differing effects on viscosity increase.

Data on the high sulfur (5.5%) asphalt AAA-1 are shown in Figure 4. It is apparent when one compares the relative amounts of ketones and sulfoxides formed in the low sulfur asphalt AAM-1 (Figure 3) with those formed in asphalt AAA-1 (Figure 4), that a much higher ratio of ketones to sulfoxides are formed in the high sulfur asphalt. Note also, except for a slight lowering of the rate of ketone formation at 60°C from physicochemical effects, that the relative amounts of ketones to sulfoxides are almost the same at both high and low temperatures. This has been found to be true for the eight SHRP core asphalts during PAV oxidation, again confirming that the kinetics and

mechanisms of oxidation are similar at all temperatures studied and are not dependent on oxygen concentration, as previously mentioned.

Examination of the data in the kinetic plot at the left in Figure 4 suggests that the relatively small increase in the rate of ketone formation between the 60°C and 100°C may not be sufficient to account for the larger rate of viscosity increase between the two temperatures. These results suggest that the sulfoxides have a greater effect on viscosity increase at the higher temperature in this higher sulfur, less compatible asphalt than in the two asphalts previously considered. An explanation for this is found in the microstructural model. A relatively greater proportion of the reactive sulfides that are precursors to sulfoxides should also be found in more associated species in this less compatible asphalt. Therefore, their formation on more associated molecular agglomerates should have a greater effect of viscosity. Also, since sulfoxides compete with ketones for hydroperoxide precursors to form sulfoxides, the molecular dissociation occurring at the higher temperature would make sulfoxides "deeper" in the associated phase more available for reaction. Therefore, if the sulfoxides were formed deeper in the associated phase at 100°C than at 60°C, then when the viscosity of the 100°C sample is measured at 60°C, sulfoxides would be buried deeper in the associated phase and have a greater effect on viscosity increase. The greater sensitivity of viscosity increase to ketone formation at 100°C than at 60°C (right side of figure) could also be explained using the same argument for ketones as was just presented for sulfoxides, in that at higher temperatures ketones are formed deeper in the microstructure, thus having a greater relative effect on viscosity. Probably physicochemical effects involving both sulfoxides and ketones are responsible for the larger increase in viscosity sensitivity during oxidation at the higher temperature.

Effects of Oxidation at Atmospheric Pressure on Oxidation Kinetics. As previously discussed, high pressure oxidation (PAV procedure) produced sulfoxides and ketones at nearly the same ratios, independent of temperature. However, in a diffusion controlled system at atmospheric pressure in which oxygen concentration within the asphalt is low, the ratio of sulfoxides to ketones produced following the spurt are highly dependent on oxidation temperature. This temperature sensitivity can be seen by comparing the data in Figure 5 for asphalt AAF-1 with the PAV aging data for the same asphalt shown in Figure 2. Aging data for AAF-1 in Figure 5 were obtained using the Thin Film Accelerated Aging Test (TFAAT) in which the asphalt was oxidized as a 160 micrometer film at ambient air pressure. In general, as the oxidation temperature is lowered, the ratio of sulfoxides to ketones increases. Space do not permit comparison of the data for the other seven SHRP core asphalts, but a comparison is planned in a future publication.

The sensitivity to temperature of the ratio of sulfoxides to ketones appears to be related to the degree of molecular association at a given temperature. This is evidenced by the fact that those asphalts which exhibited a reduction of ketone formation and viscosity increase from the physicochemical effects of molecular association at the lower 60°C temperature in the PAV oxidations, as discussed earlier, are more sensitive to an increase in the sulfoxide-to-ketone ratio as temperature is lowered. The effect is pronounced during TFAAT oxidation at 85°C, but almost disappears above 113°C where molecular dissociation is high as indicated by similar ratios (not shown) for a given asphalt at both 113°C and 130°C oxidations. It was also found, and also not shown, that 65°C TFAAT oxidation data obtained on SHRP asphalts AAD-1 (6.9% sulfur) and AAG-1 (1.3% sulfur) oxidation kinetics were quite similar to those for 85°C TFAAT oxidation. Thus, the large change in the TFAAT oxidation kinetics attributed to physicochemical effects occurs between 85°C and 113°C. This is in contrast with results from PAV oxidation where the change occurs between 60°C and 80°C. Although not shown in graphical form, ketone and sulfoxide concentrations at 400 hours of TFAAT oxidation at 85°C for the highly compatible asphalt AAG-1 are 0.15 and 0.21 mol/L, respectively. Corresponding data for ketone and sulfoxide concentrations after a comparable oxidation of 120 hours at 113°C are 0.33 and 0.14 mol/L, respectively. Thus, at higher temperatures and low oxygen concentrations, ketones seem to be formed to some extent at the expense of sulfoxides; however, the total ketone plus sulfoxide concentration is higher at 113°C (0.47 mol/L) than at 85°C (0.36 mol/L). The known thermal instability of sulfoxides at higher temperatures and the dissociation of

more reactive ketone precursors, thus increasing their concentration in the dissociated phase, are possible contributors to this difference.

At the right in Figure 5, note also the large difference between the slopes of the ketone-viscosity plots for oxidation at 85°C and 113°C. As previously discussed, this is again evidence that at higher temperatures ketone precursors dissociate deeper in the asphalt microstructure, and when oxidized to ketones, have a relatively greater influence on viscosity increase. Comparison of Figures 2 and 5 show that this effect is greatly amplified at atmospheric pressure oxidation compared with PAV oxidation.

While theorizing on the mechanism is difficult, the fact remains that the large change in the ratio of sulfoxides to ketones as a function of temperature is primarily influenced by a change in the oxygen pressure (concentration) in the asphalt. Since oxidation in pavements is diffusion controlled at ambient pressures, and oxidative aging characteristics of asphalts may be evaluated using the SHRP procedure at high pressures in which the asphalt is saturated with oxygen, the correspondence between aging at low and high oxygen pressures needs to be rationalized.

Related to the above discussion, Liu and coworkers (10) found a significantly lower level of carbonyl absorption (CA) versus time in asphalts oxidized at 0.2 atmospheres oxygen pressure than at 20 atmospheres pressure at the same temperature for asphalt AAF-1. Linear extrapolation of the CA versus time plot to zero oxidation time (roughly corresponding to the oxidation level at the end of the spurt) shows significantly lower levels of CA (ketones) in the low pressure oxidation. Since CA correlates directly with log viscosity for a given asphalt, there is some question, as Lin, et al. also point out, that aging characteristics predicted from PAV aging may not always correspond well with aging predicted from aging tests run at lower pressures. Our results regarding the effects of temperature on the aging kinetics using high and low pressure aging, particularly for less compatible asphalts, seem particularly germane.

Effects of Oxidation at Low Temperatures and at Atmospheric Pressure.

Several years ago the principle author and coworkers (G. Miyake, H. Plancher, and P.M. Harnsberger) at WRI oxidized a series of asphalts as thin films (5 wt%) in Ottawa sand briquettes. These asphalts were the unmodified control samples prepared in connection with a kinetic study to evaluate an oxidation accelerator in asphalt. Oxidations were performed at 45°C. The data obtained on extracted samples for one of these asphalts are shown in Figure 6. Since this oxidation was performed at a relatively low temperature, reaction rates were slow and oxidation during the spurt could be looked at in more detail because a number of data points were obtained during the spurt. When comparing these data with data in the previous figures, it should be noted that very little oxidation occurred following the spurt at the 45°C temperature during the 100 day aging period. Ketone levels never exceeded about 0.025 mol/L. This level is below ketone levels reached at the first data point near the end of the spurt during oxidation at the higher temperatures. It should be noted that although the oxidation temperature was low, the viscosity measurements were made at the same temperature (60°C) as was used for the kinetic studies at the higher temperatures, making these data comparable for interpretation with the higher temperature data.

Important information regarding oxidation during the spurt is apparent in Figure 6. First, the formation of sulfoxides is extremely rapid, even at 45°C, with the virtual exclusion of ketone formation. This is in agreement with the work of Huh and Robertson (19) in which it was shown that the slope of the Arrhenius plot for sulfoxide formation was smaller than that for ketone formation, thus indicating that the activation energy for sulfoxide formation is less sensitive to temperature change than is the activation energy for ketone formation. In the absence of ketone formation, one can conclude that the initial oxidation mechanism during the spurt under near ambient conditions is not a typical hydrocarbon free radical chain reaction which always produces ketones and more free radicals. This result is consistent with the observation of van Gooswillen, et al. (20) who oxidized asphalt in solution and measured the reaction rate by oxygen uptake. They noted no induction period in the oxidation kinetics which is characteristic of classical hydrocarbon chain reactions; they concluded that asphalt oxidation was not of the classical hydrocarbon type.

What is most revealing in Figure 6 is that the viscosity increase corresponds with the

formation of sulfoxides with virtually no ketones being formed. This shows that under the conditions of this experiment, that viscosity increase during the spurt is largely controlled by the formation of sulfoxides, suggesting that the sulfoxides are being formed on associating molecules deep in the polar, highly associated components during the spurt and not in the dispersing phase as may occur for sulfoxide formation following the spurt. In times past at WRI, samples taken from the surface of asphalt stored for and extended periods in sample cans at ambient temperatures have been observed to have sulfoxide concentrations of over 0.3 mol/L with no ketones having been formed.

A Proposed Two-Stage Mechanism for Asphalt Oxidation. As discussed above, sulfoxides were the primary oxidation product formed during the spurt with the virtual exclusion of ketones. The reaction of sulfides to form sulfoxides was also very rapid, yet sulfides in an inert solvent do not react with atmospheric oxygen under these conditions. A highly reactive precursor inherent in the asphalt that reacts with oxygen to form a hydroperoxide intermediate which then reacts with the asphalt sulfide to form sulfoxides (16) is proposed. Sulfides are well recognized to be very reactive hydroperoxide scavengers and react with hydroperoxides to form sulfoxides with no free radical products. Sulfides are used commercially in hydrocarbon plastics such as polypropylene as hydroperoxide scavengers to prevent the further reaction of hydroperoxides in promoting further hydrocarbon chain reactions. It has recently been proposed by Mill (21) that oxygen initially reacts with a highly reactive hydrocarbon in asphalt such as a hydroaromatic. This type of moiety can be exemplified by saturated, nonaromatic bridgehead carbons fused between aromatic ring structures to form a strained ring between the aromatic rings. Because of the steric strain imposed on the saturated carbon atoms, the hydrogens on these carbons are highly reactive toward abstraction by the oxygen to form hydrogen peroxide and/or hydroperoxides (as proposed by Mill), resulting in aromatization of the nonaromatic ring component. Thus, hydroperoxides are generated which then react with the asphalt sulfides with little or no production of ketones, consistent with the observed asphalt oxidation during the initial stages of the spurt. Then, as the oxidation continues toward the end of the spurt, initiation of a hydrocarbon chain-reaction begins with abstraction of a hydrogen from a benzylic carbon, which is a precursor to ketones, forming benzyl free radicals. These radicals can then compete with the sulfides for the available hydroperoxides. These radicals can also begin to react with oxygen to form peroxy radicals, and then continue on to form hydroperoxides with the generation of more benzylic carbon free radicals. Thus, in the latter case, a free radical hydrocarbon chain reaction has begun. Many reaction paths are possible; however, one route is for the hydroperoxide to decompose to form ketones or react with sulfides to form sulfoxides. Once the supply of the highly reactive hydrocarbon precursors previously described is exhausted, the spurt is over, explaining the rapid reduction in the oxidation rate and viscosity increase following the oxidation spurt. After the spurt, ketones form at a much slower, but nearly constant rate via typical hydrocarbon free radical chain reactions. Such chain reactions have previously been proposed (6). Reactive sulfides, as long as available, compete with the hydroperoxide ketone precursors to form sulfoxides.

Figure 7 shows the ketone and sulfoxide concentrations in the eight SHRP core asphalts at the end of the spurt during PAV oxidation at 100°C. Except for the low sulfur asphalts, the concentrations of ketones plus sulfoxides are nearly constant, indicating that these asphalts all have about the same concentration of reactive hydrocarbon precursors. Asphalt AAM-1, which is low in aromatics, might be expected to have a smaller concentration of the highly reactive hydrocarbon precursor, thus explaining its low level of oxidation during the spurt.

As previously mentioned in the discussion of Figure 6, the sulfoxides formed during the spurt appeared to control the viscosity increase during this stage of oxidation. This is explained as follows. If the reactive hydrocarbon precursors are indeed hydroaromatics, as suggested by Mill, then they would be expected to be present in the highly associated molecular agglomerates in which the more aromatic components are found. The formation of a polar sulfoxide group in the microstructure should cause the association of relatively large molecular agglomerates, thus significantly increasing effective molecular weight, and thus viscosity. Sulfoxides formed after the spurt would have less effect on viscosity if they were formed in the weakly associated dispersing phase or on rather nonpolar molecules as previously explained.

The relative abundance of ketones and sulfoxides following the spurt should be a

function of sulfide (related to sulfur) content of the asphalt. Higher sulfide concentrations provide more competition for the hydroperoxide at the expense of ketone formation. This is illustrated by the data in Figure 8 for sulfoxide and ketone formation in asphalts following the spurt. Note the ketone and sulfoxide data in the figure for the high sulfur asphalts AAK-1 and AAD-1. They cease to follow the trend as a function of sulfur content. More ketones begin to be formed at the expense of sulfoxides. Data for 80°C are shown as solid data points to provide evidence that this change in product ratios occurs somewhere between 80°C and 100°C.

As confirming evidence for a dual, two-stage oxidation mechanism for asphalts, the data in Figure 9 are submitted. These unpublished data were obtained several years ago at WRI by H. Plancher in scouting experiments on potential antioxidants in asphalts. In this experiment, a Boscan asphalt was oxidized as a thin film at 130°C with and without 2% of a potential antioxidant, triphenyltin hydroxide (TPTH). It is apparent that the TPTH had no effect on sulfoxide formation during the spurt; however, following the spurt, ketone and sulfoxide formation rate were both significantly reduced, indicating that the reaction mechanism during and after the spurt were not the same.

The Pragmatic Benefit of Sulfur in Asphalts. It has been reported (22) that asphalt sulfur content correlates with asphalt component compatibility as defined by relative viscosity measurements. In general, the less compatible asphalts are more sensitive to oxidative age hardening. Further, it has been shown in this paper that the ratio of sulfoxides to ketones formed on oxidation increases with increasing sulfur content, with sulfoxides being formed at the expense of ketone formation. This is illustrated in Figure 8 for PAV oxidation. The increasing sulfoxide to ketone ratios with increasing sulfur content is further intensified in atmospheric, diffusion controlled oxidation, particularly as the temperature is lowered. This phenomenon was explained in connection with Figure 5, but is characteristic of the SHRP core asphalts. It has also been pointed out that oxidizable asphalt sulfides are potent hydroperoxide scavengers, and thus interfere with the production of free radicals in the hydrocarbon chain reaction following the oxidation spurt. Finally, it has been shown that following the spurt, ketones have a much greater effect on viscosity increase than sulfoxides.

The pragmatic conclusion to all this is that sulfides in asphalts are effective antioxidants and reduce the effect of oxidation on age hardening. Since sulfides compete with ketone precursors, increased sulfide content in the asphalt means that more sulfoxides and less ketones are formed, a favorable situation for reduction in the rate of viscosity increase. This increased sulfoxide content and reduced ketone content tends to offset the increased sensitivity to age hardening of the less compatible asphalts, particularly at low aging temperatures. The effect of temperature on this phenomenon is illustrated in Figure 1 for the low sulfur (1.3%), highly compatible asphalt AAG-1 and the high sulfur (6.9%), rather incompatible asphalt AAD-1. The above arguments could explain why asphalts made from some high sulfur crudes harden and become brittle so rapidly in hot climates, but perform quite well in more moderate climates. With regard to age hardening, it is our belief that the maximum pavement temperature reached during hot days is more critical to eventual age hardening than are the average temperatures. Careful analysis of the data from the extensive California simulated field study of Kemp and Prodoehl (23) seem to confirm this conclusion.

SUMMARY AND CONCLUSIONS

The oxidative hardening of asphalts is a direct result of the formation of ketones and sulfoxides. The relative amount of amount of hardening that they produce depends upon the state of dispersion of the molecules on which they are formed. When formed on a molecule in a highly associated molecular agglomerate, they produce, through association with other associated agglomerates, a much larger molecular weight entity, thus significantly increasing effective molecular weight. When formed on weakly associated molecules, as in highly compatible asphalts or on molecules in the dispersing phase, their association has minimal effect on molecular weight, and thus viscosity increase. The hyperbolic-like plot of property change versus time observed for asphalt oxidation kinetics is the result of two sequential and different oxidation mechanisms. The rapid increase at the onset of the kinetic plot is attributed to reaction of highly reactive hydrocarbon precursors of limited concentration which react with oxygen to form hydroperoxides. The hydroperoxides then react primarily with asphalt sulfides to form sulfoxides with the virtual exclusion of ketone formation during the

initial stages of the spurt. Sulfoxides are the major contributor to viscosity increase during the initial stages of the spurt, at least below 45°C at atmospheric pressure. Towards the end of the spurt, a classical free radical hydrocarbon chain reaction begins to take over. When all of the highly reactive hydrocarbon precursors are exhausted, the spurt is over, after which ketones are formed at a nearly constant rate and are the major determinants of viscosity increase. As asphalt sulfur content increases, the sulfoxide contribution to viscosity increases. Following the spurt, sulfides compete for the hydroperoxide ketone precursors. Thus, less compatible, high sulfur asphalts produce more sulfoxides and less ketones than highly compatible, low sulfur asphalts. Because asphalt viscosity increase is more sensitive to ketone than sulfoxide formation, the production of more sulfoxides and less ketones in high sulfur asphalts tends to offset their increased sensitivity to age hardening, particularly at low temperatures. Sulfides in asphalt are effective antioxidants. The ratios of sulfoxides to ketones produced at high oxygen concentrations, as during PAV aging, were found independent of oxidation temperature, indicating that the mechanism of oxidation does not change with temperature. The ratio of sulfoxides to ketones, however, increased as sulfur content increased. At lower temperatures, physicochemical effects inhibit ketone formation and thus viscosity increase. During atmospheric pressure oxidation (low oxygen concentrations), the ratio of sulfoxides to ketones is not independent of temperature, but increases as oxidation temperature is lowered. The effect is intensified as the asphalt sulfur content increases and could have pragmatic implications when PAV aging is used to predict pavement aging under atmospheric, diffusion controlled condition.

ACKNOWLEDGMENTS

The authors express thanks and appreciation to the Federal Highway Administration (FHWA) for financial support of this work under FHWA Contract No. DTFH61-92-C-00170. Acknowledgement and thanks are also extended to Western Research and the Strategic Highway Research Program (SHRP) for much past data used in this paper. Janet Wolf is much appreciated for her major contributions to the laboratory work. Dr. Jan Branthaver provided many helpful discussions.

DISCLAIMER

This document is disseminated under the sponsorship of the Department of Transportation in the interest of information exchange. The United States Government assumes no liability for its contents or use thereof.

The contents of this report reflect the views of Western Research Institute which is responsible for the facts and the accuracy of the data presented herein. The contents do not necessarily reflect the official views of the policy of the Department of Transportation.

REFERENCES

1. Dorrence, S.M., F.A. Barbour and J.C. Petersen. Direct Evidence of Ketones in Oxidized Asphalts, Anal. Chem., **46**, 2242-2244 (1974).
2. Petersen, J.C., S.M. Dorrence, M. Nazir, H. Plancher and F.A. Barbour. Oxidation of Sulfur Compounds in Petroleum Residues: Reactivity-Structural Relationships, Preprints, Div. Petrol. Chem., ACS, **26(4)**, 898-906 (1981).
3. Petersen, J.C., F.A. Barbour and S.M. Dorrence. Identification of Dicarboxylic Anhydrides in Oxidized Asphalts, Anal. Chem., **47**, 107-111 (1975).
4. Petersen, J.C. and H. Plancher. Quantitative Determination of Carboxylic Acids and Their Salts and Anhydrides in Asphalts by Selective Chemical Reactions and Differential Infrared Spectroscopy, Anal. Chem., **53**, 786-789 (1981).
5. Petersen, J.C. Quantitative Functional Group Analysis of Asphalts Using Differential Infrared Spectrometry and Selective Chemical Reactions --- Theory and Practice, Transportation Research Record No. 1091, 1-11 (1986).
6. Petersen, J.C. Chemical Composition of Asphalt as Related to Asphalt Durability: State of the Art, Transportation Research Record No. 999, 13-30 (1984).

7. Petersen, J.C. Asphalt Oxidation --- An overview Including a New Model for Oxidation Proposing That Physicochemical Factors Dominate in Oxidation Kinetics, Fuel Science and Technol., Int'l., 11(1), 57-87 (1993).
8. Petersen, J.C., J.F. Branthaver, R.E. Robertson, P. M. Harnsberger, J.J. Duvall and E.K. Ensley. Effects of Physicochemical Factors on Asphalt Oxidation Kinetics, Transportation Research Record No. 1391, 1-10 (1993).
9. Lau, C.K., K.M. Lundsford, C.J. Glover, R.R. Davidson and J.A. Bullin. Reaction Rates and Hardening Susceptibilities as Determined from Pressure Oxygen Vessel Aging of Asphalts, Transportation Research Record No. 1342, 50-57 (1992).
10. Liu, M., K.M. Lundsford, R.R. Davidson, C.J. Glover and J.A. Bullin. The Kinetics of Carbonyl Formation in Asphalts, AIChE Journal, 42(4), 1069-1076 (1996).
11. Martin, K.L., R.R. Davidson, C.J. Glover and J.A. Bullin. Asphalt Aging in Texas Roads and Test Sections, Transportation Research Record No. 1269, 9-19 (1990).
12. Plancher, H., E.L. Green and J.C. Petersen. Reduction of Oxidative Hardening of Asphalts by Treatment with Hydrated Lime --- A Mechanistic Study, Proc., Assn. Asphalt Paving Technol., 45, 1-24 (1976).
13. Lee, D.Y. and R.J. Huang. Weathering of Asphalts as Characterized by Infrared Multiple Reflectance Spectra, Applied Spectroscopy, 27, 435 (1973).
14. Lin, M.S., K.M. Lundsford, C.J. Glover, R.R. Davidson and J.A. Bullin. The Effects of Asphaltenes on the Chemical and Physical Properties of Asphalts, Asphaltenes, Fundamentals and Applications, E.Y. Sheu and O.C. Mullins, ed., Plenum Press, N.Y. (1995) pp. 155-176.
15. Lee, D.Y., Development of a Durability Test for Asphalts, Highway Research Record No. 231, 34-49 (1968).
16. Branthaver, J.F., J.C. Petersen, R.E. Robertson, J.J. Duvall, S.S. Kim, P.M. Harnsberger, T. Mill, F.A. Barbour and J.F. Shabron. Binder Characterization and Evaluation, Volume 2: Chemistry, Strategic Highway Research Program, Final Report No. SHRP-A-368 (1993) p. 204.
17. Jaeger, D.A., J.R. Wyatt and R.E. Robertson. Monochlorination of n-Alkyl Phenyl Ethers in Micellar Sodium Dodecyl Sulfate, J. Org. Chem., 50(9), 1467-1470 (1985).
18. Netzel, D.A., Western Research Institute, Laramie, Wyoming, private communication.
19. Huh, J.D. and R.E. Robertson. Modeling of Oxidative Aging Behavior of Asphalts from Short Term, High Temperature Data as a Step Toward Prediction of Pavement Aging, Paper No. 961112, Presented at the Annual Transportation Research Board Meeting, January, 1996, Washington, D.C., Transportation Research Record (in press).
20. van Gooswillen, G., H. Berger and F. Th. de Bats. Oxidation of Bitumens in Various Tests, Proceedings, European Bitumen Conference, 1985, pp. 95-101.
21. Mill, T. Oxidation Pathways in Asphalts, Presentation at the Thirty-Second Annual Petersen Asphalt Research Conference, Laramie, Wyoming, July 10-12, 1995.
22. Branthaver, J.F., J.C. Petersen, J.J. Duvall and P.M. Harnsberger. Compatibilities of Strategic Highway Research Program Asphalts, Highway Research Record No. 1323, 22-31 (1991).
23. Kemp, G.R. and Prodoehl. A Comparison of Field and Laboratory Environments on Asphalt Durability, Proc., Assn. Asphalt Paving Technol., 50, 492-537 (1981).

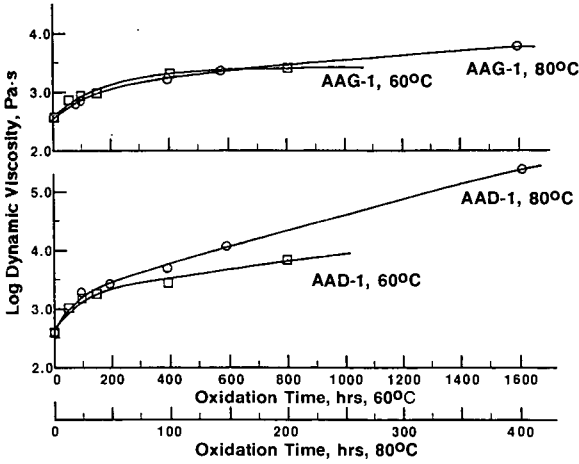


Figure 1. Effects of Temperature and Compatibility on Aging Characteristics

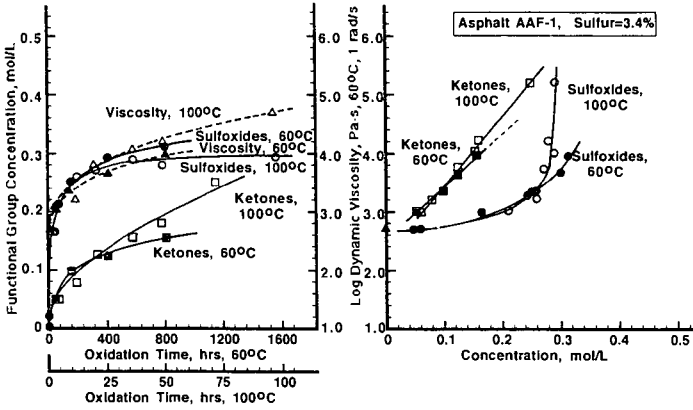


Figure 2. Kinetics and Viscosity-Functional Group Relationships, PAV Oxidation of Asphalt AAF-1

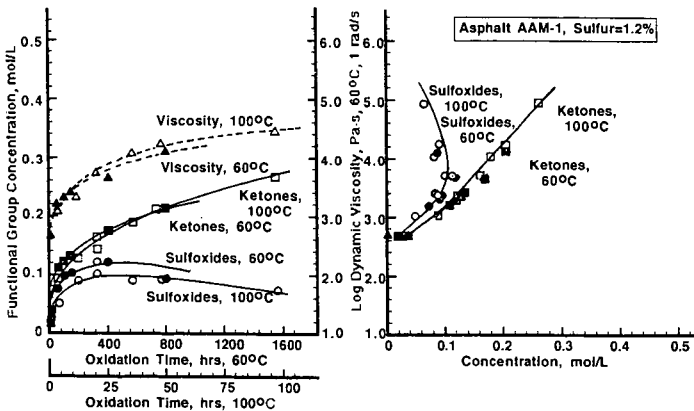


Figure 3. Kinetics and Viscosity-Functional Group Relationships, PAV Oxidation of Asphalt AAM-1

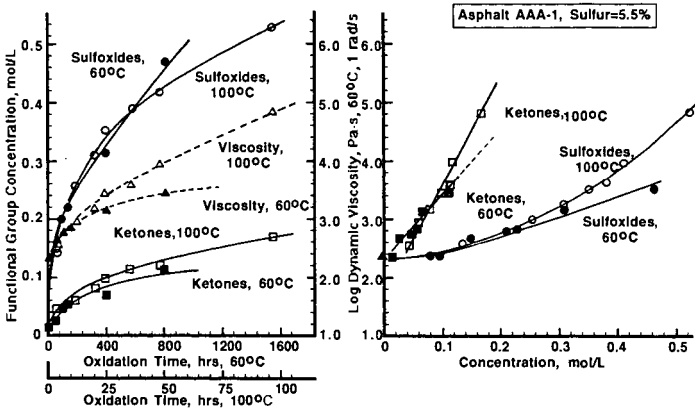


Figure 4. Kinetics and Viscosity-Functional Group Relationships, PAV Oxidation of Asphalt AAA-1

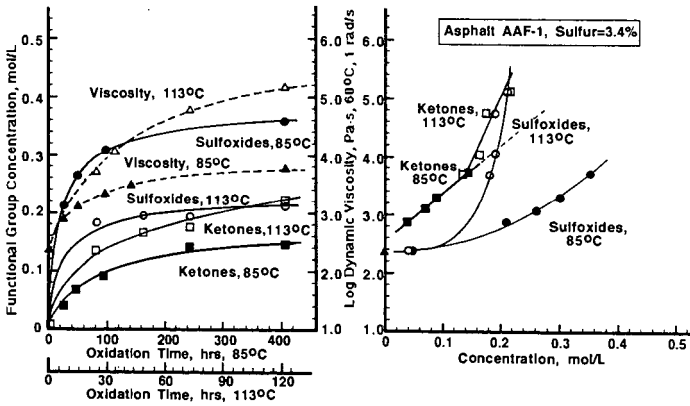


Figure 5. Kinetics and Viscosity-Functional Group Relationships, TFAAT Oxidation of Asphalt AAF-1

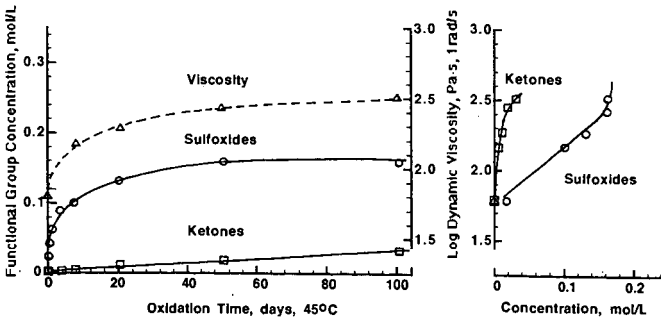


Figure 6. Kinetic Data and Viscosity-Functional Group Relationships for Shell Wood River Asphalt Oxidized at Atmospheric Pressure as a Thin Film on Ottawa Sand at 45°C

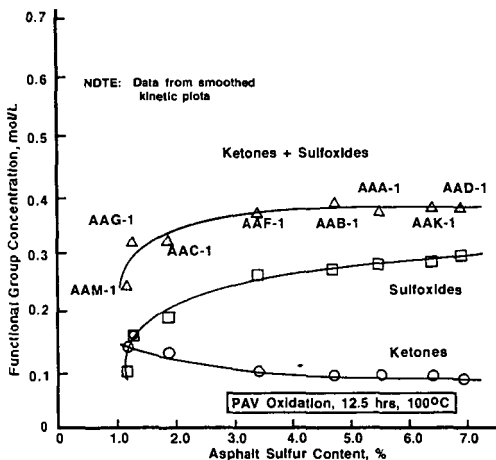


Figure 7. Ketone and Sulfoxide Concentrations at End of Oxidation Spurt

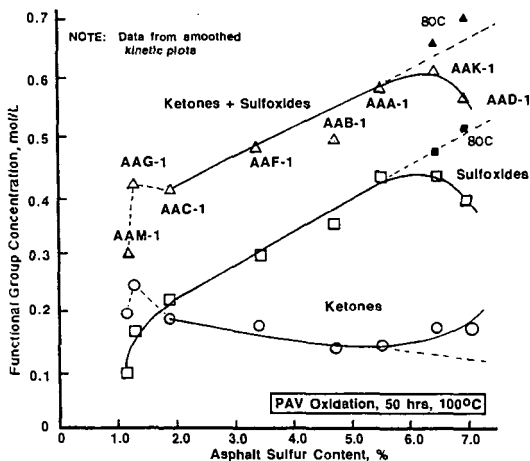


Figure 8. Ketone and Sulfoxide Concentrations at a Moderate Oxidation Level

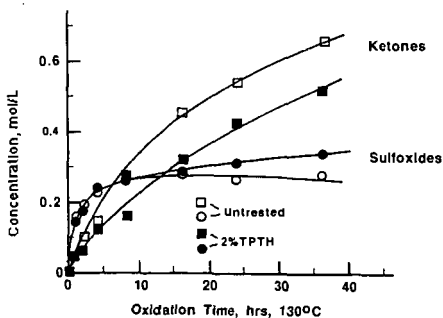


Figure 9. Effect of the Potential Antioxidant Triphenyltin Hydroxide on Oxidation Kinetics of a Boscan Asphalt

THE ROLE OF HYDROAROMATICS IN OXIDATIVE AGING IN ASPHALT

Theodore Mill
Chemistry and Chemical Engineering Laboratory
Stanford Research Institute
Menlo Park, CA 94025

Keywords: Hydroaromatics, Oxidation, Thermochemical kinetics

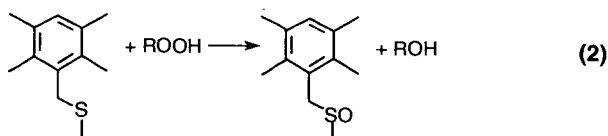
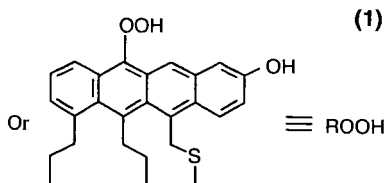
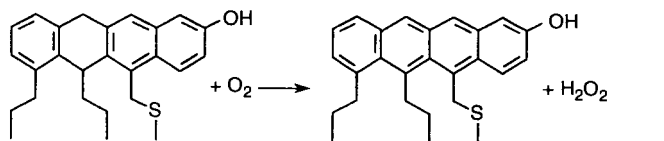
INTRODUCTION

The pavement engineering community recognized fifty years ago that age hardening and embrittlement of asphalt during service is a primary cause of road failure [Welborn, 1984] and that oxidation of asphalt is the major cause of age hardening [Nicholson, 1937; Traxler, 1961]. Oxidative aging is characterized by oxygen uptake, the formation of sulfoxide and carbonyl groups (as shown by IR spectra), and marked increases in dynamic viscosity and other rheological properties. [Petersen, 1975, 1981 and 1986]. Different asphalts show markedly different rheological changes for similar amounts of oxidation, although elemental analyses indicate a similarity in CHO ratios as well as in molecular weights, with variability only in the heteroatoms, functional groups, and trace metal compositions [Branthaver et al., 1993].

In a SHRP-supported research program, we developed a new hypothesis to account for the oxidation of asphalt, in which hydroaromatic groups in asphalt react with oxygen to form peroxides which are the proximate cause of chemical and physical changes induced by oxidative aging. The purpose of this paper is to examine how oxidation of hydroaromatic groups might proceed and whether hydroaromatics in asphalt fulfill the requirements in asphalt oxidation.

OXIDATION PATHWAYS AND AN OXIDATION MODEL

Triplet oxygen reacts with most organic compounds through free radical pathways, initiated with peroxides and metals [Mill and Hendry, 1980; Mill et al., 1995]. The unusual reactivity oxygen exhibits toward asphalt at temperatures below 100°C must be associated with some highly reactive structural features, such as polycyclic hydroaromatics. Reactions (1) and (2) illustrate the proposed reaction sequence during oxidation of asphalt.



(2)

A model for dihydroaromatic reaction with oxygen is found in the smooth reaction of dihydroanthracene ((DHA) with air or oxygen at 100°C in benzene to form hydrogen peroxide and anthracene [Mill et al., 1992]. Figure 1 shows the loss of DHA and the formation of anthracene at 100°C. Added dibutyl sulfide ((DBS), unoxidized by itself at 100°C with air, oxidizes rapidly in the presence of DHA and air at 100°C at rates that correspond to oxidation of DHA to form the peroxide. This induced oxidation is very similar to the induced oxidation of DBS by asphalt heated in air. Although asphalt contains no DHA, we believe that DHA-like hydroaromatics may be present in amounts sufficient to account for the greater part of the direct reaction with oxygen.

KINETICS OF HYDROAROMATIC-OXYGEN REACTIONS

Thermochemical kinetic estimates of the rates of reaction of oxygen and hydroaromatics start with the simple H-atom transfer from the hydroaromatic to oxygen to form the radical pair shown in Reaction (3).

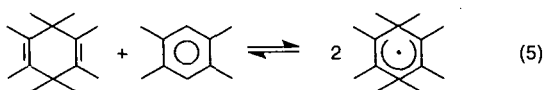


Using heats of formation of these four species, Reaction (1) has a heat of reaction ranging from 130 kJ/mole for DHA and dihydronaphthalene-like hydroaromatics to 159 kJ/mole for tetralin and tetraphenylethane-like hydroaromatics [Benson, 1968; McMillen et al., 1987]. These values correspond to the activation energies of the forward reactions, which, when combined with reasonable estimates for entropy changes, have kinetic parameters corresponding to

$$k_3 = 10^{8.5} \exp(-130,000/RT) \text{ to } 10^{8.5} \exp(-159,000/RT) \quad (4)$$

For DHA and tetralin, $k_3 = 2 \times 10^{-10} \text{ M}^{-1} \text{ s}^{-1}$ and $1.7 \times 10^{-14} \text{ M}^{-1} \text{ s}^{-1}$, respectively at 100°C. The rate constant for DHA corresponds to a half life for DHA in the presence of 25 atm of oxygen (~1 M) of about 100 years, and for tetralin, a million years! Clearly, this simple scheme fails by a wide margin to predict the experimental half life of 30-40 hours found for DHA in benzene at 100°C with 1 atm of air (see Figure 1).

An alternative model for oxidation of DHA and hydroaromatic analogs involves prior formation of the hydroaromatic (DHA) radical from the molecule assisted homolysis of the hydroaromatic (DHA) by the corresponding aromatic (anthracene) [Bilmers et al., 1986]. The resultant radicals then react with oxygen.



NM-320525-12

For DHA, Bilmers et al [1986] estimate this process to have an activation energy and log A-factor close to 151 kJ/mol and 8.5, respectively, giving a rate constant at 100°C similar to the value for the tetralin-oxygen reaction and much too slow to be important, even if equimolar amounts of anthracene and DHA were initially present.

Concerted transfer of two hydroaromatic H-atoms to oxygen (Reaction (1)) is exothermic by 63 and 84 kJ/mol with DHA and dihydrophenanthrene,

respectively, and might account for the observed oxidation of DHA, although we do not know what the intrinsic activation energy is for the process. The fast radical-chain oxidation of DHA examined by Bickel and Kooyman [1956] and by Mahoney [1966] to give the corresponding hydroperoxide is difficult to reconcile with the non-initiated oxidation we observed for DHA in benzene. Moreover, radical chain oxidation of hydroaromatics in asphalt is unlikely owing to the presence of effective radical scavenging phenols [Branthaver et al., 1993]; the oxidation would proceed, but much more slowly with a chain length of one. We should point out that a related oxidation of anthrahydroquinone to anthraquinone is the basis for commercial production of hydrogen peroxide from oxygen [Kirchner, 1981]. Asphalts, however, have low concentrations of isolated phenols and probably much lower concentrations of hydroquinones [Branthaver et al., 1993], but we cannot rule out some contribution from this reaction.

HYDROAROMATIC CONTENT OF ASPHALTS

An additional test of the validity of the hydroaromatic model for oxidation of asphalts is the extent to which oxygen uptake is related to the known hydroaromatic content of asphalts. Oxygen uptake data for several SHRP standard asphalts including AAD-1 show that up to one mole of oxygen/kg is taken up over about 100 hrs at 100°C [Branthaver et al., 1993], a significant amount of oxygen, but a small fraction of the aromatic or aliphatic units in typical asphalts with molecular weights ranging from 700 to 1300 Daltons.

Although large numbers of studies of the hydroaromatic content of coals have been published in connection with liquefaction of coal and the role of H-atom donors in the process (Bilmers et al., 1986), few estimates of the hydroaromatic content of asphalts appear to be available. In one recent study, Farcasiu and Rubin [1987] determined the formation of polycyclic aromatic compounds on dehydrogenation of vacuum residues, using uv spectra and mass spectrometry. They found that some fractions of the resid were easily dehydrogenated to give polycyclic aromatic compounds; in one case an average of 13 saturated ring carbons were readily converted to aromatic carbons, indicating that a fairly abundant supply of reactive hydroaromatics are available in some asphalts for the proposed oxidation scheme.

REFERENCES

- Bateman, L. and K. R. Hargrave, 1954a, Oxidation of Organic Sulfides I, J. Chem. Soc. 389-398.
- Bateman, L., and K. R. Hargrave, 1954b, Oxidation of Organic Sulfides II., J. Chem. Soc., 399-411.
- Benson, S. W., 1968, Thermochemical Kinetics, John Wiley and Sons, New York.
- Bickel, A. F. and E. C. Kooyman, 1956, Inhibition of the Oxidation of Dihydroanthracene by Alkyl Phenols, J. Chem. Soc. 2215-2226.
- Bilmers, R., Griffith, L. L. and Stein, S. E., 1986, Hydrogen Transfer between Anthracene Structures, J. Phys. Chem., 90: 517-523.
- Branthaver, J. F., J. C. Petersen, R. E. Robertson, J. J. Duvall, S. S. Kim, P. M. Harnsberger, T. Mill, E. K. Ensley, F. A. Barbour, and J. F. Schabron, 1993, Binder Characterization and Evaluation, SHRP Report SHRP-A-368, Vol. 2, Chemistry.

- Farcasiu, M. and Rubin, B. R., 1987, Aliphatic Structures in Petroleum Resids, Energy Fuels 5: 381-386.
- Kirchner, J. R., 1981, Hydrogen Peroxide in Kirk-Othmer Encyclopedia of Chemical Technology, M. Grayson, Ed., John Wiley and Sons, New York, Vol. 13, pp. 12-38.
- Mahoney, L. R., 1965, Reactions of Peroxy Radicals with Polynuclear Aromatic Compounds II, Anthracene in Chlorobenzene, J. Amer. Chem. Soc. 87: 1089-1095.
- Mahoney, L. R., 1966, Inhibition of Free Radical Reactions. II. Kinetic Study of the Reaction of Peroxy Radicals with Hydroquinones and Hindered Phenols, J. Amer. Chem. Soc. 88: 3035-3041.
- McMillen, D. F., Malhotra, R., Chang, S.-J., Nigenda, S. E., Fleming, R. H., 1987, Mechanisms of hydrogen transfer and bond scission of strongly bonded coal structures in donor-solvent systems, Fuel, 66: 166611-1620.
- Mill, T. and Hendry, D. G., 1980, Kinetics and Mechanism of Free Radical Oxidation of Alkanes and Olefins in the Liquid Phase, in Comprehensive Chemical Kinetics, Vol. 16., C. H. Bamford and C.F.H. Tipper, Ed., Elsevier, Amsterdam, pp. 1-83.
- Mill, T., D. S. Tse, B. Loo, C. C. D. Yao, and E. Canavesi, 1992, Oxidation Pathways in Asphalt, 204th Meeting of the ACS, Washington DC, ACS Div. Fuel Chem. Preprints 37: 1367-1375
- Mill, T., Jayaweera, I., and Ross, D. S., 1995, Hydrothermal Oxidation of Phenol, in Physical Chemistry of Aqueous Solutions, H. J. White, J. V. Sengers, and J. C. Bellows, Eds., Begell House, New York, pp. 589-592.
- Nicholson, V., 1937, A Laboratory Oxidation Test for Bitumens, Proc. A.A.P.T. 9: 208-213.
- Petersen, J. C., 1975, Quantitative Methods Using Differential IR for Determining Compound Types Absorbing in the Carbonyl Region in Asphalts, Anal. Chem. 47:112.
- Petersen, J. C., 1986, Quantitative Differential Group Analysis of Asphalts Using Differential Infrared Spectrometry and Selective Chemical Reactions-Theor. and Applications, Preprint, 65th Ann. Tran. Res. Board Meeting, Washington, D.C., Jan. 13-17.
- Petersen, J. C., S. M. Dorrence, M. Nazir, H. Plancher, and F. A. Barbour, 1981, Oxidation of Sulfur Compounds in Petroleum Residues: Reactivity-Structural Relationships, Div. Petrol. Chem., 181st Meeting of the ACS, New York, NY.
- Traxler, R. N., 1961, Relation Between Asphalt Composition and Hardening by Volatilization and Oxidation. Proc. Assoc. Asphalt Paving Technologists 30: 359-373.
- Walling, C., 1963, Free Radicals in Solution. John Wiley and Sons, New York.
- Welborn, J. Y., 1984, Physical Properties as Related to Asphalt Durability: State of the Art. Trans. Res. Record 999: 31-37.

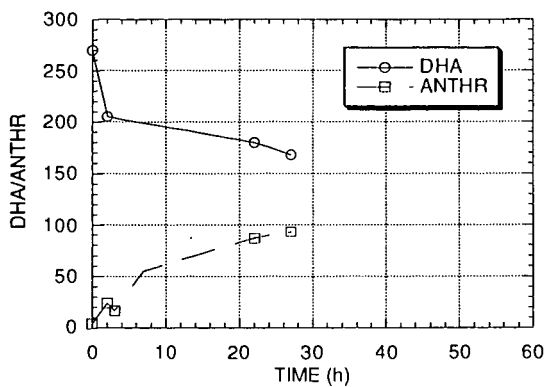


Figure 1. Conversion of 250 μ M DHA to A in benzene in air at 100°C

**POLYPROPYLENE - ASPHALT MIXTURES
FOR WATERPROOFING MEMBRANES**

Paolo Italia, Ernesto Brandolese
Production process and modified asphalt project leaders
EURON S.p.A. (Research Company of AGIPPETROLI - ENI Group)
Via F. Maritano 26 - 20097 S. Donato Milanese (MI)
Italy

Keywords: polypropylene-asphalt mixtures, waterproofing membranes, Colloidal Instability Index

Abstract

In any field of polymer-asphalt mixtures application is extremely important to achieve a very good compatibility between the components in order to improve as much as possible the performances due to the polymer content.

In the case of waterproofing membranes application this compatibility reduce, moreover, the amount of polymer required to obtain the best performances.

Using the Colloidal Instability Index I_c , as measured by the Iatroskan device, we propose a correlation between asphalt's chemical characteristics and the polymer minimum amount sufficient to disperse in a stable way the asphalt itself in the polymeric matrix.

As a result, through the proposed correlation, with a simple asphalt composition analysis it is possible to predict its performance when mixed with polypropylene.

In the paper, beside the description of the Iatroskan analytical technique, we also present a method for determining phase inversion based on optical fluorescence microscopy performed on about 30 different samples of asphalt.

We also present the experimental correlation laws between the polymer amount at phase inversion and the asphalt single components content.

1 - Introduction

As a waterproofing material, the asphalt can be used in the industrial field in many different ways: it can be found in finished products such as waterproofing membranes, paints, pastes, mastics and oxidated asphalts.

In Europe, the waterproofing membranes are the most important market; according to the modern manufacture processes these membranes consist of a rigid support (for instance, polyester) impregnated with a mixture of asphalt, polymer and mineral filler.

Each company has its products and its processes and tries to minimize the polymer content (the most expensive material), maintaining at the same time some essential requirements as cold flexibility, thermal stability, and resistance to degradation caused by the atmospheric agents.

It is therefore very important the research for asphalts with good characteristics of compatibility with the polymers in use (mostly atactic polypropylene, a refuse of the isotactic polypropylene, or similar products); compatibility is the capability of the asphalt to combine homogeneously with the polymer, in order to achieve a morphologic structure in which the polymer prevails.

As a matter of fact, even if the mixture consists mostly of asphalt, the so-called reverse phase of the mixture can be achieved with the right quantity of polymer: in fact, the polymer incorporates the particles of asphalt. Only when the polymer prevails the characteristics of elasticity and resistance reach their maximum.

2 - Preparation and valuation of the asphalt/polymer mixtures

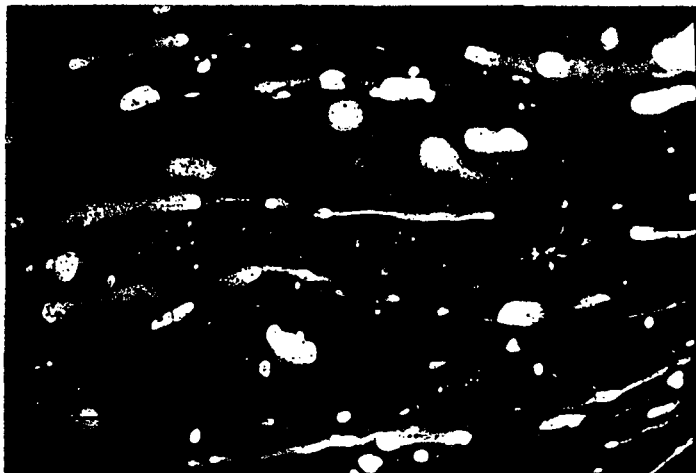
In the polymer-asphalt tests carried out in the Asphalt Laboratory of EURON, research company of AGIPPETROLI for energy sector, was used a propylene-base product, having the following characteristics:

melt viscosity at 190°C	mPas	100.000
softening point R. and B.	°C	>150
needle penetration	dmm	20
density at 23°C	g/cm ³	0.9
viscosity number "J"	cm ³ /g	100
molecular weight	Mv	85.000
intrinsic viscosity	g/100ml	1,0
glass transition temperature	°C	<-30

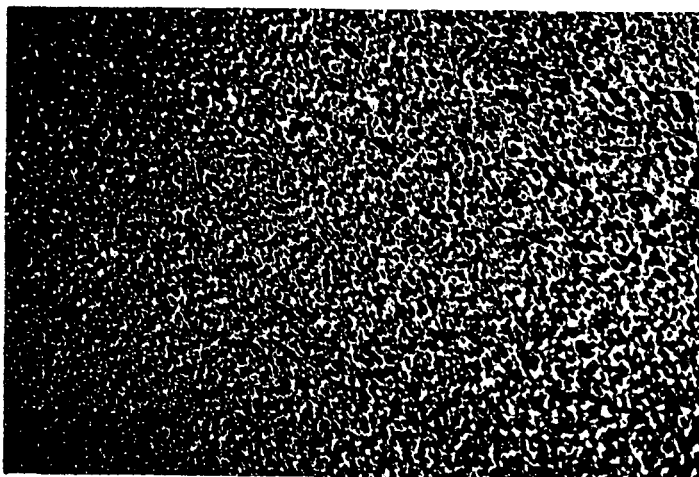
The additivition was carried out according to the following procedure, starting with 200g of mixture at 10% of polymer and adding 2g of polymer each time:

- preheat the asphalt in a nitrogen flow at a maximum temperature of 120°C, in order to transfer 180g in a 250g can. Heat in a thermostated bath at 185°C with air and mix for 15 minutes with a slanted-pallet stirrer, at a speed of 600 rpm;
- add 20g of polymer (10% in the mixture) in small doses, stirring it for 60 minutes, at a constant temperature of 185°C;
- take two drops of the mixture with a glass rod and place them on a slide; these drops must be at once cooled in distilled water, and then dried with a compressed air flow;
- observe then with a fluorescence microscope: observe at least three areas in order to remark possible cases of dishomogeneity (take a small part of the second drop in order to verify the reverse phase even in the sample). Two characteristics must be found in order to ascertain the reverse phase: the continuous polymer phase (white field) with small black drops representing the discontinuous asphalt phase, and the homogeneous scattering of the small drops (see the following pictures);
- if there is no reverse phase, add 2g more of polymer (about 1% more than the previous mixture), and, after stirring for 30 minutes at the constant temperature of 185°C, observe with the fluorescence microscope according to the previous procedure. The test continues according to the procedure until the reverse phase is determined.

In the following pictures it's possible observe no reverse phase (13% of polymer) and reverse phase (16% of polymer) for sample number 9.



Sample number 9, 13% of polymer: no reverse phase



Sample number 9, 16% of polymer: reverse phase

3 - Asphalts characteristics

For each asphalt used in the previous mixtures (27 samples), was determined the usual characteristics and the Colloidal Instability Index with the thin layer chromatographer Iatroscan. The index is the ratio between asphaltenes + saturated and resins + aromatic compounds.

The Iatroscan analysis (mod. MK-5) is a thin layer chromatography (TLC) connected to a patented Flame Ionization Detector, similar to the FID used in gaschromatography. The main difference between the usual TLC and the Iatroscan analysis is that the plate is substituted by a frame consisting of ten small quartz bars, covered by a thin layer of silicon dioxide or sintered alumina, applied with a special technique.

At the end of each bar place with a microsyringe a microliter of the solution at 1% of asphalt in dichloromethane; after completing the frame, put it under elution with solvents in a series of three spot resolution chambers for TLC. After each resolution, eliminate the eluent through stove evaporation. Using the stationary phase of the silicon dioxide and the action of the mobile phase, it is possible to separate the substances according to the degree of polarity and similarity to the solvent. For the asphalts, start with the normal-hexane in order to separate the saturated compounds, then use a mixture toluene/normal-hexane for the aromatic compounds, and finish with a mixture of dichloromethane/methanol for the resins which have strong polar characteristics. All that remains on the glass rod is asphaltene.

At the end of the resolution phases, the frame must be placed in an appropriate part of the instrument; here the small bars keep on passing between the two poles of the detector for all its length at constant speed; the process is fully automatic. The organic substances which have been separated on the thin layer are therefore ionized by the flame and their quantity can be measured. The instrument software makes also possible the data elaboration and the calculation of the per cent composition of the mixture using the method of the normalization of the peak area.

In the following tables the characteristics of the asphalts used in this experimentation are reported together with the chemical composition, the Colloidal Instability Index and the polymer amount necessary to achieve the reverse phase according to the previously described procedure.

sample number		1	2	3	4	5	6	7	8	9
penetration	dmm	257	254	190	194	182	193	185	217	190
softening point R. B.	°C	40.5	41	42.5	39	42	38.5	38.5	39	43
asphaltenes	%wt.	27.4	25.4	20.7	24.1	28.4	23.7	24.5	25.4	25.0
saturated	%wt.	8.8	8.9	3.6	2.4	4.2	6.6	3.4	4.2	5.3
resins	%wt.	25.8	27.8	18.7	24.5	21.9	28.3	33.1	30.8	34.3
aromatics	%wt.	38.0	37.9	57.0	49.0	45.5	41.4	39.0	39.6	35.4
index Ic	-	0.57	0.52	0.32	0.36	0.48	0.43	0.39	0.42	0.43
polymer	%wt.	11	13	20	18	14	16	17	16	16

sample number		10	11	12	13	14	15	16	17	18
penetration	dmm	175	172	167	190	165	206	174	155	134
softening point R. B.	°C	40.5	42	45	39	43	39	42	45	43
asphaltenes	%wt.	21.1	25.2	25.5	24.7	23.8	14.8	25.0	28.3	21.6
saturated	%wt.	4.1	4.4	2.2	3.6	4.8	4.0	4.7	5.3	3.8
resins	%wt.	37.2	40.1	23.6	33.5	22.2	23.3	18.8	24.1	22.8
aromatics	%wt.	37.6	30.3	48.7	38.2	49.2	57.9	51.5	42.3	51.8
index Ic	-	0.34	0.42	0.38	0.39	0.40	0.23	0.42	0.51	0.34
polymer	%wt.	18	16	18	16	16	24	16	14	22

sample number		19	20	21	22	23	24	25	26	27
penetration	dmm	165	245	168	190	205	155	163	199	190
softening point R. B.	°C	45.5	36	40.5	39	37.5	45	42.5	41	42
asphaltenes	%wt.	28.0	23.2	19.8	19.0	24.9	19.4	21.7	31.9	17.8
saturated	%wt.	7.3	4.7	3.6	7.1	3.7	5.3	4.7	6.3	2.7
resins	%wt.	26.2	19.9	23.2	18.6	21.1	24.5	24.2	22.3	16.8
aromatics	%wt.	38.5	52.2	53.4	55.3	50.3	50.8	49.4	39.5	62.7
index Ic	-	0.55	0.39	0.31	0.35	0.40	0.33	0.36	0.62	0.26
polymer	%wt.	13	17	21	18	16	19	18	10	22

4 - Conclusions

Averaging the previously reported data, for each polymer amount at the reverse phase used in the present work, an optimum distribution of the four main asphalt's components has been calculated and related to the Colloidal Instability Index Ic.

content of polymer		10%	11%	13%	14%	16%	17%
asphaltenes	%wt.	31.9	27.4	26.7	28.3	24.6	23.2
saturated	%wt.	6.3	8.8	8.1	4.8	4.8	4.7
resins	%wt.	22.3	25.8	27.0	23.0	28.0	19.9
aromatics	%wt.	39.5	38.0	38.2	43.9	42.6	52.2
index Ic	-	0.62	0.57	0.53	0.49	0.42	0.39

content of polymer		18%	19%	20%	21%	22%	24%
asphaltenes	%wt.	22.9	19.4	20.7	19.8	19.7	14.8
saturated	%wt.	3.2	5.3	3.6	3.6	3.2	3.9
resins	%wt.	23.9	24.5	18.8	23.2	19.8	23.4
aromatics	%wt.	50.0	50.8	56.9	53.4	57.3	57.9
index Ic	-	0.35	0.33	0.32	0.31	0.30	0.23

From figures of the previous table, it could be concluded that:

- 1) A poor compatibility is mainly related to an high aromatic and low saturated and asphaltenes content.

In fact, in the interval of polymer content at the phase inversion from 10 to 24%, we observe a 50% of aromatic increment and a 50% of saturated compounds and asphaltenes decrement, while resins change only about 10%.

- 2) Only asphalts having an Ic > 0.5 (more then 1/3 of asphaltenes + saturated compounds and less then 2/3 of resins + aromatic compounds) give high polimer compatibility, with reverse phase from 10 to 13% of polymer.

In the next figures it is possible to obtain the trend of the polymer content at the reverse phase as a function of colloidal instability index Ic and as a function of asphaltenes, saturated components, resins and aromatics.

According to the values reported in the Figure 1, it is possible to define the following law of correlation between the polymer amount at the reverse phase and the colloidal instability index:

$$\% \text{ polymer} = 33.9 - 41.7 \times \text{Ic}$$

Using this correlation is further possible to calculate the polymer amount at reverse phase for each asphalt type avoiding to prepare and evaluate various experimental mixture.

Figure 1

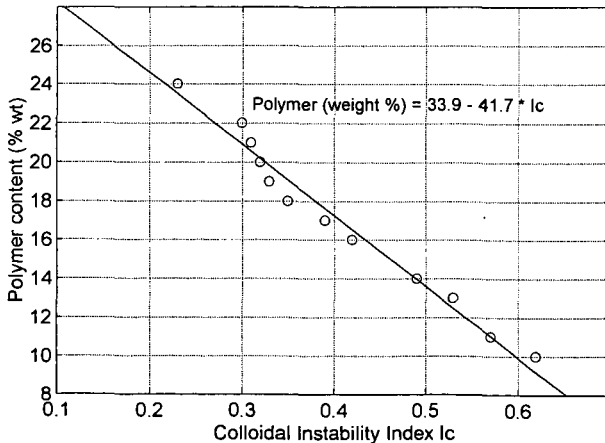


Figure 2

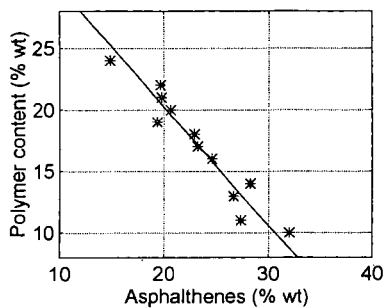


Figure 3

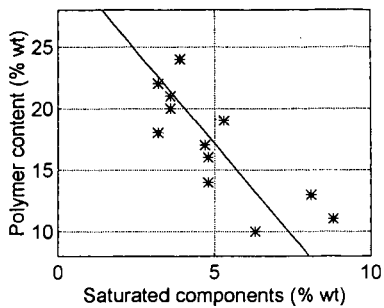


Figure 4

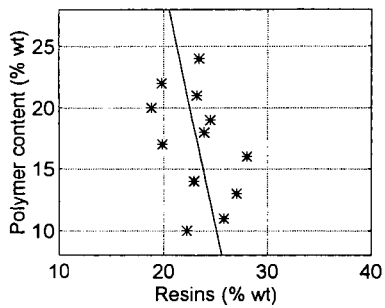
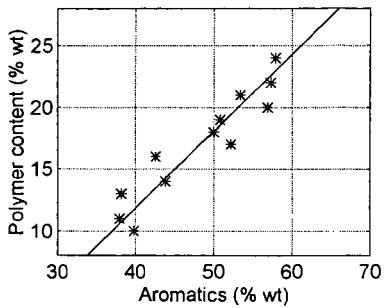


Figure 5



SLOW MECHANICAL RELAXATION IN ASPHALT

J. Stastna and L. Zanzotto

Department of Civil Engineering, The University of Calgary
Calgary, Alberta, Canada T2N 1N4

Key words: asphalt, stretched exponential, dynamic functions

INTRODUCTION

Asphalt (or bitumen) is one of the earliest construction materials used by mankind. However, despite the long history of its use and the important role it plays at the present time, in the construction of pavements, the composition and especially the structure of asphalt is still not fully understood. It is generally believed that asphalt is a multiphase system in which the large and polar molecules called asphaltenes, or their agglomerates are dispersed in the medium consisting of the smaller molecules with low or no polarity. Opinions on how the asphalt structure is arranged vary (1, 2, 3). The study of asphalt structure is made extremely difficult by the nature of this material. Non-invasive methods such as dynamic mechanical or electric testing, which investigate the asphalt in its original state may greatly contribute to our knowledge of the asphalt internal structure.

STRETCHED EXPONENTIAL RELAXATION

Around 1835, in Gottingen, Wilhelm Weber made the first systematic investigation of elastic "after-effect" in silk and glass threads (4). He noted that a weight suspended from such fibres generates an instantaneous elongation followed by an additional time dependent strain which recovered when the load was removed. For the dependence of displacement x on time t , Weber used a power law. The problem of after effect (creep in modern terminology) has been further studied by Rudolf Kohlrausch. He noticed the analogy with time dependent electric displacements, q , in charged capacitors and proposed for this effect the stretched exponential law: $q(t) = q_0 + \exp(-t/\lambda)^\beta$. In 1863 Frederick Kohlrausch (5) (the son of Rudolf) used the stretched exponential as an empirical fit for creep and relaxation data in silk and glass fibres and in rubber. The stretched exponential law has been revived after more than one hundred years in the study of dielectric relaxation. Usually the analysis of dielectric relaxation in polymers is focused on the complex dielectric "constant" $\epsilon^*(\omega)$ and its deviation from the form derived from a single relaxation time (6). A change of interest from frequency to time, i.e. from ϵ^* to the relaxation function $\phi(t)$ has been generated by the work of G. Williams and D. Watts (7). They found that the stretched exponential can fit data for many glassy and polymeric materials. In the past decade this form has been used to fit a wide variety of experimental data, dielectric, enthalpic, dynamic light scattering, magnetic relaxation, reaction kinetics, etc. (8). The possibility to use the stretched exponential in regular and polymer modified asphalts is discussed in the next paragraph.

STRETCHED EXPONENTIAL AND DYNAMIC MATERIAL FUNCTIONS

As usually we assume that for small deformations, the general linear viscoelastic constitutive equation is valid, i.e.

$$\underline{\tau}(t) = \int_{-\infty}^t -M(t-t') \underline{\dot{\gamma}}(t, t') dt' = \int_{-\infty}^t G(t-t') \underline{\dot{\gamma}}(t, t') dt' \quad 1)$$

Here, $M(t-t') = M(s) = -dG(s)/ds$; M represents the fluid memory, and G is the relaxation modulus (relaxation function). Extra stress tensor $\underline{\tau}$ is related to the strain tensor $\underline{\gamma}$, or to the rate of strain tensor $\underline{\dot{\gamma}}$ via 1). In the case of small amplitude oscillatory shear motion the complex modulus $G^*(\omega)$ is given as (9)

$$G^*(\omega) = i\omega \int_0^{\infty} G(s) \exp(-i\omega s) ds \quad 2)$$

Assume that the relaxation function, $G(s)$ has the form of stretch exponential,

$$G(s) = C \exp(-(s/\lambda)^\beta) \quad 3)$$

where C , λ , and β are constants.

Using the series representation of exponential function, and the definition of gamma function, the complex modulus $G^*(\omega)$ corresponding to the stretched exponential relaxation can be formally written as

$$G'(\omega) = C \sum_{k=0}^{\infty} \frac{\Gamma(\beta k + 1)}{k!} \cos\left(\frac{\pi}{2}(2-\beta)k\right) \left(\frac{1}{\omega\lambda}\right)^{\beta k} + iC \sum_{k=0}^{\infty} \frac{\Gamma(\beta k + 1)}{k!} \sin\left(\frac{\pi}{2}(2-\beta)k\right) \left(\frac{1}{\omega\lambda}\right)^{\beta k} \quad 4)$$

Introducing

$$\lambda^{-\beta} \equiv \alpha \quad 5)$$

the storage and the loss moduli generated by the stretched exponential relaxation function 3) are given as follows:

$$G'(\omega) = C \sum_{k=0}^{\infty} \frac{\Gamma(\beta k + 1)}{k!} \left(\frac{\alpha}{\omega\beta}\right)^k \cos\left(\frac{\pi}{2}(2-\beta)k\right) \quad 6)$$

$$G''(\omega) = C \sum_{k=0}^{\infty} \frac{\Gamma(\beta k + 1)}{k!} \left(\frac{\alpha}{\omega\beta}\right)^k \sin\left(\frac{\pi}{2}(2-\beta)k\right) \quad 7)$$

It is clear that these series representations of the components of the complex modulus do not converge for all $\omega \in (0, \infty)$. However, by choosing a finite frequency subinterval $\omega \in (a, b)$ one can always find the values of parameters λ , β , and C in such a way that the series in 6) and 7) will approximate, with the prescribed precision, G' and G'' on (a, b) . This idea is applied in the next paragraph to one regular and one polymer modified asphalt.

REGULAR ASPHALT MODIFIED BY SBS POLYMER

Dynamic material functions of a regular asphalt 200/300 Pen grade have been dynamically tested at different temperatures and the master curves of G' and G'' (ref. $T=0^\circ\text{C}$) prepared by the time temperature shifting. The mentioned regular asphalt has been modified by SBS copolymer. It is known (10) that SBS copolymer exhibits a rheological transition from Newtonian to non-Newtonian behavior at a region of higher temperature. In the low temperatures the SBS system is plastic with a yield stress. It is believed (10) that such a transition is generated by a transition of the structure from microphase-separated state to the homogeneous state.

Again the dynamic material functions of this PMA (polymer modified asphalt) have been measured and the master curves of G' and G'' prepared. The shift factor a_T for these master curves was fitted to Arrhenius and WLF forms.

The domain of experimental master curves G' and G'' for the regular 200/300 Pen grade asphalt, is $\log \omega \in [-5.6, 7]$ and we have found that the series representations 6) and 7) can be used for this sample if the domain is subdivided into three subdomains. These subdomains are: $A = \{\log \omega \in [-5.6, 1]\}$, $B = \{\log \omega \in [-1, 2.5]\}$, $C = \{\log \omega \in [2.5, 7]\}$. The given subdomains represent a minimum number of subintervals covering the domain of the master curve for regular asphalt 200/300 Pen grade, in the sense that minimally three stretched exponential; relaxation functions 3) are necessary for the description of the whole master curves G' and G'' . The parameters of the stretched exponentials in all three subdomains are: in A, $\alpha = 7.479$, $\beta = 0.0857$, $C = 4.075e+09$; in B, $\alpha = 6.1826$, $\beta = 0.1346$, $C = 9.4056e+08$; in C, $\alpha = 10.0824$, $\beta = 0.237$, $C = 4.231e+08$

The storage, G' , and the loss, G'' , moduli were calculated according to Equations 6) and 7). In these calculations the sums of series were terminated when the absolute value of the next term was less than 10^{-9} , thus strictly speaking the calculated values of G' and G'' are approximations. The compositions of calculated G' and G'' are compared with the experimental data (master curves at reference $T = 0^\circ\text{C}$) in Figs. 1, 2. The high frequency (low temperature) behavior is better seen in Fig. 2. The graph of G'' clearly shows the maximum of G'' . The high frequency behavior of G' is probably overestimated by the series approximation in the subdomain C. However, it is also possible that the last three experimental points of Fig. 1 represent the region which is difficult to access experimentally - these points are measured at $T = -30^\circ\text{C}$, i.e. roughly around the glass transition temperature ($T_g = -27^\circ\text{C}$).

The domain of experimental master curves G' and G'' , for the PMA is $\log \omega \in [-8, 7.4]$. The minimum number of subdomains, covering this domain in the sense of data fit to the least number of stretched exponentials, is four. The subdomains are: $\bar{A} = \{\log \omega \in [-8, -2.8]\}$; $\bar{B} = \{\log \omega \in [-2.8, 3.5]\}$; $\bar{C} = \{\log \omega \in [3.5, 5.4]\}$; $\bar{D} = \{\log \omega > 5.4\}$. The last subdomain, \bar{D} , covers the interval of low temperatures (again around the T_g of the base asphalt 200/300) Pen grade, and the caution is in place in considering the experimental data in this region. Experimental data were

again fitted to the stretched exponential relaxation, i.e. the series representation 6) and 7) were used in each subdomain. Parameters of the stretched exponentials in these subdomains are: in \bar{A} , $\alpha = 4.369$, $\beta = 0.0792$, $C = 3.76e+07$; in \bar{B} , $\alpha = 7.931$, $\beta = 0.081$, $C = 4.186e+09$; in \bar{C} , $\alpha = 11.112$, $\beta = 0.2174$, $C = 3.92e+08$; in \bar{D} , $\alpha = 27.03$, $\beta = 0.3034$, $C = 3.02e+08$. The compositions of calculated G' and G'' are compared with the experimental data (master curves) in Figs. 3, 4. It is clear that at highest frequencies (lowest temperatures) the fit is not as good as in frequencies $\log \omega \leq 6$. Again one has to stress the experimental difficulties in this region of temperatures.

DISCUSSION

The stretched exponential relaxation function seems to be able to generate reasonably accurate storage and loss moduli for both regular and polymer modified asphalts. The series representation 6) and 7) can be used for the estimates of $G'(\omega)$ and $G''(\omega)$ on any finite subinterval of frequencies. It is clear from the results obtained in the previous paragraph that the parameters of the stretched exponential relaxation function depend on the temperature. Not surprisingly the "relaxation" time λ is very low (order 10^{-11} for regular asphalt, and order 10^{-9} for PMA) at the lowest reduced frequencies (highest temperatures) where asphalts have a Newtonian behavior. On the other hand, at high reduced frequencies (temperatures around T_g in the studied case) the value of λ , in both neat and modified asphalts is of order 10^{-5} .

There are now several mechanisms proposed for the stretched exponential (6), one of the most interesting is the defect diffusion model (7). According to this model, mobile defects move randomly through the medium and generate local conformal abnormalities in the system. On leaving the site of such a local disturbance the defect will cause a disturbance at some other site of the medium. After some time, the neighbourhood of the disturbed "particle" will relax, as the system returns to equilibrium. Thus the migration of defects may cause a mechanical relaxation. If there is a finite concentration (c) of defects, the probability that the "particle" will be reached at time t by one of the N defects in a volume N/c is given as (12).

$$\phi(t) = \exp(-cI(t)) \quad 8)$$

Here $I(t)$ is the number of distinct "particles" attacked by a defect at time t . If each defect undergoes a random walk with the pausing-time distribution $\psi(t)$ there are two important classes of $\psi(t)$. In the first case the form of ψ is exponential

$$\psi(t) \sim \exp(-\lambda t), \quad \lambda = \text{const.} \quad 9)$$

After some time this becomes a classical diffusion which leads to Debye's result (6), $\phi(t) = \exp(-t/\lambda)$, in three-dimensional case. The second case are distributions with an inverse-power tail

$$\psi(t) \sim t^{-(1+\alpha)}, \quad 0 < \alpha < 1 \quad 10)$$

In this case

$$I(t) \sim \begin{cases} t^\alpha & \text{in 3 dimensions} \\ t^{\alpha/2} & \text{in 1 dimension} \end{cases} \quad 11)$$

Substituting 11) into 8) one obtains the stretched exponential form. The defect diffusion model is based on the movement of defects. However, the nature of defects is not known, and many possibilities have been suggested. For example, it has been suggested that a mobile carbonate (CO_3) bond is the "defect" in some high-impact resins, (13). In the case of studied asphalts one can see that the exponent β is of order 10^{-2} at higher temperatures and almost four times larger at low temperatures (around T_g of the base asphalt). Thus the "defect" seems to move in a quasi-one-dimensional motion at higher temperatures and perform a three-dimensional walk at temperatures close to T_g .

In conclusion, it appears that the stretched exponential is important not only in theoretical analysis of complex systems, but can also be successfully used in direct modelling of the stress relaxation in such systems. Such modelling in crack sealants will be discussed elsewhere.

ACKNOWLEDGMENT

The authors would like to express their gratitude to Husky Oil Ltd. and to the Natural Sciences and Engineering Research Council of Canada for their financial support of this project.

LITERATURE CITED

- (1) Yen, T.F., *Advances in Chemistry Ser.*, Ed. M.J. Comstock, ACS, **195**, 139 (1981).
- (2) Speight, J.G., Moschopedis, S.E., *Advances in Chemistry Ser.*, Ed. M.J. Comstock, ACS, **195**, 1 (1981).
- (3) Neuman, H.J., Rahimian, J., *Bitumen*, **35**, 1 (1973).
- (4) Mandelbrot, B.B., "The Fractal Geometry of Nature", Freeman, NY, (1982).
- (5) Kohlrausch, F., *Pogg. Ann. Phys.*, **119**, 352 (1863).
- (6) Debye, P., "Polar Molecules", Lancaster Press, Lancaster, Pa., (1929).
- (7) Williams, G., Watts, D.C., *Trans. Farad. Soc.*, **66**, 80 (1970).
- (8) Kakalios, J., "Hopping and Related Phenomena", World Scientific, Singapore, (1990).
- (9) Stastna, J., Zanzotto, L., Ho, K., *Rheol. Acta*, **33**, 344 (1994).
- (10) Watanabe, H., Kawahara, S., Kotaka, T., *J. Rheol.*, **28**, 393 (1984).
- (11) Palmer, R.G., Stein, D., Abrahams, E.S., Anderson, P.W., *Phys. Rev. Lett.*, **53**, 958 (1984).
- (12) Shlesinger, M.F., Montroll, E.W., *Proc. Natl. Acad. Sci. USA*, **81**, 1280 (1984).
- Bendler, J.T., *Ann. N.Y. Acad. Sci.*, **371**, 299 (1981).

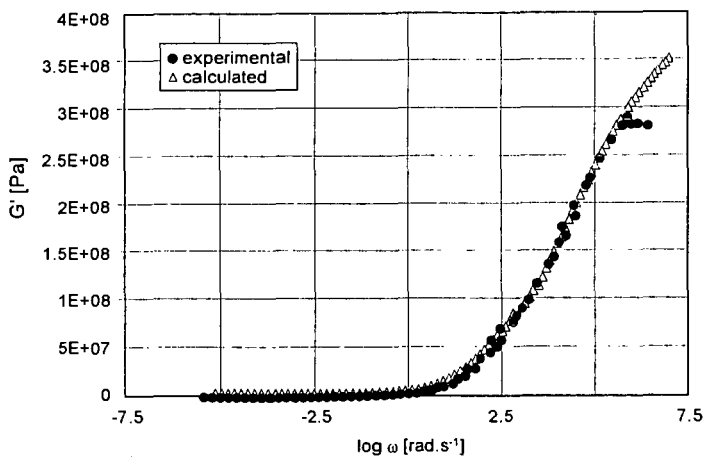


Figure 1. Regular asphalt, G' .

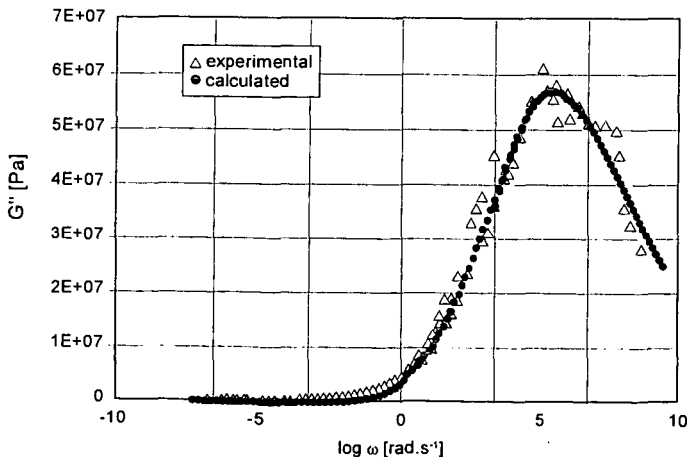


Figure 2. Regular asphalt, G'' .

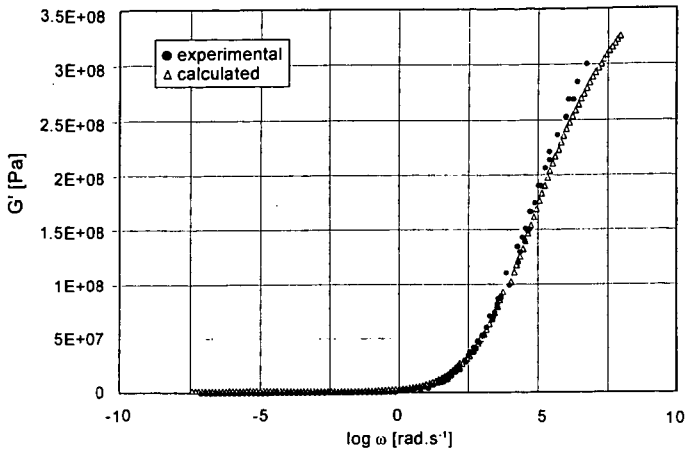


Figure 3. Polymer modified asphalt, G' .

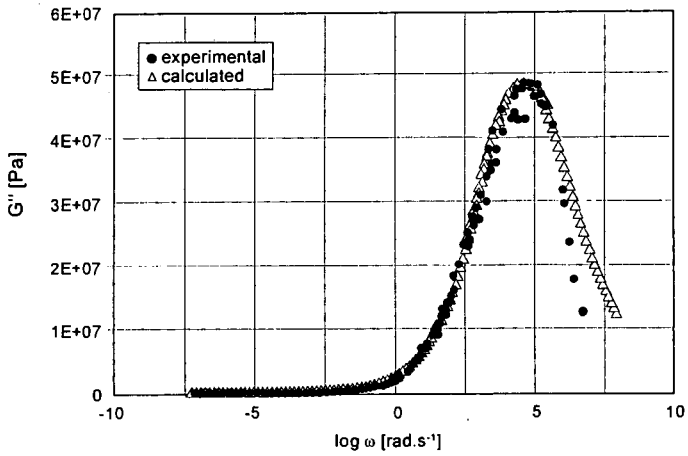


Figure 4. Polymer modified asphalt, G'' .

MOLECULAR DYNAMICS AND THE STRUCTURE OF ASPHALTS AND MODIFIED ASPHALTS AT LOW TEMPERATURES

Daniel A. Netzel, Thomas F. Turner, and Francis P. Miknis
Western Research Institute
365 North 9th Street
Laramie, WY 82070

Jeni Soule and Arland E. Taylor
Chemical and Petroleum Engineering Dept.
University of Wyoming
Laramie, WY 82071

Keywords: Asphalts, NMR, Molecular Dynamics

INTRODUCTION

One important fundamental molecular property of an asphalt, which dictates its temperature dependent performance, is the nature of molecular motions associated with the asphalt molecular components. At any given temperature, the extent of molecular motions depends on the intramolecular configuration of the various asphalt components and the manner in which they interact by intermolecular association. Molecular association tends to restrict molecular motions. Changes in structure and composition brought about by chemical reaction with oxygen as a result of aging also strongly affect overall molecular motion in asphalts through enhanced molecular association, which, in turn, affects the overall long term road performance behavior of asphalts.

On a macro scale the performance behavior of asphalts is manifested in changes in the viscoelastic nature of asphalts, that is, changes in their rheological properties. Thus, an understanding of the molecular dynamics should be helpful in the understanding of the viscoelastic nature of asphalts and in predicting the asphalt composition which optimize binder performance. The molecular mobility can be altered through modification of the asphalt chemically, by the physical blending of two or more asphalts, or the introduction of polymeric materials or other additives to asphalts.

The type and extent of molecular motions can be obtained from hydrogen-1 and carbon-13 nuclear magnetic resonance (NMR) relaxation time measurements. These measurements can provide quantitative information on the molecular structure and degree of molecular motions associated with the hydrogen and carbon types and/or groups in asphalts. Because asphalts are solid-like materials, the molecular motions of interest are low frequency, on the order of 1-50 kHz. The motions of most interest for components of asphalt are methyl rotation, segmental motions (full and/or partial rotation of segments) of the long-chain aliphatic hydrocarbons, and phenyl twisting (torsional oscillation). Figure 1 illustrates the different kinds of motions in a complex asphaltic-like molecule. The structure shown in Figure 1 is a simplification of the "average" structure of the molecules found in asphalt as determined from liquid-state NMR parameters. The structure in Figure 1 consists of polycondensed aromatic carbons with methyl and long-chain hydrocarbon group substituents. The complete "average" structure consists of several methyls and long-chain hydrocarbon groups attached to the aromatic carbon cluster. Generally, there are ~ 30% aromatic carbons and ~ 70% aliphatic carbons in an average "asphaltic" molecule. Not shown in the figure are the heteroatoms which are also of major importance to asphalt chemistry.

EXPERIMENTAL

Solid-state ^{13}C NMR measurements were made using a Chemagnetics 100/200 solids NMR spectrometer operating at a carbon frequency of 25 MHz. Variable contact times experiments were conducted using a 7.5 mm rotor spinning at a rate of 4.5 kHz. Other parameters included a pulse width of 5 μs , pulse delay of 1 s, a sweep width of 16 kHz, 1024 data acquisition points, and between 3000 and 7200 transients. Dipolar dephasing spectra were obtained at a contact time of 1 ms. Low temperatures were obtained using a FTS systems XR Series Air-Jet Sample Cooler. The asphalts were selected from the Strategic Highway Research Program (SHRP) Materials Reference Library.

RESULTS AND DISCUSSION

A stack plot of the dipolar dephasing NMR spectra for asphalt AAM-1 at -45°C is shown in Figure 2. These spectra illustrate the chemical shift position of the different carbon types and clearly show the different relaxation rates at -45°C for the different carbon types. The aromatic carbon region (110-150 ppm) is resolved into quaternary (C, ~ 130-150 ppm) and tertiary (CH, 110-130 ppm) carbon types. The tertiary carbon signals decay much faster than the quaternary carbons. At a dephasing time of 160 μs , the only remaining aromatic carbons are the quaternary carbons which span

the region from 110-150 ppm. Thus, it appears that about 50% of total aromatic quaternary carbons are hidden under the tertiary carbon peak at a dephasing time of 1 μ s which approximates a standard cross-polarization experiment. The amount of quaternary carbons dictates the size of the aromatic cluster. Thus, a simple integration of the aromatic region will underestimate the total aromatic quaternary carbons.

The rate of change of the aliphatic carbon types is quite dramatic. Almost all of the methine (CH) and methylene carbons (CH₂) (30-50 ppm) have decayed after a dephasing time of 80 μ s. In addition, the sharp methylene peak at 32 ppm decays much faster than the methylene shoulder at 30 ppm. The decays of the methyl carbons (15-30 ppm) are much slower than the other carbon types.

The methyl (CH₃) carbons attached to aromatic rings and branched to a linear main-chain hydrocarbon have resonance peaks in the region of 20-30 ppm. These methyl carbons decay faster than the terminal methyl carbons (15 ppm) of a long chain hydrocarbon. The longer relaxation rates for the two methyl carbon types relative to the methylene and methine carbons are due to the faster rotation motions of the methyl carbons compared to the much slower segmental motions of the methylene and methine carbons. It should be noted that the branched methyl carbons decay faster than the terminal methyl carbons indicating that the branched methyl carbons are rotating slower because of hindrance to rotation than the terminal methyl carbons.

T_{1 ρ} ^H of Asphalts and Modified Asphalts

The hydrogen rotating-frame spin-lattice relaxation time constants (T_{1 ρ} ^H) have been used as a probe to study the structure of polymer blends.^{1,2} The T_{1 ρ} ^H values are determined by the rate of hydrogen spin-diffusion throughout the sample, which in turn depends upon the homogeneity of the blends and extent of molecular motion.

Figure 3 shows the NMR variable contact time CP/MAS data for Conoco Denver Asphalt and the asphalt modified with 2% Elvaloy® AM (an ethylene acrylate copolymer). The T_{1 ρ} ^H values are derived from the slope of the lines between contact times of 0.5 and 6 ms. The T_{1 ρ} ^H for the Conoco asphalt at 23°C was found to be 1.34 ms and for the 2% Elvaloy AM® modified asphalt the T_{1 ρ} ^H value was found to be 0.92 ms. The smaller relaxation time for the modified asphalt suggests that the correlation time for molecular motion is faster. That is, the overall molecular motions within the asphalt were increased at 23°C. With the limited data, it appears that the modified asphalt is a homogeneous blend based on the fact that only one T_{1 ρ} ^H value represents the data.

Figure 4 shows the variable contact time CP/MAS data for Cenex asphalt (a Wyoming AC-20 asphalt) and the asphalt modified with 3% Butonal® NS175 polymer (a cold polymerized anionic styrene-butadiene dispersion). The T_{1 ρ} ^H values for the asphalt and modified asphalts were found to be 1.41 and 1.09 ms, respectively. Based on the smaller relaxation time for the modified asphalts, the molecular motions were enhanced at 23°C. There is evidence that a second T_{1 ρ} ^H could be fitted to the data suggesting therefore that two domains exist in the asphalts. Additional data will be needed to confirm the observation.

The conclusion of enhanced molecular motions (as suggested from the T_{1 ρ} ^H measurements) for the modified asphalts was limited to one temperature (23°C). To fully understand the dynamic behavior of the polymer modified asphalts, measurements must be made over a range of temperatures. The next section describes the methodology used to quantify the extent of molecular motion in asphalts over a temperature range from +20 to -45°C.

Molecular Mobility in Asphalts at Low Temperature

An important feature in the NMR spectra of any material is the increase in the signal-to-noise ratio as the temperature is decreased. The increase in the signal is due to the difference in the population of nuclear spins in the ground state relative to a higher energy state. That is, as the temperature is lowered, the number of spins increases in the ground state increasing the spin differences between the energy states resulting in an increase in the intensity of the NMR signal. The increase in signal can be predicted from the Boltzmann distribution equation and nuclear spin theory. The total spin magnetization, M₀, at any given temperature is given by equation 1.³

$$M_0 = N\gamma^2\hbar^2H_0/4kT \quad (1)$$

where:

- N = The number of spins in the sample
- γ = gyromagnetic ratio of carbon
- \hbar = Planck's constant divided by 2 π
- H₀ = Static magnetic field
- k = Boltzmann constant
- T = Temperature

Because the carbon-13 magnetization is proportional to the NMR spectral integrated area of the carbon moiety of interest ($M_o \propto A$), the relative increase in carbon magnetization (integrated signal area) can be obtained from the ratio of the two temperatures at which the NMR spectra were obtained (Eq. 2).

$$A_2/A_1 = T_2^{-1}/T_1^{-1} \quad (2)$$

Sullivan and Maciel⁴ used equation 2 to show that the increase in the NMR signals for Powhatan #5 coal at temperatures below 21°C is due only to the Boltzmann factor (ratio of the absolute temperature). Coal is a very rigid solid without any apparent or significant molecular motion in the range of 10 to 50 kHz throughout the low temperature range. Because of the lack of molecular motion in coal, the dipolar interaction of the carbons and hydrogens in a cross-polarization experiment is very efficient, whereby, most of the carbons are observed at all temperatures and the increase in signal intensity in coal with decreasing temperature is due only to the Boltzmann factor. Figure 5 shows the change in the CP/MAS spectra of asphalt AAA-1 obtained at temperatures of 20 and -45°C. For the same set of conditions, the signal-to-noise ratio in the NMR spectrum at -45 is considerably better than for the spectrum taken at 20°C. Note also that the signal of the methylene carbons (32 ppm) at -45°C is greatly enhanced relative to the signal at 20°C. The signal enhancement is greater than that predicted by the Boltzmann Factor.

Table I lists the relative signal enhancement, $A_{\max}(t) / A_{\max}(20^\circ\text{C})$, normalized to 20°C data, for the aliphatic carbons in asphalts AAA-1, AAB-1, and AAM-1 at 20, 0, -10, -20, -30, and -45°C. Also given in the table is the theoretical signal enhancement (T^{-1}/T_{293}^{-1}) expected based upon the ratio of temperatures relative to 20°C (293K). The maximum signal for aliphatic carbons was obtained at a contact time of 0.22 ms (independent of temperature). Figure 6 shows the NMR molecular-mobility/temperature profile plots of the aliphatic area ratios as a function of temperature for the three asphalts. Also shown in Figure 6 is the plot of the theoretical relative signal enhancement as a function of temperature based upon the Boltzmann spin population distribution relative to 20°C.

The ratio of the integrated areas for the aliphatic carbons of the three asphalts differ significantly from coal and from the theoretical signal enhancement due to the Boltzmann factor. These differences are the result of extensive molecular motions in asphalts which prevents effective cross-polarization of the carbon and hydrogen spins. However, as the temperature decreases, the molecular motion decreases, the molecular structure of asphalt becomes more rigid-like, the cross-polarization mechanism becomes more effective and, thus, more carbons are observed resulting in an increase in the integrated area ratio with decreasing temperature. Thus, the area ratio can be defined as a molecular rigidity parameter. That is, as the temperature decreases, the molecular structure becomes more rigid-like.

Asphalt AAA-1 shows a greater enhancement of the aliphatic carbon NMR signal over the temperature range from +20 to -45°C than asphalt AAB-1 which, in turn, shows a greater enhancement than asphalt AAM-1. The greater the relative enhancement at any given temperature the more molecular motion involved for the asphalts. Thus, the extent of segmental and rotational motions of the aliphatic carbons in the asphalts can be ranked as follows: AAA-1 > AAB-1 > AAM-1. This ranking is in the same relative order as the glass-transition temperature, viscosities, and various other rheological properties. As shown in Figure 6, for asphalt AAA-1, the relative signal intensity continues to increase after -45°C. A part of this increase is due to the increase in the Boltzmann factor for the rigid-like carbons. In addition, the signal is expected to increase until the motions due to the presence of a significant amount of methyl rotation and some residual main-chain segmental motions of the aliphatic carbons are stopped. Much lower temperatures will be needed to stop most of these molecular motions. The data for asphalt AAM-1 shows a decrease in signal after -30°C. It has not yet been established whether or not the signal will continue to decrease after -45°C (due to temperature effects on other relaxation mechanisms which can affect the cross-polarization rate) or continue rising at a rate dictated by the Boltzmann factor.

The distinction among asphalts based upon the extent of molecular motions over the temperature range of 65°C for the aliphatic carbons suggest that asphalts modified with small percent of rubber or polymers may be amenable to this NMR technique. In addition, the NMR mobility/temperature profile methodology may be useful to study the rate of oxidation as it affects the motions of the aromatic and/or aliphatic carbons.

The NMR molecular-mobility/temperature profile plots of the asphalts follow qualitatively, but inversely, their DSC thermograms throughout the glass-transition region. The NMR plots describe the change in molecular mobility (molecular dynamics) with changing temperature, whereas, the DSC thermograms measure the changes in the thermal energy (molecular energetics) associated with molecular transitions with changing temperature. Both NMR and DSC data can be expressed using

a cumulative-Gaussian equation. A modified form of the equation was used to fit the NMR data shown in Figure 6 (see equation 3):

$$\rho = A_i/A_{20^\circ\text{C}} = 0.5\rho_o (1 + \text{erf} [(t - T_{\text{NMR}})/(2^{0.5}\sigma)]) + 293.15/(273.15 + t) \quad (3)$$

where:

- ρ = relative signal enhancement ($A_i / A_{20^\circ\text{C}}$)
- ρ_o = maximum change in relative signal enhancement
- t = temperature, °C
- T_{NMR} = Inflection point temperature, °C
- σ = standard deviation of the distribution
- erf = error function

The term, $293.15/(273.15 + t)$, applies the Boltzmann factor to the fit of the data. The coefficients (ρ_o , T_{NMR} and σ) in equation 3 for the aliphatic and aromatic carbons in the three asphalts are given in Table II. Also given are the onset temperatures for molecular motion for the carbon types in each asphalt. The onset temperature was obtained using equation 4.

$$T_{\text{os}}^{\text{NMR}} = T_{\text{NMR}} + (-2\sigma) \quad (4)$$

The standard deviation of the mean (2σ) encompasses 95% of the observed changes in molecular motion.

The NMR inflection point temperatures and the onset temperatures for significant molecular motions of the aromatic carbons are several degrees higher than the aliphatic carbons. That is, upon cooling the motions of the carbon atoms in the polycondensed aromatic rings are slowed down significantly while the long-chain aliphatic carbons and methyl carbons continue to have considerable segmental and rotational motions. In addition, the NMR inflection point temperature and the onset temperatures were found to be higher than the glass-transition temperature and onset temperature measured using DSC. The NMR inflection point temperatures were found to match more closely the defining temperatures of the asphalts.

The increase in the NMR inflection point temperatures and the onset temperatures going from asphalt AAA-1 to AAM-1 is in agreement with their known rheological and performance predictive properties. Asphalt AAA-1 is the softest (considerable amount of molecular motion) of the three asphalts and asphalt AAM-1 the hardest (the least amount of molecular motions). Thus, the softer the asphalt, the lower the temperature needs to be to stop most of the molecular motion.

CONCLUSIONS

Preliminary $T_{1\rho}^{\text{H}}$ data on asphalts and polymer modified asphalts suggest that this NMR relaxation technique can be used to measure the extent of the compatibility of the asphalts and polymer on the overall molecular motions of the asphalts. It is the extent of molecular motion which governs many of the rheological properties of the asphalts. NMR molecular-mobility/temperature profile plots of asphalts were found to follow qualitatively their DSC thermograms. Both the NMR inflection point temperature and the onset temperature for molecular motion were found to be higher than the glass transition temperature and the DSC onset temperatures. Because of the high degree of distinction for the different asphalts, the NMR profile plots should be useful in studying the molecular dynamics in modified asphalts.

REFERENCES

1. Natansohn, A., 1992, *Polymer Engineering and Science*, 32(22), 1711.
2. Simmons, A., and A. Natansohn, 1992, *Macromolecules*, 25, 1272.
3. Harris, R. K., 1983, "Nuclear Magnetic Resonance Spectroscopy," Pitman Publishing Inc., Marshfield, MA, p. 9.
4. Sullivan, M. J., and G. E. Maciel, 1982. Spin Dynamics in the Carbon-13 Nuclear Magnetic Resonance Spectrometric Analysis of Coal by Cross Polarization and Magic-Angle Spinning, *Anal. Chem.*, 54, 1615-1623.

ACKNOWLEDGMENT

The authors express their appreciation to the Federal Highway Administration for their support of this program under FHWA Contract No. DTFH61-92C-00170. The authors express their thanks to Dr. Robert Statz and Dr. Richard Liu for supplying the polymer modified asphalts. Elvaloy® AM is a tradename of Dupont Company and Butonal® NS 175 is a tradename of BASF Corporation.

DISCLAIMER

This document is disseminated under the sponsorship of the Department of Transportation in the interest of information exchange. The United States Government assumes no liability for its contents or use thereof.

The contents of this report reflect the views of Western Research Institute which is responsible for the facts and the accuracy of the data presented herein. The contents do not necessarily reflect the official views of the policy of the Department of Transportation.

Table I. Carbon-13 NMR Aliphatic Carbon Area Ratios for SHRP Core Asphalts AAA-1, AAB-1 and AAM-1 from Variable Temperature Cross-Polarization Experiments

Temperature (t), °C (K)	Temperature Ratio, T^1/T^{-293}	AAA-1		AAB-1		AAM-1	
		Integrated Area, $A_{max}^{Al}(t)$	Area Ratio, $A_{max}^{Al}(t)/A_{max}^{Al}(20^\circ)$	Integrated Area, $A_{max}^{Al}(t)$	Area Ratio, $A_{max}^{Al}(t)/A_{max}^{Al}(20^\circ)$	Integrated Area, $A_{max}^{Al}(t)$	Area Ratio, $A_{max}^{Al}(t)/A_{max}^{Al}(20^\circ)$
20 (293)	1.00	14.54	1.00	19.19	1.00	26.13	1.00
0 (273)	1.07	24.51	1.69	30.05	1.57	39.33	1.51
-10 (263)	1.11	28.75	1.98	34.99	1.82	46.36	1.77
-20 (253)	1.16	35.48	2.44	43.00	2.24	53.67	2.05
-30 (243)	1.20	39.44	2.71	46.67	2.45	57.59	2.20
-45 (228)	1.29	44.75	3.08	52.06	2.71	56.75	2.17

* From maximum signal intensity for aliphatic carbons (ct = 0.22 ms)

Table II. NMR Parameters from the Molecular-Mobility/Temperature Profile Plots for the Aliphatic and Aromatic Carbons in Asphalts AAA-1, AAB-1, and AAM-1

Asphalt	Maximum Change in Signal Enhancement, ρ		Inflection Point Temperature, T_{NMR} , °C		Mean Standard Deviation, 2σ , °C		Onset Temperature for Molecular Motion* T_{on} , °C	
	Aliphatic	Aromatic	Aliphatic	Aromatic	Aliphatic	Aromatic	Aliphatic	Aromatic
AAA-1	1.83	1.42	-10.6	-9.5	±38.5	±32.7	-49.1	-42.2
AAB-1	1.44	0.86	-9.1	-7.7	±35.4	±25.9	-44.5	-33.6
AAM-1	0.94	0.61	-2.2	+1.6	±23.9	±19.2	-26.1	-17.6

* Based on 2σ (95%) and excluding CH_3 rotation below -50°C.

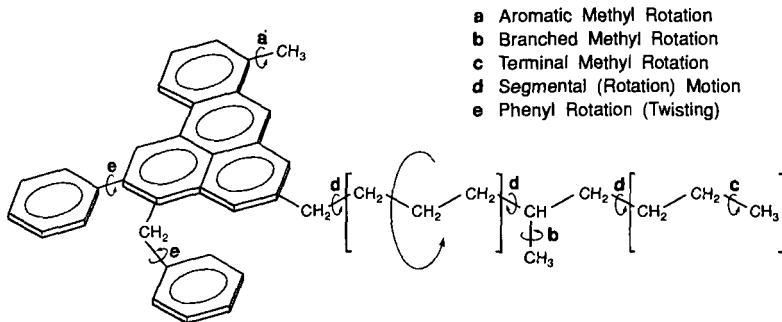


Figure 1. A Simplified "Average" Molecular Structure of Asphalt

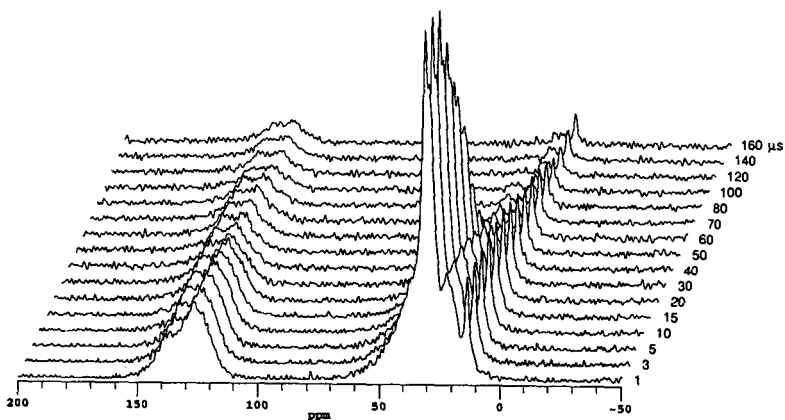


Figure 2. Stack Plot of the ^{13}C Dipolar-Dephasing NMR Spectra for Asphalt AAM-1 at -45°C

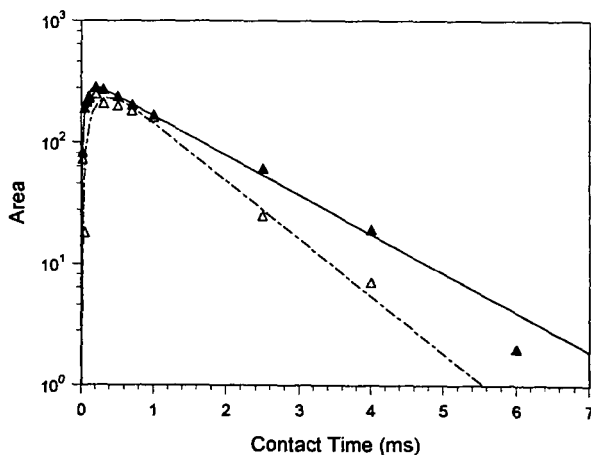


Figure 3. Carbon-13 NMR CP/MAS Variable Contact Time Data at 23°C for Aliphatic Carbons in (\blacktriangle) Conoco Denver Asphalt, and (\triangle) Asphalt Modified with 2% Elvaloy $^{\text{TM}}$ AM

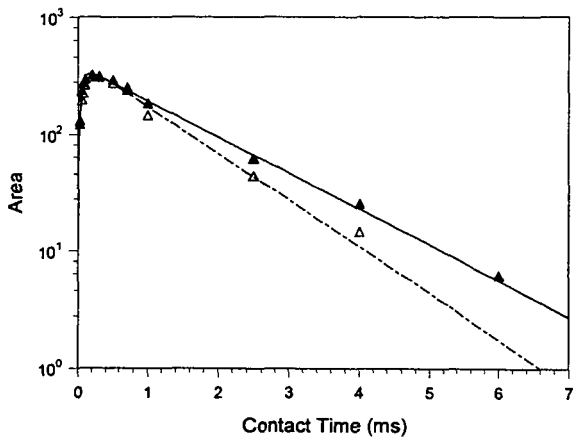


Figure 4. Carbon-13 NMR CP/MAS Variable Contact Time Data at 23°C for Aliphatic Carbons in (▲) Cenex Asphalt and (Δ) Asphalt Modified with 3% Butanol@ NS 175

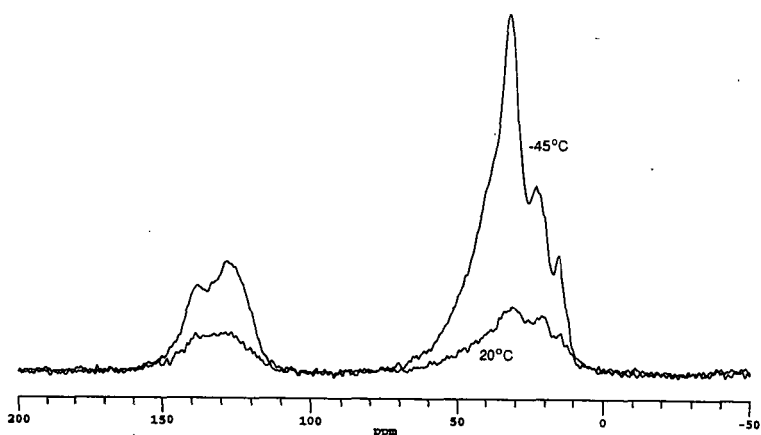


Figure 5. Carbon-13 CP/MAS Spectra of Asphalt AAA-1 at 20 and -45°C

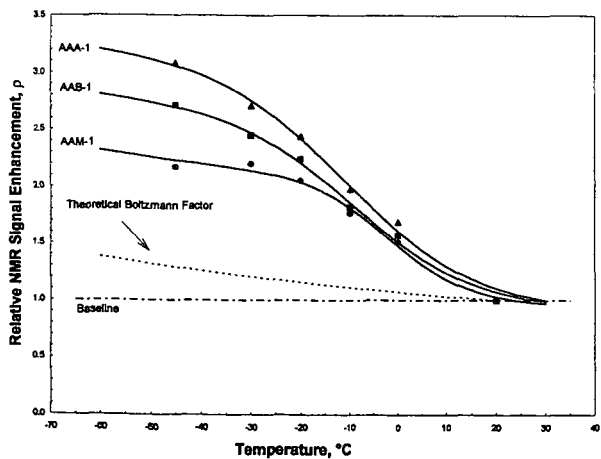


Figure 6. NMR Molecular-Mobility/Temperature Profile Plot for Aliphatic Carbons in Asphalts AAA-1, AAB-1, and AAM-1

SIZE EXCLUSION CHROMATOGRAPHY OF AGED AND CRUMB RUBBER MODIFIED ASPHALTS

John J. Duval
Western Research Institute
365 North Ninth
Laramie, WY 82070

Keywords: SEC of asphalts, SEC of aged asphalts, SEC of crumb rubber modified asphalts

INTRODUCTION

Preparative size exclusion chromatography (SEC) has been used for several years in our laboratory to provide samples for further analysis and for use in other testing procedures (1). Asphalts have been separated into a first fraction (F-I) that contains nonfluorescing (at 350 nm) materials, and the rest of the asphalt, which is collected in one or more fractions (F-II or F-IIa, F-IIb, etc). The nonfluorescing materials have been shown (1) to contain strongly associating molecules, while the fluorescing materials consist of weakly associating individual and smaller molecules. The fractionation data from these analyses have been related to the rheological property $\tan \delta$, and thereby, to rutting and premature pavement cracking. We have developed a high performance liquid chromatography (HPLC) technique that yields these analytical data more rapidly and efficiently than preparative SEC and yet gives chromatograms similar to those derived from preparative SEC. The HPLC procedure described here uses toluene as the carrier as does the preparative procedure.

SEC is a chromatography technique in which separation depends specifically on molecular size and where molecular polarity is a factor only if it promotes molecular association or if the material is of a type to bind to the chromatographic substrate. The column packing has pores of varying sizes that molecules can or cannot enter depending on their size. As a result, the largest molecules, which cannot enter the pores, emerge first from the column(s) and the smallest molecules in the sample, which do enter the pores of the packing and are, therefore, slowed in their passage through the column, emerge last. Some polar molecules may form associated species of varying strengths and if these associations persist under the column conditions they will behave as though they were true molecules with a size similar to the associated species.

A number of other workers have used HPLC/SEC, also known as HPLC-GPC (gel permeation chromatography), to analyze asphalts, among them Jennings et al. (2), who attempted to quantify the data they obtained using a UV/visible diode array detector (DAD). They used tetrahydrofuran (THF) as the carrier and also related their results to highway performance. They also grouped asphalts into four groups according to the asphalts' MSD (molecular size distribution) profiles. Glover et al. (3), used both THF and toluene in their investigations of the HPLC/SEC of asphalts. Brúlé and coworkers published several papers (4) on the HPLC/SEC of unaged and aged asphalts. Bishara et al. (5) have related molecular size data, obtained using an HPLC with a gravimetric finish, to PVN (penetration-viscosity-number), viscosity at 135° C, and other physical properties. Garrick (6) developed a mathematical model from GPC data that predicts GPC profiles from physical properties of asphalts and suggests that a strong relationship exists between GPC profiles and these physical properties, especially rheological properties. Different combinations of columns with different sized pores have been used in the various investigations.

EXPERIMENTAL

The HPLC equipment consists of a Hewlett Packard Series II 1090 liquid chromatograph with its associated computer hardware and software. There are a DAD, a differential refractive index detector (DRID), a fluorescence detector (FLD), and a fraction collector in place with the HPLC. However, because the sample concentrations used in this work are so large (the DAD, except at high wavelengths, and the FD are swamped), only data from the DRID and gravimetric data are reported here. Fractions are collected using the fraction collector, divested of solvent, and weighed on a balance to provide quantitative data not available from the other detectors.

The column combination in use consists of 2 - 500 Å and 1 - 100 Å 7.8 by 300 mm columns in series. The columns are packed with Phenomenex Phenogel with a 5 μ particle size. Toluene is used as the carrier at a flow rate of 1.00 mL/min and the columns are maintained at 40° C. Sample size is around 24 mg of asphalt dissolved in about 220 μ L of toluene. The sample is eluted in an hour. However, there is some tailing, so three hours are allowed between sample injections.

Because the samples are quite concentrated, back pressure, probably caused by adsorption of asphalt components in the frits at the ends of the columns, tends to build up after about 75 to 100 runs.

Cleaning is accomplished by backflushing the columns with 25 mL of a 3% methanol in toluene solution at 80° C followed by about 400 mL of toluene. Several samples of an asphalt then are run under normal conditions to condition the columns.

The column combination was calibrated by determination of retention times of several polystyrene standards with known peak molecular weights. Several other compounds of known molecular weight were also examined.

Samples of both unaged, at different concentrations, and asphalts aged to three levels (100°C (212°F) for 12, 20, or 36 hours at 2.07 MPa (300 psi)) were analyzed. Aging was accomplished using the thin film oven/pressure aging vessel technique described earlier (7). Samples of Strategic Highway Research Program (SHRP) asphalts AAB-1 and AAF-1 containing an AC 2.5 Amoco/Wilmington asphalt as a recycling agent were weighed out and then dissolved in toluene. Crumb rubber/asphalt mixtures were prepared by heating a weighed amount of asphalt (SHRP asphalts AAB-1, AAM-1, AAK-2, ABD-1, and ABL-3 were used) at 200°C (392°F) until liquid and then adding a weighed amount of crumb rubber followed by thorough mixing. The crumb rubbers used are both prepared from used tires and include one containing natural rubber designated NR (80 mesh) and one containing both natural and synthetic rubbers designated CR#4 (40 mesh). A sample was then taken which was labeled the zero hour sample. The rest of the CRM was heated under argon at 200°C (392°F) with samples removed at the desired time intervals. As a control, a sample of neat asphalt was heated and sampled under the same conditions as the CRM's. The CRM samples were then treated with toluene in about a 10:1 ratio of toluene to mixture. The partially dissolved samples then were centrifuged for an hour followed by filtration through a 0.22 μ filter using vacuum. The materials left in the centrifuge tube were rinsed further with toluene, centrifuged again, and filtered through the same filter as previously. The rinsing step was repeated and the combined filtrates were divested of solvent, weighed, and the requisite amount of solvent added to give the desired concentration. For all of the asphalts except AAM-1, strings of rubber were seen in the zero and one hour at 156°C (223°F) samples, rubber and carbon black were seen in the samples heated for 24 and 48 hrs, and samples that were heated for longer times seemed not to contain any rubber particles but an increased amount of finely divided carbon black was apparent. For asphalt AAM-1, carbon black first appeared in the 24 hour sample, for the NR mixtures, and increased through the 192 hour sample, while for the CR#4 mixtures, carbon black did not begin to appear until the 168 hour sample and a larger amount was seen in the 192 hour sample.

RESULTS AND DISCUSSION

A calibration curve for the column combination used is shown in Figure 1. The curve shows that the main area of separation for this system lies in the molecular weight range of around 1200 to 14000 Daltons. This is the range seen for SEC fractions F-I through F-IIb for the SHRP core asphalts as reported previously (1).

Early in this work it was necessary to determine the effect of sample size on the chromatogram. Figure 2 shows the results of this study in which it was found that a quite concentrated sample solution was necessary to achieve the desired result, i.e., emulate preparative SEC results. Apparently molecular associations were broken up in the more dilute solutions of asphalt in toluene that occurred when smaller samples were run.

It was necessary to demonstrate the effectiveness of the technique on unaged and aged asphalts so the SHRP core asphalts, both unaged and aged, were all analyzed. Examples of chromatograms of the unaged asphalts AAD-1 and AAF-1 both from the preparative SEC procedure and the HPLC/SEC procedure are shown in Figures 3 and 4 respectively. These figures show the similarity of the chromatograms produced for asphalts for both methods for two quite different asphalts.

Figure 5 shows the overlaid chromatograms of asphalt AAF-1 unaged and aged to three levels as an example of the results for aged asphalts from the technique described here. The chromatograms are drawn so that the largest peak for all four chromatograms is at the same level so that the change in the first part of the chromatogram is readily apparent. The amount of nonfluorescing associating material increases with increased aging. This is in agreement with earlier reports (1, 2, 5).

It was thought desirable to see if this technique could easily differentiate between an untreated asphalt and an asphalt treated with a recycling agent such as a lower viscosity asphalt. Figure 6 shows the overlaid chromatograms of the recycling agent and unaged asphalt AAF-1. As is evident, the recycling agent has as wide an MSD as does the higher viscosity asphalt. The major difference is in the highest molecular size material where the lower viscosity asphalt predominates. Therefore, addition of the recycling agent to the higher viscosity asphalt should show a difference in that region of the chromatogram. However, in Figure 7, where mixtures (5, 10, 25, and 50% AC 2.5) of the

recycling agent and AAF-1 are shown, no difference is apparent until the mixture reaches 25% recycling agent. Differences at the 50% level are easily seen in the figure.

Figure 8 shows data from the mixtures of the two grades of asphalt described above for the first five of nine SEC fractions. These curves show that SEC F-I does indeed grow with the addition of increasing concentrations of recycling agent while fractions F-IIa and F-IIb decrease somewhat but, again, the differences are only apparent at concentrations of 25% and above. This suggests that this particular column combination would not be useful to analyze mixtures of recycling agents with broad MSD's, such as low viscosity asphalts, and another asphalt except at high concentrations. It appears that only recycling agents that have a narrow MSD might be usefully analyzed by this system.

Mixtures of asphalts modified by addition of various crumb rubbers (CRM's) are being studied extensively in our laboratory and it was suggested that HPLC/SEC might be appropriate to determine the fate of the rubber in the CRM's, i.e., where in the MSD does the dissolved rubber appear? Figures 9 through 12 show chromatograms from the study of the separation of mixtures of crumb rubber (CRM's) and asphalt ABD-1. For example, Figure 9 shows overlaid chromatograms for the neat asphalt and the two CRM's before they had been heated except that necessary for mixing. It can be seen that the chromatogram of the mixture containing NR shows a small increase in the chromatogram in the area of large molecular size indicating that some high molecular size material had been incorporated into the asphalt. The other two chromatograms are essentially the same showing no addition of soluble CR#4 to the asphalt prior to further heating. This suggests that the difference in the crumb rubbers is demonstrated very early in the heating regimen, i.e., that NR is solubilized more easily with asphalt ABD-1 than CR#4. Figure 10 shows the effect of heating on the chromatograms of the neat ABD-1. A very small change in the area of large molecular size is seen for the neat ABD-1 on heating from 0 to 96 to 192 hours. Figure 11 shows chromatograms for the mixture of ABD-1 and NR. As can be seen, changes occur in the large molecular size region of the chromatograms. Heating this mixture for as little as an hour has made a significant change in the very large molecular size region of the chromatogram, that is, a peak is seen at the front edge of the chromatogram. Further heating of the sample gradually fills in the area between that peak and the rest of the chromatogram. This suggests that the rubber particles break down to a initially yield relatively large molecular size material followed by further breakdown to smaller molecular size material. Figure 12 shows chromatograms for the mixture of ABD-1 and CR#4. In this case, the 0 and 1 hour chromatograms are virtually identical, while the leading edge peak of the 24 hour chromatogram and those for higher levels of oxidation show that CR#4 does not begin to break down as early in the heating regimen with ABD-1 as does NR.

Figures 13 and 14 show chromatograms for both neat asphalt AAB-1 and a mixture of AAB-1 and NR respectively. Figure 13 shows chromatograms how the neat asphalt reacted to different periods of heating at 200°C (392°F). Interestingly, the amount of large molecular size materials formed on heating AAB-1 for 48 hours gradually diminished on further heating suggesting these materials broke down to lower molecular weight materials on sustained heating or became materials that are incapable of forming intermolecular associations. Of the asphalts studied so far, this result is peculiar only to AAB-1 and may be a result of the aging occurring in an argon atmosphere. The chromatograms in Figure 14 show that heating the AAB-1/NR mixture leads to an increase in large molecular size materials with increased heating time. Chromatograms are shown for a heating period of up to only 48 hours because further heating showed no further changes in the chromatograms. This lack of further change suggests that further breakdown of the rubber did not occur after 48 hours of heating with asphalt AAB-1 at 200°C (392°F). Similar chromatograms are obtained for the AAB-1/CR#4 mixture.

Chromatograms similar to those shown for asphalt AAB-1 could be shown for neat SHRP asphalts AAK-2 and ABL-3. Asphalt ABL-3 was supposed to be a replacement for SHRP asphalt AAK-2 but SEC chromatograms show significant differences. At any rate, the chromatograms for both the neat asphalts and the CRM's show a steady increase in the large molecular size region with increased heating time with the mixtures showing the larger increase.

Figures 15 and 16 show chromatograms for asphalt AAM-1 and asphalt AAM-1 with NR respectively. Figure 15 shows the chromatograms for the neat asphalt as a function of heating time and demonstrate that heating neat AAM-1 for 72 hours at 200°C (392°F) causes little change but, additional heating to a total of 96 hours caused a significant increase in the area of large molecular size material. On the other hand, heating the AAM-1/NR mixture showed small but significant changes in the large molecular size region through 24 hours of heating at 200°C (392°F) and, after 48 total hours of heating, a very large change. The chromatograms for the neat asphalt after 96 hours of heating and for the asphalt with NR after 48 hours of heating are similar, but very different from those for the other asphalts. This suggests that the source for the additional large molecular size material is the asphalt, not the rubber, and that large molecular size materials from the rubber

seen in the chromatograms from the other asphalts are "buried" under the curve for the materials from the asphalt. However, because the material appears at a shorter heating time for the CRM than for the neat asphalt, it seems possible that something in the rubber catalyzes the formation of large molecular size materials from the asphalt. This could possibly be explained by the presence of finely divided carbon black in the rubber that begins to make its appearance as the rubber breaks down. Perhaps the carbon black particles supply a focal point for potential SEC F-I materials to associate as dust particles do in crystallization. These associations must be stable in toluene in order to be detected by the DRID.

CONCLUSIONS

The HPLC/SEC technique described, i.e., the column combination, column temperature, solvent, and flow rate, has demonstrated the ability to emulate preparative SEC for unaged asphalts and also give chromatograms for aged asphalts that show an increase of large molecular size material is produced on aging in the TFO/PAV. Calibration of the column combination with materials of known molecular weight shows the major separation occurs in the large molecular size material area of the MSD. In addition, analysis of the CRM's has shown that the breakdown products from the heating of the rubbers of the CRM's at 200°C (392°F) appear in the large molecular size region of the MSD. The response of the two crumb rubbers to heating with the asphalts varies in that NR seems to solubilize sooner than does CR#4 for the same asphalt. In addition, the two crumb rubbers respond differently to being heated with different asphalts, i.e., solubilizing more rapidly in one asphalt than in another. This HPLC/SEC system has easily shown these differences.

REFERENCES

1. J.F. Branthaver, J.C. Petersen, R.E. Robertson, J.J. Duvall, S.S. Kim, P.M. Harnsberger, T. Mill, E. K. Ensley, F.A. Barbour, and J.F. Schabron, "Binder Characterization and Development. Volume 2: Chemistry. SHRP-A-368. Strategic Highway Research Program, National Research Council, Washington, DC, 39-76 (1993).
2. P.W. Jennings, J.A. Pribanic, M.F. Raub, J.A. Smith, and T.M. Mendes, "Advanced High Performance Gel Permeation Chromatography Methodology", SHRP AIIR-14 Final Report (1991).
3. G.R. Donaldson, M.W. Hlavinka, J.A. Bullin, C.J. Glover, and R.R. Davison, *J. Liquid Chrom.*, **11**, 749 (1988).
4. B. Brûlé, G. Raymond, and C. Such, "Relationships among Composition, Structure, and Properties of Road Asphalts", in "Asphaltenes and Asphalts, 1. Developments in Petroleum Science, 40" (T.F. Yen and G.V. Chilingarian, Ed.), Elsevier Science B.V. (1994).
5. S.W. Bishara, R.L. McReynolds, and E.R. Lewis, "Interrelationships between Performance-Related Properties of Asphalt Cement and Their Correlation with Molecular Size Distribution", *Transport. Res. Rec.*, **1323** (1991).
6. N.W. Garrick, *J. Mat. Civ. Eng.*, **6**, 376 (1994).
7. AASHTO Designation PPI, Edition 1A, September 1993, "Standard Practice for Accelerated Aging of Asphalt Binder Using a Pressurized Aging Vessel (PAV).

DISCLAIMER

This document is disseminated under the sponsorship of the Department of Transportation in the interest of information exchange. The United States Government assumes no liability for its contents or use thereof.

The contents of this report reflect the views of Western Research Institute which is responsible for the facts and the accuracy of the data presented herein. The contents do not necessarily reflect the official views of the policy of the Department of Transportation.

ACKNOWLEDGEMENTS

The author thanks the Federal Highway Administration for financial support under Contract No. DTFH61-92C-00170. The author also thanks J.C. Petersen, coworkers J.F. Branthaver and R.E. Robertson for encouragement and helpful suggestions in the preparation of this report, J. Greaser for help in preparation of the manuscript, and Anthony Munari for help in preparation of the figures.

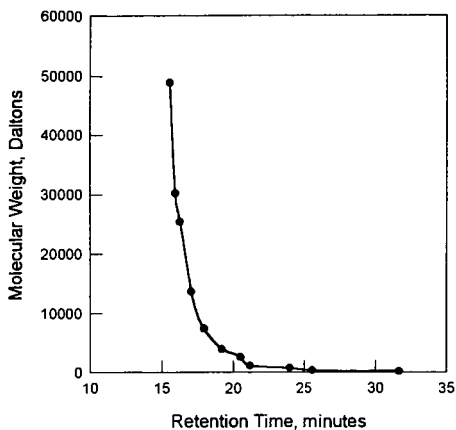


Figure 1. Calibration for column configuration of 2-500 Å and 1-100 Å Phenogel (5 μ) columns in series at 40°C (104°F) with 1.0 mL/min toluene carrier

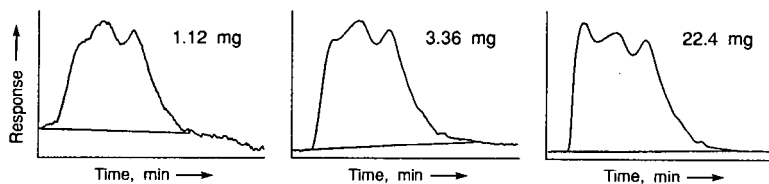


Figure 2. HPLC/SEC chromatograms of asphalt AAD-1 at three sample sizes

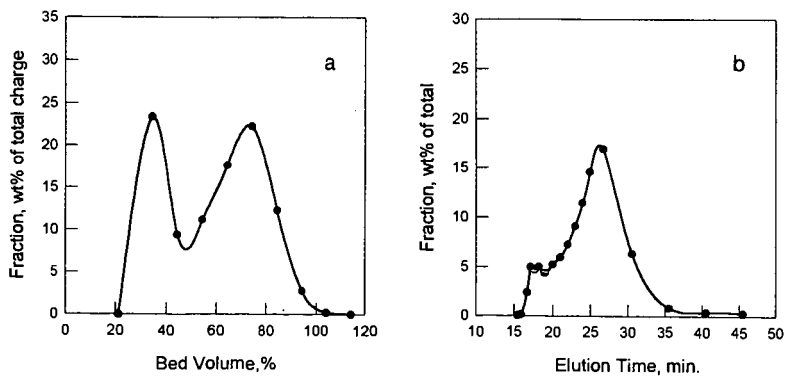


Figure 3. Chromatograms for asphalt AAD-1 from (a) preparative SEC and (b) HPLC/SEC

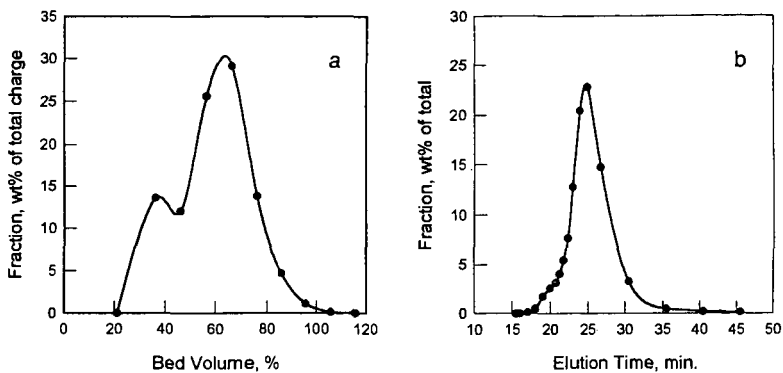


Figure 4. Chromatograms for asphalt AAC-1 from (a) preparative SEC and (b) HPLC/SEC

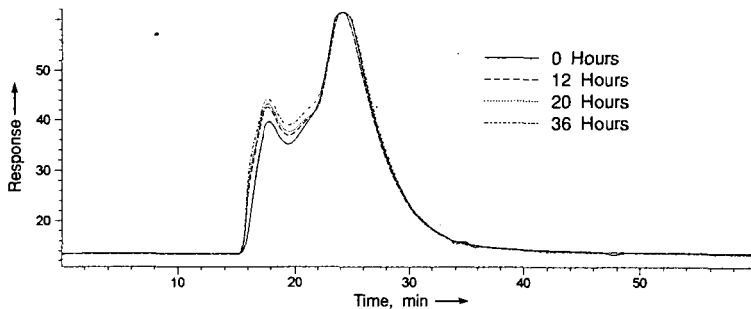


Figure 5. HPLC/SEC chromatograms for asphalt AAC-1 TFO/PAV aged at 100°C (212°F) for different times

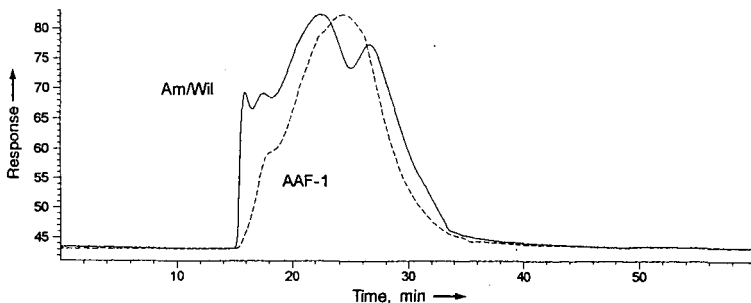


Figure 6. HPLC/SEC chromatograms for asphalt AAF-1 and Amoco/Wilmington AC 2.5

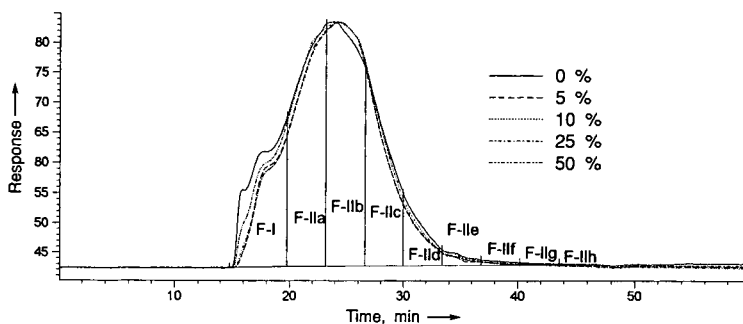


Figure 7. HPLC/SEC chromatograms for asphalt AAF-1 and various percentages of Amoco/Wilmington AC 2.5, showing fraction cutpoints

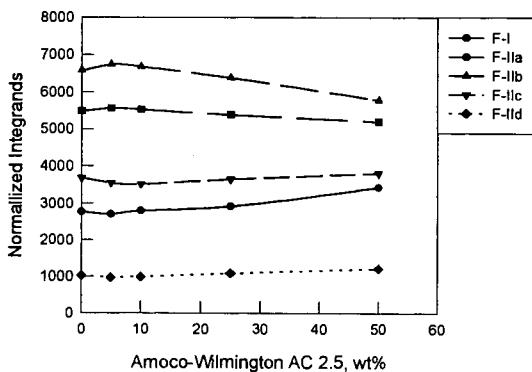


Figure 8. Normalized integrands versus wt% Amoco/Wilmington AC 2.5 in asphalt AAF-1 for various HPLC/SEC fractions

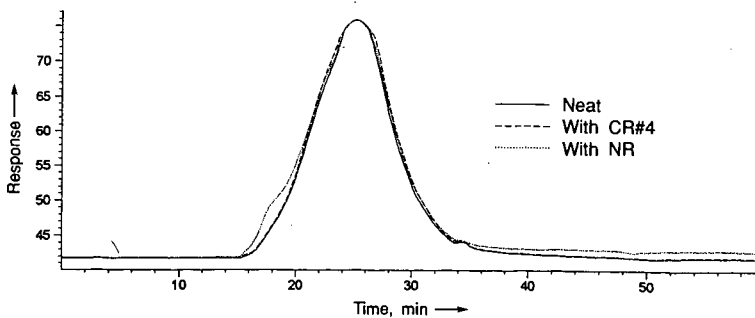


Figure 9. HPLC/SEC chromatograms for asphalt ABD-1 neat and with 12% crumb rubber NR or CR#4 mixed but with no additional heating

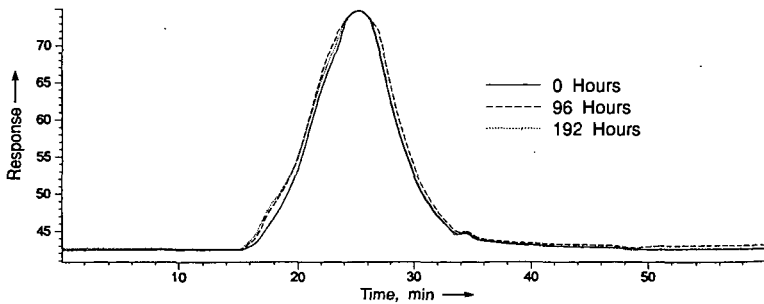


Figure 10. HPLC/SEC chromatograms for neat asphalt ABD-1 heated at 200°C (392°F) for various times

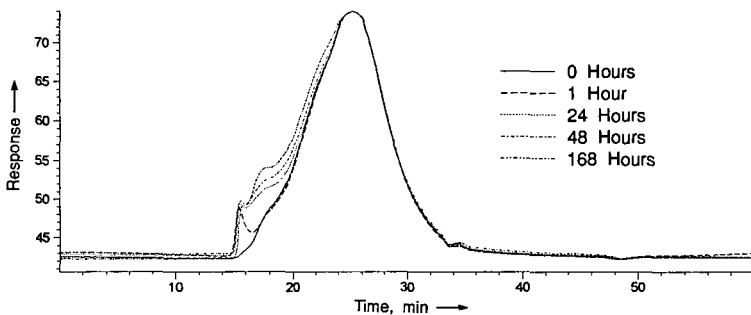


Figure 11. HPLC/SEC chromatograms for asphalt ABD-1 with 12% crumb rubber NR, heated at 200°C (392°F) for various times

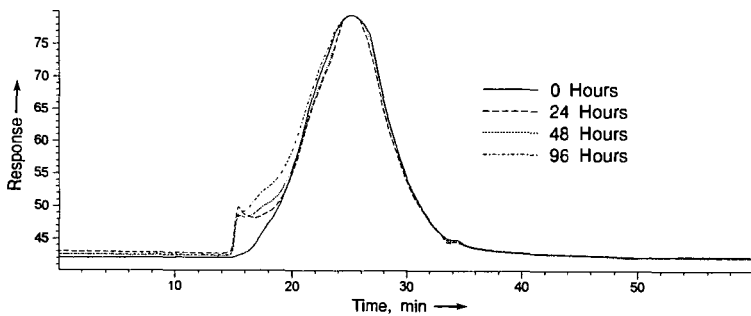


Figure 12. HPLC/SEC chromatograms for asphalt ABD-1 with 12% crumb rubber CR#4, heated at 200°C (392°F) for various times

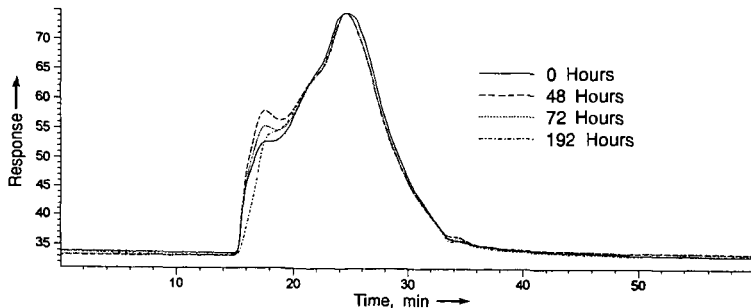


Figure 13. HPLC/SEC chromatograms for neat asphalt AAB-1 heated at 200°C (392°F) for various times

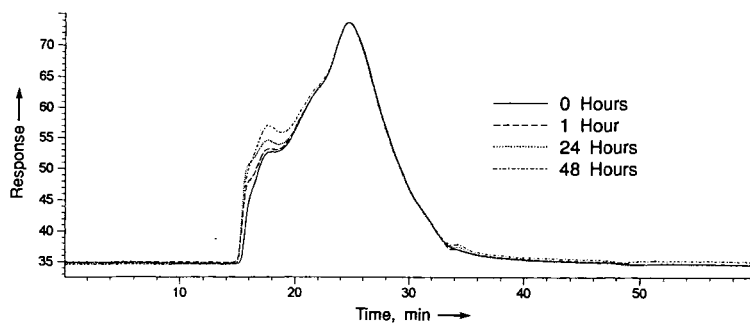


Figure 14. HPLC/SEC chromatograms for asphalt AAB-1 with 12% crumb rubber NR, heated at 200°C (392°F) for various times

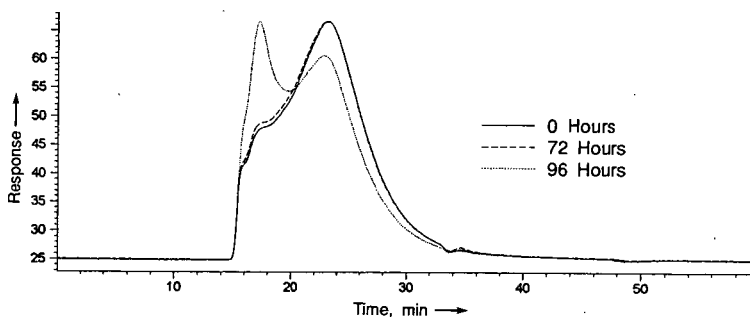


Figure 15. HPLC/SEC chromatograms for neat asphalt AAM-1 heated at 200°C (392°F) for various times

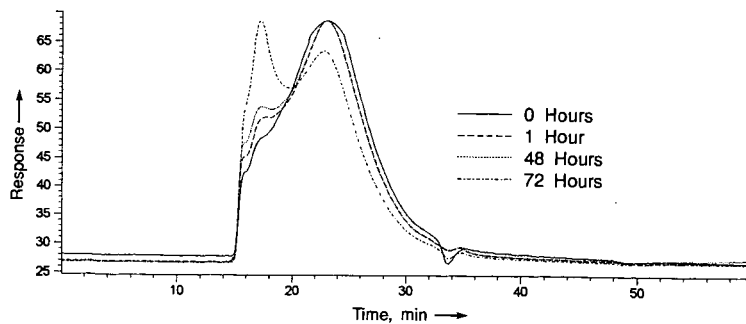


Figure 16. HPLC/SEC chromatograms for asphalt AAM-1 with 12% crumb rubber NR, heated at 200°C (392°F) for various times

ASPHALT COMPATIBILITY TESTING USING THE AUTOMATED HEITHAUS TITRATION TEST

Adam T. Pauli
Western Research Institute
365 North 9th Street, Laramie, WY 82070-3380

Key words: asphalt compatibility, peptization, flocculation

ABSTRACT

The Heithaus titration test or variations of the test have been used for over 35 years to predict compatibilities of blends of asphalts from different crude sources. Asphalt compatibility is determined from three calculated parameters that measure the state of peptization of an asphalt or asphalt blend. The parameter p_a is a measure of the peptizability of the asphaltenes. The parameter p_o is a measure of the peptizing power of the maltenes, and the parameter P , derived from p_a and p_o values, is a measure of the overall state of peptization of the asphalt or asphalt blend. In Heithaus' original procedure, samples of asphalt were dissolved in toluene and titrated with n-heptane in order to initiate flocculation. The onset of flocculation was detected either by photography or by spotting a filter paper with a small amount of the titrated solution. Recently, an "automated" procedure, after Hotier and Robin,¹ has been developed for use with asphalt. In the automated method UV-visible spectrophotometric detection measures the onset of flocculation as a peak with the percent transmittance plotted as a function of the volume of titrating solvent added to a solution of asphalt. The automated procedure has proven to be less operator dependent and much faster than the original Heithaus procedure. Results from the automated procedure show the data to be consistent with results from the original, "classical" Heithaus procedure.

INTRODUCTION

Historically, asphalts have been classified into gel-type asphalts and sol-type asphalts.² Gel-type asphalts usually are characterized by non-Newtonian rheological behavior, relatively low variation of viscosity with temperature, and low ductility. Sol-type asphalts exhibit more Newtonian rheological behavior, are highly temperature susceptible, and are more ductile. The two classifications represent extremes, and most asphalts are of intermediate nature. Sol-type asphalts have been designated as compatible asphalts, while gel-type asphalts have been designated as incompatible asphalts.

The terms "compatible" and "incompatible" (or sol-gel) arose from what became known as the colloidal model of asphalt structure. This model considers asphalts to be dispersions of what are termed "micelles," consisting of polar, aromatic molecules in viscous oils. The degree to which the so-called "micelles" form extended gel structures, unstable to heat and shear, will determine the relative degree of incompatibility. In a compatible asphalt, the dispersed materials are well peptized by the oils (maltenes), either because the dispersed materials are small in amount and/or tend not to form strong associations, and/or because the solvent effectively disperses the "micelles." In an incompatible asphalt, associations are more extensive and are not so efficiently peptized by the solvent.

The colloidal model has been subjected to much criticism in recent years. The principal objection is that there is no direct evidence for "micellar" structures, either classical or inverse, in asphalts. The term "micelle," which implies existence of a separate phase with distinct boundaries, may be inappropriate when applied to asphalts. Recently, a microstructural model of asphalt structure has been proposed.³ In this model, associations of polar molecules of varying sizes are considered to be dispersed in a polar moiety composed of less polar, relatively small molecules. No distinct phase boundaries are believed present. Nevertheless, the concept of compatibility as a measure of mutual miscibility of different chemical components of asphalts is useful. Compatible asphalts do differ from incompatible asphalts in their physical properties and in pavement performance. Highly compatible asphalts are not necessarily good to achieve all important performance related properties and likewise for low compatible asphalts. This makes compromises in compatibility necessary for optimum overall pavement performance.

Asphaltenes are solid materials which precipitate when asphalts are treated with solvents such as n-pentane, n-hexane, n-heptane, etc. Maltenes are the components of asphalts not precipitated by n-alkane solvents. Asphaltenes are more aromatic than maltenes and contain more heteroatoms. Thus intermolecular interactions are more extensive in asphaltenes than in maltenes. This is reflected in the greater molecular weights of asphaltenes compared with maltenes.⁴ In the colloidal model of

asphalt structure, asphaltenes are believed to correspond to the dispersed materials and maltenes to the solvent. Therefore, asphaltenes will be mainly responsible for the internal structure of asphalts and will dominate many physical properties.³ Thus the amount of asphaltenes in an asphalt is a rough measure of compatibility. Compatible asphalts generally have smaller amounts of asphaltenes than incompatible asphalts. Oxidative aging of an asphalt will decrease compatibility by formation of polar molecules, which cause increasing associations and result in more asphaltenes. The ease with which asphaltenes are dispersed is highly dependent on the dispersing power of maltenes, which are also a contributing factor to asphalt compatibility. The best known measurement of compatibility of asphalts that takes all the above factors into account is the Heithaus^{6,7} test. In this test, flocculation behavior of asphaltenes is measured. The method is tedious and does not work with waxy asphalts, so a study of asphaltene flocculation behavior to develop an improved compatibility test was implemented.

EXPERIMENTAL

What has been termed the classical Heithaus titration procedure is described below. Four 1.0 g samples of a test asphalt are placed into four 125 mL Erlenmeyer flasks. To the four flasks are added amounts of 1.0, 2.0, 4.0, and 6.0 mL toluene, respectively. After dissolution of the asphalt is completed, the flasks are immersed in a water bath maintained at 25°C (77°F) for 30 minutes. The flasks are titrated with 1.0 mL aliquots of n-heptane. After each addition of n-heptane, the contents of the flask are stirred for several minutes, and then inspected to observe if flocculation has taken place. Flocculation is detected by transferring a drop of the solution to a filter paper with a glass rod. The development of two rings on the filter paper signifies the onset of flocculation. Heithaus parameters p_a , p_o , and P are calculated from the flocculation ratio and the concentration, respectively. The flocculation ratio (FR) and concentration (C) are calculated as:

$$FR = \frac{V_s}{V_s + V_T} \quad (1)$$

$$C = \frac{W_a}{V_s \cdot V_T} \quad (2)$$

where V_s is the volume of solvent, V_T is the volume of titrant required to initiate flocculation and W_a is the weight of the asphalt. In the classical Heithaus procedure, FR values are calculated for solutions of asphalt at various concentrations, and concentration values are plotted versus flocculation ratio values. The x and y intercept values FR_{max} and C_{min}^{-1} extrapolated from the FR vs. C line are used to calculate Heithaus parameters p_a , the peptizability of asphaltenes; p_o , the peptizing power of maltenes; and P , the state of peptization of the asphalt, as follows:

$$p_a = 1 - FR_{max} \quad (3)$$

$$p_o = FR_{max}(C_{min}^{-1} \cdot 1) \quad (4)$$

$$P = \frac{p_o}{1 - p_a} \quad (5)$$

The automated Heithaus procedure differs somewhat from the classical procedure. In the automated procedure three to five samples of a test asphalt are weighed into 30 mL vials with Teflon sealed caps. Contrasting with the classical procedure, in which the weight of asphalt is held constant and the volume of solvent is varied, the automated procedure uses different weights of asphalt from sample to sample, and the volume of solvent is held constant. To the vials are added 0.5000 g to 1.0000 g \pm 0.0005 g of asphalt in 0.1 to 0.2 gram increments, respectively. Toluene (LC-grade) is added to each vial in 1.000 mL \pm 0.005 mL aliquots and the vials are capped and the asphalt sample is allowed to dissolve. Figure 1 depicts the apparatus that has been assembled to perform the automated procedure. The vials containing asphalt solutions are loaded into a reaction vessel maintained at 25°C (77°F) with a temperature controlled water bath and stirred for ten minutes. The temperature controlled solutions are circulated through a 0.1 mm flow cell housed within a UV-visible spectrophotometer using 0.16 cm (1/16") ID viton tubing and a metering pump. The titrant, either iso-octane (LC-grade) or n-heptane (LC-grade) which is also maintained at a constant temperature of 25°C \pm 0.1°C (77°F) is introduced into the vial through 0.055 cm (0.022") ID viton tubing with a second metering pump set at a fixed flow rate in the range of 0.300 mL/min to 0.500 mL/min. The change in the percent transmittance at an absorbance wavelength of 740 nm is plotted as a function of titrant flow rate and chart speed on a strip chart recorder. Figure 2 shows a typical

series of titration curves for asphalt AAD-1, one of the Strategic Highway Research Project (SHRP) core asphalts. The volume of titrant added is related to the distance from the start of a curve, when titrant is first introduced, to the apex of the peak (the onset of flocculation), L_p . Heithaus parameters are calculated using values of V_T that are calculated as:

$$V_T = \left(\frac{L_p}{v_c} \right) v_T \quad (6)$$

where L_p is the distance to the apex of the peak measured in centimeters, v_c is the chart recorder speed in cm/min and v_T is the titrant flow rate in mL/min.

Crossblend mixtures were prepared by mixing an arbitrary amount of maltenes from either asphalt with a specified amount of asphaltenes at the natural abundance level of the asphaltenes in either asphalt, resulting in eight different mixtures. Four of the mixtures have either AAF-1 or AAG-1 asphaltenes, four have either AAF-1 or AAG-1 maltenes, and four are mixed at either the AAF-1 or AAG-1 natural abundance level. Sample mixtures were labeled in terms of maltene type (M), asphaltene type (A), and asphaltene natural abundance level (L). Asphaltene and maltene fractions were mixed in round bottom flasks along with dichloromethane, used to dissolve and disperse the materials. Crossblend mixtures were dried using heat and vacuum distillation.

RESULTS AND DISCUSSION

Repeatability in the automated method is influenced by several variables. These are as follows: **Sample concentrations:** It was observed that with concentrations less than 0.50 g/mL, that plots of flocculation ratio (FR) versus concentration (C) deviated from linearity. This is assumed to be related to the pathlength of the flow cell; 0.10 mm used in this work. And when solutions greater in concentration than 1.1 g/mL are tested, several hours are required for complete sample dissolution, increasing the likelihood for sample oxidation due to prolonged exposure to the aerated solvent. This left only a narrow range of solution concentrations with which to work with, thus placing a greater emphasis on accuracy in other variables relevant to the procedure, such as accurate sample weights, consistency in titrant flow rate, and consistency in circulation flow rate. **Temperature:** It was found to be necessary to control both solution temperature and the titrant temperature as well to within 0.1°C. Fluctuations in lab temperature were also found to affect repeatability in data, making recording lab temperature standard practice. **Titrate flow rate and flow rate consistency:** It was found that in order to achieve an accuracy of approximately 0.05 in the value of P that the flow rate had to be steady to within 0.005 mL/min over a 20 minute period or longer, and that the flow rate had to be below 0.500 mL/min with the sample sizes that were being used. **Circulation flow rate:** It is necessary to control flow rate because solution viscosities increase with increasing concentrations. It was found that the circulation flow rate needs to be as fast as possible, at minimum the circulation flow rate needed to run at a rate of 10 mL/min and to vary no less than 0.5 mL/min when more concentrated solutions were tested. **Stirring rate, for mixture homogeneity and temperature control:** The stirring rate needed to be fast enough to adequately mix the solution, but not so fast as to heat the solution. **Titrate solvent (iso-octane in place of n-heptane):** It was found that certain waxy asphalts (AAC-1 and AAM-1 for example) were difficult or impossible to test using n-heptane as the titrating solvent. When iso-octane, which has a lower solubility parameter ($\delta = 6.90$) than n-heptane ($\delta = 7.46$), was used in place of n-heptane, all SHRP core asphalts could be tested. For non-waxy asphalts, n-heptane is a suitable titrant.

It was determined from a statistical analysis that poor repeatability in the classical procedure was due to systematic error. Figure 3 shows that a correlation, $R^2 = 0.94$ may be drawn between the weight percent of n-heptane asphaltenes for six SHRP core asphalts when plotted versus sample standard deviations in P parameters obtained using the classical procedure. It was surmised that removal of sample from solution for the purpose of performing the spot test to detect the onset of flocculation was the source of operator error in the classical procedure. With more compatible asphalts this error would be more pronounced because, for compatible asphalts (relatively low levels of asphaltenes) more titrant is required to promote the onset of flocculation and the spot testing is performed more often throughout the titration.

Table 1 shows Heithaus parameter and sample standard deviation data collected by three different operators using the automated procedure titrated with iso-octane, and sample standard deviation data collected by a single operator using the classical procedure, titrated with n-heptane for SHRP core asphalt AAD-1. It is seen from Table 1 that data gathered on this asphalt by three different operators using the automated procedure is almost as repeatable as data gathered by a single operator using the classical procedure. It has been found that compatibility data gathered for asphalts having

higher concentrations of asphaltenes (incompatible) generally give repeatable results using the classical procedure.

The problem that arises in the classical procedure lies in gathering repeatable data for asphalts having lower concentrations of asphaltenes (compatible). Thus, Table 1 shows a notable improvement in data gathered for a compatible SHRP core asphalt; AAM-1, in terms of sample standard deviation values of Heithaus compatibility parameters using both procedures.

Figure 4 depicts P-values for seven SHRP core asphalts using the classical procedure and titrated with n-heptane, plotted versus P-values using the automated procedure and titrated with iso-octane as being consistent with one another. It is not to be expected that the Heithaus parameters obtained by either method will be identical when different titrants are used. Similar plots using p_a and p_o values for the same seven SHRP core asphalts were not in as good agreement. According to Branthaver et al.⁸ asphaltenes precipitated from asphalts using iso-octane were found to have different physical properties than asphaltenes precipitated using n-heptane. This raised the question of what p_a and p_o values actually measure. Two hypotheses were formulated. First, p_a and p_o values are representative of the types of asphaltenes and maltenes, respectively found in a particular asphalt; or alternatively, p_a and p_o values are representative of the amount of asphaltenes present in an asphalt.

To verify which hypothesis was correct, asphaltene/maltene crossblend mixtures were prepared from asphaltene and maltene fractions separated from a compatible asphalt (AAG-1) and a somewhat less compatible asphalt (AAF-1). Table 2 shows compatibility data collected on eight AAG-1/AAF-1 crossblend mixtures that were titrated with n-heptane using the automated procedure. Results in Table 2 show p_a -values being more closely related to natural asphaltene abundance levels (L) and P-values also somewhat related to natural asphaltene abundance levels. Table 2 also shows p_o values being weakly related to asphaltene type (A), but not asphaltene concentration (C).

CONCLUSION

The application of an automated procedure to test asphalt compatibility appears feasible. Results show the automated procedure to be less operator dependent and more rapid than the classical procedure. Several variables relating to the repeatability of the automated procedure have been isolated, among them; sample concentrations, temperature, circulation, stirring and titrant flow rates, and titrating solvent. Heithaus P parameters measured for seven SHRP core asphalts using both automated and classical procedures show the data to be consistent from one procedure to the other. Asphaltene/maltene crossblend mixtures prepared using SHRP core asphalts AAG-1 and AAF-1 were tested using the automated procedure. Results for crossblend mixtures show that measured values of p_a relate more closely to an asphalt's asphaltene concentration, whereas, p_o values appear to be influenced by asphaltene type.

DISCLAIMER

This document is disseminated under the sponsorship of the Department of Transportation in the interest of information exchange. The United States Government assumes no liability for its contents or use thereof.

The contents of this report reflect the views of Western Research Institute which is responsible for the facts and the accuracy of the data presented herein. The contents do not necessarily reflect the official views of the policy of the Department of Transportation.

ACKNOWLEDGMENTS

The author gratefully acknowledges the Federal Highway Administration for its financial support of this work as part of contract No. DTFH61-92-C-00170 at Western Research Institute, Laramie, Wyoming. Automated Heithaus titrations were performed by A.T. Pauli, P. Holper, J. Hart, S. Salmans, and C. Wright. Classical Heithaus titrations were performed by D. Colgin, and M.W. Catalfomo. Asphaltene/maltene crossblend mixtures were prepared by J.F. Branthaver and S. Salmans. The manuscript was prepared by A.T. Pauli and J. Greaser. Figures and tables were prepared by T. Munari and A. T. Pauli. The author gratefully acknowledges C. Petersen, R.E. Robertson and J.F. Branthaver for a thoughtful review.

REFERENCES

- Hoiter, G., and M. Robin. Action De Divers Diluants Sur les Produits Petroliers Lourds: Mesure, Interpretation et Prevision de la Flocculation des Asphaltenes. Revue de L' Institut Francais du Petrole, **38**, 1983, pp. 101-120.
- Traxler, R. N. Asphalt: Its Composition, Properties and Uses. Reinhold, New York, 1961.
- SHRP A-367, Binder Characterization and Evaluation, Volume I. Strategic Highway Research Program, National Research Council, Washington D.C., 1994, pp. 9-25.
- Koots, J. A. and J. G. Speight (1975), Relationship of Petroleum Resins to Asphaltenes. Fuel, **54**, pp. 179-184.
- Boduszynski, M. M. Asphaltene in Petroleum Asphalts: Composition and Formation. In "Advances in Chemistry Series: Chemistry of Asphalts," J. W. Bunger and N. C. Li, eds., Am. Chem. Soc., Washington, D.C., **195**, 1981, pp. 119-135.
- Heithaus, J. J. (1960), Measurement and Significance of Asphaltene Peptization. Am. Chem. Soc., Div. Petrol. Chem. Prepr., **5**, pp. A23-A37.
- Heithaus, J. J. (1962), Measurement and Significance of Asphaltene Peptization. J. Inst. Petrol., **48**, pp. 45-53.
- Branthaver, J. F., J. C. Petersen, J. J. Duvall, and P. M. Harnsberger. Compatibilities of Strategic Highway Research Program Asphalts. Transportation Research Record 1323. TRB, National Research Council, Washington D.C., 1991, pp. 22-31.

Table 1. Comparison of the repeatability in data obtained using either the automated or classical procedure.

Asphalt, procedure, operator:		Heithaus parameters		
		P _a	P _o	P
AAD-1, automated:	Operator-1	0.688	0.682	2.18
	Operator-2	0.686	0.731	2.32
	Operator-3	0.701	0.637	2.13
	Average	0.691	0.683	2.21
	Std. Dev.	0.008	0.047	0.10
AAD-1, classical, single operator:	Average	0.61	1.33	3.43
	Std. Dev.	0.01	0.02	0.04
AAM-1, automated, single operator:	Average	0.907	0.66	7.08
	Std. Dev.	0.006	0.10	0.59
AAM-1, classical, single operator:	Average	0.89	1.26	12.19
	Std. Dev.	0.03	0.04	2.59

Table 2. Heithaus parameters of AAG-1/AAF-1 asphaltene-maltene crossblend mixtures.

Crossblend Mixture Design M A L *	Heithaus parameters		
	P _a	P _o	P
G F F	0.67	1.11	3.35
F F F	0.67	1.03	3.09
G F G	0.76	1.07	4.48
F F G	0.64	2.72	7.59
G G G	0.77	1.37	6.02
F G F	0.66	1.45	4.28
G G F	0.68	1.43	4.41
F G G	0.77	1.04	4.46

*M: maltene type, A: asphaltene type, L: natural abundance level of asphaltenes in asphalt listed.

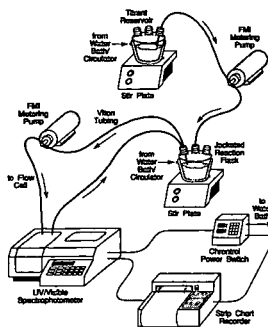


Figure 1. Apparatus used in automated Heithaus procedure.

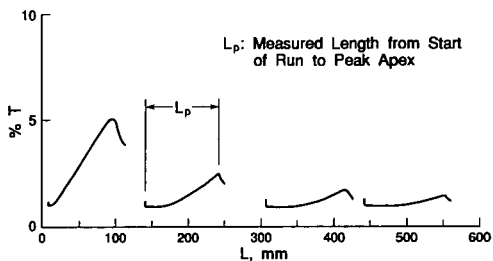


Figure 2. Flocculation peaks of one SHRP core asphalt; AAD-1.

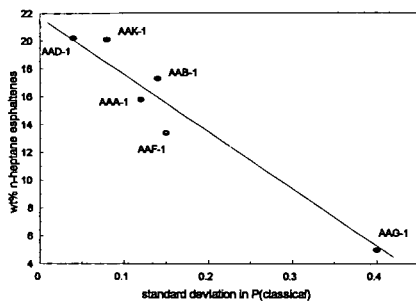


Figure 3. The relationship between asphaltene concentration and sample standard deviations in average values of the parameter.

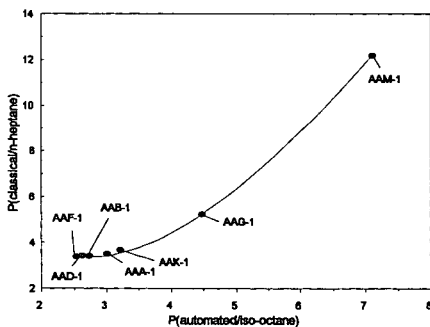


Figure 4. Relationship between Heithaus P parameters obtained using the automated procedure and the classical procedure.

RHEOLOGICAL PROPERTIES OF ASPHALT CROSSBLENDS

Jan F. Branthaver and Stephen L. Salmans
Western Research Institute,
365 North 9th Street, Laramie, WY 82070-3380

Key words: asphalt compatibility, size exclusion chromatography, rheology

ABSTRACT

Properties of blends of asphalts from different sources can not necessarily be predicted by averaging properties of the components. Asphalts may be considered to be combinations of a dispersed and a solvent moiety, the nature and amounts of which vary among asphalts. Asphalt properties will be determined by the manner in which the two moieties interact. In this work, dispersed and solvent moieties were generated from eight asphalts by size exclusion chromatography. Crossblended mixtures of dispersed and solvent moieties from different asphalts were prepared and their rheological properties measured. The influence of the relative amounts and nature of the two moieties on rheological properties were determined. It was found that rheological properties of the crossblended mixtures were greatly affected by the relative amounts of the two moieties. The nature of the two moieties also was influential in determining rheological properties, as the solvent components of some asphalts were found to be compatible with the dispersed moieties of some asphalts but incompatible with others.

INTRODUCTION

The compatibility of asphalt systems long has been of interest to researchers. Traxler¹ discusses the difference in properties among what are designated as compatible (sol-type) and non-compatible (gel-type) asphalts. According to Traxler, well-dispersed, compatible asphalts exhibit high temperature susceptibility of viscosity, high ductility, low elasticity, and low rates of oxidative age hardening. Non-compatible asphalts, which are poorly dispersed, are characterized by low temperature susceptibility, low ductility, pronounced elasticity, and high aging rates. These and other physical properties serve to categorize asphalts according to compatibility. The two fundamental types of asphalts will, of course, vary markedly in pavement performance.

Asphalt compatibility also is related to chemical composition. Non-compatible asphalts tend to be high in asphaltene and sulfur content compared with compatible systems. Heithaus² published a laboratory method that assigns numerical values to asphalts and asphalt blends according to compatibility. Heithaus considered asphalts to be dispersions of asphaltenes in a maltene solvent, and asphalt and asphalt blend properties therefore should be determined by the relative amounts of the two materials and the effectiveness by which maltenes disperse asphaltenes. The properties of asphalt blends thus are not necessarily computed additively from properties of their parent asphalts.

Properties of blends of various fractions of different asphalts have been studied. Altgelt and Harle³ measured rheological properties of various asphaltene-maltene combinations. Traxler⁴ studied mixtures prepared using solvent-derived fractions. During the Strategic Highway Research Program (SHRP)⁵, mixtures of asphalt fractions prepared by size exclusion chromatography (SEC) were studied. Very large differences in rheological properties of crossblended mixtures of asphalt SEC fractions from different sources were observed. The SEC fractions were chosen because the separation method fractionates solutions of asphalts according to molecular size. If asphalts consist of a dispersed and a dispersing component, the dispersed component should consist of the more polar, aromatic constituents of asphalts, which should be of higher apparent molecular weight than the dispersing, or solvent, component.⁶ The two components thus should be to some degree separable by SEC. A large number of asphalts have been separated into two SEC fractions that are believed to approximate asphalt dispersed and solvent components. The properties of the two components have been measured for these asphalts and vary according to source.⁵ Relative amounts of the two fractions also vary considerably among asphalts, and this relative abundance of the two SEC fractions in an asphalt is termed the natural abundance ratio. The two fractions are designated SEC Fraction-I and SEC Fraction-II, which correspond to the dispersed and solvent components of asphalts respectively. The relative amounts of the two SEC fractions in an asphalt do not correspond to asphaltene and maltene yields.

Rheological properties of asphalts depend on relative amounts of dispersed and solvent components. The solvent component is much less viscous and less elastic than the dispersed component, which contains the viscosity-building constituents. Presumably, the nature of the two components and the manner of their interaction also affect rheological properties. Another physical property, the glass transition temperature, is determined by the relative amount of the two components and the source

of the solvent component, but not the source of the dispersed component.⁷ Other properties conceivably might depend more on the source of the dispersed component than the solvent. It is the goal of this study to quantify the influence of these three factors, source of solvent component, source of dispersed component, and relative amounts of the two, on asphalt rheological properties.

EXPERIMENTAL

The separation of asphalts into two fractions by SEC has been described previously.⁸ The SEC Fraction-I materials are friable solids, and the SEC Fraction-II materials are viscous liquids. Crossblended mixtures were prepared by dissolving weighted fractions of each of two different SEC fractions in dichloromethane and combining the two solutions in a round-bottom flask. The flask was attached to a rotary evaporator and was immersed in a water bath. Most solvent was removed by heating the flask to 90°C (194°F) for one hour under vacuum. Residual solvent was removed by replacing the water bath with an oil bath and heating the flask to 130°C (266°F) under vacuum for one hour. The flask and contents were flooded with an inert gas and stoppered. Rheological measurements on the crossblended mixtures were obtained at 25°C (77°F) using a Rheometrics mechanical spectrometer. Usually, 8 mm plates were used, and strain rates of 3-15% were employed, depending on sample stiffness. Phase angles and dynamic shear modulus values were obtained over a wide range of shear rates to generate the Black plots in Figures 1-7. Each sample was annealed before rheological analysis.⁸ If this step is not performed, erratic viscosity determinations are observed.

DISCUSSION

As stated above, the purpose of this work is to evaluate the compatibilities of crossblended mixtures of SEC fractions of asphalts and evaluate the influence of three factors on crossblend rheology. The three factors are the source of SEC Fraction-II (solvent), the source of SEC Fraction-I (dispersed component), and relative amount of each fraction in the crossblended mixture.

Eight asphalts studied in SHRP were separated into SEC Fractions I and II by SEC. These eight asphalts, called core asphalts, were intensively studied. They are coded as listed in Table 1, which also lists amounts of each of the two SEC fractions in each asphalt. These amounts are the natural abundance levels, and they vary considerably.

Seven sets of crossblended mixtures were prepared. Each set consists of eight members. In each set, the SEC Fraction-II component is the same. The SEC Fraction-I component is varied among members of the set. The ratio of components for each set is that of the parent asphalt of the SEC Fraction-II component. No set of crossblends was prepared from the SEC Fraction-II of asphalt AAM-1, because of the high natural abundance of SEC Fraction-I in this asphalt. Crossblends involving the SEC Fraction-II of AAM-1 have very high viscosities.⁵

Table 2 lists absolute viscosities of seven sets of crossblended mixtures at 25°C (77°F) and 1.0 rad/s. Each column in Table 2 corresponds to one of the seven sets of crossblends, in which the relative abundance of the two SEC fractions and the nature of the SEC Fraction-II are constant. In each column of data, only the source of the SEC Fraction-I changes from entry to entry down a column. Each row in Table 2 lists viscosities of crossblends in which the SEC Fraction-I source is constant. The SEC Fraction-II source and the relative abundance of the two fractions change from entry to entry along a row.

The entries in Table 2 in which both the SEC fractions are derived from the same source correspond to reconstituted parent asphalts. The viscosities of these mixtures are observed to be two to three times larger than the original asphalts. This is because light ends are lost in the workup process, resulting in somewhat enhanced viscosities in the reconstituted mixtures.

Figures 1-7 are Black plots of rheological data collected on the mechanical spectrometer for the seven sets of crossblends. Dynamic moduli (G^*) values at 25°C (77°F) were measured for each mixture at numerous rates of shear, and the value of the phase angle (δ) at each rate of shear was plotted against the G^* value. Low δ values indicate substantial elastic components in an asphalt, and vice versa. Asphalts whose Black plots exhibit large δ changes for a given range of G^* are shear susceptible. All crossblended mixtures whose Black plots are illustrated in Figure 1 contain 78.3 mass % of SEC Fraction-II of AAA-1. The Black plots of the eight different mixtures vary greatly. The mixture containing SEC Fraction-I of AAD-1 is very distinct from the other seven in that δ values in the Black plot are lower for a given G^* value and do not range over wide values of δ . This means that the mixture containing SEC Fraction-I of AAD-1 contains the largest elastic component and is least shear susceptible. On the right side of Figure 1, the mixture containing SEC Fraction-I of AAM-1 is characterized by much larger δ values and lower G^* values. The Black plot of this mixture

indicates that its rheological properties will be very different from those of the mixture containing SEC Fraction-I of AAD-1. Due to the composition of the mixtures, the difference must be caused by the nature of the SEC Fraction-I materials. In Figure 1, the curve corresponding to the mixture containing SEC Fraction-I of AAG-1 also is somewhat distinctive. This curve ranges over a wide δ range, indicating that the mixture is highly shear susceptible. The curves corresponding to mixtures containing SEC Fraction-I of AAA-1, AAB-1, AAC-1, and AAF-1 are virtually superimposable. The curve corresponding to the mixture containing SEC Fraction-I of AAK-1 shows that this mixture is not as shear susceptible as most of the other mixtures.

The Black plots of the other six sets of mixtures exhibit similar trends to those observed in Figure 1 (Figures 2-7). Curves representing rheological data for mixtures containing SEC Fraction-I of AAD-1 lie at the lowest values of δ for a given range of G^* values, and curves representing rheological data for mixtures containing SEC Fraction-I of AAM-1 exhibit contrary characteristics. In Figure 6, the differences are not very pronounced. This is because the concentration of SEC Fraction-I materials in asphalt AAG-1 is low. The mixtures containing SEC Fraction-I of AAG-1 are most shear susceptible, based on inspection of the Black plots. Again, the lines in Figure 6 are not sufficiently differentiated to demonstrate this tendency. Curves representing rheological data for mixtures containing SEC Fraction-I of the other five asphalts are more or less similar and are intermediate between the other three curves. In Figures 1, 2, 4, and 8, the Black plots of mixtures containing SEC Fraction-I of AAK-1 indicate that these mixtures are relatively less shear susceptible.

The Black plots of the mixtures, and correspondingly their rheological properties, become more distinct as the concentration of SEC Fraction-I in the mixture increases, and vice-versa.

Reduced specific viscosities of all the crossblended mixtures have been calculated and are listed in Table 3. In order to do this, relative viscosities of the mixtures first were calculated. The relative viscosity of a mixture is the ratio of the viscosity of the solution divided by the viscosity of the solvent, both measured at the same temperature and rate of shear. For the crossblended mixtures, it is assumed that the SEC Fraction-II component is the solvent, and so relative viscosities may be calculated by dividing each entry in Table 2 by the appropriate entry in Table 1. The viscosities of the SEC Fraction-II materials vary considerably and affect the absolute viscosities of the mixtures. Specific viscosities then are calculated from relative viscosities by subtracting unity (one) from the relative viscosities. Reduced specific viscosities are calculated by dividing specific viscosities by the mass fraction of SEC Fraction-I, the solute, in a mixture. For example, the mass fraction of SEC Fraction-I in the eight mixtures listed in column 1 of Table 3 is 0.217.

Reduced specific viscosities are measures of compatibility of a system. Inspection of Table 3 reveals that the values range from 10, indicating a highly compatible system, to over 1,600, indicating a highly non-compatible system. Four of the sets of eight crossblends (columns 1, 2, 4, and 7 in Table 3) contain ~ 0.21 - 0.25 mass fraction of SEC Fraction-I, so that the concentrations of the dispersed components in these mixtures are more or less equivalent. The other three sets of crossblends (columns 3, 5, and 6 in Table 3) have lower concentrations of SEC Fraction-I (0.11 - 0.14). In most cases, the entries in columns 1, 2, 4, and 7 in Table 3 are much higher than the entries in columns 3, 5, and 6. The exceptions are the last entries in the columns, corresponding to mixtures in which the SEC Fraction-I component is derived from asphalt AAM-1. Therefore the concentration of SEC Fraction-I in a mixture usually strongly influences compatibility of the mixture. The AAM-1 SEC Fraction-I obviously is an unusual material. In columns 1, 2, 4, and 7, Table 3, even if the AAM-1 entries are discounted, reduced specific viscosity values vary greatly. Those mixtures in which SEC Fraction-I is derived from AAG-1 usually have relatively low reduced specific viscosities. Those mixtures in which the SEC Fraction-I is derived from AAD-1 have high reduced specific viscosities. The same trends are observed in the entries in columns 3, 5, and 6, Table 3. In the discussion on Black Plots above, it was emphasized that mixtures containing SEC Fraction-I components of AAD-1, AAG-1, and AAM-1 are unique, but in different ways. Reduced specific viscosities of mixtures containing SEC Fraction-I of the other five asphalts do not appear to vary as systematically. This indicates that specific interactions of these SEC Fraction-I materials with SEC Fraction-II materials influence compatibilities of mixtures. Inspection of columns 1, 2, 4, and 7 shows that the reduced specific viscosity values in column 1 tend to be somewhat higher than those in the other three columns. Therefore the SEC Fraction-II of AAA-1 is the least effective solvent of the four SEC Fraction-II materials. Similar considerations lead to the conclusion that SEC Fraction-II of AAF-1 is a better solvent than that of AAC-1. Concentrations of SEC Fraction-I in the two sets of crossblends are almost identical, and reduced specific viscosities in column 3 are much lower than those in column 5.

If the values in Table 3 are read across in rows instead of columns, it is evident that the nature of the SEC Fraction-II component of a particular mixture does not influence reduced specific viscosities as much as does the nature of the SEC Fraction-I component or the relative amounts of the two

components. Nevertheless there is some influence of the SEC Fraction-II source. The data in Table 3 indicate that certain combinations of materials lead to unexpectedly large incompatibilities or the reverse.

CONCLUSIONS

Crossblended mixtures of asphalts have been prepared from two size exclusion chromatography fractions derived from eight different asphalts. The rheological properties of the mixtures were determined and it was found that, with one exception, the nature of the fraction assumed to correspond to the asphalt dispersed component and its relative abundance strongly influences rheological properties. These materials, which are the initial size exclusion chromatography eluates, are known to contain most of the polar, aromatic viscosity-building components of asphalts. The nature of the fraction corresponding to asphalt solvent components has a lesser influence on measured rheological properties of most crossblended mixtures, again with the exception of one set of mixtures.

REFERENCES

1. Traxler, R. N. Asphalt, Its Composition, Properties, and Uses, Reinhold, New York, 1961. Chapter 5.
2. Heithaus, J. J. (1962), J. Inst. Petrol., 48, pp. 45-53.
3. Altgelt, K. H., and O. L. Harle (1975), Ind. Eng. Chem., Prod. Res. Dev., 14, pp. 240-246.
4. Traxler, R. N. (1960), Preprints, Div. Petrol. Chem., Am. Chem. Soc., 5, pp. A71-A77.
5. SHRP-A-368, Binder Characterization and Evaluation, Volume 2: Chemistry. Strategic Highway Research Program, National Research Council, Washington, D.C., 1993.
6. SHRP-A-367, Binder Characterization and Evaluation, Volume 1. Strategic Highway Research Program, National Research Council, Washington, D.C., 1994, pp. 9-25.
7. Turner, T. F., S. S. Kim, J. F. Branthaver, and J. F. McKay, Symposium on Chemistry and Technology of Asphalt-Containing Materials, 210th Meeting of the Am. Chem. Soc., Chicago, IL, Aug. 22, 1995.
8. SHRP-A-370, Binder Characterization and Evaluation, Volume 4: Test Methods. Strategic Highway Research Program, National Research Council, Washington, D.C., 1994.

DISCLAIMER

This document is disseminated under the sponsorship of the Department of Transportation in the interest of information exchange. The United States Government assumes no liability for its contents or use thereof.

The contents of this report reflect the views of Western Research Institute which is responsible for the facts and the accuracy of the data presented herein. The contents do not necessarily reflect the official views of the policy of the Department of Transportation.

ACKNOWLEDGMENTS

The authors thank the Federal Highway Administration for supporting this work under Contract No. DTFH61-92C-00170. Rheological measurements were performed by P. M. Harnsberger and F. A. Reid. J. Greaser prepared the manuscript. Figures were prepared by S. S. Kim.

Table 1. Yields of SEC Fractions of Eight SHRP Asphalts and Viscosities of SEC Fraction-II

Asphalt	Natural Abundance of SEC Fraction, Mass %		Viscosity (25°C; 1.0 rad/s) of SEC Fraction-II, Pa·s
	SEC Fraction-I	SEC Fraction-II	
AAA-1	21.7	78.3	506
AAB-1	20.8	79.2	1,367
AAC-1	13.6	86.4	8,602
AAD-1	21.2	78.8	336
AAF-1	13.3	86.7	53,350
AAG-1	11.2	88.8	62,380
AAK-1	24.8	75.2	1,124
AAM-1	31.8	68.2	26,350

Table 2. Viscosities (Pa·s) of Crossblended Mixtures of SEC Fractions of Asphalts, 25°C, 1.0 rad/s

Parent asphalt of SEC Fraction-I component of mixture	Parent asphalt of SEC Fraction-II component of mixture						
	AAA-1	AAB-1	AAC-1	AAD-1	AAF-1	AAG-1	AAK-1
AAA-1	65,200	179,600	230,100	36,100	642,400	204,400	155,100
AAB-1	90,500	148,400	220,800	36,800	384,900	403,600	198,600
AAC-1	95,900	148,000	156,100	43,300	571,900	362,950	251,300
AAD-1	177,300	223,100	225,400	59,200	884,300	764,800	240,700
AAF-1	101,400	185,400	225,900	50,000	507,000	466,300	217,400
AAG-1	36,700	97,300	138,600	26,600	502,400	405,500	164,750
AAK-1	95,800	145,100	185,700	31,300	344,600	332,250	165,450
AAM-1	3,500	10,200	26,500	3,000	114,900	125,900	10,600

Table 3. Reduced Specific Viscosity Values of Crossblended Mixtures of SEC Fractions of Asphalts, 25°C, 1.0 rad/s.

Parent asphalt of SEC Fraction-I component of mixture	Parent asphalt of SEC Fraction-II component of mixture						
	AAA-1	AAB-1	AAC-1	AAD-1	AAF-1	AAG-1	AAK-1
AAA-1	590	630	190	500	80	20	550
AAB-1	820	520	180	510	50	50	710
AAC-1	870	520	130	600	70	40	900
AAD-1	1,610	780	185	830	120	100	860
AAF-1	920	650	185	700	60	60	770
AAG-1	330	340	110	370	60	50	590
AAK-1	870	510	150	430	40	40	590
AAM-1	30	30	15	40	10	10	30

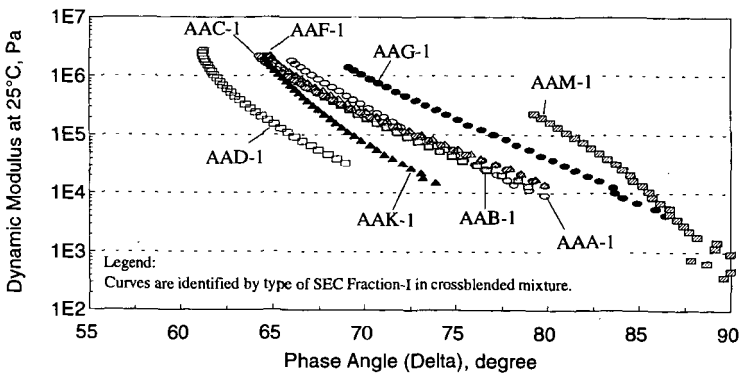


Figure 1. G^* vs. phase angle for mixtures of SEC Fraction-II of AAA-1 (78.3%) with SEC Fraction-I (21.7%) of eight different asphalts.

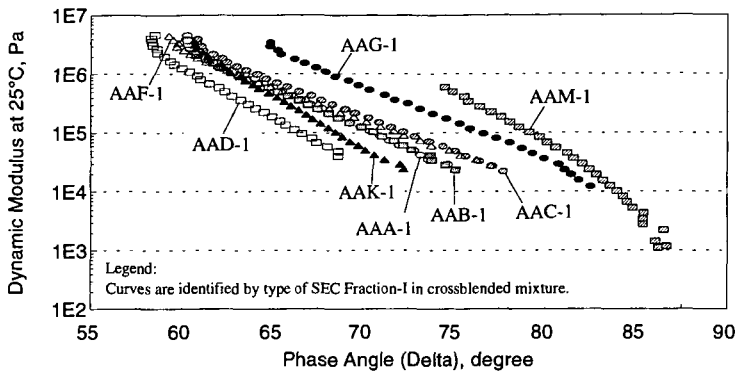


Figure 2. G^* vs. phase angle for mixtures of SEC Fraction-II of AAB-1 (79.2%) with SEC Fraction-I (20.8%) of eight different asphalts.

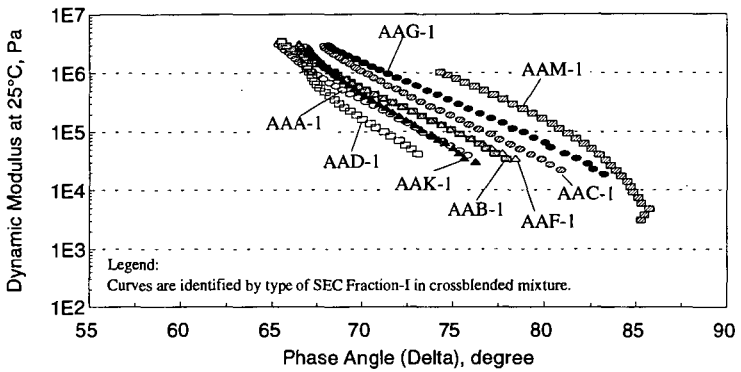


Figure 3. G^* vs. phase angle at 25°C for mixtures of SEC Fraction-II of AAC-1 (86.4%) with SEC Fraction-I (13.6%) of eight different asphalts.

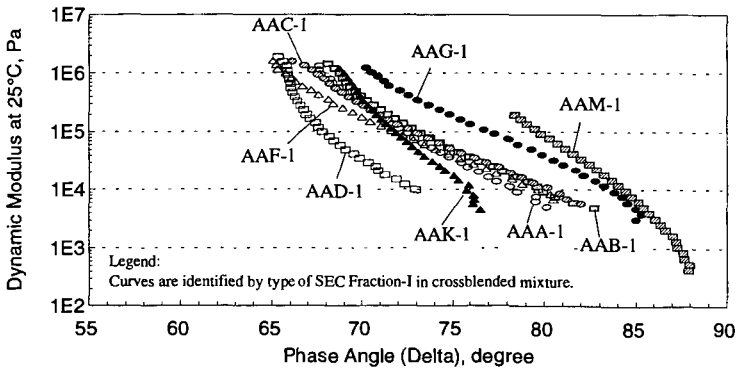


Figure 4. G^* vs. phase angle for mixtures of SEC Fraction-II of AAD-1 (78.8%) with SEC Fraction-I (21.2%) of eight different asphalts.

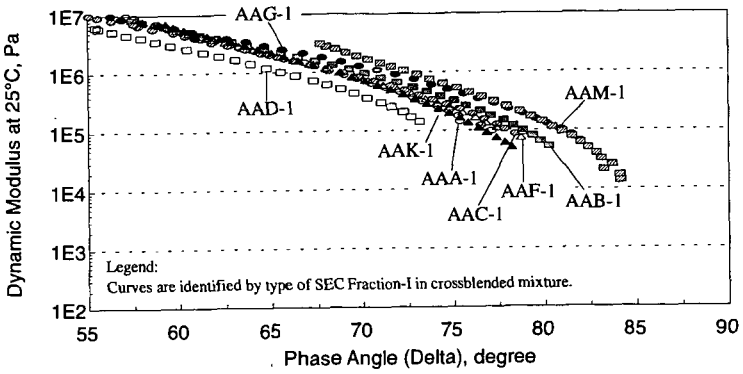


Figure 5. G^* vs. phase angle for mixtures of SEC Fraction-II of AAF-1 (86.7%) with SEC Fraction-I (13.3%) of eight different asphalts.

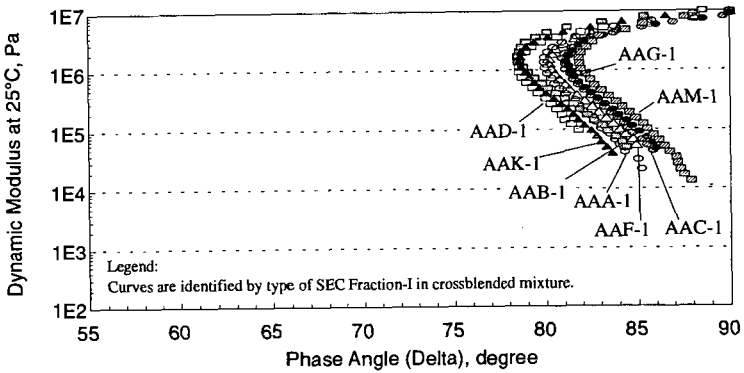


Figure 6. G^* vs. phase angle for mixtures of SEC Fraction-II of AAG-1 (88.8%) with SEC Fraction-I (11.2%) of eight different asphalts.

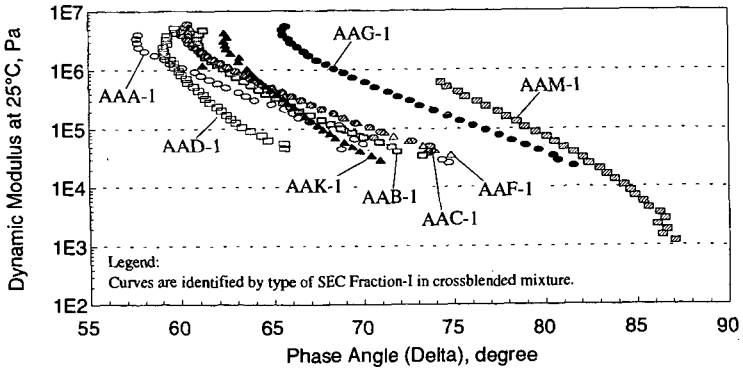


Figure 7. G^* vs. phase angle for mixtures of SC Fraction-II of AAK-1 (75.2%) with SEC Fraction-I (24.8%) of eight different asphalts.

**CHARACTERIZATION
OF RHEOLOGICAL AND THERMAL BEHAVIOR
OF ASPHALT CEMENTS MODIFIED BY ETHYLENE COPOLYMERS**

Dr Bernard Brulé, Engineer

Dr Sabine Gazeau, Engineer

Entreprise Jean Lefebvre
11 Boulevard Jean Mermoz,
92200 Neuilly sur Seine, France
Entreprise Jean Lefebvre
Laboratoire Central, Dourdan, France

Keywords: Polymer modified bitumens, differential scanning calorimetry (DSC), rheological behaviour, ethylene copolymers.

1. INTRODUCTION

The rheological properties of bituminous binders govern the subsequent performance of special hot mixtures in pavements. In the case of road pavements, the constraints engendered by moving vehicles are of dynamic origin, and dynamic rheology can be used to analyze the visco-elastic behaviour of the materials subject to loadings whose frequencies are close to those to which the road is subjected.

Differential scanning calorimetry (DSC) can be used to analyze the thermal behaviour of ethylene-copolymer-modified bitumens, and reveals there to be a good match between the melting range of the copolymer and the zone of transition between visco-elastic behaviour and purely viscous behaviour of the material [1].

As a result of SHRP work, dynamic rheology can be used to determine an isomodulus temperature that can be proposed for monitoring performance at high temperatures.

The results given in this paper concern ethylene copolymer/bitumen blends whose melting (and crystallization) ranges and visco-elastic behaviour depend on the type of ethylene copolymer, among other things.

2. ETHYLENE-COPOLYMER-MODIFIED BITUMENS STUDIED

Binders made with a pure straight run bitumen (70/100) and different ethylene copolymers were studied.

The ethylene copolymers used have the following characteristics:

- | | |
|---------------------|--|
| Copolymer A: | ethylene and methyl acrylate copolymer (EMA) with high crystallinity and molecular weight. |
| Copolymer B: | ethylene and vinyl acetate copolymer (EVA) with moderate crystallinity and molecular weight. |
| Copolymer C: | ethylene and vinyl acetate copolymer (EVA) with low crystallinity and molecular weight. |

These bitumens modified with 10% ethylene copolymers have a continuous polymer matrix within which are dispersed bitumen globules of different sizes (see Figure 1).

3. DIFFERENTIAL SCANNING CALORIMETRY

Ethylene copolymers are semi-crystalline copolymers. They are made of polyethylene crystallites separated from each other by amorphous regions caused by the co-monomer. The peak of ethylene copolymer melting is at lower temperatures than that of the polyethylene, for the co-monomer results in a reduction in the length of crystallizable sequences. The amorphous region is characterized by a glass transition temperature. All these characteristics can be determined by differential scanning calorimetry (DSC).

3.1. Test method

The thermal behaviour of ethylene-copolymer-modified bitumens is characterized by differential scanning calorimetry (DSC) using a Mettler DSC 30 analyzer.

This technique can determine the enthalpy of changes in the physical state of the copolymer such as:

- | | |
|------------------|--|
| melting: | first-order transition characterized by an endothermic signal, |
| crystallization: | first-order transition characterized by an exothermic signal. |

The glass transition temperature (T_g), which is an important characteristic of amorphous materials, is a second-order transition. The glass transition temperature of ethylene copolymers is between -20 and -40°C , depending on the ethylene copolymer. This paper will deal only with first-order transitions.

In the experiments the ethylene-copolymer-modified bitumens are softened by heating them, and are placed in a sealed aluminum crucible. They have to be left to stand 24 hours before the sample can be analyzed (time for the structure to stabilize).

All the tests are carried out with a cooling rate of $5^\circ\text{C}\cdot\text{min}^{-1}$ to -80°C . The sample is then heated to 120°C at a rate of $5^\circ\text{C}\cdot\text{min}^{-1}$, then cooled to -20°C at a cooling rate of $5^\circ\text{C}\cdot\text{min}^{-1}$.

3.2 Thermograms of ethylene-copolymer-modified bitumens

The thermograms in Figure 2 show the melting ranges of the three ethylene copolymers solvated with a maltenic fraction of the bitumen.

From the thermograms of Figure 2 it would appear that the temperature range defining the melting ranges varies appreciably, depending on the type of ethylene copolymer:

Melting range of ethylene copolymer A: $63-99^\circ$ \rightarrow Melting peak : 86°C

Melting range of ethylene copolymer B: $35-81^\circ$ \rightarrow Melting peak : 53°C

Melting range of ethylene copolymer C: $27-62^\circ$ \rightarrow Melting peak : 48°C

Like the melting ranges, the crystallization ranges depend on the type of ethylene copolymer, as can be seen from the thermograms in Figure 3.

The kinetics of ethylene copolymer crystallization are slow because of copolymer dispersion in the bitumen, which explains the shift between the melting ranges and crystallization.

4. DYNAMIC RHEOLOGICAL TESTS

Pure bitumens and polymers are visco-elastic materials, i.e. their behaviour is between that of an elastic solid and that of a viscous liquid.

Dynamic rheology is an oscillation technique that can be used to study the structure of materials in accordance with frequency (isotherms) and/or temperature (isochrones). It involves submitting the sample to a sinusoidal stress or deformation and measuring the material's response to this loading.

4.1. Test method

Measurements are taken with a Bohlin rheometer which uses plane-plane geometry. The temperature of the sample (immersed in water) is controlled by a thermoregulator. The sinusoidal deformation is chosen after a stress scan in order to locate it within the range of linear visco-elasticity. The results are given in the form of a modulus, G^* , for which the imaginary part is the loss modulus, G'' (viscous component of the modulus), and the real part is the storage modulus, G' (elastic component of the modulus). The delta phase angle, δ , represents the lag between the stress and deformation.

4.2. Interpretation of results

Examination of the isochrones of the modulus (G^*) at 1.5 Hz, under the conditions proposed by the SHRP [2], and by means of analysis of the gradient of variation of modulus G^* with temperature, provides an assessment of the temperature susceptibility of bituminous binders [3].

Examination of the isochrones of the delta phase angle, δ determines the temperature range between the visco-elastic region and the flow region of the ethylene-copolymer-modified bitumen.

In addition, examination of G^* and δ isochrones allows for assessment of a temperature at which $G^*/\sin\delta = 1$ kPa, the figure the SHRP specifications propose for the verification of binder performance at high temperatures [2].

5. DSC/DYNAMIC RHEOLOGY RELATIONSHIP

The isochrones of the modulus and of the phase angle of bitumen mixes with ethylene copolymers A, B, and C are shown in Figures 4 and 5.

Visco-elastic range

The temperature at which the test begins (15°C) is within the visco-elastic range of the materials.

The rheological behaviour of the pure bitumen is different to that of the highly modified bitumens: its modulus decreases rapidly with the temperature, and it proves to be highly temperature-susceptible. The isochrone of the phase angle does not have a rubbery plateau, contrary to ethylene-copolymer-modified bitumens: its structure collapses gradually as the temperature rises. Its phase angle increases parabolically up to the asymptotic value of 90°. At as little as 18°C, more than 90% of the modulus of the pure bitumen is accounted for by the viscous component (phase angle greater than 65°).

From the isochrones of the modulus, G^* , of highly modified bitumens (Figure 4), it can be seen that the reduction of the modulus in accordance with temperature is much lower than that seen with pure bitumens, which is a reflection of the improvement in thermal susceptibility brought about by addition of ethylene copolymer. Additionally, the degree of this variation depends on the type of ethylene copolymer A.

Thus, examination of the isochrones of the modulus allows for classification of binders in decreasing order of temperature susceptibility [4]: pure 70/100 bitumen, bitumen with copolymer C, bitumen with copolymer B, bitumen with copolymer A.

The isochrones of the phase angle in the modified binders (Figure 5) show that these binders are substantially more elastic than pure bitumen (lower phase angles across the whole range of temperatures studied). However, the contribution of the elastic component of the modulus is specific to each ethylene copolymer. It becomes negligible when the phase angle exceeds 65°.

Thus, the bitumen blend with copolymer A is the most elastic of the three modified bitumens studied. This is true for the entire temperature range. The bitumen mix with copolymer B is more elastic than that with copolymer C.

The significant increase in the phase angle of the modified bitumen is observed above 53°C for copolymer B, and above 43°C for copolymer C. This increase is linked to the melting of the ethylene copolymer, as detected by DSC analysis.

Flow region

The flow region corresponds to melting of the ethylene copolymer.

From the thermograms of Figure 2 and the phase-angle isochrones of Figure 5, it can be seen that the increase in the phase angle of the bitumens with copolymers B and C is close to the melting peak (Pf) determined by DSC analysis (53°C and 43°C respectively). The increase in the phase angle induces a decrease in elastic effects and a rise in viscous phenomena. This is because more than 90% of the modulus is attributable to its viscous C component when the phase angle is higher than 65°C [4].

The temperature corresponding to a phase angle of 65° is close to 68°C for bitumen modified with copolymer B and 53°C for bitumen modified with copolymer C.

As for the bitumen modified with copolymer A, its melting range is at higher temperatures (melting peak at 86°C). This is why the phase angle is low (major elastic effects) in the temperature range studied (10-70°C), for the copolymer does not melt.

Copolymer melting therefore results in a major modification in the rheological behaviour of the binders. It shows the temperature range between the visco-elastic field and the flow field. The less temperature-susceptible the ethylene copolymer is, the later flow will start.

It thus appears to be possible to guide the choice of the ethylene copolymer in accordance with the climatic conditions of the site (maximum temperature of the pavement).

6. PROCEDURE FOR DYNAMIC RHEOLOGICAL TESTING

Knowledge of the melting and crystallization ranges of ethylene-copolymer-modified bitumens allows for informed discussion of the effect the procedure for dynamic rheological testing (Bohlin) has on results. This comment particularly concerns modified binders with high copolymer contents, i.e. with a continuous polymer matrix, for binders with a continuous bitumen matrix behave in much the same way as the bitumen itself.

If a sample is placed on the rheometer at a temperature either in the melting range or in the crystallization range, the modulus measured will depend on the temperature history of the material (overmelting phenomenon).

The usual procedure for studying rheological behaviour involves placing the sample at a temperature of around 30°C.

To study the effect of the temperature history on rheological behaviour, isochrones were determined for 15 to 95°C for the bitumen modified with copolymer A, and for 15 to 70°C for the bitumen modified with copolymer C. The sample was then cooled to 15°C and a second isochrone was determined.

Ethylene copolymer A had a melting peak at around 86°C, and its crystallization range is from around 73 to 53°C (Figure 3).

The two isochrones of the modulus were identical, as can be seen in Figure 6.

Ethylene copolymer B has a melting peak around 53°C, and its crystallization range is from around 81 to 35°C (Figure 3). The two isochrones of the modulus are identical, just as for copolymer A.

As for copolymer C, its melting peak is around 43°C, and it starts to crystallize at around 12°C, as is shown in Figures 2 and 3. When the second isochrone starts at 15°C, the crystallization of copolymer C has not yet started. The copolymer overmelts, resulting in a significant reduction of the modulus (Figure 7). The moduli become identical as they enter the flow region.

Knowledge of the thermal behaviour of the ethylene copolymers is therefore very important for proper interpretation of their rheological behaviours (thermal and rheological) depending on the characteristics of the copolymer.

7. SHRP HIGH SERVICE TEMPERATURES

The new SHRP specifications [2] propose that at the mean maximum weekly temperature of the pavement, the value of $G^*/\sin \delta$ of the binder as is should be 1 kPa at a frequency of 1.6 Hz. This value ($G^*/\sin \delta = 1$ kPa) expresses a minimum rigidity, as shown by the following expressions [5]:

$$\begin{aligned}G^* &= 1/J^* \\ G^*/\sin \delta &= 1/J^*\sin\end{aligned}$$

where J^* is the complex compliance (1/Pa).

Associated with an SHRP performance criteria, this temperature can replace the ring and ball (R & B) softening point test in the case of polymer-modified bitumens for which it has been largely demonstrated that the test was not appropriate.

Through interpretation of their isochrones, the rheological behaviour characterization tests presented above allow for easy evaluation of the temperature for which $G^*/\sin \delta = 1$ kPa, and for identification of δ and G^* for that temperature (Table 1).

From Table 1 it can be seen that at temperatures where $G^*/\sin \delta = 1$ kPa, the difference between $G^*/\sin \delta$ and G^* is negligible. The phase angles are sufficiently great to allow the following simplification:

$$\begin{aligned}\sin \delta &\rightarrow 1 \\ G^*/\sin \delta &\rightarrow G^* \\ G^*/\sin \delta &\rightarrow 1/J^*\end{aligned}$$

The isomodulus temperatures are considerably higher than the ring and ball softening points [4]. It is clear that the ring and ball temperatures for ethylene-copolymer-modified bitumens are not isomodulus temperatures.

8. CONCLUSION

Differential scanning calorimetry (DSC) is seen to be a promising technique for characterizing and understanding the behaviour of ethylene-copolymer-modified bitumens.

Dynamic rheology provides an appreciation of the temperature susceptibility of bituminous binders, on the basis of modulus isochrones.

In the case of highly modified ethylene-copolymer-modified bitumens (continuous polymer matrix), the melting ranges of the copolymers and the isochrones of the phase angle are used to determine the temperature range between the visco-elastic region and the flow region. Melting of the copolymer engenders an increase in the phase angle, which is reflected by a gradual decrease in elastic effects and an increase in viscous phenomena. The greater the

crystallinity and the molecular weight of the copolymer, the higher the temperature of the flow area will be.

In addition, knowledge of the thermal behaviour of ethylene copolymers in bitumen makes it possible to discuss the effect of the test procedure on the rheological behaviour analysis of modified binders and the interpretation of results.

The temperature for which $G^*/\sin \delta = 1$ kPa, which is the value proposed in SHRP specifications for checking high-temperature performance, also depends on the characteristics of the copolymer.

BIBLIOGRAPHY

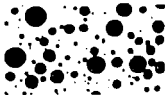
- [1] R. SHUTT, C. TURMEL, "Analyse Thermique Différentielle et Propriétés Rhéologiques de Bitumes Modifiés par les Polymères Semi-cristallins", 5th Eurobitume Symposium, Stockholm, Abstracts and Reports, June 1993, pp. 76-80.
- [2] D.A. ANDERSON, "Programme SHRP: Méthodes d'essai et spécification des liants", Revue Générale des Routes et Aérodrômes, No. 714, January 1994, p. 48.
- [3] G. RAMOND, M. PASTOR, C. SUCH, "Recherche des performances d'un liant à partir de son module complexe", 5th Eurobitume Symposium, Stockholm, Abstracts and Reports, June 1993, p. 81.
- [4] B. BRULE, M. MAZE, "Les bitumes polymères pour enrobés spéciaux: élastomères ou plastomères?", Revue Générale des Routes et Aérodrômes, No. 726, 1995, p. 42.
- [5] C. SUCH, G. RAMOND, "Les spécifications SHRP en termes plus usuels - Tentative de décryptage", LCPC, Communication presented to the SHRP Seminar in Lille, Sept 1994.

	R&B (°C)	G^* at R&B temp. (Pa)	Phase angle at R&B temp.	$T(G^*/\sin \delta) = 1$ kPa (°C)	G^* (Pa) at isomodulus temp.	Phase angle at isomodulus temp.
Bitumen	45	9.65E + 03	83	62	998	83
Bitumen with copolymer A	86	1.85E + 03	63	96	974	75
Bitumen with copolymer B	68	3.63E + 03	69	79	996	79
Bitumen with copolymer C	56	2.67E + 03	70	70	998	80

Table 1: Conventional and SHRP characteristics at high service temperatures



Ethylene copolymer A-bitumen



Ethylene copolymer B-bitumen



Ethylene copolymer C-bitumen

Figure 1: Microstructure of ethylene-copolymer-modified bitumens (10% blends)

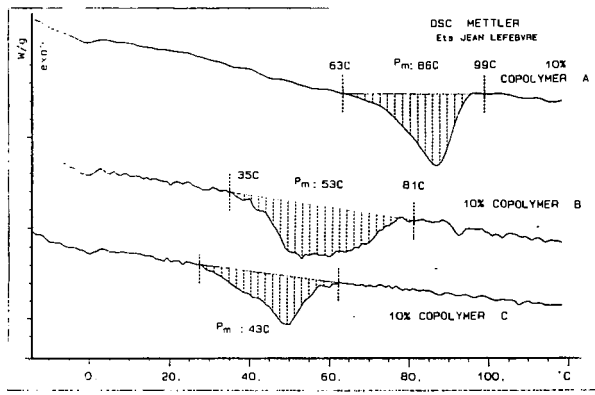


Figure 2: Thermograms of bitumen blends with ethylene copolymer A, B, and C Melting ranges

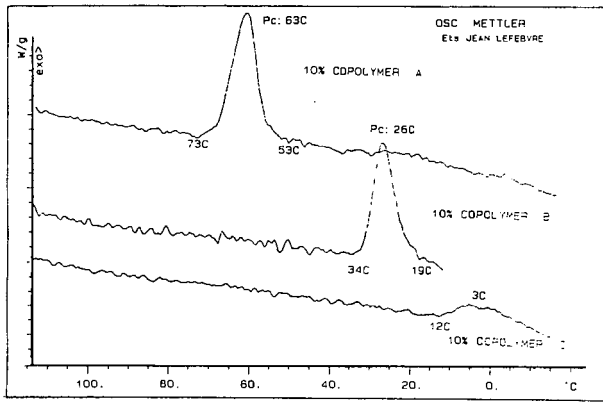


Figure 3: Thermograms of bitumen blends with ethylene copolymer A, B, and C Crystallization ranges

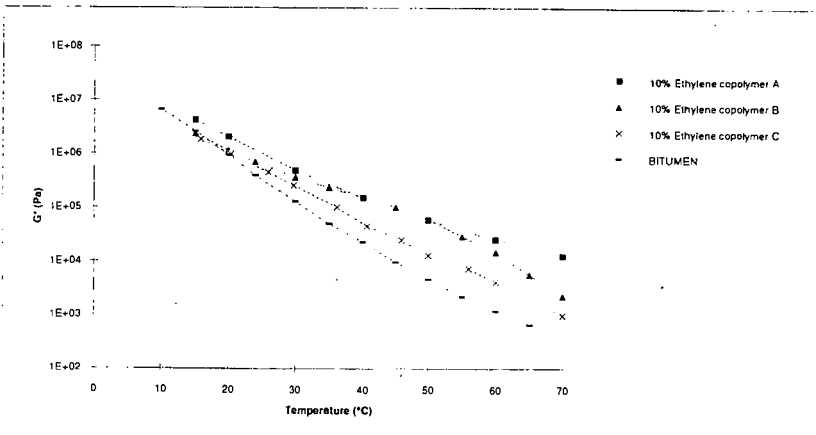


Figure 4: G* isochrones (1.5 Hz) for bitumen blends with ethylene copolymer A, B, and C

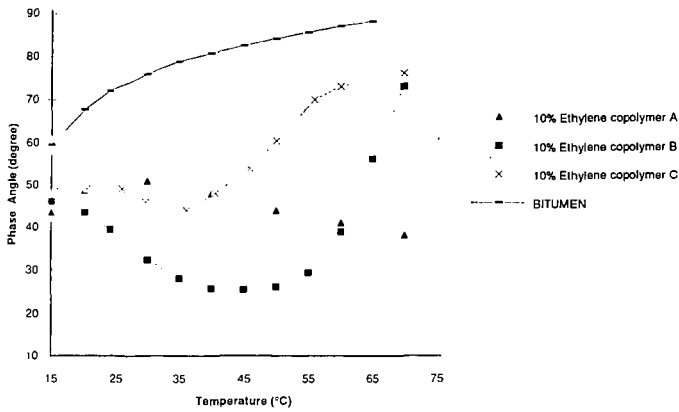


Figure 5: δ isochrones (1.5 Hz) for bitumen blends with ethylene copolymers A, B, and C

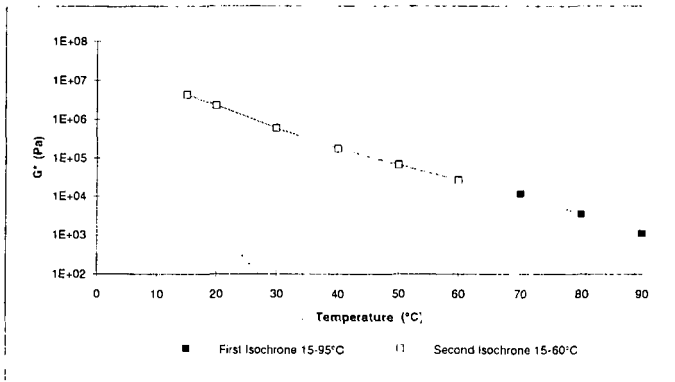


Figure 6: G^* isochrones for bitumen modified with 10% of copolymer A

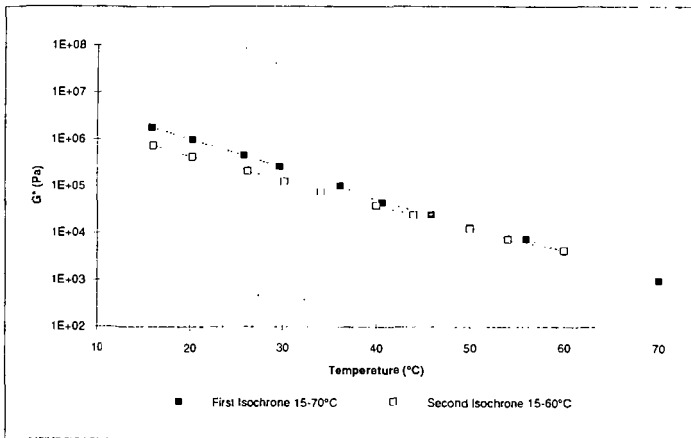


Figure 7: G^* isochrones for bitumen modified with 10% of copolymer C

**HP-GPC CHARACTERIZATION OF ASPHALT AND MODIFIED ASPHALTS
FROM GULF COUNTRIES AND THEIR RELATION
TO PERFORMANCE BASED PROPERTIES**

H. I. Abdul Wahhab, Mohammad F. Ali,
I. M. Asi, and I. A. Dubabe
King Fahd University of Petroleum and Minerals
Dhahran 31261, Saudi Arabia

Keywords: Modified Asphalts, HP-GPC Characterization, Gulf Countries Asphalts

INTRODUCTION

Asphalt producing refineries in the Gulf countries include Ras Tanura and Riyadh (Saudi Arabia), Al-Ahmadi (Kuwait), and BAPCO (Bahrain). Riyadh and Ras Tanura refineries are located in the central and eastern Saudi Arabia respectively. Arabian light crude oil is used to produce 2000 to 3000 tons of asphalt per day using vacuum distillation, air blowing and grade blending techniques to produce 60/70 penetration grade asphalts in each of these two Saudi refineries. All of the asphalt cement used in Saudi Arabia, Qatar and parts of the United Arab Emirates is supplied by Riyadh and Ras Tanura refineries.

Al-Ahmadi refinery supplies all of the asphalt cement needed for construction in the state of Kuwait. Ratwi-Burgan crude oil mix is used to produce 750 to 1000 tons of asphalt per day using vacuum distillation and air blowing processes.

BAPCO refinery, Bahrain, utilizes crude oils produced from Saudi oil fields and supplies asphalt cement needed for construction in Bahrain, Oman and parts of United Arab Emirates.

The roadway network in Gulf countries has developed more rapidly than in many industrialized countries. The entire roadway network is built using flexible pavements due to the availability of relatively low cost asphalt binders. The asphalt binder plays a significant role in pavement ability to withstand thermal and fatigue cracking and contribute to permanent deformation behavior. Fatani et al [1] in a study about permanent deformation in Saudi Arabia have concluded that the asphalt cement is responsible for a major part of rutting in the region, and that extreme weather conditions of the Gulf countries has promoted an inferior performance of asphalt concrete mixes in the field.

Asphalt binders are thermo-visco-elastic materials where temperature and rate of load application has a great influence on their behavior. Asphalt consistency and hence ability to sustain and hold their fundamental cementing mechanism changes depending on temperature. The pure asphalt lack the proper balance of viscous fluid-elastic sponge properties which usually occur due to an effective elastic network created by molecular association. In recent years various studies have shown that polymer modification can be successful in forming this viscous fluid-elastic sponge balance by creating molecular entanglement in an asphalt.

This study was initiated to evaluate different locally available polymer materials in order to identify potential polymers to modify asphalts to satisfy the performance requirements in the Gulf countries' environmental conditions. The storage stability of the asphalt-polymer blends and the life cycle cost analysis of the polymer modification were also studied.

EXPERIMENTAL

1. Temperature data collection and temperature zoning: Metrology and Environmental Protection Agencies, Directorate of Climatology and other similar agencies in the Gulf countries were approached to provide the research team with the available historical annual environmental data covering the Gulf countries (GC). These data were analyzed and used to build temperature data base and to develop suitable temperature zoning for the GC.
2. Asphalt samples collection: Asphalt binder samples were collected from all asphalt cement producing refineries in the Gulf which include Ras Tanura and Riyadh (Saudi Arabia), Al-Ahmadi (Kuwait), and BAPCO (Bahrain) and an additional sample was collected from Awazel private company which modifies asphalt produced by Riyadh refinery.
3. Asphalt testing: Collected asphalt samples were subjected to comprehensive testing to determine their physical and chemical properties. Testing included:

- a. Consistency testing; viscosity at 25°C (ASTM D 3570), 60°C (ASTM T-202-80) and 135°C (AASHTO T-201-80), penetration at 25°C and 4°C (AASHTO T-49-80), softening point (AASHTO T-53-81) and ductility (AASHTO T-51-81). Testing was carried out on fresh and rolling thin film oven (RTFO) residue (AASHTO T-240-78).
 - b. Performance based testing which was performed on original binder, RTFO residue and pressure aging vessel (PAV) residue [2]. Tests included flash point, rotational viscosity, dynamic shear, mass loss after RTFO, flexural creep stiffness and direct tension failure strain [2].
 - c. Chemistry, chemical composition of collected samples were determined using Corbett's method, ion exchange chromatography and high pressure gel permeation chromatography (HP-GPC).
The HP-GPC procedure for this study utilized four μ -styragel columns connected in the following order according to size: 10,000, 1000, 500 and 100 μ . Two kinds of detectors, a differential refractometer and a UV absorbance detector (230 nm and 340 nm) were used. HPLC grade tetrahydrofuran (THF) was used as a solvent mobile phase at ambient temperature (24°C) at a flow rate of 1.0 ml/min. the data were accumulated by a millennium 2010 chromatography manager.
4. Asphalt Modification: Asphalt cement which has a performance grade that does not satisfy the binder specification as determined by temperature zoning was modified to improve its quality. Modified binders were subjected to the same set of tests as virgin asphalts.

RESULTS AND DISCUSSION

Asphalt Testing: The complete test results for the collected asphalt samples, temperature data and contour map were published in Al-Abdul Wahhab et al [3].

Results indicate that asphalt cement produced in the Gulf satisfies the low temperature requirement but can only satisfy one zone of 64°C average seven day consecutive maximum temperature. Awazel air blown asphalt met the requirement of PG 70-10 while PG 58-10 and PG 76-10 zones have not been met. This indicates the necessity of modifying locally produced asphalts to meet the performance requirements of these temperature zones.

ASPHALT MODIFICATION

The asphalt modification work was carried out in two phases. The first phase focused on identifying potential polymers while the second focused on the optimization of modification process for the following selected polymers:

LLDPEX - Linear low density polyethylene grade 1182

PP500C - Polypropylene grade 500V

SBS - Styrene - butadiene - styrene

A fourth polymer, crumb rubber from truck tires (CRT) was also included for this study. The polymer modified samples were subjected to physical tests.

Results showed that addition of the polymer material significantly improves the physical and rheological properties of Arab asphalt binders for all sources and all polymer types.

HP-GPC Analysis

A typical HP-GPC profile is shown in Fig. 1. The variable on the x-axis is the time required of a particular size to emerge from the system. The reading on the y-axis is the detector response, which is an indicator of the concentration of asphalt molecules in solution. In order to distinguish HP-GPC profiles, the area under the curve is divided into different sections. Most frequently this is divided into three sections and the area under each section is determined. These three areas are referred to as large-molecular size (LMS), medium-molecular size (MMS), and small-molecular size (SMS) material. However, other researchers felt that these three parameters could not adequately model the subtle differences between the HP-GPC profiles of the asphalts used. Accordingly, for this study a procedure was used in which the area under the curve was divided into eight sections (see Fig. 1). This number was selected as the optimum needed to provide an accurate quantitative model of the HP-GPC profiles.

The cut-off points were selected to have equal elution times. The eight sections are numbered from left to right. Consequently, apparent molecular size decreases progressively from Section 1 to Section 8.

Fig. 1 also compares GPC profiles for fresh, RTFO and PAV aged asphalts. There are clear differences in each of the curves, with the PAV aged and RTFO aged samples showing significant

growth in the large-molecular size (LMS) region (material eluted between 24 and 30 minutes) for this sample. GPC profile Fig. 1 also shows the growth in LMS is accompanied by a gradual decrease in MMS and SMS regions. Profiles of parent asphalts, polymer modified asphalts, and RTFO/PAV asphalts are shown in Figs. 2, 3 and 4.

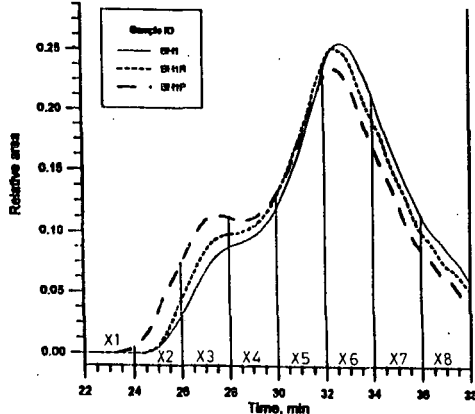


Fig. 1: HP-GPC profiles for original and oxidized asphalts

From the HP-GPC analysis it can be seen that all of the polymer modified asphalts have a larger percentage of fractions # 1, 2, 3 and 4 and a smaller percentage of fractions 5 and 6 than the parent AC-20. It is also apparent from the GPC profile that the fractions # 1, 2 and 3 have considerably increased for RTFO and PAV aged samples (Fig. 4) than modified non-aged asphalt.

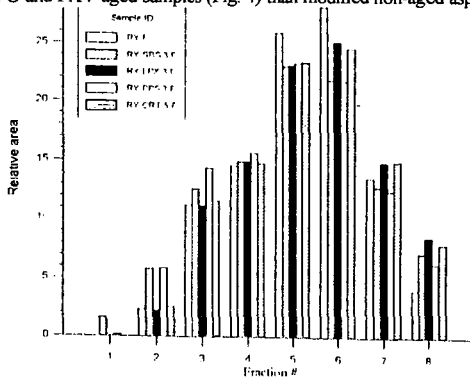


Fig.2: HP-GPC partitions into Eights of parent AC-20 and polymer modified asphalts

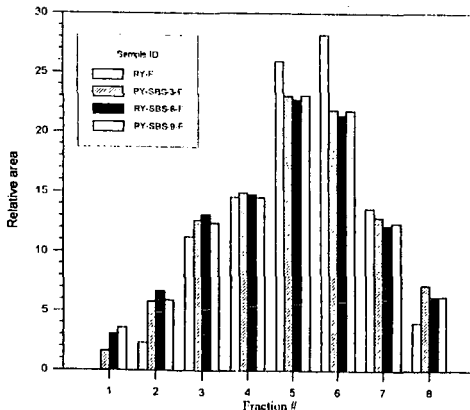


Fig. 3: HP-GPC partitioned into Eights of parent AC-20 and SBS-modified asphalts

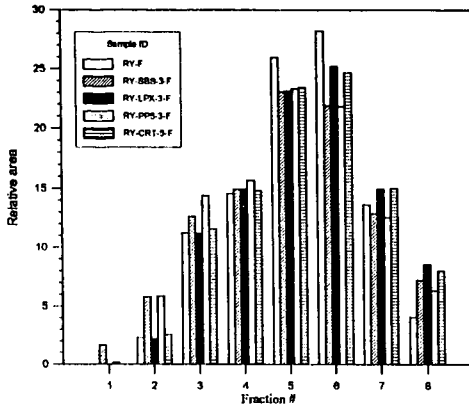


Fig. 4: HP-GPC partitioned into Eights of parent AC-20 and SBS-modified and their RTFO and PAV aged asphalts

Correlation Studies of Asphalt Composition with Its Performance-Related Characteristics :

This sub-task aims at finding the mathematical relation - if it exists - between the physical properties of the asphalt and its chemical composition. The physical properties which are included in this sub-task are shown in Table 1. The chemical composition is represented by the eight fractions (X_1 to X_8) into which the HP-GPC chromatograms were divided. X_1 was dropped from the analysis to get rid of interdependency between the eight fractions of the chromatograms, i.e. if X_1 is kept in the analysis, the sum of X's is always 100.

Table 1: Included physical properties

Used Symbol	Property
SG	Specific Gravity
PEN25	Penetration at 25°C
RPEN25	Retained Penetration at 25°C
PEN4	Penetration at 4°C
RPEN 4	Retained Penetration at 4°C
SP	Softening Point
FP	Flash Point
DUC	Ductility
VIS25	Sliding Plate Viscosity at 25°C
VISR25	Viscosity Ratio at 25°C
VIS60	Absolute Viscosity at 60°C
VISR60	Viscosity Ratio at 60°C
RVIS135	Rotational Viscosity at 135°C
VIS135	Kinematic Viscosity at 135°C
VISR135	Viscosity Ratio at 135°C
PI	Penetration Index
PIS	Penetration Temperature Susceptibility
PR	Penetration Ratio
PVN	Penetration Viscosity Number
PVNI	Penetration Viscosity Number for VTS calculation
VTS	Viscosity Temperature Susceptibility
ω_c	Cross Over Frequency
R	Rheological Index
T_d	Defining Temperature
G*	Complex Dynamic Modulus, KPa
S	Flexural Creep Stiffness, MPa
m	Flexural Creep Slope

The purpose of the analysis is to help select from the 7 candidate variables X_2, X_3, \dots, X_8 a smaller subset that will adequately explain the response. A number of variable selection procedures are available in the statistical literature. The most commonly used ones are the search over all possible subsets, the forward selection procedure and the stepwise selection procedure. The corresponding SAS PROC RSQUARE, SAS PROC FORWARD and SAS PROC STEPWISE were used and their results are noted. It is generally accepted that all stepwise procedure is vastly superior to the others and thus it is the one relied upon in this analysis.

Table 2 presents models for the different variables, together with their R^2 value and P-value for fresh and polymer modified samples.

Table 2: Regression analysis for fresh samples

Variable	Modifi- cation	Model	R ²	P-value
SG	No	$1.09 - 0.003X_1 - 0.002X_2$	0.51	0.0011
PEN25	No	$74.04 + 1.02X_1 - 1.67X_2$ P-value for testing significance of X_1 is 0.12	0.32	0.0297
RPEN25	No	$1.99 + 0.04X_1 - 0.09X_2 - 0.01X_3$ P-value for testing significance of X_1 is 0.10	0.85	0.0001
PEN4	No	$44.1 + 1.43X_1 - 0.9X_2$	0.71	0.0001
RPEN4	No	$0.14 + 0.03X_1 + 0.02X_2$	0.31	0.0316
SP	No	$-44.23 + 2.93X_1 + 0.47X_2 + 1.96X_3 + 1.55X_4$ P-value for testing significance of $X_1 = 0.11$	0.76	0.0001
FP	No	$971.44 - 2.05X_1 - 14.14X_2 - 33.45X_3 - 11.8X_4 + 8.06X_5$	0.97	0.0001
DUC	No	$205.67 - 7.96X_1 - 2.46X_2$	0.68	0.0001
VIS25	No	NO MODEL		
VISR25	No	NO MODEL		
VIS60	No	$(-48.722 + 1.758X_1 + 0.969X_2 + 0.958X_3) \times 10^2$	0.67	0.0002
VISR60	No	$2.66 - 0.04X_1$ P-value for testing significance of $X_1 = 0.10$	0.13	0.0001
RVIS135	No	$560 - 18.22X_1 + 49.64X_2 - 21.5X_3$	0.80	0.0001
VIS135	No	$-493.82 + 49.03X_1 + 18.39X_2$	0.35	0.0008
VISR135	No	$1.02 + 0.03X_1$	0.28	0.0126
PI	No	$-6.35 + 0.11X_1 + 0.15X_2$	0.74	0.0001
PTS	No	$0.05 - 0.001X_1 - 0.0006X_2$	0.77	0.0001
PR	No	$218.18 - 4.74X_1 - 4.14X_2$	0.63	0.0001
PVN	No	$-3.67 + 0.18X_1 + 0.018X_2$	0.63	0.0001
PVNI	No	$1.18 - 0.06X_1$	0.57	0.0001
VTS	No	$4.38 + 0.048X_1 - 0.1X_2$	0.43	0.0063
R	No	$2.132 + 0.17X_1$	0.76	0.0001
a _s	No	$8.32 \times 10^{-1} + 1.64 \times 10^{-5} X_1$	0.41	0.0023
T _s	No	No Model		
PEN25	Yes	$87.15 - 5.22X_1$	0.63	0.0021
SP	Yes	No Model		
G*@76	Yes	$31776-3300X_1$	0.44	0.0107
G*@80	Yes	$20516-2089X_1$	0.38	0.0344
SG@-18	Yes	$-1207.3 + 66.6X_1 + 85.5X_2$	0.77	0.0006
SG@-12	Yes	$-678.6 + 44.22X_1 + 40.04X_2$	0.70	0.0018
m@-18	Yes	$0.191-0.0114X_1$	0.46	0.0077
m@-12	Yes	$0.489-0.0158X_1$	0.52	0.0082

It is worth noting that the R^2 value for any model can be increased on the expense of entering variables that are correlated with ones already in the model or that are not significant, and this is one problem the stepwise procedure tries to avoid. For those variables with a very low R^2 , for example VISR60 (an R^2 -value of 0.13 for fresh samples and in fact no fitted model for aged samples), an explanation would be that either a linear model does not provide a good fit for the data or that there is really no relationship between the dependent variable, in this case viscosity ratio at 60°, and the independent variables, the molecular size distribution. The latter may well be the case, because in that regard a logarithmic transformation was done on the data for all the variables and different statistical procedures were run and the results are a lot like those from a linear model. As a matter of fact, for some there was a slight decrease in the R^2 value. On the other hand, a high value of R^2 , for example 0.97 for the variable FP for fresh samples, may not necessarily mean that the given model represents the true relationship if there is no physical evidence to indicate that. This may just be a purely mathematical result with no physical evidence but may warrant further study. An important point that is worth noting is the non-uniformity in the models found for fresh and aged samples. By that, we mean for any variable the model fitted for fresh samples may differ in the number and the nature of the independent variables entered and thus in the magnitude of the regression coefficients and in the R^2 value. That may be attributed to the fact that aged samples are inherently different from fresh ones and thus molecular size distribution is different.

It should be noted that the physical properties of asphalts are measured on whole homogenized sample, whereas the R^2 values reported in Tables 5 and 6 are based on the regression analysis of randomly picked GPC fractions. We conclude by noting that although some of those models may look good, they should be examined carefully and interpreted in accordance with physical results.

CONCLUSION

Addition of polymers significantly improve the physical and rheological properties of Arab asphalts. HP-GPC characterization can be used to predict physical properties of asphalts and modified asphalts.

ACKNOWLEDGMENT

The authors would like to thank King Abdulaziz City for Science and Technology (KACST) for providing support for this research and to the King Fahd University of Petroleum and Minerals for providing the laboratory space and facility.

REFERENCES

- (1) Fatani,M.N., Al-Abdul Wahhab,H.I., Balghunaim,F.A., Bubshait, A., Al-Dubabe ,I. and Nouredin, A. S., "Evaluation of Permanent Deformation of Asphalt Concrete Pavement in Saudi Arabia". Final Report, National Res. Proj., KACST, Saudi Arabia, 1992.
- (2) Strategic Highway Res. Prog., "The Superpave Mix Design System Manual of Specification, Test Methods and Practices", Report No. SHRP-A-379, Washington, D.C. 1994.
- (3) Al-Abdul Wahhab,H.I., Ali, M. F., Asi, I.M., and Al-Dubabe,I. A., "Adaptation of SHRP performance based asphalt specification to the Gulf countries". Progres Report No. 4,AR-14-60, King Abdul Aziz City for Science And Technology, Saudi Arabia, 1995.

EVALUATION OF VALIDITY OF CONVENTIONAL TEST METHODS IN CASE OF POLYMER-BITUMENS

Dr Dariusz SYBILSKI

Road and Bridge Research Institute, Warsaw, Poland

Key-words: polymer-bitumens, non-linear behavior, conventional tests

INTRODUCTION

When testing polymer-bitumens, non-linear behavior of material is observed in test conditions at behavior of conventional, plain bitumens is linear. Polymer-bitumen systems show non-Newtonian behavior in a wider range of temperature and shear than plain bitumens. Paper presents results of testing of polymer-bitumens with discussion of validity of conventional test methods when applied for polymer-bitumen systems. Several polymer-bitumen systems were tested including bitumens modified with SBS elastomers (elastomer-bitumens) and polyolephinic plastomer PO (plastomer-bitumens). Test program contained: penetration at 5, 10, 15, 25, 40, 50°C and at 25°C under load 50, 100, 200g, Softening Point R&B, Fraass Breaking Point, viscosity at 60°C, ductility at 5, 15, 25°C. Viscosity was measured in rotational viscometer at various shear rates. Zero-shear viscosity was calculated from viscosity-shear rate relationship according to simplified Cross Equation [1]:

$$\eta = \frac{\eta_0}{1 + (K \cdot d\gamma / dt)^m}$$

where: η - apparent viscosity, mPas, η_0 - zero-shear viscosity, mPas, $d\gamma/dt$ - shear rate, 1/s, K - constant, s , m - constant.

Wheel-tracking test was conducted on asphalt concrete with polymer-bitumens and plain bitumens in LCPC apparatus at 45°C, load 0.5 kN, contact pressure 0.6 MPa. Rutting resistance was expressed as a number of wheel passes to rut depth 10mm, N_{10} , calculated according to Equation:

$$h = a \cdot \ln^b N$$

where: h - rut depth, mm, N - number of wheel passes, a, b - constants. N_{10} was related to binder properties.

PENETRATION

Elastomer-bitumens show non-linear relationship of $\log(\text{penetration})$ vs temperature above 25°C (Fig. 1). Penetration is lower than expected. Bitumen and plastomer-bitumen show linear relationship in temperature range from 5 to 50°C. The same conclusion comes out from penetration test under various load (Fig. 2). In case of elastomer-bitumens relationship of penetration vs load deviates from linear when increasing load. This is not observed in case of bitumen or plastomer-bitumen. Penetration tests showed that elastomer-bitumens are less temperature and load susceptible than bitumen or plastomer-bitumen.

Zero-shear viscosity at 60°C shows a very weak relationship with penetration at 25°C (Fig. 3). Two separate group of polymer-bitumens may be easily recognized depending on consistency of base bitumen used for modification. A great variety in viscosity is observed among polymer-bitumens of equal penetration. In a group of binders of penetration at 25°C from 40 to 70x0.1mm, viscosity at 60°C varies from 4×10^5 mPas to 1.5×10^7 mPas, i.e. the highest value is 38 times of the lowest!

SOFTENING POINT

There is a doubtful relationship between R&B Softening Point and Penetration at 25°C (Fig. 4). The same Softening Point may be obtained by elastomer-bitumens of significantly different penetration. Soft base bitumen highly modified with elastomer (i.e. 6-7% by mass) results in a binder of very high Softening Point, above 70°C, comparative with that obtained by harder base bitumen low modified (i.e. 3-4%).

Relationship of Plasticity Range and Penetration Index in case of some elastomer-bitumens deviates significantly from linear observed in case of plain bitumens and plastomer-bitumens (Fig. 5) as a result of deviation of Softening Point and Fraass Breaking Point as well as Penetration from relationships found for bitumens by Heukelom [2].

When relating Softening Point to Zero-shear viscosity at 60°C an interesting shape of relationship was found as linear but with a break point at 68.2°C (with respective Zero-shear viscosity 7380000 mPas) - Fig. 6. The relationship is much stronger than for penetration. A sharp change in slope is

observed at this point which means that below this point increase in Softening Point reflects increase in viscosity of binder while above this point increase in Softening Point does not bring increase in viscosity. This observation may explain doubts in significance of Softening Point in case of some soft highly modified elastomer-bitumens. For a polymer-bitumen of Softening Point 60°C its zero-shear viscosity at this temperature would be 2164000 mPas which is much above 1300000 mPas as determined by Heukelom for plain bitumens.

LOW-TEMPERATURE PROPERTIES

Vonk et al. [3] analysed validity of Fraass Breaking Point for evaluation of low-temperature behavior of elastomer-bitumens. Fraass Breaking Point temperature was compared with acoustic emission test results, showing that the first did not reflect low-temperature behavior in some cases. Fraass Breaking Point reflects a certain stiffness of binder not its ability to combat tensile strain. Fig. 7 presents results of tests of ductility at various temperatures related to penetration measured at the same temperature. A group of results obtained for penetration below 20x0.1mm has been chosen which represent hard binders tested at 15 or 25°C or soft binders tested at 5°C. Significant difference may be noted when comparing materials of the same penetration from two groups. Plain bitumens and plastomer-bitumens are grouped in the first while elastomer-bitumens in the second. At the same penetration elastomer-bitumen shows higher ductility than plain bitumen or plastomer-bitumen. In average, at penetration of 10x0.1mm bitumen or plastomer-bitumen shows ductility of 5.0cm while elastomer-bitumen of 28.2cm. When considering that ductility test was conducted on hard bitumen, these results may be regarded as reflecting low temperature behavior of binders. No relationship of ductility at low temperature and Fraass Breaking Point was found. Conclusion is similar to that which came out from SHRP: low-temperature properties of bituminous binder shall be characterized by stiffness but also tensile strain.

RUTTING RESISTANCE OF ASPHALT CONCRETE VS BINDER PROPERTIES

Comparison of rutting resistance of asphalt concrete with Softening Point of bituminous binder showed a weak relationship (Fig. 8). Much higher regression coefficient was achieved in case of zero-shear viscosity at 60°C (Fig. 9). However in both cases the same phenomenon may be noted: elastomer-bitumens from soft base bitumen highly modified may be overestimated in terms of rutting resistance when evaluating on base of Softening Point or zero-shear viscosity. In case of the latter the potential reason lies in equipment possibilities which do not allow to approach sufficiently low shear rates [1]. In case of Softening Point a break point may be noted at a point of about 70°C which is the value of break point of relationship of Softening Point and zero-shear viscosity at 60°C. The best rutting resistance was obtained with harder grade elastomer-bitumen with a lower modification or with highly modified plastomer-bitumen based on hard bitumen.

CONCLUSIONS

Non-linear non-Newtonian behavior of polymer-bitumens may be found in conventional tests depending on temperature and load conditions. All conventional test methods as penetration, R&B Softening Point, Fraass Breaking Point have validity limited to relatively low modified polymer-systems, especially in case of elastomer-bitumens. In case of Softening Point, the limiting value was found as 68.2°C. Zero-shear viscosity calculated from viscosity-shear rate relationship reflects susceptibility of binder to permanent deformation. The test method is limited with equipment potentials to approach zero shear conditions in case of highly modified polymer-bitumen systems.

REFERENCES

1. Sybilski D.: *Zero-Shear Viscosity of Bituminous Binder and its Relation to Bituminous Mixtures Rutting Resistance*. 75th TRB Annual Meeting, 1996
2. Heukelom W.: *An Improved Method of Characterizing Asphaltic Bitumens with Aid of their Mechanical Properties*. Proc. AAPT, Vol. 42 (1973)
3. Vonk W.C., Robertus C., Jongeneel D.J., Korenstra J.: *Acoustic emission: a new tool for assessing the relative performance of binders and asphalts at low temperatures*. The East-West European Road Conference, Warsaw, 22-24 Sept. 1993

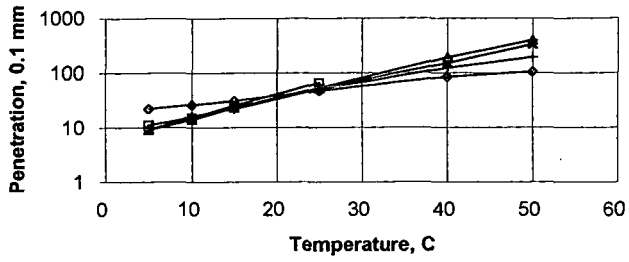


Fig. 1. Penetration vs Temperature of plain bitumen and polymer-bitumens

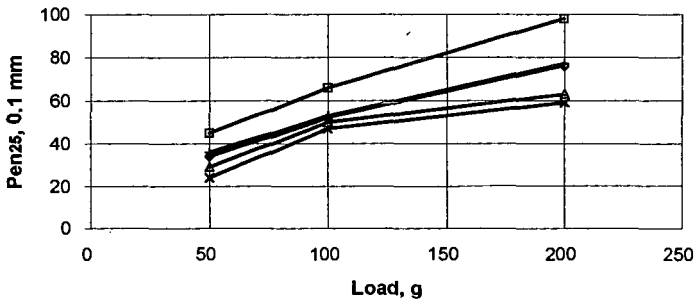


Fig. 2. Penetration vs Load of plain bitumen and polymer-bitumens

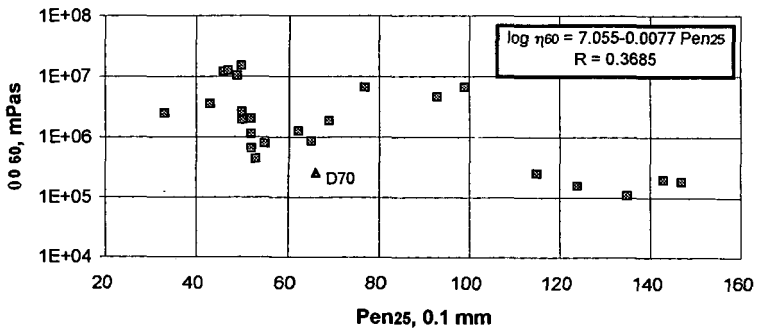


Fig. 3. Zero-shear viscosity at 60°C vs Penetration at 25°C

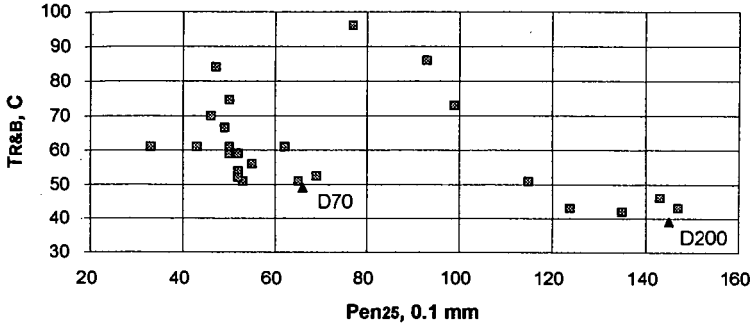


Fig. 4. R&B Softening Point vs Penetration at 25°C

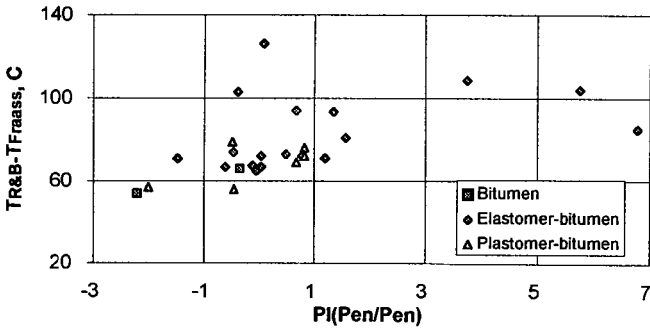


Fig. 5. Plasticity Range ($T_{R\&B} - T_{Fmass}$) vs Penetration Index

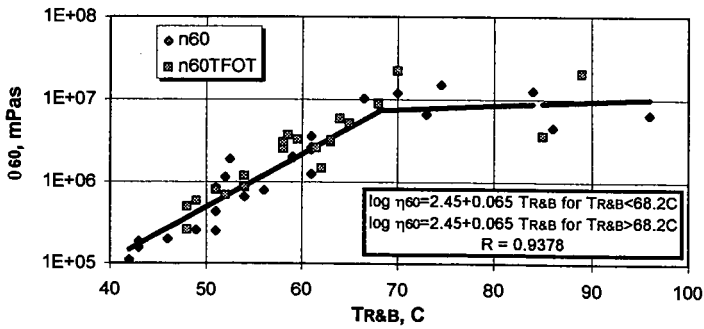


Fig. 6. Zero-shear viscosity at 60°C vs R&B Softening Point

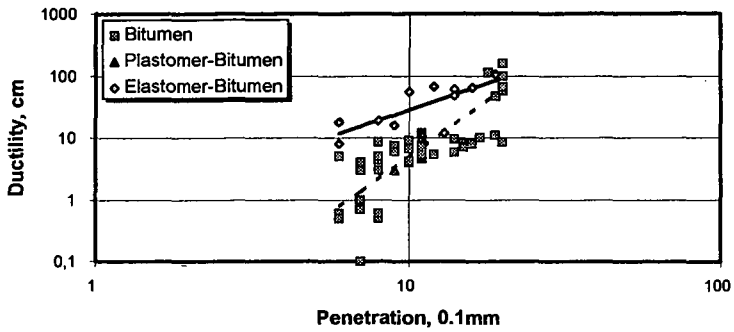


Fig. 7. Ductility vs Penetration at the same temperature (Penetration below 20x0.1mm)

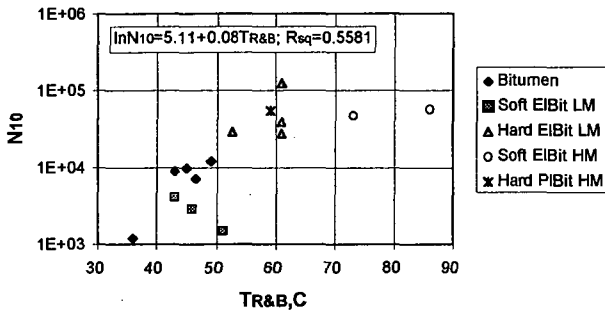


Fig. 8. Rutting Resistance of Asphalt Concrete vs R&B Softening Point of Binder

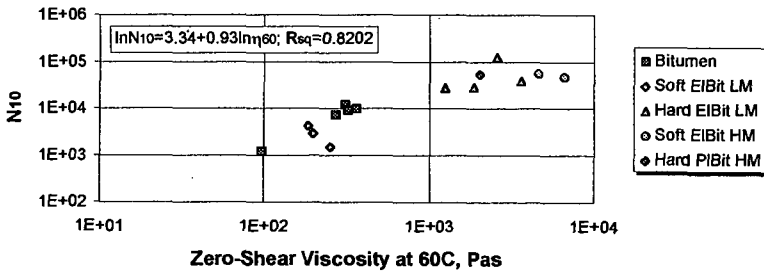


Fig. 9. Rutting Resistance of Asphalt Concrete vs Zero-Shear Viscosity at 60°C of Binder

RHEOLOGICAL PROPERTIES OF ASPHALTS WITH PARTICULATE ADDITIVES

N. Shashidhar
EBA Engineering
5800 Metro Drive
Baltimore MD 21215

Brian H. Chollar
Federal Highway Administration, HNR-20
6300 Georgetown Pike
McLean VA 22101

Keywords: Mastic, particulate composite, rheological properties

INTRODUCTION

The Superpave asphalt binder specifications are performance-based specifications for purchasing asphalt binders for the construction of roads. This means that the asphalt is characterized by fundamental material (rheological) properties that relate to the distress modes of the pavements. The distress modes addressed are primarily rutting, fatigue cracking and low temperature cracking. For example, $G^*/\sin(\delta)$ is designed to predict the rutting potential of pavements, where G^* is the magnitude of the complex shear modulus and δ is the phase angle. The binder for a road that is situated in a certain climatic zone requires the binder to have a minimum $G^*/\sin(\delta)$ of 2200 Pa at the highest consecutive 7-day average pavement temperature the road had experienced. Implicit in such a performance based specification is that the fundamental property, $G^*/\sin(\delta)$, of the binder correlates with rutting potential of the pavement regardless of the nature of the binder. In other words, the specification is transparent to the fact that the binder can simply be an asphalt, or an asphalt modified by polymers, particulates and other materials that can form a two-phase mixture.

There has been limited amount of research to validate the correlation of the Superpave binder parameters with laboratory mix tests and fewer still with pavement performance. The use of modified binders in such validation studies is further limited. Rarer still are studies that use particulate modifiers. Anderson and Kennedy¹ presented the basis for Superpave binder specification and validated these with mix tests. They did not specifically use modified systems, except when talking about low temperature cracking specifications. King et. al.² showed a good correlation between the low-temperature cracking predictors, namely, the temperature at which the failure strain is 1% and the temperature when creep stiffness is 200 MPa, to the thermal stress restrained specimen test (TSRST) for various asphalts and polymer modified binders. Hicks et. al.³ validated the binder specifications with laboratory mixture testing using only unmodified binders. Bouldin et. al.⁴ show excellent correlation between $G^*/\sin(\delta)$ and wheel tracking tests, but limit the asphalts to unmodified and styrene butadiene-styrene (SBS) copolymer. In conclusion, the Superpave binder specifications were developed considering primarily unmodified asphalts. Though some validation studies (with laboratory mix tests) consider polymer modified asphalts, they are limited to binders containing modifiers that form a macroscopically homogenous system with the asphalt.

When the Intermodal Surface Transportation Efficiency Act of 1991 was passed, some testing of asphalt modified with ground tire rubber or crumb rubber modifiers (CRM) were reported^{5,6}. In these papers the Superpave binder testing was simply applied to testing binder with fairly large (up to -10 mesh = 2 mm) particulates. It was not shown in these papers that the Superpave binder test methods can be used to predict the performance of such binders.

AASHTO provisional procedure PP5⁷ deals with the separation of modifiers from asphalt on storing either by formation of the film on the surface or a sludge on the bottom. The practice further ensures that the base asphalt that is used to make modified binder is over 99% soluble. This implies that after passing this test any modifier (including a particulate modifier) can be used provided the modifier does not separate when left standing at 163°C for 48 hours. In a move to limit the kinds of modifiers that could be used, the FHWA Superpave Binder Expert Task Group (ETG)⁸ decided "that the material being evaluated using the Superpave binder specifications must be tested to satisfy the ASTM D5546 solubility criteria. If the material fails this test, it is up to the purchasing agency to accept or reject the material." Although such specifications on the use of particulates do impose some restrictions, they do not absolutely disallow the use of particulates. This perhaps should not be done since it will stifle any innovation. However, a basic understanding of the behavior of particulates in asphalt will allow for a more objective evaluation on the benefits (or lack thereof) of particulates in pavements.

Given that the development and validation of Superpave binder tests did not rigorously consider binders with particulate additives, several questions must be answered before the adoption of the Superpave binder specification nationally. These questions broadly fall into three categories:

- (1) When particulates are added to asphalt there are issues relating to segregation of the particulates due

to settling or other phenomena. There is the issue of maximum particle size below which the accuracy of measurements with the Superpave testing equipment will not be affected. There may also be other unknown issues that could affect the results. These issues can be summarized by the questions "Can the present Superpave testing procedures be used to test binders with particulate additives? Under what limitations can such modified binders be tested?"

- (2) How does modification of binders with particulate additives affect the Superpave grading of these binders? Can the changes in grading be predicted with the knowledge of parameters that completely characterize the rheology of particulate-binder system?
- (3) Will a binder whose PG (performance grade) grading is achieved by adding particulate modifiers perform the same as another binder of the same PG grade that is unmodified? In other words, will the changes in binder specification due to particulate modifiers truly reflect on the performance of mixes containing such modified binders in laboratory mixture tests and on the pavement performance?

Obviously, these are loaded questions and require extensive research. The third question above, is the most significant, for, if adding particulates to binders changes a property such as $G^*/\sin(\delta)$ but does not really change the pavement performance, then the binder will have an inflated grade that will not be reflected in the performance. On the contrary, if the addition of certain particulates does enhance the performance of the roads, but this is not truly reflected in the current specifications, then methods must be developed to capture this enhanced performance.

An understanding of the asphalt-particulate system is fundamental to answering any of the above questions. This is the subject of this paper.

Evaluation of particulates in asphalt in the form of fines and mineral dust is not new, nor is the evaluation of particulate composites in polymers and other materials. There are hundreds of research papers that deal with this topic in the materials science literature. In asphalt literature, several investigators have tried to evaluate the effect of fines in asphalt concrete and have attempted ways to predict the stiffening power of fillers in asphalt. Tunnicliff⁹ has reviewed the literature for mineral filler-asphalt systems prior to 1962. Another noteworthy paper is the report by Anderson¹⁰ who gives insight into the role of mineral filler in asphalt. In the field of polymers, two recent reviews^{11,12} and a book¹³ summarize the developments in polymer-melt systems, highly filled systems and general treatment, respectively. The above is not meant to be a complete literature survey, but just a reference to key review papers.

Description of asphalt with particulate additives

The description of the behavior of filled systems in polymer matrices has traditionally been approached from two directions—Einstein's equation¹⁴ and its modifications for polymer liquid and melt systems, and the Kerner's equation¹⁵ and Hashin and Shtrikman's equation¹⁶ and their variations for polymer solid systems. These two approaches were brought together with the expression

$$\left(\frac{\eta}{\eta_1} - 1 \right) = \frac{2.50(8 - 10\nu_1)}{15(1 - \nu_1)} \left(\frac{G}{G_1} - 1 \right) \quad (1)$$

for the relation between viscosity and shear modulus¹⁷. Here, η is the viscosity, G the shear modulus, ν is the poisson's ratio. When the Poisson's ratio is 0.5, then

$$\frac{\eta}{\eta_1} = \frac{G}{G_1} \quad (2)$$

Thus, the equations developed for η/η_1 should be applicable to G/G_1 , and vice-versa. The convention used above will be that used in equations henceforth—subscript 1 denotes the matrix, 2 denotes the particulates, and the unsubscripted variables denote the binders with particulates (a composite property).

After an evaluation of many equations in the literature including the Einstein¹⁴, Mooney¹⁸, Roscoe¹⁹, Eilers-van Dijk²⁰ etc. (which will not be described in this paper) equations, the generalized Nielsen's equation^{13,21} was selected for further analysis of asphalts. Nielsen's equation is a modification of Kerner's equation for elastic materials. However, this equation has been applied to many viscoelastic polymers successfully¹³. The Nielsen's equation describes the stiffness dependence on the volume fraction of particulates in terms to two fundamental properties of the system. It further provides a way to account for differences in the stiffness of fillers themselves, the particle-matrix interface energy, and other materials parameters. Such knowledge will help isolate the the various causes for stiffening of binders when particulates are added.

Nielsen's equation describes the modulus ratio between the filled and unfilled system as follows:

$$\frac{M}{M_1} = \frac{1 + AB\phi_2}{1 - B\psi\phi_2} \quad (3)$$

where M is any modulus and ϕ_2 is the volume fraction of the filler. The constant A takes into account such factors as geometry of the filler phase and poisson's ratio of the matrix, the constant B takes into account the relative moduli of the matrix and filler phases; its value is 1.0 for very large M_2/M_1 ratios.

$$B = \frac{M_2/M_1 - 1}{M_2/M_1 + A} \quad (4)$$

The factor ψ depends on the maximum packing fraction, ϕ_m , of the filler. An empirical equation that satisfactorily describes the relation between ψ and ϕ_m is

$$\psi = 1 + \frac{1 - \phi_m}{\phi_m^2} \phi_2 \quad (5)$$

The constant A is related to the generalized Einstein Coefficient K_E by

$$A = K_E - 1 \quad (6)$$

In the case of mineral fillers in asphalt, since the modulus of the filler is much higher than the asphalt, the value of B is unity. Substituting $B=1$ and equation 5 in equation 3 will yield

$$\frac{M}{M_1} = \frac{1 + A\phi_2}{1 - (1 + C\phi_2)\phi_2} \quad (7)$$

where

$$C = \frac{1 - \phi_m}{\phi_m^2} \quad (8)$$

By curve-fitting equation 7 to the data, the constants A and C can be estimated. From these parameters, the generalized Einstein coefficient K_E and the maximum packing fraction, ϕ_m , can be calculated.

Thus, if Nielsen's equation, obtained for filled polymer systems, can be used for asphalts, it is then possible to characterize an asphalt-particulate system using two fundamental properties, K_E and ϕ_m . A knowledge of the variation of K_E and ϕ_m for different asphalt-modifier systems as a function of properties of interest then lead to the selection of appropriate powders for better such properties. Although, this paper restricts the analysis to mineral fillers, this approach can be used for all modifiers used for asphalts as long as they do not completely dissolve in asphalt, but form a discrete, but dispersed phase.

EXPERIMENTAL

Thirteen fillers that were used in a prior study²² were used with an AC-20 from Venezuela's Lagoven base stock supplied by Koch Material's company, Pennsauken, NJ. Some of the properties of these fillers are listed in Table 1. The particle size distributions for all these fines are reported in a prior study²³

The asphalt was used in its unaged state for all the experiments. Fines were added to asphalt to make 10 g batches of 4, 8, 12, 16, 20 and 24 volume percent particulates. Care was taken not to form agglomerates during the mixing process. The mastic was continuously stirred as it cooled down to prevent any settling. When the mastic thickened due to cooling, it was then transferred to silicone rubber molds to make pellets for testing with the dynamic shear rheometer (DSR).

Testing of the mastic was done with a Rheometrics RDA II dynamic shear rheometer (DSR) with a FTS torque transducer. The transducer was used in its most sensitive range (200 g-cm full scale). Strain

Table 1. Particulates used in this study[†]

Code	Sp. Gr.	Rigden Voids	Material
SWE2	2.84	36.5	Granite
SWE3	2.74	38.2	Granite
SWE5	2.91	37.3	Granite
SWE6	2.84	40.0	Granite
SWE7	2.74	33.1	Limestone
CHE1	2.76	38.5	Sandstone
CHE2	2.76	32.8	Limestone
GER1	2.74	35.2	Pure Limestone
GER2	2.87	34.8	Dolomitic Limestone
GER3	2.74	34.5	V. Pure Limestone
GER4	2.76	45.7	Granite
GER7	3.18	69.2	Fly Ash
GER9	2.74	38.2	Limestone

[†]Data from Reference 19

sweeps were measured at 25°C and 10 rad/s frequency with 8 mm parallel plate geometry and 2 mm gap and at 70°C with a 25 mm parallel plate and 1 mm gap. There has been discussion as to the maximum size particulates that can be used between parallel plates with 1mm gap. In these experiments we have avoided this issue by choosing fine particulates that have over 90 wt% below 75 μ m. The issue of maximum particle size will be addressed in later research.

RESULTS

The strain sweeps obtained for asphalt with varying amount of fines are shown in Figures 1 (25°C) and 2 (70°C). This is a representative of data obtained for all the fines. The data was linear to over 1% strain at 25°C and to over 10% strain at 70°C. For further analysis, values at 0.1 % strain for 25°C and 1% strain at 70°C were considered.

When the ratio of G^* to G_1^* was plotted as a function of volume fraction of particulates (ϕ_2), behaviors such as illustrated in Figures 3 and 4 were observed. These figures also illustrate the curve-fit according to equation 7 And the 95% confidence limits for these curves. The curve-fit parameters are listed in Tables 2 and 3 for measured parameter G^* and G' , respectively. It must be noted that for the fines studied, the constant A varied from 1.2 to 6.6 with the exception of GER7 which had A values between 10.5 and 15.2. The constant C varied from 1.0 and 4.7 not including GER7.

The generalized Einstein coefficient K_E and the maximum packing fraction ϕ_m calculated from the curve-fit parameters are listed in Table 2. The variation in constant A is reflected in variation of K_E . The ϕ_m varied from 0.32 to 0.52 for all the powders. It is also interesting that ϕ_m varied as little as 0.04 and as much as 0.12 between measurements at the two temperatures for a given particulate and asphalt. The key to using this approach is in the success in the interpretation of K_E and ϕ_m .

Figure 5 shows the phase angle as a function of ϕ_2 at both 25°C and 70°C. This curve is typical of those of the thirteen mastic mixes in that there is no systematic variation in the phase angle with ϕ_2 . Also, the magnitude of variation is $\pm 1^\circ$. We can therefore conclude that the phase angle is not effected by the addition of mineral particulates up to 25 volume percent fines.

DISCUSSION

When a powder fills a container, a fraction of the volume of the container is occupied by the powder particles while the rest are voids. The fraction of the volume of the container actually occupied by the powder is defined as the packing fraction, ϕ_2 . If the powder packs efficiently, then the volume fraction of

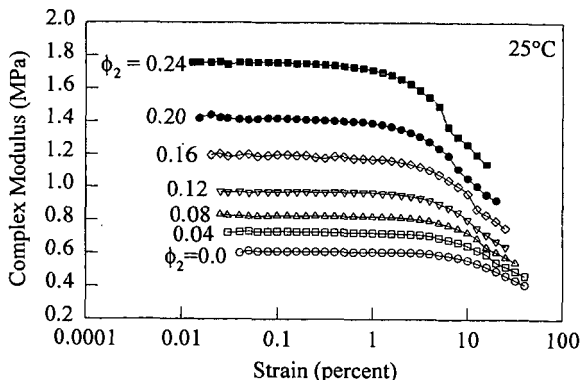


Figure 1. Strain Sweeps at 25°C for asphalt with different amounts of GER9. This is representative of all the powders.

	25°C		70°C		25°C		70°C	
	A	C	A	C	K_E	ϕ_m	K_E	ϕ_m
CHE1	2.2	3.1	2.6	4.5	3.2	0.43	3.6	0.37
CHE2	4.2	1.8	4.7	3.7	5.2	0.52	5.7	0.40
GER1	2.5	2.7	3.0	3.4	3.5	0.45	4.0	0.41
GER2	4.0	3.2	3.3	3.5	5.0	0.43	4.3	0.41
GER3	1.6	3.8	2.0	4.2	2.6	0.40	3.0	0.38
GER4	2.5	5.1	2.6	5.3	3.5	0.36	3.6	0.35
GER7	10.5	6.8	12.8	8.5	11.5	0.32	13.8	0.29
GER9	3.0	2.7	2.2	3.8	4.0	0.45	3.2	0.40
SWE2	1.9	5.5	1.6	5.9	2.9	0.35	2.6	0.33
SWE3	2.5	2.7	2.3	3.9	3.5	0.45	3.3	0.39
SWE5	1.0	6.7	2.6	2.8	2.0	0.32	3.6	0.45
SWE6	1.7	4.1	3.4	3.6	2.7	0.39	4.4	0.41
SWE7	1.8	5.3	2.9	4.4	2.8	0.35	3.9	0.37

powder in the container, and, hence, the packing fraction, ϕ_m increases. The maximum packing fraction, ϕ_m , is the highest value ϕ_2 can have, and is a function of the average particle size and particle size distribution. Anderson described two refined techniques for measuring ϕ_m , namely, the dry compaction method and the kerosene method¹⁰. Since ϕ_m is a fundamental property, ϕ_m measured by an independent technique (such as Anderson's) should compare with the value from Nielsen's equation.

Figures 6 and 7 plots the correlation between the ϕ_m from the dry compaction method of Anderson and the ϕ_m obtained as described in this paper. This figure shows there is a poor correlation between the two techniques. The ϕ_m from Equation 6 is consistently lower than the measured value.

In another example, we fit viscosity (25°C) measurements from Traxler²⁴ to Nielsen's equation and estimated the ϕ_m . The correlation between the estimated ϕ_m and the value measured experimentally²⁴ (by dry compaction in a glass graduate technique) is plotted in Figure 8. This, in contrast to the data in Figures 6 and 7, shows very good correlation.

Apparently, the success of Equation 7 in estimating ϕ_m in Figure 8 indicates that the equation works in some situations. The problem is to identify when the equation works and how to best use it to gain an insight into the mastic.

A likely reason for disparity between the measured and calculated values of ϕ_m is the fact that the ϕ_m calculated from Nielsen's equation measures the true state of packing for particulates in asphalt, while the

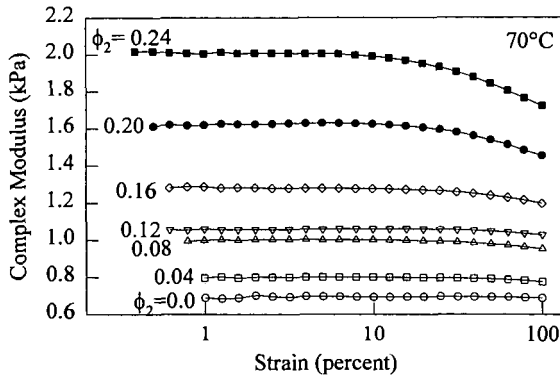


Figure 2. Strain sweeps at 70°C for asphalt with different amounts of GER9. This is representative of the behavior of all the particulates.

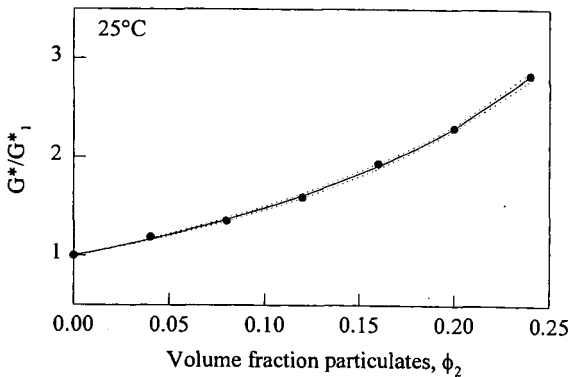


Figure 3. The change in G^* ratio as a function of ϕ_2 at 25°C. The solid line is a fit with the Nielsen's equation and the dotted lines are 95% confidence limits for the curve-fit.

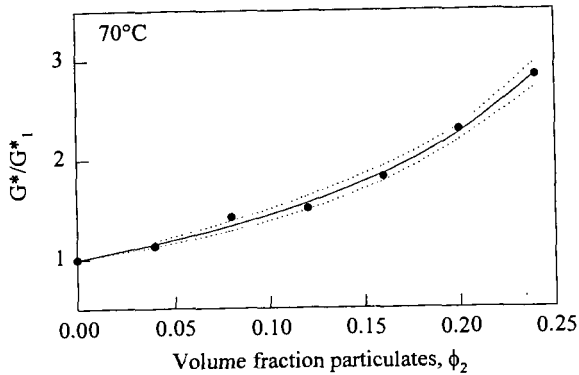


Figure 4. The change in G^* ratio as a function of ϕ_2 at 70°C . The solid line is a fit with the Nielsen's equation and the dotted lines are 95% confidence limits for the curve-fit.

dry compaction technique of Anderson measures an ideal case, a state that is unnatural for asphalt systems. The following factors would effect the packing of particulates in asphalt and, hence, the estimates of K_E and ϕ_m ¹³:

1. Any particle-particle interaction causing networks (structuring) among particles or formation of agglomerates would decrease the packing of particulates (decreasing ϕ_m). Such interactions will also reflect on higher estimates of K_E .
2. The aggregate shape and aspect will also effect the packing of powders. Higher aspect ratio of particles would increase the K_E and decrease the packing efficiency (decreasing ϕ_m).

On the other hand, the K_E measured for all the powders are close to the theoretical value of 2.5 derived for very dilute spheres¹⁴. This indicates that the approach is fairly successful in describing the mastic, and there are differences between the powders in terms of shape of particles, their interaction with the asphalt, etc.

Although there are several issues to be resolved, the use of Nielsen's equation allows for a fundamental approach to analyzing particulates and fillers in asphalts. In the asphalt literature, it has been reported that the Rigden voids (which is equivalent to $1-\phi_m$) correlate most with the stiffening power of asphalts^{10,22}. The approach presented in this paper indicate that a factor other than Rigden voids (and its equivalent ϕ_m), namely, the generalized Einstein coefficient K_E , also is an important property that predicts the stiffening power of the fines. In fact, both these parameters are equally important in predicting the stiffening power of particulates. These two parameters are a function of the asphalt-particulate system and characterize the system completely. The effect of both these parameters on the stiffening of asphalts will be discussed next in this paper.

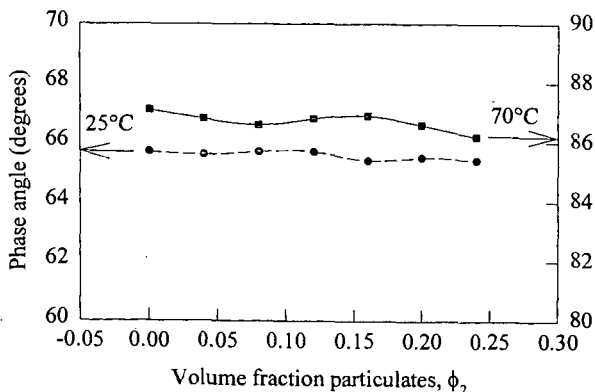


Figure 5. The change in phase angle as a function of ϕ_2 at 25°C and 70°C .

Effect on PG grading

It has been shown that the increase in G^* with addition of particulates can be described if we know ϕ_m and K_E . It was shown that for most of the mineral powders used in this study, ϕ_m varied between 0.32 and 0.52 and K_E varied between 2 and 5. By analyzing how G^* varies for a range of ϕ_m and K_E , one can predict to what extent the addition of mineral fillers are likely to effect the PG grading if the ϕ_m and K_E are known.

In Figure 5, it was shown that the phase angle did not change with addition of particulates. This indicates that by the addition of particulates the master curve for the asphalt merely shifts towards higher G^* without undergoing any change in time dependence. Such a behavior is assumed for low temperature region as well. Since the m -value is equivalent to the phase angle, the independence of phase angle to the addition of particulates can be reasonably expected to reflect the independence of m -value also. This assumption has to be tested with actual experimental data. This is planned for future work.

The procedure described below was used to evaluate the effect of the addition of mineral fillers on the PG grade of asphalt:

1. The $G^*/\sin(\delta)$ was plotted as a function of temperature and fit with a quadratic equation of the form $\log(G^*/\sin(\delta)) = \alpha + \beta T + \chi T^2$. From this equation the fractional grading (the temperature when $G^*/\sin(\delta) = 2200$ Pa) for the binder was determined.
2. For $G^*/\sin(\delta)$ at each temperature (52, 58, 64 and 70°C), the $G^*/\sin(\delta)$ for binder with particulates were calculated for given values of ϕ_m and K_E using Nielsen's equation.
3. We now have the estimated $G^*/\sin(\delta)$ vs. temperature data for asphalt with different amount of particulates. For each ϕ_m , a quadratic equation was fit as before to calculate the continuous grade of the mastic. It was found that only the constant α varied with ϕ_m , the constants β and χ being invariant. The fraction grading thus estimated is plotted as a function of ϕ_m and K_E in Figures 9 and 10, respectively.
4. A similar procedure was carried out for creep stiffness at 60 s. The change in fractional grade with the addition of particulates as a function of ϕ_m and K_E are plotted in Figures 11 and 12, respectively.

The invariance of constants B and C with ϕ_m is the result of assuming that ϕ_m and K_E does not change with temperature. This assumption is consistent with our earlier reasoning that the addition of particulates merely shifts the master curve to higher stiffness. It can however be seen from Table 2 that ϕ_m and K_E do not seem to be different at 70°C than it is at 25°C, which leads us to give credence to this assumption.

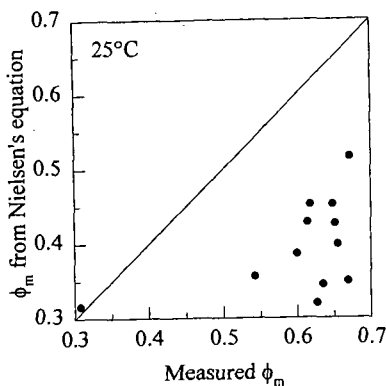


Figure 6. A comparison of ϕ_m estimates from Nielsen's equation (25°C data) and measured by dry-compaction method.

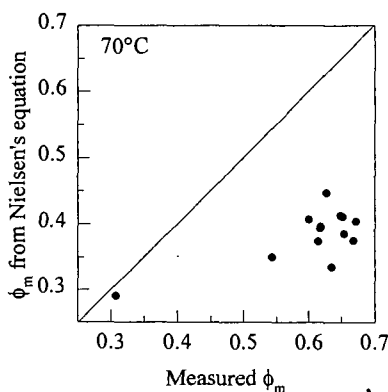


Figure 7. A comparison of ϕ_m estimates from Nielsen's equation (70°C data) and measured by dry-compaction method.

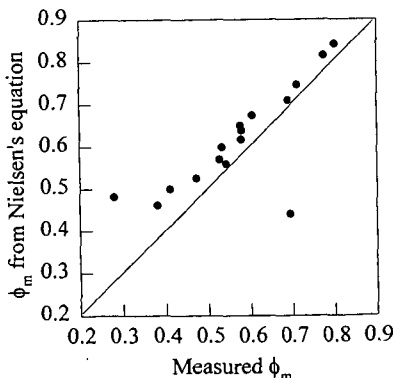


Figure 8. A comparison of ϕ_m estimates from Nielsen's equation (25°C data) and measured by a different dry-compaction method. (Data from Ref. 22)

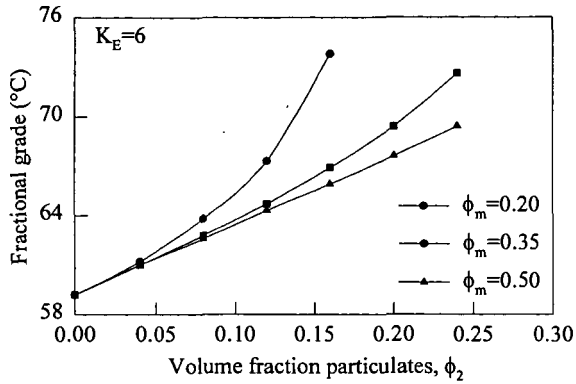


Figure 9. The effect of increasing ϕ_m on the high temperature grade for RTFOT aged asphalts.

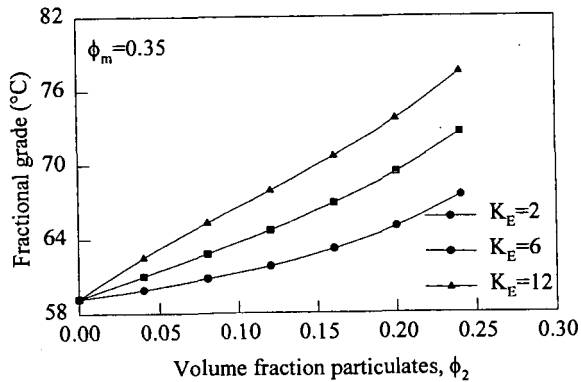


Figure 10. The effect of increasing K_E on the high temperature fractional grade on RTFOT aged asphalts.

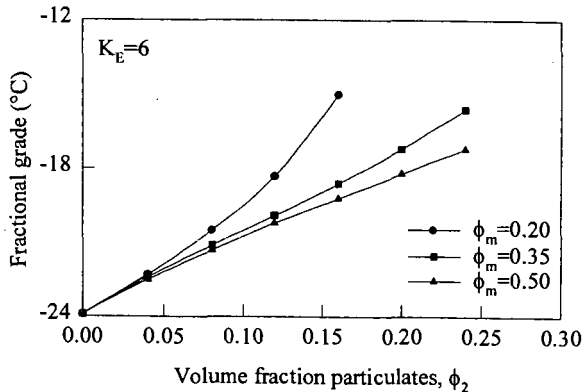


Figure 11. The effect of increasing ϕ_m on the low-temperature fractional grading based on S.

The range of ϕ_m and K_E selected for our study should represent many non-agglomerating mineral fillers. Close packing of particulates can yield a value of ϕ_m higher than 0.5. Very poor packing caused by the hygroscopic nature of the particulates or existence of agglomerates can cause ϕ_m to be less than 0.2. If the particulates are extremely fine, then the ϕ_m and K_E can be very different.

From Figure 9 it can be seen that as fines are added to the asphalt, the high temperature grade increases

by six degrees (one grade) with the addition of 13% particulates when ϕ_m is 0.35 and another grade with additional 10% fines. When the ϕ_m is 0.5, it requires 16% for the first grade and additional 10% for the next grade. On the other hand, if ϕ_m is closer to 0.2, it takes just 8% to increase $G^*/\sin(\delta)$ by a grade and additional 5% for the next grade. Thus as ϕ_m is reduced, $G^*/\sin(\delta)$ becomes more sensitive to the addition of particulates.

Similarly, when $K_E=2.0$ (Figure 10) it takes as much as 22% particulates to increase $G^*/\sin(\delta)$ by one grade, 13% when K_E is 6, and only 9% when K_E is 12. Since most of the powders studied had K_E between 2 and 6, it can be stated that between 13 and 22% particulates change the high temperature grade by 6°C. Higher the K_E , the more sensitive is the grade to the addition of fillers (stiffening effect).

At the lower end, a similar behavior can be observed. However, it is much subdued at this end for it takes 18% particulates to increase S by one grade at ϕ_m of 0.35 and K_E of 6. It is not known if these parameters ϕ_m and K_E , will remain the same as the temperature is lowered. If this behavior can be controlled then it is possible to tailor the fines to effect the high temperature grade while not causing a change in the low temperature properties.

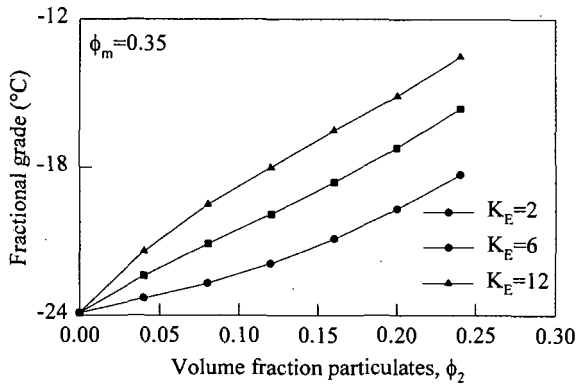


Figure 12. The effect of increasing K_E on the low-temperature grade of binders based on S.

CONCLUSIONS

The following conclusions were made from this study:

1. Nielsen's equation was shown to fit the dependence of stiffness on volume fraction particulates, ϕ_2 , for thirteen fillers. The parameters in the equation estimates the maximum packing fraction ϕ_m and generalized Einstein coefficient, K_E . Thus the dependence of stiffness on volume fraction can be predicted by knowing these two fundamental parameters.
2. The phase angle did not vary systematically with ϕ_2 . The overall change in the phase angle with the addition of up to 25 volume percent particulates was less than 2 degrees.
3. The ϕ_m estimated from Nielsen's equation did not correlate with the ϕ_m measured by compaction technique for the measured data. However, when such a comparison was made for data from literature very good correlation was observed. Thus, more study is required to completely understand the Nielsen's equation for asphalt mastics.
4. For the powders used in our study ϕ_m had values of 0.29 to 0.52, and K_E had values 2.04 to 13.8.
5. The high temperature and low temperature continuous grade increased with addition of fillers. This increase was more sensitive as ϕ_m decreased and as K_E increased. In other words, if ϕ_m is reduced or K_E is increased, the continuous grade increased more rapidly with the addition of particulates.
6. The continuous grade which is synonymous with stiffening power is affected by not just ϕ_m (which is equivalent to Rigden voids) but also to K_E , another independent parameter.

REFERENCES

1. D. A. Anderson and Thomas W. Kennedy, "Development of SHRP binder specifications," *J. Assoc. Asphalt Paving Technol.*, 62, 481-555, (1993).

2. G. N. King, H. W. King, O. Harders, W. Arand and P. P. Planche, "Influence of asphalt grade and Polymer Concentration on the Low Temperature Properties of Polymer Modified Asphalt," *J. Assoc. Asphalt Paving Technol.*, **62**, 1-22, (1993).
3. R. G. Hicks, F. N. Finn, C. L. Monismith and R. B. Leahy, "Validation of SHRP binder Specification through mix testing," *J. Assoc. Asphalt Paving Technol.*, **62**, 565-614, (1993).
4. M. G. Bouldin, G. M. Rowe, J. B. Sousa and M. J. Sharrock, "Mix Rheology—A Tool for Predicting the High Temperature Performance of Hot Mix Asphalt," *J. Assoc. Asphalt Paving Technol.*, **63**, 182-223, (1994).
5. H. U. Bahia and R. Davies, "Effect of Crumb Rubber Modifiers (CRM) on Performance-related Properties of Asphalt Binders," *J. Assoc. Asphalt Paving Technol.*, **63** 414-49, 1994.
6. H. U. Bahia and R. Davies, "Factors Controlling the Effect of Crumb Rubber on the Critical Properties of Asphalt Binders," *J. Assoc. Asphalt Paving Technol.*, **64** 130-162, (1995).
7. AASHTO provisional Specification PP5-93, "Standard Practice for the Laboratory Evaluation of Modified Asphalt Systems," American Association of State Highway and Transportation Officials, March (1995).
8. Minutes of Superpave Binder Expert Task Group meeting, December (1994).
9. D. G. Tunnickliff, A review of Mineral Filler," The Proceedings of the Assoc. Asphalt Paving Technologists," **31**, 118-50, (1962).
10. D. A. Anderson, "Guidelines on the Use of Baghouse Fines" National Asphalt Pavement Association. Information Series 101-11/87. Lanham, Maryland, (1987).
11. Yu. G. Yanovsky and G. E. Zaikov, "Rheological Properties of Filler Polymers," Encyclopedia of Fluid Mechanics. Volume 9: Polymer Flow Engineering, Gulf Publishing Company, Houston, 243-76, (1990).
12. A. V. Shenoy, "Rheology of Highly filled Polymer Melt Systems," Encyclopedia of Fluid Mechanics. Volume 7: Rheology of Non-Newtonian Flows, Ed. N. P. Cheremisinoff, Gulf Publishing Company, Houston, 667-701, (1988)
13. L. E. Nielsen and R. F. Landel, "Mechanical Properties of Polymers and Composites" Chapter 7: Particulate-Filled Polymers, 377-459 Marcel Dekker, Inc. New York (1992).
14. A. Einstein, *Ann. Phys.*, **17**, 549 (1905); **19**, 289, (1906); **34**, 591, (1911)
15. E. H. Kerner, *Proc. Phys. Soc.*, **B69**, 808 (1956)
16. Z. Hashin and S. Shtrikman, *J. Mech. Phys. Solids*, **11**, 127 (1963)
17. L. E. Nielsen, "The Relation Between Viscosity and Moduli of Filled Systems," *J. Composite Mater.* **2**, [1] 120-23, (1968).
18. M. Mooney, *J. Colloid Sci.*, **6**, 162 (1951)
19. R. Roscoe, *Brit. J. Appl. Phys.*, **3**, 267 (1952)
20. H. Eilers, "Viscosity of Emulsions of a Highly Viscous Substance as a Function of Concentration," *Kolloid Z.*, **97**, 313 (1941).
21. L. E. Nielsen, "Generalized Equation for the Elastic Moduli of Composite Materials," *J. Appl. Phys.*, **41** [11] 4646-7, (1970).
22. B. M. Harris and K. D. Stuart, "Analysis of Filler Materials and Mastics Used in Stone Matrix Asphalt," *J. Assoc. Asphalt Paving Technol.*, **64** 54-95, (1995).
23. B. H. Harris, "Analysis of Minus 150 μm Aggregates for Stone Matrix Asphalt," Internal Report (1994).
24. R. N. Traxler, "Evaluation of Mineral Fillers in Terms of Practical Pavement Performance," *Assoc. Asphalt Paving Technologists Proc.* **8**, 60-77 (1937).

FRACTURE ENERGY SPECIFICATIONS FOR MODIFIED ASPHALTS

Joseph E. Ponniah*
Ministry of Transportation, Ontario
1201 Wilson Avenue, Downsview, ON. M3M 1J8

Ralph A. Cullen and Simon A. Hesp*
Department of Chemistry, Queen's University
Kingston, ON. K7L 3N6

Keywords: fracture, modified asphalts

INTRODUCTION

Low temperature cracking of asphalt pavements is a major performance problem in North America. In the past, extensive research has been done in this area to mitigate this problem. Recent findings by the Strategic Highway Research Program (SHRP) show that asphalt binder properties are by far the dominant factor controlling thermal cracking. Thus, the determination of these binder properties that affect thermal cracking is the key to the successful development of performance-based specifications for asphalt binders.

Traditionally, thermal cracking in asphalt pavements is controlled by using soft grades of asphalt cement based on penetration and viscosity measurements. Although, this approach has met with some success, it did not solve the problem completely. Besides, the emergence of modified asphalts has created a need for developing a suitable testing method for the characterization of binders containing additives. In general, asphalt pavement layers have built-in flaws (construction cracks). In addition, micro-cracks develop at the asphalt-aggregate interface due to differential thermal contraction of asphalt and mineral aggregates [1]. Micro-cracks can cause a localized stress concentration near discontinuities within the binder under thermally induced tensile loads. These stresses often reach a limiting value which leads to premature failures. Current binder specification limits do not consider the material resistance to these failure modes due to localized stress concentration. As a result, the actual performance often varies significantly from that anticipated by the design. What is required is a rational approach by which asphalt binders can be properly evaluated for their effectiveness to resist locally induced premature cracking.

There is some concern that the binder tests developed by SHRP may not be adequate to accurately predict the low temperature performance of modified asphalts. SHRP binder tests are mainly focussed on determining the creep stiffness or failure strains of asphalt binders at selected temperatures. Although these properties are necessary to globally characterize the low temperature behaviour of asphalt binders, they alone are not sufficient to reliably measure the resistance of asphalt binders to premature cracking. A complete knowledge of the damage process both at the micro and macro levels, is required to address the problem of premature fatigue cracking due to localized stress concentration, particularly in modified asphalts.

A review of the literature shows that fracture mechanics principles can be effectively used to control the fracture of materials which occur prematurely due to built-in flaws or cracks. The main objectives of this study are: a) to apply the fracture mechanics principles to characterize the low temperature fracture behaviour of asphalt binders; b) to develop a rational routine testing method using the fracture mechanics principles suitable for evaluating neat and modified asphalt binders with respect to low temperature cracking; (c) to analyze the correlation between the fracture properties and the low temperature performance.

SCOPE

The scope of the work includes: a) determination of binder properties and performance grade (PG) temperatures for the different asphalt binders using conventional and SHRP test methods; b) measurement of fracture properties (fracture toughness, fracture energy) of the asphalt binders selected in (a), using the newly developed fracture test method; c) determination of fracture temperatures of asphaltic concrete specimens containing the same binders as in (a) and (b), using the Thermal Stress Restrained Specimen Test (TSRST); and d) establishment of a correlation among the binder properties (determined from SHRP tests and the fracture test method) and the mix fracture temperature.

* To whom the correspondence may be addressed

APPLICATION OF FRACTURE MECHANICS PRINCIPLES

Fracture mechanics is a technique which identifies the cause of premature failure of materials due to built-in flaws, such as micro-cracks, under a load much smaller than the design load. If the material is homogeneous and behaves in a linear elastic manner, the effect of stress concentration around a micro-crack can be measured in terms of a parameter, called stress intensity factor (K_I). K_I increases with an increase in the external load and when it reaches a critical value, K_{Ic} , unstable fracture occurs. The parameter, K_{Ic} , called the fracture toughness, decreases with an increase in specimen thickness reaching a constant minimum value when plane-strain conditions are reached. This lower level of K_{Ic} is reproducible and can be used as a material property to evaluate the brittle fracture of materials in the same manner as the yield strength is used for structural analyses. This means that the fracture toughness can also be used to study the brittle fracture behaviour of asphalt binders at low temperatures. However, when polymers are added to the asphalt, the modified binder exhibits different failure behaviour at low temperatures, ranging from brittle fracture to plastic deformation or excessive elongation. This is because the modified asphalts usually contain finely dispersed secondary phases within the polymer matrix which contribute to shear yielding mechanisms and thereby prevent brittle failure. Fracture mechanics suggests that, when a material undergoes yielding (creep), it is the rate of energy dissipation (fracture energy) which controls the failure mode from crack initiation to full depth crack propagation. As explained later, fracture energy can be calculated once the fracture toughness and the stiffness modulus values are obtained. Thus, it appears that fracture energy will give valuable and consistent information on the effectiveness of modifiers in increasing the fracture resistance of asphalt binders. The question still remains how effective the fracture energy specification is as compared to the SHRP binder specification with respect to low temperature cracking. An experimental investigation was carried out to compare the correlation between the low temperature performance and the binder properties determined from the fracture test and those from SHRP tests. As well, trial sections were installed in Northern Ontario to compare the findings of the laboratory investigation with the long term low temperature performance of the modified asphalts in the field.

EXPERIMENTAL INVESTIGATION

Materials

Two types of conventional asphalts (85-100 pen and 150-200 pen) and five different modified asphalts were used in the experimental program. These modified asphalts were specifically selected or designed in such a way to give a wide range of performance levels. For this purpose, different modifiers and various grades of base asphalts, ranging from hard (85-100 pen) to soft (300-400 pen) asphalts were used in this study. As such, the performance of different modifiers will not be addressed. The suppliers who participated in this study include: Petro Canada, Huskey Oil, Bitumar, Polyphalt, and McAsphalt.

TESTING PROCEDURES

Thermal Stress Restrained Specimen Test (TSRST)

The Thermal Stress Restrained Specimen test is intended to simulate conditions that a mix would experience in the field. The test specimens of approximately 100x35x35 mm size were made from asphaltic concrete briquettes prepared using the plant mix from the trial sections. Each specimen was glued to the end plates of a test frame located within a temperature controlled chamber. The specimen was restrained by the end plates while the temperature in the chamber was gradually reduced at $-10^{\circ}\text{C}/\text{hour}$ until the specimen failed due to thermally induced stresses. However, the potential change in specimen length due to the thermal shrinkage was compensated by the computer software system which was linked to two linear variable displacement transducers (LVDT) placed in between the end plates. The software uses the signals from the transducers to maintain a constant specimen length during testing. The output gives the temperature and the stress within the material at failure. The measured specimen failure temperature due to low temperature shrinkage is a good performance indicator of different binders used in the specimens.

Table 1: TSRST Results

Binder	Failure Stress (MPa)	Failure Temp (C)
Control 150-200	not tested	not tested
Control 85-100	2.24	-25.7±5.7
A	2.83	-45.4±2.5
B	2.65	-42.8±2.5
C	2.15	-42.9±4.9
D	8.31	-34.4±7.5
E	1.92	-29.5±8.1

A summary of the results together with 90% confidence intervals is presented in Table 1. The results indicate that binder A, with an average failure temperature of -45.4°C , will perform better than the rest, closely followed by binders C and B. The binder which has the lowest resistance to low temperature cracking, as expected, is the 85-100 pen asphalt. This test is time consuming and cannot be used on a routine basis; but it is a valuable research tool for investigating the low temperature performance of asphalt pavements

FRACTURE ENERGY TEST

Fracture energy testing was carried out by using a three point bending beam method (Figure 1) based on ASTM E 399-90 procedures [2]. The neat and modified binder beam samples were prepared using 25 mm wide by 12.5 mm deep by 175 mm long silicone rubber molds which have 90° starter notches, 5 mm deep, at the centre of the bottom surface. The molds were filled with asphalt binders and kept in a freezer at -20 °C for about two hours until they became solidified. The binder samples were then removed from the molds and were kept at the testing temperature for 18 hours. The starter notch in each sample was sharpened with a razor blade prior to testing. The notched beam is then placed on a three point bending apparatus of span 100 mm within an environmentally controlled chamber (Figure 1). The beam was then loaded until failure. From the output, the fracture toughness was computed according to Equation (1).

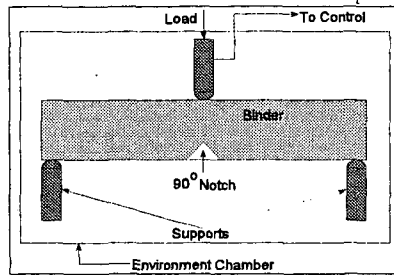


Figure 1: Fracture Toughness Apparatus

$$K_{IC} = \frac{P_f S}{BW^{3/2}} \left[\frac{3\left(\frac{a}{W}\right)^{1/2} \left[1.99 - \frac{a}{W} \left(1 - \frac{a}{W} \right) \right] \left(2.15 - 3.93 \frac{a}{W} + 2.7 \frac{a^2}{W^2} \right)}{2 \left(1 - 2 \frac{a}{W} \left(1 - \frac{a}{W} \right) \right)^{3/2}} \right] \quad (1)$$

Where: K_{IC} is the fracture toughness; P is the failure load; S is the span; B is the specimen depth; W is the specimen width; a, is the crack length .

The fracture energy can then be derived from:

$$G_R = \frac{K_{IC}^2 (1-\nu^2)}{E} \quad (2)$$

Where: G_R is the fracture energy (Jm^{-2}); ν is Poisson's ratio; E is Young's Modulus. As Poisson's ratio for asphalt cement at low temperature is very small, it is neglected in the computation of G_R using Equation 2. A couple of tests were carried out to ensure plane-strain conditions as discussed previously so that the fracture toughness values remain constant and reproducible. Secondly, the linear-elastic behaviour of the specimens was achieved by selecting the appropriate low test temperatures. For modified samples, the test temperature was -30 °C and the results are given in Table 2. Fracture toughness values in this table provide information on the type and amount of polymers used while the modulus gives information on the type of base asphalts used. Fracture energy measures the resistance of the binder to fracture. The results show that binder A has a higher resistance to thermal cracking than the rest, followed by binders C and B. The results also show that binder D, which used a harder base asphalt (85-100 pen), gives lower fracture energy while the binders A, B, and C used a softer base asphalt (150-200 pen) to give higher energy values. This supports the common believe that modified binder with a soft base asphalt is most suitable for preventing low temperature cracking.

Table 2. Fracture Energy Test Results at -30°C

Binder	Fracture Toughness (kNm ^{3/2})	Modulus (Mpa)	Fracture Energy (Jm ⁻²)
150/200 pen	*	*	*
85/100 pen	*	*	*
A	63.4	0.79	5.1
B	57.0	0.78	4.2
C	57.3	0.73	4.5
D	70.1	1.66	3.0
E	48.4	0.83	2.8

* Samples were too brittle and failed immediately

Figure 2 shows an obvious link between fracture energy and the low temperature TSRST performance. The regression analysis gives a strong correlation coefficient R^2 of 0.933. The good correlation implies that fracture energy can be used to develop a low temperature performance-based specification.

SHRP BINDER TESTS

SHRP binder tests were carried out using the control and modified samples. Table 3 provides the SHRP performance grades (PG) of the conventional asphalts and those of binders A, B, C, D, and E. Figure 3 shows the weak correlation between the PG grade values and the fracture temperatures with an R^2 value of 0.672. Alternatively, the relationship between the binder creep stiffness and fracture temperature was also investigated as shown in Figure 4. There is some improvement in the R^2 value but the correlation is still not as good as for that of G_{IC} . When the results of the SHRP direct tension test were compared with the fracture temperature it gave a very poor correlation (R^2 value = 0.004) as shown in Figure 5.

Table 3: SHRP low temperature performance grade results

Binder	Performance Grade (°C)
Control 150-200	-24
Control 85-100	-20
A	-32
B	-28
C	-26
D	-21
E	-26

PENETRATION TEST

Penetration tests were performed at 25° C after aging the binder using the Rolling Thin Film Oven Test method. Figure 5 shows that the correlation between the penetration values and the fracture temperatures is even better than that observed for the SHRP binder test results. This seems to indicate that SHRP binder testing system has not improved the existing characterization system with regards to modified binders

4.0 CONCLUSIONS

- Fracture energy shows the best correlation ($R^2 = 0.933$) with TSRST failure temperatures.
- Because of the high correlation and the fact that it is a fundamental material property, fracture energy seems to offer promise for use in the development of a low temperature performance-based specification for modified binders.
- The SHRP approach to establish a low temperature performance grade for asphalts based on binder creep stiffness, m-value, and failure strain gives a poor correlation with the TSRST failure temperatures
- The correlation between the penetration test results and the performance is comparable to that observed for the SHRP binder tests. However, the results are not conclusive because of the limited data.

Table 4: Penetration Test Results

Binder	Aged Pen 25° C
Control 150-200	85
Control 85-100	47
A	87
B	65
C	66
D	41
E	39

5.0 RECOMMENDATIONS

- Expand the study so that the effects of aging on fracture toughness / fracture energy properties can be determined
- Establish a set of critical fracture energies so that low temperature Performance Grades can be established using fracture energy testing.
- Relate the experimental data to the field observation from the Hwy 118 test sections in Northern Ontario. This should be done to verify if experimental predictions can be related to actual field performance.

6.0 REFERENCES

1. El Hussain H. Mohamed, Kwang W. Kim, and Joseph Ponniah, "Assessment of Localized Damage Associated with Exposure to Extreme Low Temperatures", Transportation Research Board, Washington, D. C., January, 1996.
2. ASTM Method E 399-90 (1984) Standard Test Method for Plane-Strain Fracture Toughness of Metallic Materials. Philadelphia: ASTM.

ACKNOWLEDGEMENT

Special thanks to Imperial Oil for their assistance in this research work.

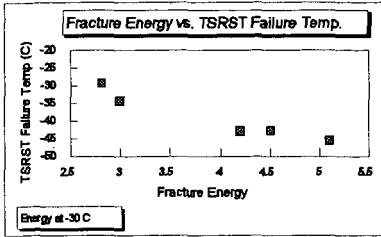


Figure 2: Fracture Energy vs TSRST Failure Temperature

$R^2 = 0.933$

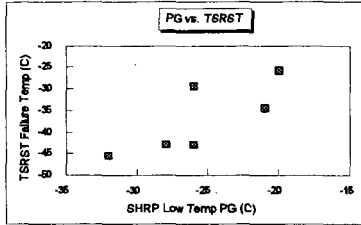


Figure 3: Performance Grade vs TSRST Failure Temperature

$R^2 = 0.617$

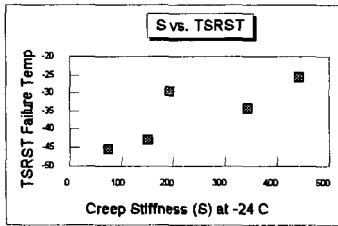


Figure 4: Creep Stiffness vs Failure Temperature

$R^2 = 0.672$

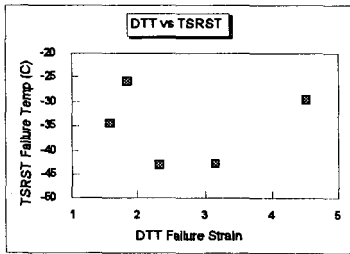


Figure 5: Failure Strain vs TSRST Failure Temperature

$R^2 = 0.0004$

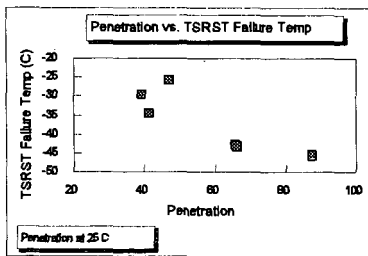


Figure 6: Correlation for Aged Binder at 25 C

$R^2 = 0.702$

HIGH TEMPERATURE PERFORMANCE OF SCRAP TIRE RUBBER MODIFIED ASPHALT CONCRETE

A. (Coom) Coomarasamy*, Research & Development Branch,
Ministry of Transportation, Downsview, Ontario, M3M 1J8, Canada,
Steven Manolis and Simon Hesp*, Department of Chemistry,
Queen's University, Kingston, Ontario, K7L 3N6, Canada.

ABSTRACT

Wheel track rutting tests on mixes modified with 30 mesh, 80 mesh, and very fine colloidal crumb rubber particles show that a very significant improvement in performance occurs with a reduction in the rubber particle size. The SHRP binder test for rutting, which was originally developed for homogeneous systems only, does not predict the performance improvement for smaller rubber particles. If these new scrap rubber binder systems are to be used in pavements then rutting tests on the asphalt-aggregate mixture should be conducted in order to accurately predict high temperature performance.

Keywords: crumb rubber modifier, particle size, rutting

1. INTRODUCTION

Excessive permanent deformation in the form of rutting associated with high temperature service and thermal cracking associated with low temperature service are two major problems affecting the performance of asphalt concrete pavements (1). Widespread adoption of radial tires, with pressures of 138 to 173 psi higher than their bias-ply predecessors and increased traffic volumes have accentuated these problems, especially rutting at high service temperatures. Without rutting, motorists would benefit from better steering control and less danger from hydroplaning in rain or skidding in icy conditions (2).

The demand for asphalt binders with a reduced temperature susceptibility is increasing, as user agencies are insisting on improved performance (3). Modification of the asphalt binder with high molecular weight polymers is one of the methods commonly employed for improving the thermal susceptibility of paving asphalts. Polyethylene, styrene-butadiene, and ethylene vinyl acetate copolymers have all been used successfully to improve upon the performance of asphalt binders (4). For the last three decades discarded rubber tires have also found end-use applications in asphalt binders in order to improve upon both the low- and high-temperature performance of the road surface. However, actual field trials have so far been inconclusive in their assessment of the performance/cost benefits of these materials (5). Use of reclaimed tire rubber for paving applications is also desirable from a solid waste management point of view.

2. BACKGROUND

Experimenting with scrap rubber for asphalt modification started in the 1920's (6). However, development of rubber modified asphalt binders, as they are now most often used throughout North America and in many other countries started in the 1960's, with the introduction of the McDonald process by the Roads Department of the City of Phoenix, Arizona (7). Since the developments in the late 1960's by McDonald and co-workers, various proprietary and generic technologies have evolved for the use of recycled rubber from scrap tires in asphalt binders and rubber modified asphalt concrete.

The dry process which was developed in the late 1960's in Sweden under the trade name Rubit was patented for use in the United States in 1978 under the trade name PlusRide (8). It differs from the wet process in that the crumb rubber is used as a portion of the aggregate and is directly mixed with the aggregate. This process uses crumbs of larger sizes (1/16-1/4 in; ~1.58-6.35 mm) at a loading of 3-4 wt% of the aggregate. This process also requires 1.5-3% more liquid asphalt than a conventional hot-mix. The increased asphalt content is needed to achieve a voids content below 3% in order to prevent premature ravelling of the pavement (9,10). The PlusRide technology has been proven effective in reducing the harmful effects of ice formation on roads (11,12). Other dry process techniques include those developed by the Army Corps of Engineers at the Cold Regions Research Laboratory (CRREL) and the Generic dry technology (13).

* To whom correspondence may be addressed.

In the wet process, when asphalt cement and crumb rubber are blended together, there is an interaction between these materials. This asphalt-rubber reaction is influenced by the blending/reaction temperature, the length of time the temperature remains elevated, the type and amount of mechanical mixing, the size and the texture of the crumb rubber modifier, and the aromatic component of the asphalt cement. Crumb rubber being a three dimensional network of natural and synthetic rubbers, reinforced with carbon black absorb the light oils from the asphalt cement during the "reaction" which results in swelling and softening of the crumbs. This in turn increases the viscosity of the modified binder (14). The wet process requires the use of at least 20% more liquid asphalt than is used in a conventional hot-mix pavement. In some cases 40-60% more asphalt is used, accounting for most of the increase in both cost and performance. The high initial cost combined with the uncertainty regarding future benefits is probably a factor which has hindered the large scale acceptance of asphalt-rubber technology. It is a fact that the cost of rubber modified pavements, in general, is currently anywhere from 60-150% above the cost of a conventional pavement (16). However, if modest amounts of fine crumb are applied to an asphalt binder, a pavement could be constructed with normal binder contents and aggregate gradations which would result in only a slight overall increase in cost. This approach has already been taken in recent years. Paving trials in Florida (17) and Ontario (18) have used asphalt binders which contain only 7-9% fine crumb rubber (80 mesh) directly blended into the asphalt cement. Initial laboratory and field results are quite promising but it is too early to draw any firm conclusions.

Crumb rubber being a cross-linked product, it has long been thought that devulcanization, partial devulcanization, or depolymerization would provide additional benefits in terms of storage stability and performance improvements. Epps (19) has found in an informal survey that there have been fewer pavements constructed with devulcanized rubber binder systems. The patent literature contains numerous claims on processes for devulcanizing waste tire matter: In 1971, Nikolinski and Dobrova (20) used various process oils to produce devulcanized rubber from waste SBR, nitrile rubber, butyl rubber and 1,4 cis polybutadiene. This is one of the earlier patents which clearly describes the use of aromatic oils in the process. Patents of C.H. McDonald (21), Nielsen and Bagley (22), Sergeeva et al. (23), and Ulicke and Cerner (24) all describe the use of aromatic oil for effecting devulcanization of scrap tire rubber in an asphalt medium. The main drawback with regards to the use of aromatic oils for devulcanization of waste rubber comes from the health hazard associated with these oils. The use of process oil or hydrocarbon liquid under high temperature and shear to render vulcanized rubber into a fluid form is described by Wakefield et al. in 1975 (25). Applications of shearing energy with addition of an aromatic oil to produce bitumen-asphalt compositions is described by van Bochove (26). According to this patent, better control over the material properties were made possible through the application of shearing forces. In 1992 and in 1994, Liang and Woodhams (27,28) described a process for devulcanization of scrap tire rubber in asphalt with the aid of aromatic oils and high shear and subsequently further stabilizing the devulcanized or disintegrated rubber particles by reacting the product with liquid polybutadiene and sulphur. The devulcanized system is mixed with a sterically-stabilized, polyethylene-modified asphalt binder as described in earlier patents by Hesp et al. (29,30). A recent paper by Zanzotto and Kennepohl (2) describes a high temperature, high shear process for devulcanizing scrap tire rubber in liquid asphalt. The authors report that the modified asphalt materials are being tested for their performance in paving mixes. It is apparent that morphology in the asphalt-rubber composition plays a crucial role in determining the properties of the crumb rubber modified binder systems and in the performance of crumb rubber modified asphaltic concrete. The work described here is concerned with achieving improved high temperature performance of asphaltic concrete mixes, taking into consideration the particle size of the asphalt rubber composition. Another paper by the same authors describes the work done on low temperature performance of the asphalt rubber mixes developed for this study (31).

3. EXPERIMENTAL

3.1 Materials

The asphalts used in this study were a 150-200 and an 85-100 penetration grade both obtained from the Lake Ontario refinery of Petro-Canada in Clarkson, Ontario made with crude from the Bow River area in Alberta, Canada.

The 30 mesh, cryogenically ground, passenger car tire rubber sample was obtained from Recovery Technologies of Mississauga, Ontario and the 80 mesh, ambiently ground, tire rubber sample was obtained from Rouse Rubber Industries of Vicksburg, Mississippi.

A dense-graded mix design meeting the Ontario HL-3 specification (32) for surface course mixtures, was used to prepare the asphalt rubber concrete samples for the evaluation of rutting resistance. Limestone coarse aggregate, limestone screenings and natural sand used for sample preparation were supplied by Dibblee Construction of Westbrook, Ontario.

3.2 Procedures

3.2.1 Sample Preparation

Two types of crumb rubber modified binders were prepared by slowly adding 10% by weight of crumb rubber (30 mesh and 80 mesh) to the 150-200 penetration grade asphalt at $170^{\circ} \pm 10^{\circ}\text{C}$ with moderate shearing. The third sample was prepared starting with 10% by weight of a 30 mesh crumb rubber in a 150-200 penetration grade asphalt. Particle size reduction was obtained with a thermo-mechanical process.

The asphalt concrete beams used, consisted of two lifts, each 38 mm from selected mix designs. The bottom lift of each beam was manufactured using a high stability (13600 N) Durham HL-4 mix. The top lift was manufactured using HL-3 mixes containing crumb rubber modified asphalt binder and the unmodified 150-200 and 85-100 penetration grade reference binders. The beams were prepared using a California Kneading compactor.

3.2.2 Dynamic Mechanical Testing

A Rheometrics Dynamic Analyzer RDA II was used for rheological testing. Hot asphalt samples were poured into a combined melts and solids (CMS) test fixture and allowed to cool to room temperature prior to testing. The CMS fixture consists of a 42 mm diameter cup and a bilevel plate which has an 8 mm diameter serrated surface concentric with and projecting from a 25 mm diameter plate. A temperature sweep was used to measure G'' , G' , G'' and $\tan\delta$ at four temperatures between 52 and 70°C in intervals of 6°C . A frequency of 10 rad/s was used. Samples were conditioned for at least 11 minutes at each test temperature. A soak time of 180 s, during which time the temperature did not vary by more than 0.1°C , was used prior to each measurement.

3.2.3 Rutting Evaluation

Rutting tests were carried out using a wheel tracking machine purchased from Petro-Canada Ltd. It consists of three parts; a constant temperature reservoir, a wheel carriage assembly and a drive linkage assembly. All of these parts work in unison to produce a back and forth movement of a tire along the lengths of the beam sample (2).

The prepared beam samples were conditioned at 70°C for 6 hours and tested at 60°C after allowing the sample to equilibrate in the constant temperature reservoir. Samples were subjected to 8000 passes (4000 cycles) using a treaded tire (pressurized at 550 kPa) at 60°C to induce rutting. Profilometers were used to obtain the rutting profiles.

4. RESULTS AND DISCUSSION

4.1 Effect of Crumb Rubber Modifier on Rutting Performance

The rut depth results obtained for individual HL-3 asphalt concrete beams and the average values for each mix are presented in Table 1. The mean particle size of the crumb rubber modifier in these systems are also given.

The results show that the resistance to rutting for crumb rubber modified binders is significantly better than that of the reference sample. Improvements over the control sample were about 37%, 51%, and 60% for modified binders containing 30 mesh, 80 mesh and $0.4 \mu\text{m}$ crumb rubber respectively. It is to be noted that the variation in rut depths between the duplicate samples are reasonable (except for the mix prepared with an 85-100 pen asphalt), considering the fact that the preparation of the concrete beams for these tests involves a series of steps which have to be carefully performed.

Table 1 also gives the rut depth values obtained for an 85-100 pen grade asphalt which is commonly used in high temperature service conditions such as in Southern Ontario. These preliminary results also indicate that, by crumb rubber modification of a softer grade (150-200 pen) asphalt, it may be possible to obtain high temperature rutting resistance comparable to that of an 85-100 pen grade asphalt.

The mean particle size for the thermo-mechanically processed sample was found to be 0.4 microns with a standard deviation of 0.4 microns. This represents a decrease of 1500 times compared to the 30 mesh (590 microns) crumb rubber used for modification. In terms of rutting performance, only about a 25% decrease in rut depth was obtained for a particle size reduction from 30 mesh (590 microns) to 0.4 microns.

4.2 Effects of Crumb Rubber Modifier in Dynamic Shear Measurements

A comparison was made between normalized average rut depths and normalized performance grades of all the three crumb rubber modified binders and the reference binder as shown in Figure 1. But this comparison does not seem to reveal any trend correlating the PG of a binder with the rutting performance.

The work of Hanson & Duncan (34) on crumb rubber binders also indicates that although the stiffness increases with concentration, there is little variation in $G^*/\sin\delta$ for different gradations of rubber. The gradations of rubber used in their work were GF 16, 40, 80 and 120 mesh sizes, as provided by Rouse Rubber Industries (33).

5. CONCLUSIONS

A thermo-mechanical process employed to incorporate larger 30 mesh size crumb rubber seems to be an effective method for the preparation of crumb rubber modified binder with significantly improved high temperature properties. A limited number of rutting experiments conducted on modified mixes, suggests that the resistance to rutting improves with a reduction in the particle size of the crumb rubber modifier. The SHRP binder test for rutting resistance, which was originally developed for homogeneous systems only, does not predict the performance improvement for crumb rubber modified systems containing smaller rubber particles. Rutting tests on a wheel tracking machine are found to be better for predicting rutting performance of crumb rubber modified systems.

6. ACKNOWLEDGEMENTS

Thanks are due to Albert Chang, Bonnie Wong and Steven Goodman all Co-op students from the University of Waterloo, for their assistance in the preparation of specimens, and to the staff of the Bituminous Section, of MTO, for their assistance in conducting rutting experiments. Financial assistance provided by Ontario Ministry of Environment & Energy to conduct part of this work is gratefully acknowledged.

7. References

1. Epps, J., Petersen, J. C., Kennedy T.W., Anderson, D. and Haas, R. (1986), TRR 1096, Washington, D.C.
2. Yacyshyn, R., Tam, K.K., and Lynch, D.F. (1990) Report EM-93 Engineering Material Office, Ministry of Transportation Ontario, Downsview, Ontario.
3. Sawatzky, H., Temperature Dependence & Complexation Process in Asphalt and Possible Influence on Temperature Susceptibility Conference on HydroCarbon Residue and Wastes Commission Utilization, Edmonton, Alberta, Sept. 4-5, 1991.
4. Wardlaw, K.R. and Shuler, S., Eds (1992) Polymer-Modified Asphalt Binders. ASTM Special Technical Publication 1108, Philadelphia: ASTM.
5. Flynn, L., Roads & Bridges, 12 (1992) 42.
6. Zanzotto, L., and Kennepohl, G. (1996). Presented at the 75th Annual Meeting of the Transportation Board, Washington, D.C.
7. Morrison, G.R., and Hesp., S.A.M. (1995) Journal of Material Science 30, 2584-2590.
8. Bjorklund, A. (1979) in Proceedings of the VII World Road Conference, Vienna.
9. Takallon, H.B. and Hicks, R.G., TRR 1171, TRB, National Research Council, Washington, D.C. (1988) pp. 113-20.
10. McQuillen, J.L., Member, J.F., Takallon, H.B., Hicks, R.G. and Esch, D., Transp. Eng. 114 (1988) 259.
11. Narusch, F.P. Alaska Department of Transportation and Public Facilities, Div. of Design and Construction, Central Region, Juneau, Alaska.
12. Esch, D., TRR 860, TRB, NRC, Washington, D.C. (1992) p. 5-13.
13. Epps, J.A. (1994), NCHRP Synthesis 198, TRB, NRC, Washington, D.C.
14. Heitzman, M., 71st Annual Meeting 12-16 January 1992, Washington, D.C. Preprint 920549.
15. Moore, W., Construction Equipment, February 1991.
16. Tarricone, P., Civil Eng., April 1993, 46.
17. Page, C.G., Ruth, B.E. and West, R.C., 71st Annual Meeting, 12-16 January 1992, Washington, D.C., Preprint 920452.

18. Joseph, P.E., and Kennepohl, G., Report PAV-91-03, Ministry of Transportation Ontario, Downsview, Ontario June 1991.
19. Epps, J., Ontario Ministry of Transportation Meeting on the Use of Crumb Rubber-Modified Asphalt Binders, April 10, MTO, Downsview.
20. Nikolinski, P., and Dobрева, R., Polim. Simp. 1971 (Pub. 1972) vol. 3, pp. 254-9.
21. McDonald (1974), US Patent 4,085,078, Filed on Dec. 1, 1970.
22. Nielsen, D.L. and Bagley, J.R. (1978), US Patent 4,068,023, Filed on May 20, 1976.
23. Sergeeva, M., Zhailovich, I.L., Tumashchik, P.I., and Orekirov, I.A. (1987), USSR Patent SU1289872 A1. Issued on Feb. 15, 1987.
24. Chemical Abstracts, Vol. 116(8) AN 61360c.
25. Wakefield, L.B., Crane, G., and Kay, E.L. (1975), US Patent 3,896,059, Filed Feb. 5, 1974.
26. Van. Bochove (1991), European Patent 0439232 A1, Filed Jan. 22, 1991.
27. Liang, Z.Z., and Woodham, R.T. (1992) GB Patent Application. Filed on December 29, 1992.
28. Liang, Z.Z., and Woodhams, R.I. (1994), World Patent Application 94/14896, Priority date: December 29, 1992 - GB 92 27035.4.
29. Hesp, S.A.M., Liang, Z.Z., and Woodhams, R.T. (1993). World Patent Application 93/07219 Priority date: September 30, 1991 - US 863,734.
30. Hesp, S.A.M., Liang, Z.Z. and Woodhams, R.T. (1994), US Patent 5,280,064, Filed on September 30, 1991.
31. Coomarasamy, A. and Hesp, S.A.M., Paving in Cold Areas, October 1996, Niigata, Japan (Paper to be presented).
32. Ministry of Transportation Ontario Laboratory Series, LS Manual.
33. Rouse Rubber Industries Inc. (1992) Company Product Literature, Vicksburg Mississippi.
34. Hanson, D., and Duncan, G.M. (1995), TRR 1488, TRB, Washington, D.C.

TABLE 1

Effect of Crumb Rubber Modified Binder on Rutting of HL-3 Mixes at 60°C after 8000 Passes of a Wheel Tracking machine				
Binder System	Run 1 Rut Depth (cm)	Run 2 Rut Depth (cm)	Average* Rut Depth (cm)	Crumb Rubber Particle Size (Microns)
150 - 200	0.84	0.71	0.77	N/A
10% 30 mesh	0.45	0.53	0.49	590 †
10% 80 mesh	0.41	0.35	0.38	177 †
10% 0.4 µm	0.34	0.27	0.31	0.41 ‡
85 - 100	0.15	0.33	0.24	N/A

* Average of Run 1 & Run 2 † Sieve size reported by Rouse Rubber Industries
 ‡ Mean particle size as determined by optical image analysis

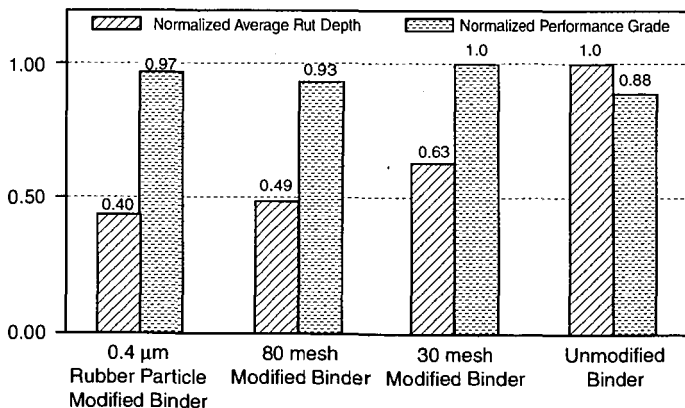


FIGURE 1. Comparison of normalized average rut depth with normalized performance grade

USE OF NUCLEAR MAGNETIC RESONANCE IMAGING TO STUDY ASPHALT

Francis P. Miknis and Daniel A. Netzel
Western Research Institute
365 North 9th Street
Laramie, WY 82070

Keywords: magnetic resonance imaging, asphalt, natural rubber, asphaltenes

INTRODUCTION

Magnetic resonance imaging (MRI) combines the basic principles of magnetic resonance with spatial encoding to obtain images of the distribution of fluids in samples. Because of the sensitivity of the hydrogen nucleus in NMR and because of its favorable relaxation times, water is the fluid most often imaged. This favorable aspect suggests that MRI might be used to obtain valuable information about water susceptibility and moisture damage mechanisms in asphalt. However, it has only been fairly recently that nonmedical applications of MRI have been increasing partly because of improvements in instrumentation and speed of data acquisition. MRI has been used to measure the distribution of fluids in porous rocks [1], ceramics [2], wood [3], other plant materials [4], synthetic polymers [5], solvent diffusion in polymers [6], coals [7,8], and bonding of adhesives [9].

In favorable circumstances, NMR imaging methods can be employed for imaging solid materials such as elastomers. NMR imaging has been used to study the morphology and defects in tire composites and the dispersion of carbon black in sections of tire tread [10] and to detect voids, gaps, and foreign particles in elastomers [11]. NMR imaging has also been used to study aging and phase separation in elastomers and to obtain the kinetics of the aging reaction [12]. In addition, inhomogeneities in natural rubber have been detected and characterized. Komorowski [13] has written a recent review of nonmedical applications of MRI. Little work has been done on the use of MRI in asphalt research.

EXPERIMENTAL

MRI measurements were made using spin echo (SE) or 3 dimensional (3D) imaging techniques. For nonviscous materials, such as water and organic solvents, the spin echo technique provided the best images because the relaxation times of nonviscous liquids were generally long and therefore more favorable for spin echo imaging. For elastomeric and viscous materials, the relaxation times of the protons were generally too short for spin echo imaging. Consequently, the 3D technique was used for these materials.

Magnetic resonance imaging experiments were carried out at a nominal proton resonance frequency of 200 MHz using a Chemagnetics/Otsuka Electronics microimaging probe. Samples for NMR imaging experiments were placed in 23 mm (OD) glass vials, which were then placed in 25 mm(OD) glass tubes. The tubes were inserted into the MRI probe and were positioned in the probe using O rings such that the cross sections to be imaged were contained in the experimental field of views (FOV).

Typical instrument parameters using the spin echo technique were echo times of 10-40 ms, a pulse delay of 1 s, a free induction decay size of 256 data points, 256 phase encodes, and a gradient strength of 34 G/cm. Eight slices, 1 mm thick and separated by 1 mm were obtained. The measuring time was ~ 1 hr. Images using the 3D method were made using an echo time of 2 ms, a pulse delay of 1 s, a free induction decay size of 256 data points, 128 phase encodes, 50 acquisitions and a gradient strength of 69 G/cm. Eight slices were usually obtained. The measuring time was 14.2 hrs for these experiments.

RESULTS AND DISCUSSION

MRI Measurements on Asphalts. MRI measurements cannot be obtained on asphalts at room temperature because the lack of molecular mobility (high viscosity), causes the NMR signal to decay away before any spin echoes can be formed. However,

there are some techniques that can be employed to decrease the viscosity and to increase the relaxation time, T_2 , so that images of asphalt are obtained. One approach is to acquire images at elevated temperatures where the asphalt viscosity is reduced and the relaxation times are lengthened. Cursory MRI experiments of this nature have been performed using a heat gun to melt asphalt and to acquire images as soon as possible while the sample is cooling. Images of asphalt have been obtained in this fashion but are not shown here. The experiments demonstrated that temperature can be used as an aid in imaging asphalts.

The use of solvents to dissolve asphalts is another approach to imaging asphalts. However, this approach poses some problems because the solvent and dissolved asphalt both contain protons so that the respective contributions from each set of protons to the NMR image is not evident. Chemical shift imaging is a possible solution in this situation, albeit a remote one given the present state-of-the-art of NMR imaging. The use of deuterated solvents is another way to circumvent this problem.

For certain applications, signals from the solvent may not present problems as illustrated by the images in Figure 1. This is a set of images for an asphalt dissolved in an equal volume of toluene and titrated with isooctane to the point at which flocculation occurs and asphaltenes begin to precipitate. After a period of time the asphaltenes settle out to form a layer, the height of which depends on the amount of isooctane used to precipitate the asphaltenes.

Figure 1 is also an example of how the experimental parameters can be chosen to enhance the signal contrast between different components of the system. In Figure 1, the spin echo time was varied from 10 to 40 ms. For the shorter echo time (10 ms), the image shows little contrast because for this echo time the NMR signals from all the components are strong. As the echo time gets longer, the contrast between the asphaltenes and solvent improves. For an echo time of 40 ms, the NMR signal from the asphaltenes has decayed considerably and appears as a dark gray band at the bottom of the vial. The NMR signals from the asphalt/toluene/isooctane components are still strong for this echo time and appear as the bright areas in the figure. If the layer of asphaltenes is of interest, the solvent and dissolved asphalt do not present a problem so long as long echo times are used to form the images. This procedure is referred to as T_2 weighting.

There is a thin black layer between the solvent and asphaltenes which is very noticeable in the images taken at a 40 ms echo time (Figure 1). To obtain some idea of the nature of the black layer, a spatula was inserted to the bottom of the vial and an "X" pattern was scribed to disrupt the asphaltene/solvent interface (Figure 2). The images of the asphaltenes show that the surface was apparently rigid as indicated by the pieces of the black layer that were broken and scattered throughout the asphaltene layer. The nature of this layer is not known at present. This layer could be a part of the asphaltene layer that is becoming more rigid with time at the asphaltene/solvent interface. A more rigid system would have shorter relaxation times and would appear darker in the NMR images. The layer could also be due to oxidation of the maltenes, which are then attracted to the highly polar surface of the asphaltenes and form a distinct layer at the interface. Other possibilities also exist and investigations are continuing to characterize this layer.

Natural Rubber in Asphalt. Although the federal mandate on the use of crumb rubber in paving applications has been removed, there still is sufficient interest to more fully understand the compatibility and physicochemical interactions of asphalt and crumb rubber materials. Preliminary MRI measurements were conducted on the feasibility of observing the presence of natural rubber in asphalt and the possibility of natural rubber dissolution in asphalt after heat treatment. A conical piece of natural rubber was submerged in an asphalt and heated to a temperature of 160 °C for 16 hrs. The asphalt had a high carboxylic acid content and carboxylic acids have been shown to dissolve different rubber materials when heated to 200 °C for extended periods of time (Tauer and Robertson, this symposium)[14]. Images of the asphalt/natural rubber system were acquired before and after heating using the 3D technique (Figure 3). Only the protons in the rubber are imaged using the 3D imaging sequence. Images of the asphalt are not obtained because the proton relaxation times of asphalt are too short. The image of the heated sample (Figure 3b) is not as clear as

that of the unheated sample (Figure 3a). The current interpretation is that the less sharp image of the heated sample is a result of reactions that have taken place at the surface of the natural rubber cone. Reactions between the natural rubber and components in the asphalt could cause the relaxation times of the protons in both materials to be slightly different at the surface than that of the bulk natural rubber leading to less sharp images. Further experiments along these lines are in progress.

Asphalt/Water/Aggregate Systems. Moisture damage in pavements generally leads to stripping, raveling and late rutting. One probable mechanism responsible for these failures is loss of adhesion of the asphalt at the aggregate interface. Water is suspected to play a major role in this damage mechanism. Direct observation of this failure mode has been difficult because of the lack of suitable instrumental techniques. Magnetic resonance imaging (MRI) methods may offer an approach to study this mechanism because of the favorable response of water in MRI experiments. However, little research has been done on the use of MRI to study asphalt/aggregate/water interactions in order to validate whether MRI methods can provide insight into moisture damage mechanisms.

MRI measurements were made on pieces of aggregates that were embedded in asphalt and covered with a layer of water. A spin echo pulse sequence was used to image the cross-sections of the asphalt/aggregate/water system in the XZ plane, before and after freeze thaw cycling, to determine whether water had any effect on the asphalt/aggregate interface. Three asphalts of differing stiffness and three different aggregate systems were studied. However, preliminary MRI measurements indicated that a limestone aggregate would be the easiest to observe changes as a result of the freeze thaw cycling. The other aggregates had varying amounts of magnetic components and therefore could not be imaged.

Of the three asphalts studied, only one showed displacement of asphalt from the aggregate after freeze thaws. This is shown in Figure 4. Comparison of the boundary at the water/aggregate/asphalt interface in the lower left center of each panel, before and after freeze thawing, shows an increase in the amount of water extending downward into the asphalt along the aggregate. The penetration began after 4 freeze thaws and increased slightly with successive freeze thaws, although there was not much difference after 6 freeze thaws.

SUMMARY

Applications of magnetic resonance imaging to study various aspects of asphalts are in their infancy. Consequently, a number of imaging methods and instrumental parameters need to be investigated to determine the feasibility of MRI to study asphalts. In this study, exploratory MRI measurements were made on the precipitation of asphaltenes from asphalt, observation of natural rubber in asphalt, and the possible interaction of water with asphalt at an aggregate interface. The MRI experiments showed that image contrast between asphaltenes and the precipitating solvent can be improved by varying the echo time used to form the images. Natural rubber in the presence of asphalt can be observed using 3D imaging methods, leading to the possibility of studying solvent swelling and possible dissolution of crumb rubber by components of the asphalt. MRI measurements of asphalt/water/aggregate systems showed evidence of water penetration at the aggregate interface. In all cases, the results were sufficiently encouraging to warrant additional investigations.

DISCLAIMER

This document is disseminated under the sponsorship of the Department of Transportation in the interest of information exchange. The United States Government assumes no liability for its contents or use thereof.

The contents of this report reflect the views of WRI which is responsible for the facts and the accuracy of the data presented herein. The contents do not necessarily reflect the official views of the policy of the Department of Transportation.

Mention of specific brand names or models of equipment is for information only and does not imply endorsement of any particular brand to the exclusion of others that may be suitable.

ACKNOWLEDGMENTS

The authors gratefully acknowledge support of this work by the Federal Highway Administration under Contract No. DTFH61-92-C-00170. Technical discussion with Dr. Joseph Ford of Chemagnetics/Otsuka Electronics was also appreciated.

REFERENCES

1. Sarkar S.N., E.W. Wooten, and R.A. Komoroski, *Appl. Spec.*, 1991, 45, 619.
2. Ackerman J.L., L. Garido, J.E. Moore, and W.A. Ellingson, *Polymer Prepr.*, 1990, 31, 145.
3. Chang S.J., J.R. Olsen, and P.C. Wang, *For. Prod. J.*, 1989, 39, 43.
4. Cofer G.P., J.M. Brown and G.A. Johnson, *J. Magn. Reson.*, 1989, 83, 608.
5. Rothwell, W.P.; Holocek, D.R.; Kershaw, J.A.
6. Weisenberger L.A., and J.L. Koenig, *NMR Investigations of Case II Diffusion in Polymers*, in *Solid State NMR of Polymers*, L.J. Mathias, ed., Plenum Press, New York, 1991, 377-386.
7. Webb A.G., K. Motsegood, and R.B. Clarkson, *Fuel*, 1993, 72, 1235.
8. Hou L.; Cody, G.D.; French, D.C.; Botto, R.E.; Hatcher, P.G. *Energy Fuels*, 1995, 9, 84.
9. Koenig J.L., *Application of NMR Imaging to Polymers*, in *Solid State NMR of Polymers*, L.J. Mathias, ed., Plenum Press, New York, 1991, 61-79.
10. Sarkar S.N. and Komoroski R.A., *Macromolecules*, 1992, 25, 1420.
11. Chang C. and Komoroski R.A., *Macromolecules*, 1989, 22, 600.
12. Blumler P. and B. Blumich, *Macromolecules*, 1991, 24, 2183.
13. Komoroski R.A., *Anal. Chem.*, 1993, 65, 1068A.
14. Tauer, J.E.; Robertson, R.E. *Prepr. Pap.-Am. Chem. Soc., Div. Fuel Chem.*, 1996, 41, *Symp. on Modified Asphalts*.

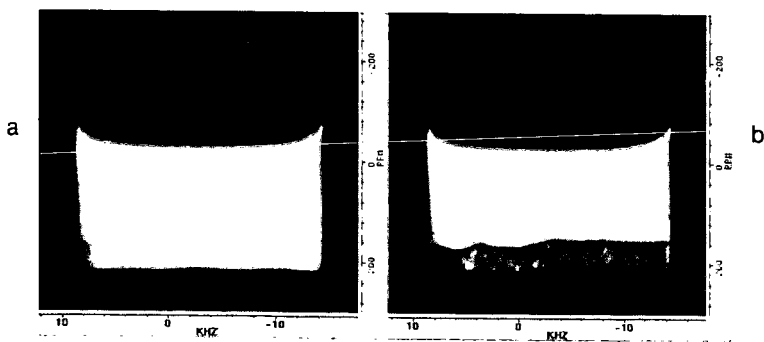


Figure 1. Spin echo images of asphaltene settling illustrating T_2 weighting to enhance image contrast: (a) 10, and (b) 40 ms echo time.

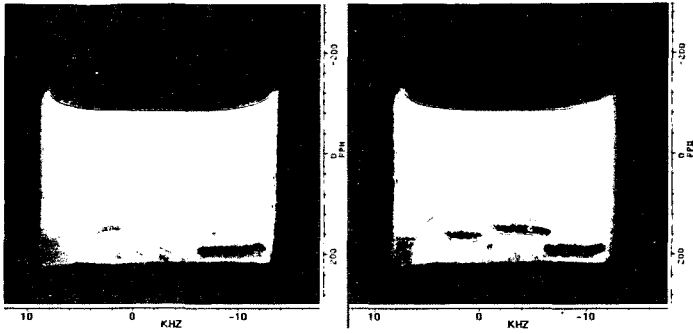


Figure 2. Spin echo images of asphaltene layer after stirring.

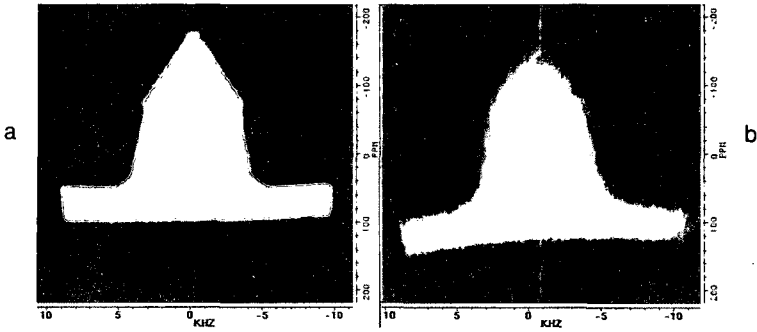


Figure 3. 3D images of natural rubber submerged in asphalt: (a) unheated, (b) heated for 16 hrs at 160 °C.

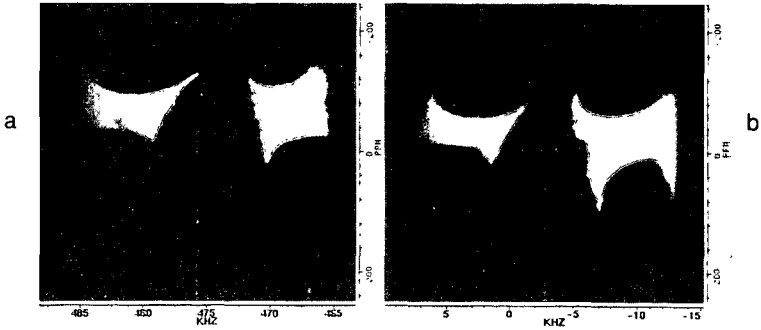


Figure 4. Spin echo images of SHRP asphalt AAM-1 and MRL aggregate RE in water after: (a) 0, and (b) 6 freeze thaws.